

149063

Reports of the Department of Geodetic Science  
Report No. 156

NASA CR-

141749

# OPTIMAL SELENODETIC CONTROL

by  
Haim Benzion Papo

(NASA-CR-141749) OPTIMAL SELENODETIC  
CONTROL Interim Report (Ohio State Univ.  
Research Foundation) 273 p

N75-73006

00/98 Unclas  
12381

Prepared for  
National Aeronautics and Space Administration  
Manned Spacecraft Center  
Houston, Texas

Contract No. NAS 9-9695  
OSURF Project No. 2841  
Interim Report No. 5



The Ohio State University  
Research Foundation  
Columbus, Ohio 43212

August, 1971

REPRODUCED BY  
NATIONAL TECHNICAL  
INFORMATION SERVICE  
U. S. DEPARTMENT OF COMMERCE  
SPRINGFIELD, VA. 22161

115

Reports of the Department of Geodetic Science

Report No. 156

OPTIMAL SELENODETTIC CONTROL

by

Haim Benzion Papo

Prepared for

National Aeronautics and Space Administration  
Manned Spacecraft Center  
Houston, Texas

Contract No. NAS 9-9695  
OSURF Project No. 2841  
Interim Report No. 5

The Ohio State University  
Research Foundation  
Columbus, Ohio 43212

August, 1971

## PREFACE

This project is under the supervision of Ivan I. Mueller, Professor of the Department of Geodetic Science at The Ohio State University, and it is under the technical direction of Mr. James L. Dragg, Mapping Sciences Laboratory, NASA/MSC, Houston, Texas. The contract is administered by the Space Sciences Procurement Branch, NASA/MSC, Houston, Texas.

A revised version of this report has been submitted to the Graduate School of The Ohio State University in partial fulfillment of the requirements for degree Doctor of Philosophy.

## ABSTRACT

This study was undertaken to solve the problem of determination of an optimal selenodetic control network on the Moon. Selenodetic control is defined by the coordinates of a network of well identifiable features on the lunar surface with respect to a selenodetic Cartesian coordinate system, which is fixed to the lunar crust, is centered at its mass center and is oriented along the three principal axes of inertia of the Moon.

The method developed for solving the problem is fully consistent with the theoretical and numerical models for the motion of the Moon in space. For this purpose, the parameters of orientation of the selenodetic system with respect to the mean ecliptic system, identified in this study with the physical librations of the Moon, are made an integral part of the solution for selenodetic control.

The solution is based on optical data obtained by photography or by direct angular observations of the Moon taken from the Earth or on board a spacecraft and on range and range-rate data obtained from tracking stations on Earth to a spacecraft orbiting the Moon. In order to achieve orientation of the control network at least part of the optical data is considered oriented with respect to a certain celestial coordinate system. Scale is introduced to the control solution through the assumption that the lunar ephemeris describes the motion of the center of mass of the Moon, or in this case, the translatory motion of the origin of the selenodetic coordinate system with respect to the geocenter. The lunar ephemeris introduced by JPL under the code-name LE-16 is used for the above purpose.

The total observational material modeled in terms of the parameters of the solution is processed by a weighted least squares adjustment procedure and results in estimates for the following parameter groups and their covariances:

- a. selenodetic coordinates of a selected number of fundamental control points on the lunar surface,
- b. parameters of orientation of the Moon (physical libration angles and time rates at a standard epoch),
- c. parameters featuring the low degree terms in the lunar gravitational field.

In case the optical data was taken on board a spacecraft, an orbit determination procedure is applied to the range and range-rate data which results in estimates for the selenocentric state vector of the spacecraft and also in estimates for the higher degree terms in the lunar gravitational field.

In order to test numerically the mathematical procedure developed in this study, a simulated environment was created which reflects very closely the true world. The Earth, the Moon and a variety of satellites move and rotate in this simulated environment strictly according to the laws of Newton and Kepler. The observational material generated is free of unaccounted phenomena and simulates very closely real observations.

Numerical tests with the simulated as well as with real data demonstrated that the solution for the physical librations of the Moon conforms very closely to existing solutions while having many advantages primarily that of being an integral part of the control network solution. A complete selenodetic control solution obtained from simulated Earth-based optical data confirmed the feasibility of the method developed in this study and introduced estimates for accuracies that could be achieved in the solution for an optimal selenodetic control.

## ACKNOWLEDGEMENTS

It gives me a great pleasure to be able to extend my gratitude and appreciation to the many persons without whom this work would not have been possible.

From my parents I inherited a deep and sincere love for learning and an acute curiosity for the unknown and the unsurveyed. The Technion, Israel's Institute of Technology and The Ohio State University provided me with the best education one could ask for in my field.

Working in Room 231, Lord Hall on the OSU campus with other graduate students like myself has been a wonderful experience. There was an atmosphere of enthusiastic learning, of a fruitful exchange of ideas, of sharing ones excitement over finding an answer to a problem, of true friendship of people working together.

The OSU Computer Center provided me generously with computer time needed for the study and through the invaluable assistance of Mr. John M. Snowden, I was able to make full use of its excellent facilities.

Discussions on many conceptual and practical problems with Doctors Peter Meissl, Dean C. Merchant and Donald H. Eckhardt helped in bringing more clarity and exactness where those were needed.

Professors Urho A. Uotila, Richard H. Rapp and Gerald H. Newsom served on the reading committee and provided noncompromising, but constructive, criticism which was indispensable in improving many portions of this work.

My advisor Professor Ivan I. Mueller played a most vital part in my work. It is only through his guidance, encouragement and unlimited confidence in me that I was able to overcome many difficult moments when it seemed that I was facing an inevitable dead end.

The difficult task of typing the text and, in particular, the many

formulae involved was done with exceptional skill and expertise by Mrs. Evelyn Rist, Mrs. Rene Tesfai and Miss Barbara Beer.

No graduate study by a married man is possible without the unconditional support and understanding of his wife and family. To my wife, Viola, and to my children, I shall be indebted forever for their patience and love which sustained me during the years of concentrated study.

This study was supported by The Mapping Sciences Laboratory NASA MSC, Houston, Texas under Contract No. NAS 9-9695 and the technical direction of Mr. James L. Dragg. Scholarships were granted me by the Hebrew Technical Institute of New York and also by the Technion, Israel's Institute of Technology.

Last, but not least, a word of thanks to The Department of Geodetic Science and The Ohio State University and in particular to the Department Chairman, Professor Urho A. Uotila, for making it possible for me to study and work in this great country.

## TABLE OF CONTENTS

	<u>Page</u>
PREFACE	ii
ABSTRACT	iii
ACKNOWLEDGEMENTS	v
LIST OF TABLES	x
LIST OF FIGURES	xi
1. INTRODUCTION	1
1.1 Statement of the Problem	1
1.2 Past Achievements and Problem Areas	3
1.21 Earth Based Methods	5
1.22 Satellite Borne Methods	7
1.3 Astronomical Models and Constants	11
1.31 Lunar Theory and Ephemeris	11
1.32 Orientation of the Moon in Space	16
1.33 Fundamental Astronomical Constants	22
1.4 General Plan for the Study	24
2. THEORETICAL SOLUTION OF THE PROBLEM	28
2.1 Introduction	28
2.2 General Adjustment Model	35
2.21 Condition Equations for an Optical Observation	39
2.22 Condition Equations for Range and Range-Rate	41
2.3 Parameters in the Solution	43
2.4 Linearization	49
2.41 Optical Observations	49
2.42 Range and Range-Rate Observations	55
2.5 Formation and Solution of the Normal Equations	57
2.51 Satellite Borne Optical Observations (Single Arc)	57

2.52	Earth Based Optical Observations	59
2.53	Combined Solution	60
2.6	Programming Considerations	62
3.	NUMERICAL INTEGRATION OF THE PHYSICAL LIBRATIONS OF THE MOON	71
3.1	Introduction	71
3.2	Equations of Rotational Motion of the Moon	74
3.21	Euler's Dynamic Equations	74
3.22	Transformation of Euler's Dynamic Equations	80
3.23	Differential Equations of the Physical Libration Angles	87
3.3	Adjustment Theory	91
3.31	Mathematical Model	92
3.32	State Transition and Parameter Sensitivity Matrices	96
3.4	Fitting Numerically Integrated Physical Libration Angles Into Existing Solutions	107
3.41	Spatial Angles Approach	108
3.42	Variational Rotations Method	114
4.	SIMULATION OF ENVIRONMENT AND OBSERVATIONS	119
4.1	Introduction	119
4.2	Fundamentals of the Simulation	123
4.3	Constants of the Simulation	127
4.31	The Earth	127
4.32	The Moon	128
4.33	Illuminating Source "Sun"	130
4.34	Initial Values for Position and Orientation of Earth and Moon, Including Linear and Angular Velocities	131
4.35	Motion of the Mass Center of the Moon	132
4.36	Eulerian Angles of the Moon	133
4.37	Eulerian Angles of the Earth	135
4.4	Equation of Motion	136
4.41	Equations of Motion of the Moon's Mass Center	138
4.42	Equations of Motion of the Selenodetic Coordinate System with Respect to a	

	Selenocentric Inertially Oriented System	143
4.43	Equations of Motion of the Average Terrestrial Coordinate System with Respect to a Geocentric Inertially Oriented Coordinate System	147
4.44	Equations of Motion of a Satellite with Respect to a Selenocentric Inertially Oriented Coordinate System	151
4.45	Numerical Integration of the Equations of Motion	154
4.5	Total Librations of the Moon	160
4.6	Observations	162
4.61	Optical Observations	162
4.62	Range and Range-Rate Observations from an Earth Station to a Satellite of the Moon	168
5.	NUMERICAL EXPERIMENTS	173
5.1	Introduction	173
5.2	Fitting Numerically Integrated to Simulated Physical Libration Angles	175
5.3	Fitting Numerically Integrated to Eckhardt's Physical Libration Angles	183
5.4	Selenodetic Control Solutions from Simulated Earth Bound Optical Observations	198
6.	SUMMARY AND CONCLUSIONS	219
	APPENDIX A: Equivalency of MacCullagh's Formula to a Spherical Harmonics Expansion	224
	APPENDIX B: Derivation of a Numerical Value for the Ratio Between the Equatorial and Polar Moments of Inertia of the Earth	228
	APPENDIX C: Design of a Set of Mascons on the Moon	231
	APPENDIX D: Considered Parameters in a Least Squares Adjustment Process	234
	APPENDIX E: Rules for Differentiation of Matrices	241
	APPENDIX F: Orbit Determination Routine for a Satellite of the Moon in the Simulated Environment	247
	REFERENCES	256

## LIST OF TABLES

	<u>Page</u>
2.1 Parameters in the General Adjustment Procedure . . . . .	45
4.1 Geocentric Cartesian Coordinates of Observatories . . . . .	128
4.2 Mass and Selenodetic Coordinates of Mascons on the Moon . . .	129
4.3 Selenodetic Coordinates of Triangulation Points on the Moon . .	130
4.4 Arguments of the Terms in the Physical Librations Harmonic Series . . . . .	134
5.1 Starting and Adjusted Physical Libration Parameters for Solutions Numbers 1 through 8 . . . . .	186
5.2 Correlation Matrices for Cases 1 through 4 . . . . .	187
5.3 Correlation Matrices for Cases 5 through 8 . . . . .	188
5.4 Covariance and Correlation Matrices for Solution of Network I from 30 Bundles. Triangulation Points . . . . .	205
5.5 Covariance and Correlation Matrices for Solution of Net I from 30 Bundles. Physical Libration Parameters . . . . .	206
5.6 Diagonal Elements of Covariance Matrix for Solution of Net I from 30 Bundles . . . . .	208
5.7 Diagonal Elements of Covariance Matrix for Solution from 6, 12, 18, 24 and 30 Bundles . . . . .	210
5.8 Effect on the Solution of Different Optical Observation Accuracies . . . . .	211
5.9 Solution Vector for Test (a) in Experiment (ii) . . . . .	214
5.10 Solution Vector for Test (b) in Experiment (ii) . . . . .	215
5.11 Solution Vector for Test (c) in Experiment (ii) . . . . .	217

## LIST OF FIGURES

	<u>Page</u>
1.1 Libration Window . . . . .	5
1.2 Mean Orbit of the Moon . . . . .	13
1.3 Optical Librations in Longitude . . . . .	17
1.4 Cassini's Laws . . . . .	18
1.5 Eulerian Orientation Angles . . . . .	19
2.1 Earth-Moon Environment . . . . .	31
2.2 Geometry of Observations . . . . .	37
2.3 Optical Observations . . . . .	40
2.4 Range and Range-Rate Observations . . . . .	41
3.1 Euler's Geometric Equations Diagram . . . . .	81
3.2 Motion of the MOD Ecliptic Coordinate System . . . . .	83
3.3 Spatial Angles Diagram . . . . .	108
3.4 Variational Rotations about the xyz Axes . . . . .	114
3.5 Equivalency between Spatial Angles and Variational Rotations . . . . .	116
4.1 Position and Orientation of the Earth and the Moon . . . . .	126
4.2 The Simulated Earth-Moon Environment . . . . .	137
4.3 Eulerian Angles of the Moon . . . . .	144
4.4 Eulerian Angles of the Earth . . . . .	148
4.5 Total Librations of the Moon . . . . .	160
4.6 Reference Frame for Optical Observations . . . . .	163
4.7 Optical Observations . . . . .	165
4.8 Determining the Eulerian Angles $\varphi_1, \varphi_2, \varphi_3$ . . . . .	165
4.9 Vector Diagram of Optical Observations . . . . .	167
4.10 Range and Range-Rate Diagram . . . . .	169
4.11 Conditions for Existence of Range and Range-Rate Observations . . . . .	171

	<u>Page</u>
5.1 Differences between Numerically Integrated and Simulated $\tau$ Angles (Physical Librations in Longitude). . . . .	182
5.2 Differences between Numerically Integrated and Eckhardt's $\tau$ Angles. . . . .	189
5.3 Differences between Numerically Integrated and Eckhardt's Physical Libration Angles . . . . .	192
5.4 Differences between Numerically Integrated and Eckhardt's Modified Physical Libration Angles . . . . .	194
5.5 Differences between Numerically Integrated and Eckhardt's Corrected Physical Libration Angles. . . . .	196
5.6 Typical Areas for Positioning Triangulation Points on the Moon .	198
5.7 Distribution of Points in Control Networks I and II. . . . .	199
5.8 Libration Subpoints of the Thirty Optical Bundles . . . . .	200
A.1 Polar Coordinates of Point Q . . . . .	225
F.1 Vector Diagram for a Satellite of the Moon . . . . .	248

## 1. INTRODUCTION

### 1.1 Statement of the Problem

Maps of the Moon have been drawn ever since the first telescopes began scanning the surface of the nearest-to-the-Earth celestial body. Coordinates of features on the front side of the Moon have been calculated for almost two centuries. Improvements in observational techniques and instrumentation as well as the perfection of mathematical theories designed to model the motions of the celestial bodies involved all have continuously enhanced the accuracy of the maps produced. Recent articles reporting on research being done in this area reveal that the interest in mapping the Moon has not subsided; on the contrary with the advent of space exploration a new dimension has been added to it. Having detailed and accurate maps of the Moon's surface is considered indispensable in view of landing missions and also in cases where certain instruments are placed and operated on the surface of the Moon.

The new dimension extends also to the types of observational material obtained. In addition to the Earth-bound optical observations, a new generation of space-borne photography and angular measurements became available. For the first time the Earth's atmosphere ceased to be a limiting factor in the overall quality of observations of the Moon.

The high degree of optimism, however, gave way to a mild disillusionment as the analysis of space-acquired data failed to conform to the previously available results. Possible reasons for the discrepancies could be named by the dozen, but no clear way for resolving the contradictions and eventually arriving at a consistent and better solution were at hand. This is the point where the study presented hereafter was initiated.

In addition to the practical aspects of obtaining better coordinates for features on the Moon and consequently defining a better coordinate system, there was a challenge in undertaking an investigation in this particular field. Traditionally, mapping of the Moon has been in the domain of astronomers and out of place for geodesists who had plenty of problems of their own to cope with. The geodetic sciences, however, have registered tremendous progress in the past several decades, and the prospects for a geodesist to contribute to the solution of the problem of mapping the Moon are at least fair. The challenge is also in venturing into and examining theories and models of celestial mechanics associated with the motion of celestial bodies in general and that of the Moon in particular. There is a certain advantage in coming into a field from the outside: The traditional approaches and solutions appear less inhibitive. It is easier for a newcomer to think of new ways to tackle old problems than it is for the home bred scientist.

The problem to be investigated can be defined as follows:

To explore known methods for mapping the Moon and to develop a procedure for the establishment of a unique solution which will be consistent with all the data types available and which will conform with the models and ephemerides for the motion of the Moon, the Earth, and other celestial bodies.

The initial stage in any mapping sequence is the definition and determination of a datum and a fundamental control network which will serve in later stages as the basis for densification of control and the actual map production. Thus the specific objective in this work is limited to the basic phase of the general problem of mapping the Moon, i. e. , the establishment of a fundamental control network on the Moon or using "geodetic" as a synonym:

"The establishment of an optimal selenodetic control."

## 1.2 Past Achievements and Problem Areas

A detailed review of past achievements in mapping the Moon is beyond the scope of an introductory chapter. As can be seen in [Mueller, 1969b], even a bibliographical list could easily extend into tens of pages. Instead, in order to put in perspective the work reported in the following chapters, typical articles have been selected to represent the past achievements and contemporary trends in this field. In what follows, the various solutions to the problem are classified according to their broader character; thus avoiding the necessity of going into exhausting details and the many delicate differences among the individual procedures.

The data considered in this section are optical data obtained by photography of the Moon or from the measurement of directions to particular features on the surface of the Moon. The methods for determining coordinates of features on the Moon are divided into two major categories according to the mode of acquiring the optical data:

- I. Methods based on data obtained from the surface of the Earth.
- II. Methods based on data acquired from a spacecraft.

Following is an outline of the main optical data types:

- (i) Heliumeter or position micrometer observations in which the quantity measured is the spatial angular distance between any two features on the surface of the Moon or between a particular feature (the crater Mösting A) and the apparent limb of the Moon at different position angles [Koziel, 1948; Hopmann, 1967].
- (ii) Photography of the Moon obtained by means of long focus (15-20 m) Earth-based astronomic telescopes with or without a superimposed star field [Arthur, 1962; Moutsoulas, 1969].
- (iii) Photography of the Moon by cameras with a principal distance of 80-240 mm taken from a spacecraft in the vicinity of the Moon.

(iv) Directions to features on the surface of the Moon measured with an optical instrument on board an orbiting spacecraft [Ransford, et al., 1970].

Although a more detailed account on the complex motion of the Moon is presented in section 1.3, one particular aspect of this motion should be mentioned in the present section due to its relevance to the Earth-based methods. The rotation of the Moon about its center of mass and its translatory (orbital) motion about the geocenter (the center of mass of the Earth) are interrelated in a way such that the face of the Moon as seen by an observer on Earth remains the same, i.e., the relative orientation of the Moon with respect to the Earth does not change. Due to various reasons (see section 1.3) the Moon oscillates about its mean orientation with respect to the Earth. These oscillations, as detected by an observer on Earth, are called in general librations of the Moon. They are composed of true or physical and of apparant librations. The true librations are deviations of the Moon from the state of steady (even) rotational motion as referred to inertial space, while the apparant librations are due to the varying position of the observer on Earth with respect to the Moon.

The maximum amplitude of the total librations as seen from the geocenter is of the order of  $7^\circ$  to  $8^\circ$ . Another way of presenting the situation would be to say that from the geocenter the Moon can be seen only through a comparatively narrow libration window measuring  $15.9^\circ$  by  $13.3^\circ$  (see figure 1.1). Due to the diurnal rotation of the Earth, an observer located on its surface could observe the Moon outside the libration window by as much as  $57'$  [Kopal, 1969]. Thus, two optical observations taken by an observer on Earth to a particular feature on the Moon can have a maximal angle of convergence of about  $23^\circ$ . However, such cases are rare and the usual angle of convergence is considerably smaller.

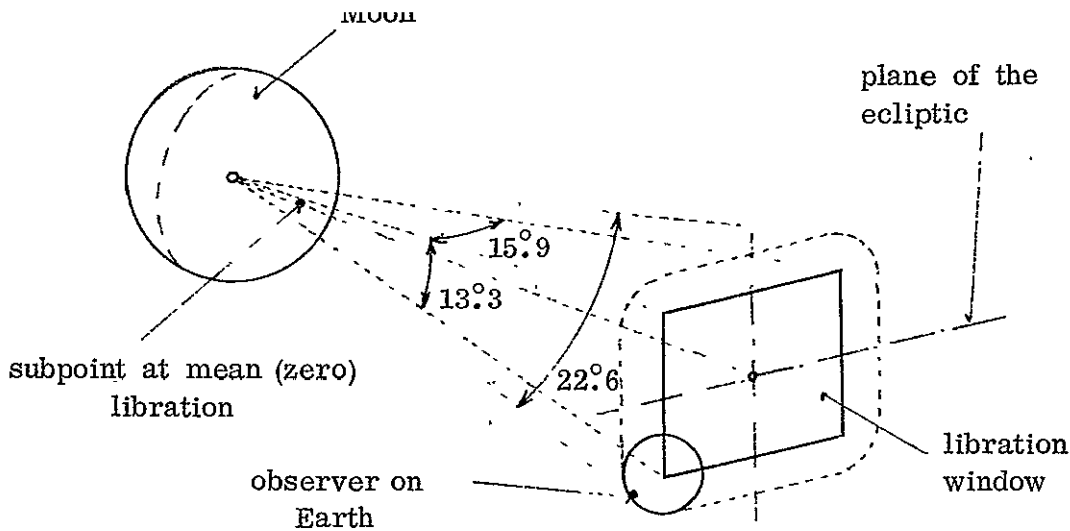


Figure 1.1 Libration Window

### 1.21 Earth-Based Methods.

(a) Heliumeter observations of the angular distances between the lunar crater Mösting A and points on the lunar limb were processed and resulted in the derivation of the parameters of physical libration and the selenographic Cartesian or polar coordinates of the point Mösting A. The coordinates of this point together with the orientation of the Moon as defined by the physical libration model (constants in a trigonometric series) define the "center of figure" datum. The center of figure is introduced by the implicit assumption made in the reduction of the heliometer observations that the center of the apparent limb corrected for local irregularities (deviations from a circle) is the projection of the point about which the Moon oscillates. The latest and most comprehensive solution for this datum had been derived by Koziel and reported in [Kopal and Goudas, 1967]. Mösting A was regarded as the "datum point" of any further extension of control on the Moon. It should be noted that the scale of the datum was

defined through the mean radius of the Moon, i.e., the radius of the best fitting circle over the irregularities of the lunar limb.

(b) Direct angular observations between Mösting A and 12 other craters on the Moon's surface, performed by heliometer or position micrometer together with a physical libration model (for the orientation of the Moon), were used to determine the coordinates of these 12 points as a fundamental control network. With small variations these points together with Mösting A served as the basis of any subsequent Earth-based control network. Observations of this type were performed some 70 years ago by two distinguished German astronomers—Franz in Königsberg [Franz, 1899] and Hayn in Leipzig [Hayn, 1904]. Franz measured 8 of the 12 points and Hayn, the remaining 4. Half a century later the Austrian astronomer, Schrutka-Rechtenstamm, readjusted the original observations of Franz and Hayn and obtained a consistent solution for the 12 fundamental points [Schrutka-Rechtenstamm, 1956]. His solution is rigorous mathematically and provides a procedure for handling the nonlinear variation of the parameter  $f$  ( for a definition of  $f$  see section 1.32 ).

(c) Photography of the Moon obtained by astronomic telescopes at extreme librations resulted in a series of convergent photos. These convergent photographs were used through the colinearity conditions of an optical bundle to determine the relative positions of secondary control points [Kopal, 1969]. The first consistent sets of such secondary control were derived by Franz and Saunder at the beginning of this century [Franz, 1901; Saunder, 1900]. Schrutka-Rechtenstamm also recalculated Franz's observations for secondary control and established a set of 150 second-order control points on the front side of the Moon [Schrutka-Rechtenstamm, 1958]. The list of second- and third-order triangulations based on this method is long. To mention a few: Breece, Hardy and Marchant [1964], Meyer and Ruffin [1965], Hathaway [1967], Mills [1968]. There is also extensive literature on intercomparison of coordinates and error evaluation.

Hallert [1962] and others [NASA MSC, 1965] concluded that, theoretically, regarding known uncertainties in the photogrammetric process, e.g., acquisition of photography through a continuously turbulent atmosphere [Edgar, 1964], poor geometry (narrow libration window), identification and measuring accuracies, the results from this method can hardly be better than 1-1.5 km; and in many cases they would probably be much worse. This could be proven to some extent also numerically by comparing coordinates of the same points as determined in various triangulations [Kuiper, Arthur et al., 1969].

(d) A modified version of method (c) is possible when the Earth-based lunar photographs have stars recorded in the background [Arthur, 1962] or superimposed on the lunar disc [Moutsoulas, 1970]. The scale and the orientation of the photos can thus be determined from the star images, and so the photogrammetric solution does not have to depend on the fundamental control as in method (c). Two series of star-oriented photographs have been obtained in the past decade: the Tucson, Arizona, "star-trailed" photographs and more recently the Manchester, England, "star-superimposed" plates. Some results of triangulations with these oriented plates have been reported [Arthur, 1968; Kuiper, Arthur et al., 1969], but it is too early to draw conclusions insofar as ultimate accuracies and datum determination are concerned.

Methods (c) and to some extent (d) depend on the datum defined by the methods (a) and (b). Accordingly, they all define an Earth-based center of figure lunar datum. An extensive review and discussion on the various third-order lunar triangulations is given in [Kuiper, Arthur et al., 1969].

## 1.22 Satellite-Borne Methods.

Distinctly different although somewhat related to the above are the satellite-borne methods. If from a spacecraft in the vicinity of the Moon a photograph is obtained or an oriented direction is observed, due to the

superior geometry (directions and photos can be taken from any conceivable angle, no atmospheric effects, closer range, etc.), a "photogrammetric" solution can be obtained for coordinates of features on the surface of the Moon. "Photogrammetric" is put between quotation marks because, as in the case of direct angular observation from an Apollo command module, though the data is reduced photogrammetrically there are no photographs involved. This comment is further expanded in section 2.1 to bring forward the idea of a general optical direction in space; see also [Rinner et al., 1967].

(e) Photographic coverage of the Moon's surface or portions thereof were treated as in ordinary aerotriangulation with existing ground control. Photographs taken with a Hasselblad camera from the Apollo spacecraft (command module) have been used to triangulate strips of photographs [Mueller, 1969b, pp. 38, 51] using control points obtained through method (c) above or by method (f) to be discussed next. Constraints on spacecraft positions were not necessarily imposed and the orientation of the photos were regarded as unknown. Along this line, D. Brown envisioned a situation where-if a complete coverage with sufficient side and forward overlapping were obtained, the peculiar geometry of the closed net would be so strong as to allow an excellent solution without any orbital or camera orientation constraints [Brown, 1968]. One problem which cannot be overlooked, however, is the datum of this perfectly determined cluster of points.

(f) The solution as of method (e) could be enhanced by the introduction of more or less rigid orbital constraints, i. e., consideration of the fact that the photos are taken from points on a trajectory of a spacecraft orbiting the Moon. Moreover, if the orientation of the camera may be assessed by an independent sensor, a stellar camera or an inertial navigator, a photogrammetric solution may be obtained which does not need fundamental control

at all. It creates its own control which stems from the orbital geometry and the orientation of the photographs with respect to inertial space. Here, however, the orientation and the rotation of the Moon come into the picture. As the Moon rotates with respect to the stars in a rather complicated manner, the projection center and the orientation of the bundle of directions created by each photograph cannot be used directly in the photogrammetric solution unless the rotation of the Moon is taken into account. This would mean that this method can define fundamental control through the use of the physical librations as derived on the basis of method (a) discussed above. Thus, this method still has to depend on information obtained from Earth-based observations. A procedure that avoids this dependence is developed in Chapter 2 where the model for a combined solution is discussed. The solutions for "independent control" from Lunar Orbiter IV photography belong to this class irrespective of the fact that the geometric integrity of the transmitted photos and the reliability of the orbital and orientation constraints may be questioned [TOPOCOM, 1969; Boeing, 1969].

(g) If instead of photography, direct angular observations were obtained from the orbiting spacecraft, a solution is possible which follows in general that of method (f). The same feature on the Moon's surface has to be observed from different points along the orbit and also, if possible, from different passes in order to acquire geometry that will allow a good solution. Observations of this type have been made successfully by Apollo astronauts and have been reduced by NASA/MSL as reported in [Ransford et al., 1970].

It should be noted that the datums defined by methods (f) and (g) are not constrained to the coordinates of Mösting A. On the other hand, these two methods define a datum which is centered at the mass center of the Moon primarily due to the orbital constraints. An excellent preview of satellite-

borne methods for moon triangulation is presented in [Doyle, 1968] which reflects to some extent thoughts and recommendations of the Santa Cruz study group on lunar exploration [NASA, 1967].

Summarizing the methods outlined above, it appears that none of them is capable of solving independently and satisfactorily the problem of a fundamental control network on the Moon. The Earth-based methods suffer from poor geometry, atmospheric turbulence and define a datum which is centered at an arbitrary "center of figure" point whatever the definition of that figure may be. The satellite-borne methods need the orientation of the Moon in space in order to relate their observations to the actual surface of the Moon although they are capable of determining the scale of the datum and associate it to the center of mass.

For one reason or another, none of the methods takes full advantage of the existence of a lunar ephemeris of a superior quality which is available today [O'Handley et al., 1969]. Although the ephemeris is used for deriving the physical libration series and also to some extent in orbit determination of the state vector of the satellite, it is not a dominant factor, and its metric potentials are ignored.

As stated at the beginning of this section, this is only a compressed review of existing methods, and it should be understood that within each method there are numerous variations in approach and treatment which, however, do not alter their basic nature as specified above.

### 1.3 Astronomical Models and Constants

The Geodesy and Cartography Working Group of the NASA 1967 Summer Study of Lunar Science and Exploration held between July 31 and August 13, 1967, in Santa Cruz, California, outlined in exceptionally lucid language certain principles which were adopted almost literally as the motto in this work. Regarding the determination of a datum and its relation to the translatory and rotational motion of the Moon as well as to its gravitational figure, it states the following [NASA, 1967, p. 298]:

The interlinked nature of the whole set of topics has the consequence that refinements in all topics must proceed at the same pace for optimum efficiency. In fact, it is difficult to singularly advance any of the topics without advancing some aspects of others. Just enough redundancy exists in the proposed program so that the solutions obtained can benefit from a consistency check within the total framework.

Indeed since August, 1967, in some of the interlinked topics mentioned above a definite progress has been registered. The brilliance and systematic efforts of scientists from JPL and USNO produced in 1969 a new lunar ephemeris which is a significant step forward toward the stated objective of 10 m accuracy. The presentation of the mascon hypothesis and the determination of a network of point masses on the near side of the Moon to model its gravitational potential are without doubt another major breakthrough.

This section summarizes the study of models for the motion of the Moon which was undertaken in order to achieve a better understanding of the interrelations between the constants involved and in general to enhance the insight into some of the problems in dynamical astronomy.

#### 1.31 Lunar Theory and Ephemeris.

The lunar theory was subjected to intensive and detailed study with the following primary objectives:

- (a) To obtain a sufficient knowledge of the mathematical procedures employed in the various solutions of the lunar theory. The rotating rectangular

coordinates method of Hill as developed by Brown was to be investigated in particular.

- (b) To settle on a minimum number of parameters which govern the lunar theory and define the relationship between those constants and the geocentric coordinates of the Moon at any epoch.
- (c) To evaluate the latest reports on the consistency of the lunar ephemeris with certain observational types and come up with reasonable estimates of the remaining uncertainties in it.

The following is condensed primarily from [Brown, 1896] and [Brouwer and Clemence, 1961]. The motion of the Moon about the geocenter is essentially a perturbed two body Keplerian motion. The main perturbations are due to the gravitational attraction of the Sun while secondary perturbations are due to the planets, the nonspherical dynamic shapes of the Earth and the Moon, and to tidal forces.

The solution of the differential equations of motion of the Moon is based on the assumption that the motion of the perturbing bodies is a known function of time and in general follows Keplerian motion (heliocentric). Small corrections for the actual deviations from Keplerian motion are added at a later stage. One way of presenting the solution is by expressions for the six osculating orbital elements containing, in general, constant, secular and periodic parts.

The mean orbital elements of the Moon are composed of the constant and secular parts, all periodic terms being removed:

$$\psi = \psi_0 + \psi_1$$

where

$$t = T - T_0$$

$\psi$  symbolizes any of the six mean orbital elements at the epoch T

$\psi_0$  is the value of  $\psi$  at the standard epoch  $T_0$  (1900.0 for example)

$\psi_1$  is the rate of secular change in  $\psi$ .

The six orbital elements are (see Figure 1.2):

L	mean longitude	n	mean motion in longitude
$\tilde{\omega}$	longitude of perigee	e	eccentricity
$\Omega$	longitude of ascending node	i	inclination

The mean longitude and the longitude of perigee are composite angles measured from the equinox to the ascending node and from the node along the orbital plane.

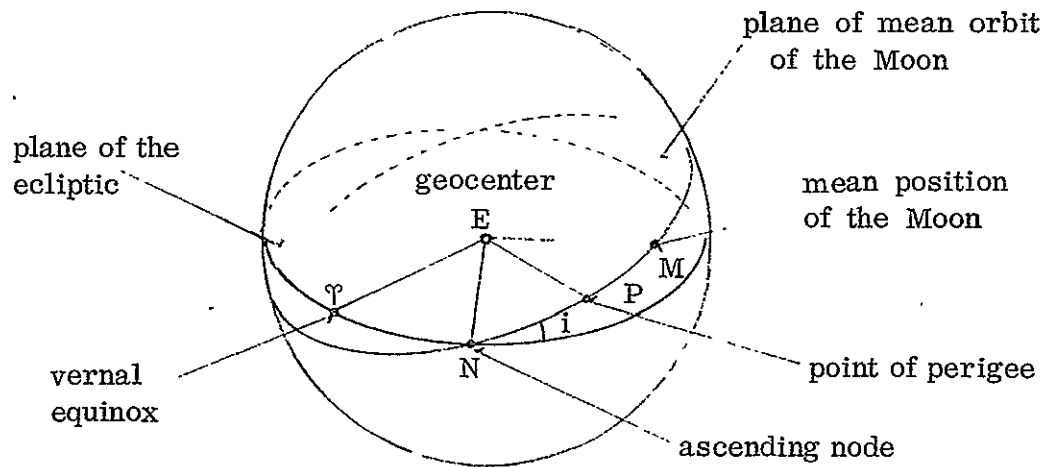


Figure 1.2 Mean Orbit of the Moon

According to Figure 1.2 and the definitions outlines above, the following relations hold:

$$\begin{aligned}\Omega &= \angle \hat{E}EN \\ \tilde{\omega} &= \Omega + \angle \hat{N}EP \\ L &= \tilde{\omega} + \angle \hat{P}EM\end{aligned}$$

The physical constant  $\mu$  may be considered as the "seventh" element and stands for

$$\mu = k^2(E + M)$$

where

$k^2$  is the Gaussian gravitational constant

$E, M$  are the masses of the Earth and the Moon, respectively.

Three more quantities are needed to define the mean orbit geometrically:

$a = (\mu/n^3)^{\frac{1}{3}}$  the mean distance

$(1-c)n$  the mean motion of perigee

$(1-g)n$  the mean motion of node, where

$c, g$  are functions of the parameters  $a, n, e, i$ , and also of the adopted constants of mass and motion of the Sun and the planets. Instead of  $i$ , a more useful parameter is  $\gamma = \tan i$ . Thus the list of the mean elements can be written as follows:

$$\begin{aligned} L &= L_0 + nt & n &= n_0 + n_1 t \\ \tilde{\omega} &= \tilde{\omega}_0 + (1-c)nt & e &= e_0 + e_1 t \\ \Omega &= \Omega_0 + (1-g)nt & \gamma &= \gamma_0 + \gamma_1 t \\ a &= a_0 + a_1 t \end{aligned}$$

$a_1, n_1, e_1, \gamma_1$  are secular variations due to tidal dissipation (Kopal, 1969). They are added at the very end of the solution. Thus for the most part of the development of the theory,  $a, n, e, \gamma$  are regarded as virtually constant.

The elements of the mean orbit at the initial epoch  $T_0$  and the values of the auxiliary constants ( $c, g$ ) are determined from observations and are known with high precision. As  $c$  and  $g$  are also functions of ( $n, a, e, \gamma$ ), the comparison of the theoretical  $c, g$  with the observed ones serves as a test of the validity of the theory. Actually for Brown's theory as corrected by Eckert's work, there are still some unexplained differences between the theoretical and observed  $c$  and  $g$  [Eckert, 1965].

The practical result of any lunar theory is the lunar ephemeris in which the geocentric coordinates of the Moon are given as a function of time.

The general form of an ephemeris is

$$Q = Q_0 + Q_1 t + \sum_i P_i \frac{\sin}{\cos} (p_i t + q_i)$$

where

- $Q$  represents any of the three coordinates (longitude, latitude, parallax)
- $Q_0 + Q_1 t$  are the coordinates in the mean orbit
- $P_1$  are algebraic functions of  $a, e, \gamma$  and corresponding solar and planetary orbital constants
- $q_1$  are linear functions of  $L_0, \tilde{\omega}_0, \theta_0$  and corresponding solar and planetary orbital constants
- $p_1$  are linear functions of  $L_1, \tilde{\omega}_1, \theta_1$  and corresponding solar and planetary constants
- $t$  is the independent variable, i. e., ephemeris time measured from the standard epoch—1900.0 (in the original Brown's theory).

Thus the objective of any lunar theory is to determine the values of  $P_1, p_1, q_1$ . In numerical theories like Hansen's, the numerical values of the parameters  $n, a, e, \gamma, c, g$ , etc. are substituted at the outset; and the series are developed numerically as far as  $P_1$  is concerned. In such a theory, the parameters of the mean orbit which are contained implicitly in the coefficients of the harmonic series cannot be separated. In a fully algebraic theory like Delauney's, the coefficients  $P_1$  are developed in a literal form in terms of the primary parameters. Brown's theory is semi-algebraic as the ratio  $m = n/n'$  ( $n'$  is the mean motion of the Sun) is substituted numerically while the other parameters are left in the development in an algebraic form. The periodic terms in Brown's theory are thus convenient for the calculation of partial derivatives of the coordinates with respect to the mean orbital parameters [Eckert, et al., 1954]. As reported by Van Flandern, very good approximations for the partial derivatives of the lunar coordinates with respect to the mean orbital elements can be obtained by differentiating the characteristic part of the major terms in Brown's series [Van Flandern, 1970]. An inadequacy was detected in Brown's theory, namely, the insufficiently developed planetary part [Mulholland, 1968]. Scientists from JPL have largely solved the problem by integrating numerically the equations of motion and fitting to quasi-observations obtained from

the theoretical Brown ephemeris. These are the so-called integrated lunar ephemerides, the latest reported version being called LE-16 [O'Handley et al., 1969]. Reports by various users of this ephemeris provide a satisfactory proof of the improvement achieved [Mulholland, 1969b; Cary and Sjogren, 1968; Garthwaite, et al., 1970] and increase the confidence in the estimated accuracies, namely: 100-150 m in position and 50 m in range [Mulholland, 1969]. This error level is of the same order of magnitude as the errors in selenocentric position of a circumlunar satellite as determined from Doppler data.

As a result of examining the various lunar theories; and in particular, after realizing the magnitude of the task of improving an existing ephemeris, the decision was made to adopt the newly developed JPL lunar ephemeris, LE-16 and to make use of it in the following manner: The Cartesian geocentric coordinates of the Moon are to be regarded as random quantities with mean at the nominal value of the coordinates as given by LE-16 and standard deviations corresponding to 50 m in range (parallax) and 150 m in direction (latitude and longitude). In other words, the uncertainties are defined as an oblate rotationally symmetric error ellipsoid with major and minor semiaxes of 150 m and 50 m respectively where the shorter (rotational) axis is oriented along the Earth-Moon vector.

### 1.32 Orientation of the Moon in Space.

In this subsection, the actual motion of the Moon around its center of mass and with respect to inertial space is discussed. As it is well-known the Moon rotates around its axis of rotation with a rather slow rate as compared to the Earth. The rotational period is equal to one sidereal month so that this rotation combined with the orbital period of one month results in the Moon facing the Earth with the same side. However, since the Moon moves around the Earth in an elliptical orbit with a varying velocity along the orbit in accordance with the second law of Kepler, while

its rotational velocity remains approximately constant, the Moon, as seen from the Earth, librates in longitude (see Figure 1.3). These are the so-called optical librations in longitude. Their period is an anomalistic month (perigee to perigee) where the amplitude is  $7^{\circ}57'$  [Kopal, 1969].

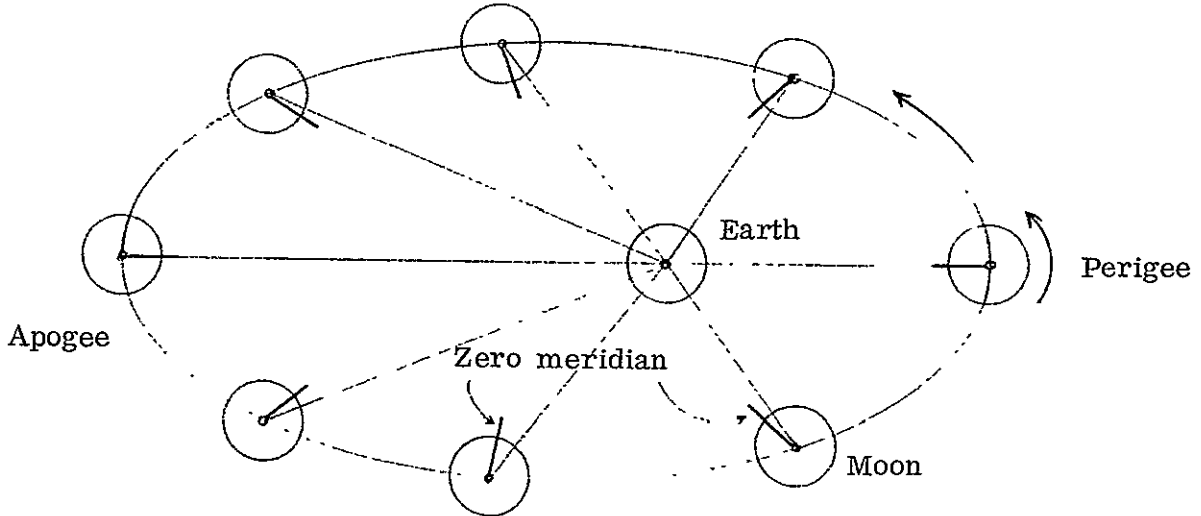


Figure 1.3 Optical Librations in Longitude

The inclination of the Moon's equator (the plane normal to the rotational axis) with respect to the ecliptic ( $1^{\circ}32'$ ) combined with the inclination of its orbit with respect to the ecliptic ( $5^{\circ}08'43''$ ) result in the so-called optical librations in latitude with a maximum amplitude of  $6^{\circ}41'$  [Kopal, 1969].

Because of the asymmetric gravitational field of the Moon, the Earth and the Sun trigger secondary true oscillations of the Moon of a much smaller amplitude but of a more complicated nature called physical or true librations.

Mathematically, the rotation of the Moon is defined through the rotational motion, with respect to the ecliptic coordinate system, of a selenodetic coordinate system which is considered fixed to the body of the Moon. The selenodetic system is centered at the Moon's mass center and its three axes are oriented along the Moon's principal axes of inertia.

In its rotation, the Moon follows very closely the three laws of Cassini (see Figure 1.4):

- (i) The Moon rotates uniformly about its axis of maximum moment of inertia with a rotational velocity identical with its mean motion around the Earth ( $n$ ).
- (ii) The inclination of the lunar equator (the plane normal to the rotational axis) with respect to the ecliptic is a constant ( $I$ ).
- (iii) The lunar equator intersects the plane of the ecliptic along the line of nodes of the Moon's mean orbit so that the plane of the ecliptic is always in between the planes of the equator and the orbit.

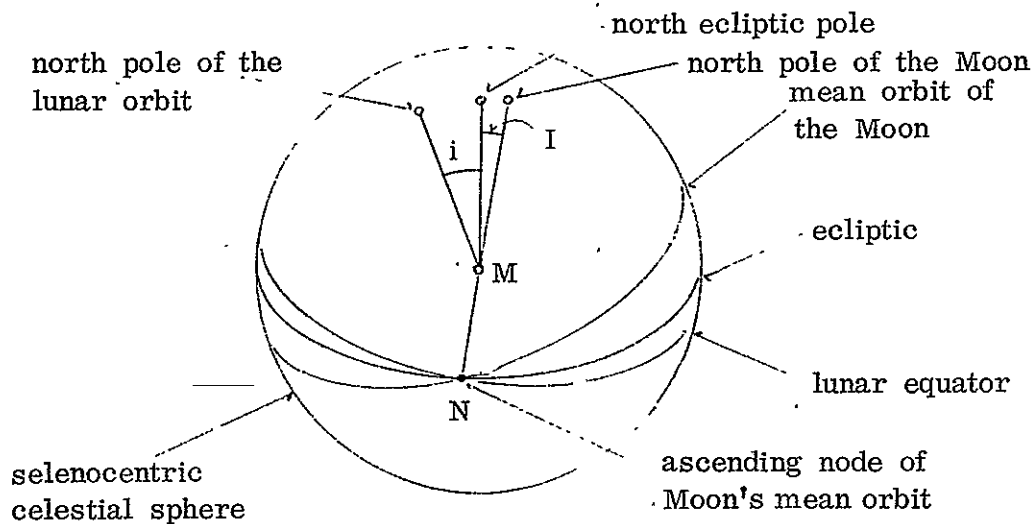


Figure 1.4 Cassini's Laws

The physical librations as defined earlier are actually the deviations of the Moon from following exactly the laws of Cassini. These are:

- $\tau$  - the libration in longitude (deviation from law (i) above);
- $\rho$  - the libration in inclination (deviation from law (ii) above);
- $\sigma$  - the libration in node (deviation from law (iii) above).

The instantaneous orientation of the Moon's selenodetic system with respect to the ecliptic system is defined by the Eulerian angles  $\varphi$ ,  $\psi$ ,  $\theta$ . The Eulerian orientation angles are composed of elements of the mean orbit (through the laws of Cassini) and of the three physical libration angles as shown in the following formulae and also in Figure 1.5:

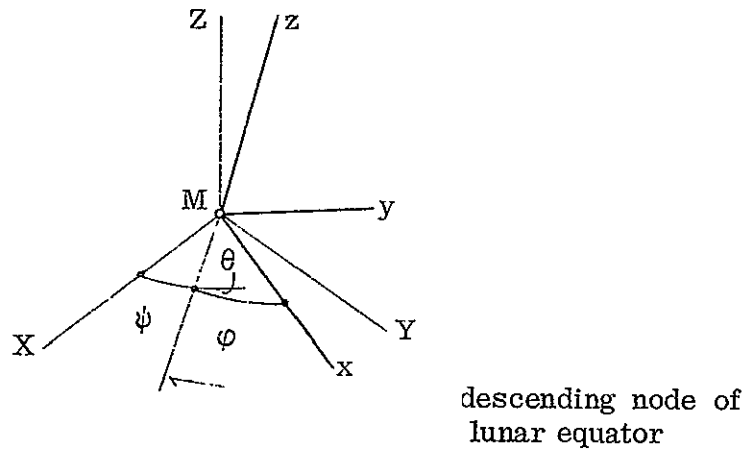


Figure 1.5 Eulerian Orientation Angles

where:

XYZ is a selenocentric coordinate system parallel to the ecliptic system

xyz is the selenodetic coordinate system as defined above.

$$\varphi = L + \Pi - \Omega + \tau - \sigma$$

$$\psi = \Omega + \sigma$$

$$\theta = I + \rho$$

where:

L is the mean longitude of the Moon

$\Pi = 3.1415\dots$

$\Omega$  is the longitude of the ascending node of the Moon's mean orbit

I is the mean inclination of the lunar equator to the ecliptic

$\tau, \sigma, \rho$  are the physical librations in longitude, node and inclination, respectively.

In formulating the differential equations for the physical librations, two assumptions are made, namely, that the Moon is perfectly rigid and that the geocentric motion of its center of mass is a known function of time. Three second-order differential equations (Euler's dynamic equations) are formed for the motion of the Moon about its center of mass. The solution of Euler's dynamic equations is obtained in terms of harmonic series having fixed coefficients with arguments which are linear functions of the mean orbital parameters of the Moon and the Sun.

$$\lambda = \sum_1 A_1 \frac{\sin}{\cos} (a_1 t + b_1)$$

where  $\lambda$  represents any of the three physical libration angles. The forced librations are defined as the particular solution of the differential equations, depending on the varying position of the Earth with respect to the Moon's selenodetic system. The general solution contains six constants of integration which are defined as the parameters of free librations. Only two of these parameters are considered non zero and are determined from analysis of observations.

The solution of Euler's equations requires the following additional information:

I - the mean inclination of the lunar equator to the ecliptic, and

$f = \frac{(C - B)B}{(C - A)A}$  - the mechanical flattening representing the ratio

between the principal moments of inertia A, B, C.

Assuming these two quantities to be known, the solution is a purely mathematical process, the final product being a model of the physical libration angles [Eckhardt, 1965]. Observations are necessary, however, in order to check the model and also for the establishment of a consistent set of constants (including I, f, the free libration constants and other auxiliaries).

The heliometer observations of the Moon were designed to provide this

observational material. They are precise measurements of the angular distances between an arbitrarily chosen crater at the center of the visible moon disc - Mösting A - and the apparent limb. As stated already, the physical librations are modeled as taking place about the center of mass of the Moon. In order to reduce the heliometer observations and obtain an estimate for the parameters ( $I$ ,  $f$ , free librations, etc.) an assumption is made in that the center of the best fitting circle to the apparent limb is a projection of the center of mass of the Moon along the Moon-Earth mass centers vector. This is equivalent to the assumption that the Moon is homogeneous and basically spherical so that its center of mass coincides with the center of the best fitting sphere. Recent observations have largely demonstrated that certain biases exist between the center of mass and the center of the best fitting sphere [Ransford, 1969]. Because of this inconsistency in modeling the heliometer observations the parameters which are being estimated in the adjustment process contain certain biases. However, determinations of the gravitational field of the Moon from Orbiter tracking data have essentially confirmed the value of  $f$  as known from reducing heliometer data and have thus demonstrated, at least for  $f$ , that even if such a bias does exist its magnitude is small [Lorell, 1969].

Another troublesome area in the current version of the solution of physical librations is in the linearization of Euler's equations prior to their solution. This creates a nonlinearity problem in the physical libration in longitude  $\tau$  for  $f = .662$  with corresponding large uncertainties in the coefficient of one of the terms in the series for  $\tau$ . A major development in this area as reported in an article by Moutsoulas [1970], is that he solves the differential equation of Euler for libration in longitude in its original nonlinearized form and thus avoids altogether the nonlinearity problem. Consequently,  $f$  can assume values near  $f = .662$ .

There are two more problems associated with the current version of a solution

for physical librations. As reported above, it appears that the future lunar ephemerides are going to be numerical, i. e., obtained by numerical integration of the equations of motion rather than by an analytical or semianalytical solution (Brown's, for example). The current solutions for the physical librations are based on the lunar ephemeris presented in a harmonic series form only and cannot be easily adopted to a numerical ephemeris. Unless the physical libration is very insensitive to variations in the lunar ephemeris, this may create serious inconsistencies between the orientation of the Moon and the position of its mass center.

A second problem exists which is of a practical nature. In order to obtain least squares estimates for the parameters of physical librations based on the minimization of the residuals of a suitable observational data, the partial derivatives of the observed quantities with respect to these parameters are needed. But the physical libration angles are related to the constants  $I$  and  $f$  only indirectly and in a rather complicated manner. Also it is not clear which are the basic (independent) parameters of the physical librations in addition to  $I$  and  $f$ . So it is evident that a method is necessary that will allow a straightforward computation of the partial derivatives of any relevant data type with respect to a carefully selected minimal set of independent parameters.

Chapter 3 gives an answer to most of the aforementioned problems.

### 1.33 Fundamental Astronomical Constants.

As in many other areas, the means for satisfying the aspiration for consistency between the astronomic constants became available only late in the 20th century. The resolutions taken at almost every congress of the IAU mark the steady progress in this area. Important in particular and relevant to the presently accepted set of constants is the resolution of the General Assembly of the International Astronomical Union at its session on September 3, 1964, in Hamburg, West Germany.

The constants adopted by the IAU are defined as follows [Transactions IAU, 1966]:

Defining: These are constants which are actually adopted without having to assess their value by observations.

Primary: These are a self-consistent set (also consistent with the defining constants) of independent constants which are obtained as the result of direct or indirect observations. As such they are subject to eventual updating when the quality of new observations and mathematical models warrant it. However such an updating is permissible only provided the consistency within the combined sets of defining and primary constants is preserved.

Secondary. These are essentially functions of the defining and primary constants. Through the functional relationships which are consistent with one another, the original consistency within the primary set is maintained throughout the secondary group [AENA Supplement, 1961].

The establishment of a fundamental coordinate system on the Moon involves more than the lunar ephemeris and the physical libration model. Most of the observations are ultimately related to the Earth, its size, its geometric and dynamic figure and its motion in space. So in order to maintain consistency between all the elements to be used in this work another parallel to the "IAU—1964" set of constants was considered as reported in JPL's [Melbourne et al., 1968]. For the most part the differences between JPL and IAU—1964 are minute, but where they do exist the JPL constants were adopted.

Thus, in summary of this section it can be stated that JPL's constants and lunar ephemeris data were adopted as a basis for the solutions developed in this report. Textbooks like [Mueller, 1969] and [AENA Supplement, 1961] were consulted insofar as definitions and interrelations between the constants were concerned.

#### 1.4 General Plan for the Study

Two basic concepts were laid down at the basis of the solution proposed in this work: consistency and uniformity. The brief analysis of existing astronomical theories and models as presented in section 1.3 made clear that consistency is indeed one of the backbones in modern astronomical theory. Practically, this means that the functional relationship between the various models as well as the constants involved have to be clearly formulated so that no contradictory assumptions are made and no constants are used which fail to satisfy these conditions. This principle extended to the definition and determination of fundamental control on the Moon creates one more branch in the list of constants and models which together constitute the comprehensive theory of the shape and the motion of the Moon. As in any other creation of man, the concept of consistency should not be regarded as absolute but rather within the limits of the presently available observational material.

It often so happens that improvements in the quality of the observational data uncover new inconsistencies in theory which in turn warrant a new reevaluation and eventually a restatement of relationships and finally an overall refinement in theory and corresponding computational procedures. Considering presently available types of observations, a careful study of the existing theories was undertaken and at the end a consistent set of constants and postulates were selected to serve as the basis for the datum solution. As the numerical treatment in this work is limited to a simulation, certain liberty was taken in ignoring known physical realities with the purpose of leaving in only the most important aspects in the situation, namely, the geometric and gravitational phenomena. A detailed exposition of this simplified environment is presented in Chapter 4. Notwithstanding the simplifications, this synthetic environment was designed to be absolutely self-consistent.

The many data types available and appropriate for use in determining a

lunar datum prompted the search for a general treatment of them all. This is what brought the quest for uniformity. Stripped from instrumental peculiarities and particular observing procedures, available data could be grouped into a few broad classes with the result that a uniform and compact solution could be worked out. Adapting such a general solution to the processing of a real data type could be done at a later stage by the introduction of a set of parameters pertaining to the particular data (error modelling) so that the uniformity in the solution would be preserved. This is the reason for grouping the existing data types into two categories:

- Optical observations from a point in space to points on the surface of the Moon.
- Range and range-rate observations from a tracking station on Earth to a spacecraft.

In the mathematical treatment of the second class certain subdivisions were necessary, but on the whole their character and contribution to the solution are such that they stand clearly as a single observational group. An odd member in the optical observations family is the heliometer observation. Although a detailed model and a computer program for their generation were developed, their incorporation into the general solution was not worked out in detail. The reasons are mainly limitations in time and the fact that this particular group of optical observations is not indispensable for achieving a solution to the problem.

There is a whole generation of new types of observations either already available or in the process of being developed (or at least being considered) which were excluded from the solution. To mention a few, these are:

- (a) Laser ranging from observatories on Earth to reflectors placed on the surface of the Moon.
- (b) Very-long-baseline interferometric observations with a base extending from an antenna on Earth to another antenna on the Moon.

(c) Satellite-to-satellite range and range-rate observations from a synchronous satellite of the Moon to a Moon-orbiting spacecraft.

An entirely new revision of astronomic theory and reduction procedures seem indispensable in order to take full advantage of the significantly higher quality of these new data types. These types of observations are treated in the work of Fajemirokun [1971].

Last but not least the old problem of orientation of the Moon in space was given another try. Although it has been treated by many distinguished scientists, it appears that a new contribution could be registered by the application of modern numerical methods and practices. The new solution as presented in Chapter 3 of this work compares fairly well with the latest and most authoritative model in use today, i. e., that of Eckhardt. It would be presumptuous to regard the new solution as superior in quality, although as demonstrated in Chapter 2, it has definite advantages in its actual use as part of the general solution for fundamental control on the Moon.

Summarizing, the structure of this study is as follows:

Chapter 2 presents the solution for an optimal selenodetic control.

Chapter 3 contains the elements of the newly proposed model for the physical librations of the Moon.

Chapter 4 displays in full detail the conceptual and mathematical basis for the creation of a simulated Earth-Moon environment and observational types.

Chapter 5 reports on some experiments made with the simulated and real data in which the theories from Chapters 2 and 3 are applied.

A number of odd topics are discussed in the Appendices. Although relevant to the subject, these topics were judged to be out of the main line of thought and were designated accordingly as Appendices.

A guiding principle in writing this report has been the creation of the chapters as independent units with minimal cross referencing. The extensive

bibliography listed at the end was continuously consulted through all stages of this work, although, in the text, referencing to it was kept to a minimum in order not to disrupt the continuity of the presentation. This was accomplished at the expense of some overlapping between chapters and also the inclusion of some theorems and procedures which can otherwise be found in the existing literature.

## 2. THEORETICAL SOLUTION OF THE PROBLEM

### 2.1 Introduction

The problem of mapping the lunar surface has attracted the attention of astronomers for many centuries. Considering the exactness of the methods employed and the quality of the results obtained, it would not be presumptuous to state that only in the twentieth century steps have been taken towards mapping with geodetic accuracy. Chapter 3 in Prof. Z. Kopal's The Moon [Kopal, 1969] contains many interesting details on the long history of lunar mapping; however, it is only the past decade of space exploration and "oriented" lunar photography which have brought a real breakthrough in this field.

The basic problem in lunar mapping and, unfortunately, the one most elusive and difficult to solve is the definition and determination of a datum on the Moon. Even if the concept of a datum is confined here to the position and orientation with respect to the lunar crust of a Cartesian coordinate system only, thus avoiding the necessity of defining a reference figure for the Moon, the problem remains far from being solved. The main reason is in the fact that there are no observations conducted from the surface of the Moon which can claim geodetic accuracy. Traditionally, the only data available have been obtained from remote observations conducted primarily from the Earth's surface, and in the past five years or so from spacecrafts in the vicinity of the Moon. The prospects for extensive geodetic measurements on the surface of the Moon in the next five or ten years appear remote at present, even if technology which could support such an undertaking has been developed. So the problem remains to explore methods which have not been considered as yet for the establishment of control of geodetic quality on the Moon.

Geodetic quality should not be interpreted merely as high relative-position accuracy of a number of features on the Moon's surface, but also and mainly as the determination of coordinates of points such that the coordinate system defined by them is unique, possesses favorable properties, and is consistent with observations and theories associated with the Moon. This would mean, for example, that the geocentric lunar ephemeris and the parameters of orientation in space of the Moon will have to be incorporated in any solution for a datum on the Moon.

The favorable properties of a datum are related to the dynamical rather than the topographical figure of the Moon. Assuming the Moon to possess a practically invariable gravitational field, the favorable datum can be defined as having its origin at the mass center of the Moon and its three axes oriented along the principle axes of inertia. As the basic dynamical figure of the Moon is that of a triaxial ellipsoid, this definition of a datum holds many advantages and appears less arbitrary than others. One important advantage is that the basically triaxial dynamic figure governs the rotation of the Moon in space as shown in chapter 3. Any other choice of orientation of the datum would complicate the equations of rotational motion of the Moon and may increase the uncertainties in their solution. There are broader problems associated with the dynamic figure and motion of the Moon, the solution of which is not enhanced by the choice of this particular datum. For example:

- (a) The  $C_{20}$  term of the Moon is about  $1/5$  of the  $-J_2$  of the Earth.
- (b) The equatorial dynamical flattening represented by the  $C_{22}$  term is much smaller than the polar flattening.
- (c) The spin of the Moon is about  $27\frac{1}{2}$  times slower than the corresponding diurnal rotational velocity of the Earth.

All these facts imply that the principal axes of the Moon ( $x, y, z$ ) are not so well defined. As a result the use of observations for the determination of a datum on the Moon is much less efficient. These considerations lead to the

preliminary conclusion that in determining a lunar datum it would be unreasonable to expect accuracies comparable to those on Earth. Even after lunar surface measurements become available, it would require observations of a much higher degree of accuracy and also the use of much more exact theories of motion in order to approach geodetic accuracies as known on Earth.

The requirement for consistency between datum solution and theories and models for the motion of the Moon can be interpreted as follows:

- (a) Constants used in the "accepted as exact" models should not be included in the list of parameters to be solved simultaneously with the datum.
- (b) The assumptions underlying the various theories and the mathematical model for the datum solution have to be fully consistent.
- (c) Limited by feasibility only, a maximum number of parameters should be solved together with the datum solution thus enhancing uniformity and implicitly satisfying requirements (a) and (b) above.

Before proceeding with the solution for a datum as presented in this chapter, a brief exposition is given of the fundamental concepts which form the basis of this work.

For a fundamental orientation frame of reference, a hypothetical inertial coordinate system is considered which coincides with the ecliptic mean coordinate system at some arbitrary standard epoch and is defined as a Newtonian Frame of Reference (Brouwer and Clemence, 1961, p. 3). The orientation of any other Cartesian coordinate system with respect to the inertial system is defined through three Eulerian angles necessary to rotate the particular Cartesian system into the inertial or vice versa (see Figure 2.1). The term inertial coordinate system, to be denoted by XYZ, is used for any coordinate system (having an arbitrary origin) which is parallel to the fundamental orientation frame. Thus, one may have a geocentric inertial system, an inertial system centered at a satellite, etc.

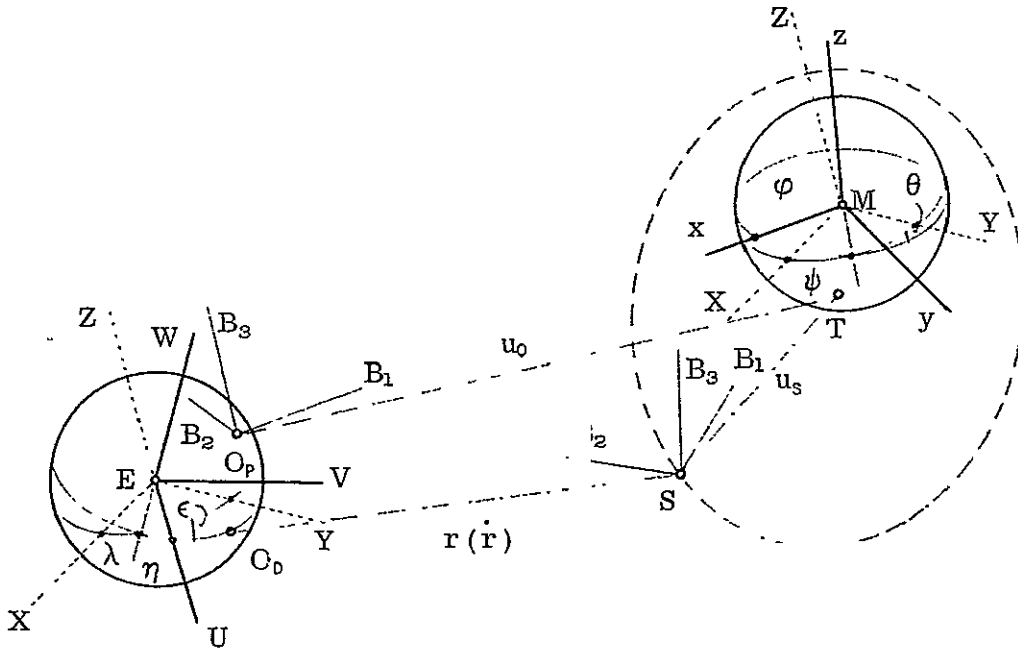


Figure 2.1 Earth-Moon Environment

- E - the geocenter
- M - the selenocenter
- S - a satellite
- XYZ - inertial coordinate systems
- UVW - average terrestrial coordinate system
- xyz - selenodetic coordinate system
- $B_1 B_2 B_3$  - reference frames for optical observations
- $\eta, \lambda, \epsilon$  - Eulerian orientation angles of the Earth
- $\phi, \psi, \theta$  - Eulerian orientation angles of the Moon
- $O_p$  - observing station for optical observations
- $O_D$  - tracking station for range and range rate observation
- T - triangulation point on the Moon

- $r(\dot{r})$  - range (range rate) between  $O_p$  and S  
 $\left. \begin{array}{l} u_o \\ u_s \end{array} \right\}$  - optical ray (direction) between  $O_p$  or S and T.

The orientation of a physical body is defined through a Cartesian coordinate system fixed to the body. Thus, for example, the orientation of the Earth is defined through the so-called average terrestrial coordinate system which is fixed to the Earth's crust and related to a geocentric inertial system by means of three Eulerian angles.

There are three Cartesian systems which are of primary importance:

(a) The average terrestrial system is centered at the mass center of the Earth and is oriented with respect to the crust through the CIO pole and the so-called mean observatory [Mueller, 1969]. It is denoted by UVW.

(b) The selenodetic system is centered at the mass center of the Moon and is oriented along its principal axes. It is denoted by xyz.

(c) The optical observations reference system is centered at the projection center (from which the optical rays emanate) and is generally oriented so that the primary axis ( $B_1$ ) points towards the Moon. It is denoted by  $B_1B_2B_3$ .

The general rotational motion of a physical body with respect to the inertial system is described by the change with time in the Eulerian orientation angles of the appropriate coordinate system (the one fixed to the body). Thus, for example, in order to study the rotational motion of the Moon, one should consider the changes in the Eulerian angles ( $\varphi, \psi, \theta$ ) which relate the Moon-fixed (xyz) system to the inertial (XYZ) system. From this definition of rotational motion, it is clear how rotation and orientation of a body are related to one another. As the body rotates, its orientation changes and by considering the instantaneous

set of Eulerian angles at a particular epoch one has the means for defining the orientation of the body at that epoch.

The rotation of a physical body is governed by a set of equations of rotational motion (second order differential equations) in which the external forces acting on the body are represented. The solution of these equations of motion results in the Eulerian orientation angles as functions of time.

The position with respect to the UVW system of points on the surface of the Earth is defined by three Cartesian coordinates. Points on the surface of the Moon are defined similarly with respect to the selenodetic (xyz) system.

The position and velocity (state vector) of points in space with respect to a particular inertial coordinate system (selenocentric, geocentric, etc.) are defined by Cartesian coordinates (XYZ). Thus, the geocentric state vector of the Moon's mass center is given by the LE-16 ephemeris [O'Handley et al., 1969] where the inertial XYZ system has been defined as identical to the mean equatorial system of 1950.0 .

All optical observations of the Moon (photographs, direction measurements, etc.) are treated as light rays emanating from a projection center whose selenocentric inertial coordinates are known or are being estimated in a least squares process. The individual ray from a bundle (the rays emanating from the same projection center form a bundle ) is related to a reference optical frame  $B_1B_2B_3$  by two angular quantities. As mentioned above, the  $B_1B_2B_3$  is related to the XYZ system centered at the projection center by three Eulerian angles or in general by an orthogonal transformation matrix.

Recapitulating, the objective of this study is to develop a model solution for an optimal datum on the Moon in the form of Cartesian coordinates of a network of topographic features on its surface. The solution is to be obtained by a simultaneous weighted least squares adjustment of presently available types of observations, where the weights are determined from

estimates of the observations statistics. Available and newly developed physical models are to be used in formulating the problem and its solution such that they would share a common basis of postulates and would be consistent with one another.

## 2.2 General Adjustment Model

In the model to be developed in this section, the Moon is regarded as a rigid body. As such its motion in space can be partitioned into two independent parts, i. e. , a translatory motion of its mass center and a rotation about its mass center.

The numerical solution of the geocentric equations of translatory motion of the Moon as provided by JPL in the form of the LE-16 ephemeris (the lunar part in the general ephemeris of the Sun and the planets called DE-69, see [O'Handley et al. , 1969]) is considered absolute and constitutes the numerical basis for the entire solution in this chapter. Future improvements in the lunar ephemeris by the incorporation of more accurate data and further perfection of the mathematical model of its translatory motion could be used to reprocess the available observations and eventually obtain a new and better determination for the lunar datum. It can be shown, however, that accepting the presently known uncertainties in the lunar ephemeris as being fair estimates, the effect of these uncertainties is well below the noise level of conventional optical observations.

The model for the rotational motion of the Earth in space as specified by generally-adopted constants [IAU, 1964] for precession and nutation and the continuously monitored polar motion and UT1 variations is considered as being exact. The nutation information is to be taken directly from the DE-69 tape where it has been computed from Woolard's series as developed in [Woolard, 1953]. The total effect of inadequacies in this model resulting in errors in the orientation of the Earth in space as well as uncertainties in the geocentric (UVW) position of Earth stations performing optical or radio observations can be shown to fall below the noise level of the optical observations.

The assumptions of adequacy of the lunar ephemeris, Earth orientation and station positions on Earth may invoke serious reservations as to their validity and

place a question mark on the solution for lunar datum as proposed in this study. There is always the possibility, however, to model the station unknowns and the Earth orientation parameters (for example, the Eulerian orientation angles) although it should be admitted that the application of such a model at this stage would require considerable work. In the present solution, however, in order to obtain realistic statistical information for the parameters that are being solved, the uncertainties in the lunar ephemeris, the orientation of the Earth and the geocentric position of the observing stations are considered in the form of covariances of the selenocentric position of the observing station on Earth. This is done following the approach of "Considered Parameters" presented in Appendix D.

The data to be used in determining coordinates of features on the Moon have been defined in general as optical observations. The idea is to regard an observation which defines a direction from a point in space, to be called the "projection center", to a point on the lunar surface as an optical observation. The directions in space are considered in principle nonoriented, and it is through the a priori covariances in the adjustment process that a distinction is made between truly nonoriented and partially - or fully - oriented directions.

Presently the selenocentric position of a spacecraft orbiting the Moon is determined by least squares adjustment of range and range-rate tracking data from stations on Earth to the satellite. The ordinary orbit determination solves for the state vector (position and velocity) at a standard (initial) epoch as well as for a number of constants. As some of these constants are dominant factors in the rotational motion of the Moon and also as the projection center from which the optical observations are made lies along the trajectory of the spacecraft, it is necessary to process the range and range-rate tracking data together with the optical data and thus obtain a solution for the trajectory and for the relevant constants which is consistent with both types of data. Thus

the uncertainties in the selenocentric position of the projection center are the combined result of the degree of incompatibility of its adjusted position and velocity with the range, range-rate, and optical observations.

Thus far the orientation of the Moon in space was not discussed. It is, however, inherent in the definition of the selenocentric coordinates of points on the surface of the Moon; and, moreover, it is instrumental in the definition of an optimal lunar datum as stated in section 2.1. For the above reasons and also from a practical point of view, i. e., the need to define the orientation of the Moon at any epoch by a minimal number of parameters, the theory for the rotation of the Moon is redeveloped; and a numerical solution is provided in Chapter 3. The solution for the rotation of the Moon as presented in Chapter 3 is consistent with the lunar ephemeris (LE-16) as it actually uses the LE-16 as an input in the numerical solution. In the least squares adjustment procedure, the parameters in the proposed solution are used to model the optical and to a certain extent the range and range-rate data. In this sense the solution for the parameters of orientation of the Moon can be regarded as an integral part of the general adjustment procedure.

The geometric situation and the observations involved are represented schematically in Figure 2.2.

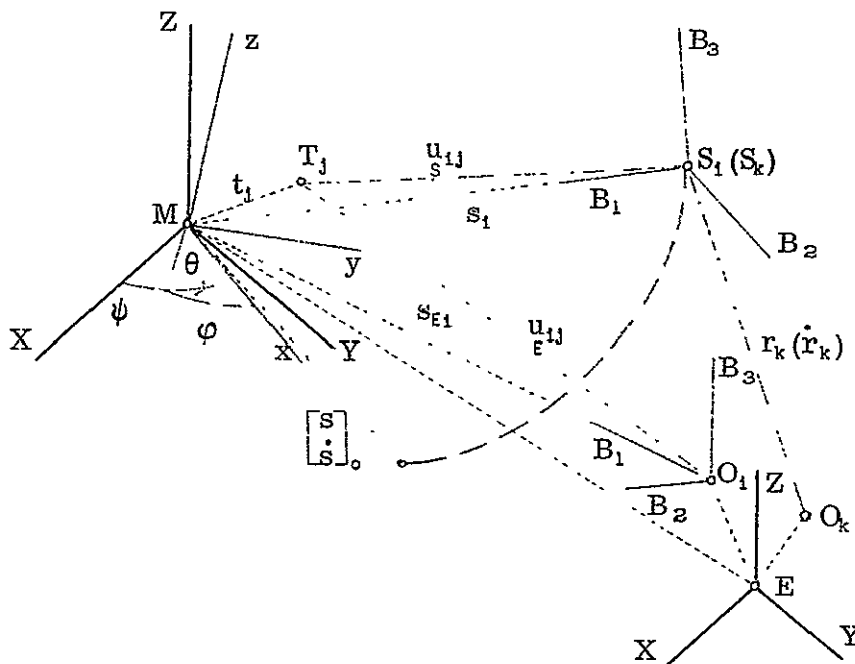


Figure 2.2 Geometry of Observations

The symbols in Figure 2.2 have the following meaning:

- E is the geocenter
- M is the selenocenter
- $S_1, (S_k)$  is the satellite
- XYZ are the inertial Cartesian coordinate systems
- xyz is the selenodetic coordinate system
- $B_1B_2B_3$  are reference frames for optical observations
- $O_1$  is an Earth-based station for optical observations
- $O_k$  is an Earth-based station for range and range-rate observations
- $T_j$  is a triangulation point on the Moon where  $t_j$  is the selenocentric position vector in components of the xyz system.
- $u_{Eij}$  are unit vectors of the optical rays to T from  $O_1$  and  $S_1$ , respectively, given in  $B_1B_2B_3$  components
- $u_{Sij}$
- $r_k(\dot{r}_k)$  are range and range-rate measurements from  $O_k$  to  $S_k$
- $\left. \begin{matrix} S_{1E} \\ S_{1i} \end{matrix} \right\}$  are the selenocentric position vectors of  $O_1$  and  $S_1$ , respectively at epoch  $T_1$  in components of the XYZ system
- $\left. \begin{matrix} \dot{s} \\ s \end{matrix} \right\}$  is the initial state vector of the satellite S at epoch  $T_0$
- $\varphi, \psi, \theta$  are the Eulerian orientation angles of the Moon

(It should be noted that  $\varphi, \psi, \theta$  change with time.)

The meaning of the subscripts is as follows:

- i indicates quantities at epoch  $T_1$
- k indicates quantities at epoch  $T_k$
- j indicates the sequential number of a triangulation point on the Moon

Two orthogonal transformation matrices are defined as follows:

- $M_B$  for a transformation from  $B_1B_2B_3$  into XYZ



two independently measured quantities which are defined in this study as the angles  $\kappa$  and  $\nu$  (see Figure 2.3). Actually, in order to assure orthogonality, the quantities  $q_{ij}$  defined below, rather than  $\kappa$  and  $\nu$ , are used. The following two equations define  $u_{ij}$  and  $q_{ij}$  in terms of  $\kappa_{ij}$  and  $\nu_{ij}$

$$u_{ij} = \begin{bmatrix} \cos \nu \\ \sin \nu \cdot \cos \kappa \\ \sin \nu \cdot \sin \kappa \end{bmatrix}_{ij} ; \quad q_{ij} = \begin{bmatrix} \nu \\ \sin \nu \cdot \kappa \end{bmatrix}_{ij}$$

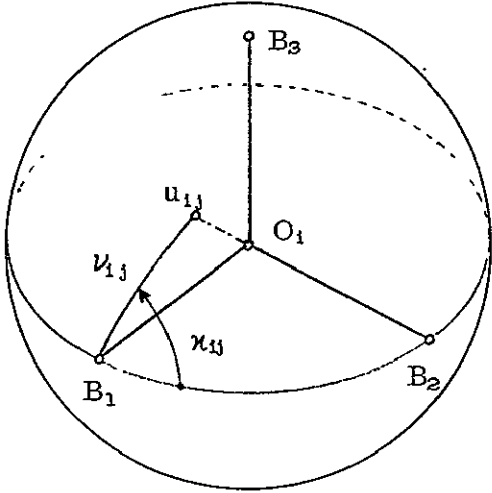


Figure 2.3 Optical Observations

As shown in Figure 2.2 the projection center can be along the trajectory of a satellite ( $S_i$ ), or it can be an observing station on Earth ( $O_i$ ). The notation for the vector equation remains unchanged except for subscript E indicating that  $\vec{s}_{Ei}$  is a selenocentric vector pointing at the station on Earth instead of  $\vec{s}_i$  being the selenocentric vector to the satellite  $S_i$ . In sections 2.3 and 2.4 this distinction is expanded further in the nomination of appropriate parameters and the subsequent linearization.



The symbols used in Figure 2.4 have the following meaning:

M selenocenter

$S_k$  satellite at epoch  $T_k$

$O_k$  radio tracking station on Earth

$\begin{bmatrix} X \\ \dot{X} \end{bmatrix}_{tp,k}$  topocentric (tracking station) state vector of Moon in X, Y, Z components.  
 Implicit in  $\begin{bmatrix} X \\ \dot{X} \end{bmatrix}$  are the following: lunar ephemeris, tracking station position, orientation and rotational velocity of the Earth.

$\begin{bmatrix} S \\ \dot{S} \end{bmatrix}_k$  selenocentric state vector of satellite in X, Y, Z components

$\begin{bmatrix} R \\ \dot{R} \end{bmatrix}_k$  topocentric state vector of satellite in X, Y, Z components.

It should be noted that in forming the equations  $G_k$  and  $H_k$  the topocentric state vector of the satellite  $\begin{bmatrix} R \\ \dot{R} \end{bmatrix}_k$  is obtained from the following vector relationship:

$$\begin{bmatrix} R \\ \dot{R} \end{bmatrix} = \begin{bmatrix} X \\ \dot{X} \end{bmatrix} + \begin{bmatrix} S \\ \dot{S} \end{bmatrix}$$

### 2.3 Parameters in the Solution

The subject treated in this section is the selection and definition of the parameters in the general adjustment model. The nature of the observational material is fairly well known. The quantities of direct interest, i. e. , the coordinates of features on the Moon in the particular (optimal) coordinate system are also well defined. A number of additional parameters are needed, however, for the purpose of modeling the observations and also for the definition of the selenodetic system itself which are not so easily available. Before describing the parameters chosen for this analysis; a short discussion is presented on the general problem of parameters in an adjustment process.

The basic relationship between parameters and observations in an adjustment process is that the observations processed have to be fairly sensitive to variations in the parameters. Unless this is so, the parameters cannot be estimated from analysis of the observations and, vice versa, there is no need for these parameters as they cannot model the observations. However, even after it is clear from experience, logic or intuition what type of parameters are necessary to model a particular physical or geometric situation, there are still a number of options left for selecting a particular set of parameters. Thus choosing a set of parameters in an adjustment problem is of necessity somewhat arbitrary. Unless there is past experience or the parameters are physically obvious, the only guidance in making the final selection is provided by physical or numerical considerations.

Once chosen and utilized, the criteria for evaluating the success of a particular set of parameters are trifold:

- (a) The estimated values for the parameters should be stable, i. e. , the solutions obtained from processing different batches of data should be consistent within the estimated covariance of the solutions.
- (b) The parameters should fully model the situation at hand.
- (c) It should be numerically possible to arrive at solutions for the parameters which are well separated.

The first and the third criteria are easy to check. The second is difficult as the only means one has of checking it is through inspection and analysis of the observational residuals after the adjustment. But even if the residuals appear well behaved, i. e. , showing no residual systematic effects, one is seldom sure that criterion (b) above has been fully met.

A case can be envisioned in which some parameters may be tolerated even if they do not satisfy criterion (a). This means that the values of these parameters are of no interest, and they are used in the adjustment as nuisance parameters. Numerically such parameters are not solved explicitly, but rather their solution is "folded in" the solution of the other parameters (see section 2.5).

As implied in section 2.2, the parameters figuring in the general model are selected so as to model only the geometric and gravitational aspects of the situation. Parameters associated with the instrumentation involved or with physical phenomena such as refraction, solar pressure, etc. are left out. The mathematical interpretation of this would be that the effect of the parameters left out is perfectly known, and the raw observed quantities involved in the process can be fully corrected prior to the adjustment. A direct result of this assumption is that the observations can be regarded as noncorrelated quantities. By a proper definition of orientation parameters, directions observed simultaneously (from the same projection center) can also be regarded as noncorrelated with one another. In accordance with the "Generalized Approach," the actual observations are regarded and treated in the adjustment as another group of parameters [Uotila, 1967].

Two broad classes of parameters are considered:

- (a) Permanent: These are the parameters which are displayed as the results of the analysis. Implied by this is that they should satisfy completely all three criteria mentioned above.
- (b) Transient: These are parameters which are necessary in constructing the mathematical model, yet they are either different for different data batches,

or their nature is such that there is no particular interest in their adjusted values and the appropriate covariance matrices. The actual observations belong to this class although it may be of interest to study their residuals after the adjustment.

The parameters chosen for this analysis are presented in Table 2.1 followed by brief comments on each of the 11 parameter groups.

Description	Class	Symbol
<u>Parameters:</u>		
1. Cartesian coordinates of triangulation points on the Moon in xyz system.	P	L <sub>1</sub>
2. Orientation parameters of the Moon at a standard epoch T <sub>00</sub>	P	L <sub>2</sub>
3. Physical constants of the Moon (low degree)	P	L <sub>3</sub>
4. Higher-degree gravitational parameters of the Moon (in mascon form)	T	L <sub>4</sub>
5. State vector of a satellite at a standard epoch T <sub>0</sub> in XYZ system.	T	L <sub>5</sub>
6. Exterior orientation elements of B <sub>1</sub> B <sub>2</sub> B <sub>3</sub> with respect to the XYZ system	T	L <sub>6</sub>
<u>Observations:</u>		
7. Optical observations (two independent quantities per direction)	T	L <sub>7</sub>
8. Range	T	L <sub>8</sub>
9. Range-rate	T	L <sub>9</sub>
<u>Considered Parameters (see Appendix D )</u>		
10. Selenocentric position of Earth observatory or tracking station in XYZ system		L <sub>10</sub>
11. Selenocentric velocity of Earth observatory or tracking station in XYZ system		L <sub>11</sub>
P - permanent ;      T - transient		

Table 2.1 Parameters in the General Adjustment Procedure

Parameters  $L_1$ . Cartesian coordinates were chosen to relate points on the surface of the Moon to the xyz selenodetic coordinate system. The advantage in the use of Cartesian coordinates is in having simpler mathematical formulation and an easy derivation of partial derivatives. Associated with Cartesian coordinates, however, is the lack of distinction between horizontal and vertical control which may be considered as a disadvantage. There is the inconvenience in analyzing the positional uncertainties of the points after an adjustment and also in case the points are to be used for densification of control or for navigation. However, transformation into polar coordinates is a simple matter for the Moon which is basically spherical in shape.

Parameters  $L_2$ . These are the physical libration angles and their time rates at a standard epoch. Variations in the orientation parameters of the Moon at a particular epoch (the Eulerian angles) are related to  $L_2$  by a  $6 \times 6$  matrix of partial derivatives called the state transition matrix (see section 3.32 in Chapter 3). This is a significant asset in the parameterization of the model. No matter at how many epochs the Moon is observed, the parameters of orientation of the Moon remain six.

Parameters  $L_3$  and  $L_4$ . These are the parameters defining the dynamic figure of the Moon. The reason for their separation into two groups is technical.  $L_3$  does figure in the equations of rotational motion of the Moon as well as in the satellite motion, while  $L_4$  affects the motion of the satellite only. Also with reference to the classification as permanent and transient,  $L_3$  are considered permanent while  $L_4$  are regarded as transient. This would mean that the adjusted  $L_4$  can be different for different satellite arcs. The values of  $L_4$  are solved implicitly by the "fold in" matrix operation (section 2.5).

Parameters  $L_5$ . This is the selenocentric state vector of a particular satellite arc at the initial epoch. This would mean that if, for various reasons, data from the same satellite are processed in several arcs, there will be several sets of initial values. For this and other reasons as shown in section 2.5, the

data are processed one arc at a time. As in the case of parameters  $L_2$ , there is a single set of six parameters for the selenocentric position and velocity of the spacecraft at any epoch along the same arc. An appropriate state transition matrix is used to relate variations in the state vector at a particular epoch to the  $L_5$  parameters (see Appendix F).

Parameters  $L_6$ . The choice for exterior orientation parameters was made following in general [Rinner et al., 1967]. These parameters are defined as three differential rotations applied to the Cartesian reference system  $B_1B_2B_3$ . These rotations together with a nominal (approximate) orthogonal transformation matrix  $M_B$  (see section 2.2) bring the  $B_1B_2B_3$  reference system into the inertial XYZ system. The mathematical treatment of these orientation parameters is much simpler than the one using the traditional gimbal axes ( $\kappa, \varphi, \omega$ ) and is more appropriate to the general model developed in this chapter. No matter how the nominal orientation of the  $B_1B_2B_3$  system is determined: by star background photography, by a separate camera, by star-lock devices, inertial navigator, etc., the mathematical treatment of the exterior orientation elements remains invariable. The only difference is in the a priori values of the covariance matrix of the orientation parameters.

Parameters  $L_7, L_8, L_9$ . These are the actual observations and need little or no explanation. The optical observations ( $L_7$ ) were chosen to be two independent quantities relating an individual ray to the reference  $B_1B_2B_3$  Cartesian system. The  $B_1B_2B_3$  system is the same for all rays observed at the same epoch (see also section 4.7 in Chapter 4). As shown in section 2.4, the linearized mathematical model does not have to be altered in order to accommodate a different choice of observed quantities.

Parameters  $L_{10}$  and  $L_{11}$ . These are the selenocentric Cartesian components of the position and the velocity of an observing station on Earth in the XYZ system. These parameters are not solved. They are used as shown in section

2.4 for deriving partial derivative matrices of the F, G, and H functions in order to be employed later in evaluating the covariances of the permanent parameters. Throughout this chapter, these are the "considered parameters" in the adjustment (see Appendix D).

## 2.4 Linearization

The linearization of the mathematical models for optical, range, and range-rate observations is obtained through partial differentiation of the  $F^*$ ,  $G$ , and  $H$  functions (equations 2.21.1, 2.22.1 and 2.22.2) with respect to the parameters. As usual, the linearization is valid provided the functions are fairly linear over the range of the corrections to the observed quantities. For the partial derivatives with respect to parameters  $L_3$ ,  $L_4$ , and  $L_6$ , use is made of the state transition and parameter sensitivity matrices as derived in section 3.32 and also in Appendix F. Accordingly, in this section, these matrices are assumed known.

### 2.41 Optical Observations:

Mathematical model for projection center on a satellite (equation 2.21.1):

$$\frac{F^*}{S} = \frac{F^*}{S}(L_1^a, L_2^a, L_3^a, L_4^a, L_5^a, L_6^a, L_7^a) = 0 \quad .$$

Mathematical model for projection center on Earth (equation 2.21.1):

$$\frac{F^*}{E} = \frac{F^*}{E}(L_1^a, L_2^a, L_3^a, L_6^a, L_7^a, L_{10}^b) = 0$$

where  $L_{10}^b$  are considered parameters ( see Appendix D ) ,

$$L_i^a = L_i^b + X_i$$

and  $L_i^a$  are the adjusted,  $L_i^b$  are the observed and  $X_i$  are the corrections to the observed parameters. The following expressions are needed for the linearization:

$$\begin{aligned} \frac{F^*}{S}(L_1^b, L_2^b, L_3^b, L_4^b, L_5^b, L_6^b, L_7^b) &= \frac{F^*}{S} \\ \frac{F^*}{E}(L_1^b, L_2^b, L_3^b, L_6^b, L_7^b, L_{10}^b) &= \frac{F^*}{E} \\ \frac{\partial F^*}{\partial L_i} = \frac{F^*}{F_i} &= \frac{\partial F^*}{\partial L_i} \quad . \end{aligned}$$

The linearized models for optical observations are as follows:

$$\overset{*}{F}_S = 0 = \overset{*}{W}_S + \overset{*}{B}_1 X_1 + \overset{*}{B}_2 X_2 + \overset{*}{B}_3 X_3 + \overset{*}{B}_4 X_4 + \overset{*}{B}_5 X_5 + \overset{*}{B}_6 X_6 + \overset{*}{B}_7 X_7 = 0 \quad (2.41.1)$$

$$\overset{*}{F}_E = 0 = \overset{*}{W}_E + \overset{*}{B}_1 X_1 + \overset{*}{B}_2 X_2 + \overset{*}{B}_3 X_3 + \overset{*}{B}_6 X_6 + \overset{*}{B}_7 X_7 = 0 \quad (2.41.2)$$

The partial derivatives matrices  $\overset{*}{B}_i$  are obtained by differentiating equation 2.21.1 with respect to the parameters  $L_i$  ( $i = 1, 2, \dots, 7, 10$ ).

$$\overset{*}{F}_{i,j} = M_{B,i} \cdot u_{i,j} + \frac{1}{\rho_{i,j}} (s_i - M_{M,i} \cdot t_j) \quad (2.21.1)$$

$$\overset{*}{B}_1 = \frac{\partial \overset{*}{F}_{i,j}}{\partial L_{i,j}} = \frac{\partial \left\{ \frac{1}{\rho_{i,j}} [s_i - M_{M,i} \cdot t_j] \right\}}{\partial t_j} = -\frac{1}{\rho_{i,j}} [I - M_{B,i} u_{i,j} u_{i,j}^T M_{B,i}^T] \cdot M_{M,i} \quad (2.41.3)$$

where

$$L_1 = \begin{bmatrix} L_{1,1} \\ L_{1,2} \\ \vdots \\ L_{1,j} \\ \vdots \end{bmatrix} \quad \text{and} \quad L_{1,j} = t_j = \begin{bmatrix} t_{j,x} \\ t_{j,y} \\ t_{j,z} \end{bmatrix}$$

$$\begin{aligned} \overset{*}{B}_2 &= \frac{\partial \overset{*}{F}_{i,j}}{\partial L_2} = \frac{\partial \overset{*}{F}_{i,j}}{\partial p_i} \cdot \frac{\partial p_i}{\partial v_i} \cdot \frac{\partial v_i}{\partial L_2} = \\ &= \frac{1}{\rho_{i,j}} \left[ M_{M,i} \cdot \mathbb{E}_3 \cdot t_j \quad ; \quad \mathbb{E}_3 \cdot M_{M,i} \cdot t_j \quad ; \quad -R_3(-\psi_i) \cdot \mathbb{E}_1 \cdot R_1(\theta_i) \cdot R_3(-\varphi_i) \cdot t_j \quad ; \quad 0 \quad ; \quad 0 \quad ; \quad 0 \right] \cdot \end{aligned}$$

$$\cdot \begin{bmatrix} 1 & -1 & 0 & \vdots & & & \\ 0 & 1 & 0 & \vdots & & & \\ 0 & 0 & 1 & \vdots & & & \\ \hline & & & & 1 & -1 & 0 \\ & & & & 0 & 1 & 0 \\ & & & & 0 & 0 & 1 \end{bmatrix} \cdot U_M \quad (2.41.4)$$

where

$$p_1 = [\varphi \psi \theta \dot{\omega} \dot{\psi} \dot{\theta}]_1^T$$

$$v_1 = [\tau \sigma \rho \dot{\tau} \dot{\sigma} \dot{\rho}]_1^T$$

$$L_2 = [\tau \sigma \rho \dot{\tau} \dot{\sigma} \dot{\rho}]_0^T$$

$$U_M^1 = \frac{\partial v_1}{\partial L_2}$$

which is the state transition matrix for the physical libration angles (see section 3.32).

$$M_{M,1} = R_3(-\psi_1) \cdot R_1(\theta_1) \cdot R_3(-\omega_1)$$

$E_1, E_2, E_3$  are Lucas matrices used to differentiate the rotation matrices (see Appendix E).

$$\begin{aligned} \begin{bmatrix} B_3^* & B_4^* & B_5^* \\ F & F & F \end{bmatrix} &= \begin{bmatrix} \frac{\partial F_{1,j}^*}{\partial L_3} & \frac{\partial F_{1,j}^*}{\partial L_4} & \frac{\partial F_{1,j}^*}{\partial L_5} \end{bmatrix} = \begin{bmatrix} \frac{\partial F_{1,j}^*}{\partial p_1} & \frac{\partial p_1}{\partial v_1} & \frac{\partial v_1}{\partial L_3} \\ \frac{\partial F_{1,j}^*}{\partial \dot{s}_1} & \frac{\partial \dot{s}_1}{\partial L_3} & \end{bmatrix} \\ &= \begin{bmatrix} \frac{\partial F_{1,j}^*}{\partial \dot{s}_1} & \left( \frac{\partial \begin{bmatrix} s \\ \dot{s} \end{bmatrix}_1}{\partial L_4} \quad \frac{\partial \begin{bmatrix} s \\ \dot{s} \end{bmatrix}_1}{\partial L_5} \right) \end{bmatrix} = \\ &= \begin{bmatrix} \frac{\partial F_{1,j}^*}{\partial p_1} & \frac{\partial p_1}{\partial v_1} & Q_M^1 \\ \frac{\partial F_{1,j}^*}{\partial \dot{s}_1} & \begin{bmatrix} Q_{s1} & Q_{s2} & U_s^1 \end{bmatrix} \end{bmatrix} \end{bmatrix} \quad (2.41.5)$$

where

$L_3 = [C_{22} \beta C_{20}]^T$  are low-degree harmonics of the gravity field of the Moon;

$\beta = (C-A)/B$ ; A, B, C being the principle moments of inertia of the Moon

$L_4 = [\mu_1, \mu_2, \dots]^T$  are mass concentrations on the surface of the Moon representing the higher-degree features of the gravity field of the Moon. The conditions imposed on the solution of  $L_4$  are as in Appendix C.

$L_5 = \begin{bmatrix} s \\ \dot{s} \end{bmatrix}_0$  is the initial state vector of the satellite arc

$Q_M^1 = \frac{\partial v_1}{\partial L_3}$  is the parameter sensitivity matrix for the rotation of the Moon

$\begin{bmatrix} Q_{s1} & Q_{s2} \end{bmatrix} = \frac{\partial \begin{bmatrix} s \\ \dot{s} \end{bmatrix}_1}{\begin{bmatrix} L_3 \\ L_4 \end{bmatrix}}$  is the parameter sensitivity matrix for the motion of the satellite

$U_{s_1} = \frac{\partial \begin{bmatrix} s \\ \dot{s} \end{bmatrix}_1}{\partial \begin{bmatrix} s \\ \dot{s} \end{bmatrix}_c}$  is the state transition matrix for the motion of the satellite

$\rho_{1,j}, v_{1,j}, \frac{\partial \rho_{1,j}}{\partial v_{1,j}}, \frac{\partial F_{1,j}^*}{\partial \rho_{1,j}}$  are the same as defined or derived for  $B_F^*$  above

$Q_{s_1}$  is derived in section 3.32

$Q_{s_1}, Q_{s_2}, U_{s_1}$  are derived in Appendix F.

In equation 2.41.5 above, the expression for  $\frac{\partial F_{1,j}^*}{\partial \begin{bmatrix} s \\ \dot{s} \end{bmatrix}_1}$  is evaluated as follows:

$$\frac{\partial F_{1,j}^*}{\partial \begin{bmatrix} s \\ \dot{s} \end{bmatrix}_1} = \frac{1}{\rho_{1,j}} [I - M_{B,i} u_{1,j} u_{1,j}^T M_{B,i}^T \quad ; \quad 0] \quad .$$

The expression for  $B_{F10}^*$  is actually part of  $\frac{\partial F_{1,j}^*}{\partial \begin{bmatrix} s \\ \dot{s} \end{bmatrix}_1}$  as follows:

$$B_{F10}^* = \frac{\partial F_{1,j}^*}{\partial L_{10,1}} = \frac{\partial F_{1,j}^*}{\partial s_1} = \frac{1}{\rho_{1,j}} [I - M_{B,i} u_{1,j} u_{1,j}^T M_{B,i}^T] \quad . \quad (2.41.6)$$

The matrix  $B_{F10}^*$  is not part of the linearized mathematical model (2.41.2) but is needed for the evaluation of the contribution of the considered parameters  $L_{10}$  to the covariances of the parameters which are being solved (see Appendix D).

The exterior orientation parameters were defined in section 2.3 as small rotations  $(e_1, e_2, e_3)$  around  $B_1, B_2, B_3$ , respectively. The approximate values of  $e_i$  are set to zero, and it is assumed that the  $M_B^T$  matrix transforms the  $B_1 B_2 B_3$  system very closely to its "true" orientation with respect to the XYZ system so that the  $e_1, e_2, e_3$  are small quantities. The derivation of  $B_F^*$  is presented in what follows:

$$u_{1,j}^* = M_{B,i} \cdot M_{e,i} \cdot u_{1,j}$$

$$M_{e_i} = R_3(e_{i,3}) \cdot R_2(e_{i,2}) \cdot R_1(e_{i,1}) \cong \begin{bmatrix} 1 & e_3 & -e_2 \\ -e_3 & 1 & e_1 \\ e_2 & -e_1 & 1 \end{bmatrix}_i \quad .$$

The approximation is based on the  $e_1, e_2, e_3$  being small angles so that  $\sin e_i \cong e_i$  and  $\cos e_i \cong 1$ .

$$\begin{aligned}
 {}^* u_{1,j} &= M_{B,1} \cdot \left( I + \begin{bmatrix} 0 & e_3 & -e_2 \\ -e_3 & 0 & e_1 \\ e_2 & -e_1 & 0 \end{bmatrix}_{1,j} \right) u_{1,j} = M_{B,1} \cdot u_{1,j} + M_{B,1} \begin{bmatrix} 0 & e_3 & -e_2 \\ -e_3 & 0 & e_1 \\ e_2 & -e_1 & 0 \end{bmatrix}_{1,j} \cdot u_{1,j} \\
 {}^* u_{1,j} &= M_{B,1} \cdot u_{1,j} + M_{B,1} \cdot \begin{bmatrix} 0 & -u_3 & u_2 \\ u_3 & 0 & -u_1 \\ -u_2 & u_1 & 0 \end{bmatrix}_{1,j} \cdot \begin{bmatrix} e_{1,1} \\ e_{2,1} \\ e_{3,1} \end{bmatrix}_{1,j}
 \end{aligned}$$

The last algebraic operation is based on the following identity:

$$\vec{e}_i \times u_{1,j} = -u_{1,j} \times \vec{e}_i$$

Using the expressions developed above and realizing that

$$L_{E,1} = e_1 = \begin{bmatrix} e_{1,1} \\ e_{1,2} \\ e_{1,3} \end{bmatrix}$$

the expression for  $B_{E,1}$  follows directly:

$${}^* B_{E,1} = \frac{\partial {}^* F_{1,j}}{\partial L_{E,1}} = \frac{\partial {}^* u_{1,j}}{\partial e_1} = \frac{\partial \left( M_{B,1} \cdot \begin{bmatrix} 0 & u_3 & -u_2 \\ -u_3 & 0 & u_1 \\ u_2 & -u_1 & 0 \end{bmatrix}_{1,j} e_1 \right)}{\partial e_1} = M_{B,1} \cdot \begin{bmatrix} 0 & u_3 & -u_2 \\ -u_3 & 0 & u_1 \\ u_2 & -u_1 & 0 \end{bmatrix}_{1,j} \quad (2.41.7)$$

The partial derivatives matrix for the optical observations is evaluated as follows:

$${}^* B_{F,7} = \frac{\partial {}^* F_{1,j}}{\partial L_{7,1,j}} = \frac{\partial {}^* F_{1,j}}{\partial u_{1,j}} = M_{B,1} \quad (2.41.8)$$

At this point a transformation will be performed from  $\bar{F}$  to  $F$  functions with corresponding transformation of the  $B_{\bar{F},1}$  matrices into  $B_{F,1}$ . The purpose of this transformation is to reduce the number of condition equations per observed direction from 3 ( $\bar{F}$ ) to 2 ( $F$ ) so that the normal matrix to be obtained subsequently from the optical observations is of full rank. The new  $L_7$  parameters are defined as follows:

$$= \begin{bmatrix} L_{7,1,1} \\ L_{7,1,2} \\ \vdots \\ L_{7,2,1} \\ \vdots \\ L_{7,1,j} \\ \vdots \\ \vdots \end{bmatrix} ; \quad L_{7,1,j} = q_{1,j} = \begin{bmatrix} \nu \\ \sin \nu \cdot \kappa \end{bmatrix}_{1,j} ; \quad \overset{*}{L}_{7,1,j} = u_{1,j}$$

$$\overset{*}{\delta} L_{7,1,j} = \delta u_{1,j} = \frac{\partial u_{1,j}}{\partial q_{1,j}} \cdot \delta q_{1,j} = \begin{bmatrix} -\sin \nu & 0 \\ \cos \nu \cos \kappa & -\sin \kappa \\ \cos \nu \sin \kappa & \cos \kappa \end{bmatrix} \cdot \delta L_{7,1,j} = E_{1,j} \cdot \delta L_{7,1,j}$$

Using this relationship

$$\overset{*}{B}_{F,1,j} \cdot \overset{*}{X}_{7,1,j} = \overset{*}{B}_{F,1,j} \cdot E_{1,j} \cdot X_{7,1,j} = \overset{*}{B}_{F,1,j} X_{7,1,j} \quad (2.41.9)$$

$$\overset{*}{B}_{F,1,j} = M_{B,1} \cdot E_{1,j} \quad (2.41.10)$$

An important property of  $E_{1,j}$  is that it is orthogonal, i. e.,

$$E_{1,j}^T \cdot E_{1,j} = I \quad .$$

As  $M_{B,1}$  is orthogonal too,  $B_{7,1,j}$  is an orthogonal matrix, i. e.,

$$B_{F,1,j}^T \cdot B_{F,1,j} = I \quad .$$

The linearized function  $\overset{*}{F}$  is premultiplied by  $B_{F,1,j}^T$ :

$$\overset{*}{F}_S = B_{F,1,j}^T \cdot \overset{*}{F}_S = B_{F,1,j}^T (B_{F,1} \overset{*}{X}_1 + \dots + B_{F,7} \overset{*}{X}_7 + \overset{*}{W}_S) = 0$$

The same is done for  $\overset{*}{F}_E$ . The resulting linearized model is denoted by the omission of (\*).

$$B_{F,1} X_1 + B_{F,2} X_2 + B_{F,3} X_3 + B_{F,4} X_4 + B_{F,5} X_5 + B_{F,6} X_6 + X_7 + W_S = 0 \quad (2.41.11)$$

$$B_{F,1} X_1 + B_{F,2} X_2 + B_{F,3} X_3 + B_{F,6} X_6 + X_7 + W_S = 0 \quad (2.41.12)$$

In what follows the expressions for  $B_{F,1}$  are summarized:

$$B_{F,1,j} = \frac{-E_{1,j}^T M_{B,2}^T}{\rho_{1,j}} [I - M_{B,1} u_{1,j} u_{1,j}^T M_{B,1}^T] \cdot M_{M,1}$$



$$G_k = ([\dot{s}_s - \dot{s}_E]_k^T \cdot [\dot{s}_s - \dot{s}_E]_k)^{\frac{1}{2}} - r_k \quad (2.42.5)$$

$$H_k = \frac{1}{r_k} \cdot [\dot{s}_s - \dot{s}_E]_k^T \cdot [\dot{s}_s - \dot{s}_E]_k - \dot{r}_k \quad (2.42.6)$$

where

$\begin{bmatrix} s \\ \dot{s} \end{bmatrix}_s$  is the selenocentric state vector of the satellite

$\begin{bmatrix} s \\ \dot{s} \end{bmatrix}_E$  is the selenocentric state vector of the tracking station on Earth.

The partial derivatives matrices  $B_G$  and  $B_H$  are derived by the differentiation of equations (2.42.5) and (2.42.6) with respect to the parameters  $L_i$  figuring in equations (2.42.1) and 2.42.2), respectively:

$$\begin{bmatrix} B_G \\ B_H \\ B_S \end{bmatrix}_{\downarrow k} = \frac{\partial G_k}{\partial \begin{bmatrix} s \\ \dot{s} \end{bmatrix}_k} \cdot \begin{bmatrix} \frac{\partial \begin{bmatrix} s \\ \dot{s} \end{bmatrix}_k}{\partial L_3} \\ \frac{\partial \begin{bmatrix} s \\ \dot{s} \end{bmatrix}_k}{\partial L_4} \\ \frac{\partial \begin{bmatrix} s \\ \dot{s} \end{bmatrix}_k}{\partial L_5} \end{bmatrix} = \frac{1}{r_k} \begin{bmatrix} [\dot{s}_s - \dot{s}_E]_k \\ 0 \end{bmatrix} \cdot \begin{bmatrix} Q_{s1} & Q_{s2} & U_s \end{bmatrix}$$

$$\begin{bmatrix} B_G \\ B_H \\ B_S \end{bmatrix}_{\downarrow k} = \frac{1}{r_k} \begin{bmatrix} [\dot{s}_s - \dot{s}_E]_k \\ -\dot{r}_k [\dot{s}_s - \dot{s}_E]_k^T \cdot [\dot{s}_s - \dot{s}_E]_k \end{bmatrix} \cdot \begin{bmatrix} Q_{s1} & Q_{s2} & U_s \end{bmatrix} \quad (2.42.7)$$

$$B_{G,s,k} = -I ; \quad -B_{H,s,k} = -I \quad (2.42.8 \text{ and } 2.42.9)$$

$$\begin{bmatrix} L_{10} \\ L_{11} \end{bmatrix}_{\downarrow k} = \begin{bmatrix} s \\ \dot{s} \end{bmatrix}_E$$

$$B_{G,10,k} = \frac{\partial G_k}{\partial L_{10,k}} = -[\dot{s}_s - \dot{s}_E]_k^T \quad (2.42.10)$$

$$B_{H,10,k} = \frac{\partial H_k}{\partial L_{10,k}} = -\frac{1}{r_k} [\dot{s}_s - \dot{s}_E]_k^T \quad (2.42.11)$$

$$B_{H,11,k} = \frac{\partial H_k}{\partial L_{11,k}} = -\frac{1}{r_k} [\dot{s}_s - \dot{s}_E]_k^T \quad (2.42.12)$$

For the derivation of  $Q_{s1}$ ,  $Q_{s2}$ ,  $U_s$ , see Appendix F.

## 2.5 Formation and Solution of the Normal Equations

The development presented in this section is based on the following premises:

- (a) A large batch of data (optical, range, and range-rate) is to be processed simultaneously. The batch includes data from several satellite arcs and also from Earth-based observations.
- (b) There have been data processed prior to the present batch so that there is an a priori knowledge of values for the parameters and their covariance matrices.
- (c) The covariance matrix of the permanent parameters  $L_1, L_2, L_3$  (see section 2.3) is nondiagonal while those of the transient parameters are diagonal or at least block diagonal.

The notation used is as in section 2.4, and the solution follows according to Appendix D. The two cases of optical observations—satellite borne and Earth-based—are treated separately, and at the end it is demonstrated how the separate normal equations are combined into the final solution for the whole batch.

### 2.51 Satellite-Borne Optical Observations (Single Arc).

The solution as developed is for processing data from a single satellite arc. The linearized models as from section 2.4 are:

$$\begin{aligned}
 F &= B_F^1 X_1 + B_F^2 X_2 + B_F^3 X_3 + B_F^4 X_4 + B_F^5 X_5 + B_F^6 X_6 + X_7 & + W_F &= 0 \\
 G &= & B_G^3 X_3 + B_G^4 X_4 + B_G^5 X_5 & - X_8 & + W_G &= 0 \\
 H &= & B_H^3 X_3 + B_H^4 X_4 + B_H^5 X_5 & - X_9 & + W_H &= 0 \\
 C &= & & C_4 X_4 & & + W_C &= 0
 \end{aligned}
 \tag{2.51.1}$$

The conditions ( $C_4$ ) imposed on the  $X_4$  parameters are identical to the ones presented in Appendix C.

The minimizing function  $\phi$  is defined in the usual way:

$$\phi = [X_1^T X_2^T \dots X_9^T] \Sigma^{-1} [X_1^T X_2^T \dots X_9^T]^T - 2 \lambda^T [F^T G^T H^T C^T]^T
 \tag{2.51.2}$$

where

$\lambda = [\lambda_F \lambda_G \lambda_H \lambda_C]^T$  is a vector of Lagrange multipliers

$\Sigma$  is the a priori covariance matrix of all the parameters involved in the adjustment ( $L_1, L_2 \dots L_9$ ).

It is clear from the formulation of  $\varphi$  that the weight matrix is obtained by inverting the covariance matrix where the variance of unit weight is defined as a dimensionless number equal to one.

In order to facilitate the formation and solution of the normal equations, the submatrices are blocked in terms of auxiliary matrices.

$$\Gamma_1 = \Sigma_{1,2,3}; \quad \Gamma_2 = \begin{bmatrix} \Sigma_4 & 0 \\ 0 & \Sigma_5 \end{bmatrix}; \quad \Gamma_3 = \begin{bmatrix} \Sigma_6 & & & & \\ & \Sigma_7 & & 0 & \\ & & & & \\ & 0 & & \Sigma_8 & \\ & & & & \Sigma_9 \end{bmatrix}; \quad \Gamma_4 = \Sigma_{10,11}$$

$$A_1 = \begin{bmatrix} B_F^1 & B_F^2 & B_F^3 \\ 0 & 0 & B_G^3 \\ 0 & 0 & B_H^3 \\ 0 & 0 & 0 \end{bmatrix}; \quad A_2 = \begin{bmatrix} B_F^4 & B_F^5 \\ B_G^4 & B_G^5 \\ B_H^4 & B_H^5 \\ C_4 & 0 \end{bmatrix}; \quad A_3 = \begin{bmatrix} B_G & I & 0 & 0 \\ 0 & 0 & -I & 0 \\ 0 & 0 & 0 & -I \\ 0 & 0 & 0 & 0 \end{bmatrix}; \quad A_4 = \begin{bmatrix} 0 & 0 \\ B_G^{10} & 0 \\ B_H^{10} & B_H^{11} \\ 0 & 0 \end{bmatrix}$$

$$Y_1 = \begin{bmatrix} X_1 \\ X_2 \\ X_3 \end{bmatrix}; \quad Y_2 = \begin{bmatrix} X_4 \\ X_5 \end{bmatrix}; \quad Y_3 = \begin{bmatrix} X_6 \\ X_7 \\ X_8 \\ X_9 \end{bmatrix}; \quad Z = \begin{bmatrix} X_{10} \\ X_{11} \end{bmatrix}; \quad U = \begin{bmatrix} W_F \\ W_G \\ W_H \\ W_C \end{bmatrix}; \quad K = \begin{bmatrix} \lambda_F \\ \lambda_G \\ \lambda_H \\ \lambda_C \end{bmatrix}$$

The normal equations are obtained [Uotila, 1967] using the auxiliary notation:

$$\begin{bmatrix} -\Gamma_1^{-1} & 0 & 0 & A_1^T \\ 0 & -\Gamma_2^{-1} & 0 & A_2^T \\ 0 & 0 & -\Gamma_3^{-1} & A_3^T \\ A_1 & A_2 & A_3 & 0 \end{bmatrix} \begin{bmatrix} Y_1 \\ Y_2 \\ Y_3 \\ K \end{bmatrix} = \begin{bmatrix} 0 \\ 0 \\ 0 \\ -U \end{bmatrix} \quad (2.51.3)$$

The solution for  $Y_1$  is according to Appendix D :

$$\begin{aligned} Y_1 &= -P A_1^T M_{2,3}^1 U \\ P &= (\Gamma_1^{-1} + A_1^T M_{2,3}^1 A_1)^{-1} \end{aligned} \quad (2.51.4)$$

where

$$M_{2,3}^1 = (A_2 \Gamma_2 A_2^T + A_3 \Gamma_3 A_3^T)^{-1} .$$

The covariance matrix of the adjusted  $Y_1^a$  parameters is

$$\Gamma_1^a = P + P A_1^T M_{2,3}^1 M_z M_{2,3}^1 A_1 P \quad (2.51.5)$$

where

$$M_z = A_z \Gamma_z A_z^T .$$

## 2.52 Earth-Based Optical Observations.

In this case there are no accompanying range and range-rate observations; the parameters  $X_4, X_5$  do not appear in the model, and the solution is consequently much simpler. Auxiliary notation similar to that for the satellite observations is used:

$$\Gamma_1 = \Sigma_{1,2,3}; \quad \Gamma_3 = \begin{bmatrix} \Sigma_6 & 0 \\ 0 & \Sigma_7 \end{bmatrix}; \quad \Gamma_z = \Sigma_{10,11}$$

$$A_1 = [B_1 \ B_2 \ B_3]; \quad A_3 = [B_6 \ I]; \quad A_z = [B_{10} \ 0]$$

$$Y_1 = \begin{bmatrix} X_1 \\ X_2 \\ X_3 \end{bmatrix}; \quad Y_3 = \begin{bmatrix} X_6 \\ \\ X_7 \end{bmatrix}; \quad Z = \begin{bmatrix} X_{10} \\ \\ X_{11} \end{bmatrix}$$

$$U = W_f; \quad K = \lambda_f .$$

The solution for  $Y_1$  and the covariance matrix of the adjusted parameters  $Y_1^a$  are:

$$Y_1 = -P A_1^T M_3^1 U \quad (2.52.1)$$

$$\Gamma_1^a = P + P A_1^T M_3^1 M_z M_3^1 A_1 P \quad (2.52.2)$$

where

$$P = (\Gamma_1^{-1} + A_1^T M_3^1 A_1)^{-1}$$

$$M_3 = A_3 \Gamma_3 A_3^T$$

$$M_z = A_z \Gamma_z A_z^T$$

2.53 Combined Solution.

In case more than one satellite arc are processed, the parameters  $L_4, L_5$  are different for each arc.  $L_4$  may end up being the same for all the arcs although this is not enforced by the solution, i. e.,  $L_4$  are allowed to adjust to different values for different arcs. The a priori values and covariance matrix for  $L_4$  used for the different arcs are the same. This is so as the processing of the arcs is regarded as simultaneous even if numerically the arcs are processed one by one.

The normal equations of all the observations in the batch ( $k$  satellite arcs and Earth observations) can be written as follows (see normal equations for a single arc (2.51.3) ):

$$\begin{bmatrix} -\Gamma_1^{-1} & 0 & A_1^T \\ 0 & -\Gamma^{-1} & A^T \\ A_1 & A & 0 \end{bmatrix} \cdot \begin{bmatrix} Y_1 \\ Y \\ K \end{bmatrix} + \begin{bmatrix} 0 \\ 0 \\ U \end{bmatrix} = 0 \quad (2.53.1)$$

where

$$\Gamma = \begin{bmatrix} \Gamma_2 & 0 & & & & \\ 0 & \Gamma_3 & & & & \\ \hline & & \Gamma_2 & 0 & & \\ & & 0 & \Gamma_3 & & \\ \hline & & & & \Gamma_2 & 0 \\ & & & & 0 & \Gamma_3 \\ \hline & & & & & & \Gamma_{3,E} \end{bmatrix}$$

$$A_1 = \begin{bmatrix} A_{1,1} \\ A_{1,2} \\ \vdots \\ A_{1,k} \\ A_{1,E} \end{bmatrix}; \quad A = \begin{bmatrix} A_2 & A_3 & & & & \\ \hline & A_2 & A_3 & & & \\ & & & & & \\ \hline & & & & & \\ & & & & A_2 & A_3 \\ \hline & & & & & & A_{3,E} \end{bmatrix}$$

$$K = \begin{bmatrix} K_1 \\ K_2 \\ \vdots \\ K_k \\ K_E \end{bmatrix}; \quad U = \begin{bmatrix} U_1 \\ U_2 \\ \vdots \\ U_k \\ U_E \end{bmatrix}$$

The solution of such a mammoth system of normal equations is a straightforward matter due to its banded block diagonal structure [Brown, 1969]. The operations with the large matrices are replaced by a summation. The procedure is well known and at the end the adjusted values of the permanent parameters and their covariance matrix are as follows:

Setting  $P$ ,  $P_E$ ,  $P_i$  as

$$P = [\Gamma_1^{-1} + P_E + \sum_{i=1}^k P_i]^{-1}; \quad P_E = (A_1^T M_3^{-1} A_1)_E; \quad P_i = (A_1^T M_{2,3}^{-1} A_1)_i$$

it follows

$$Y_1^a = Y_1^b - P \cdot [(A_1^T M_3^{-1} U)_E + \sum_{i=1}^k (A_1^T M_{2,3}^{-1} U)_i] \quad (2.53.2)$$

$$\begin{aligned} \Gamma_1^a = & P + (\Gamma_1^{-1} + P_E)^{-1} (A_1^T M_3^{-1} M_z M_3^{-1} A_1)_E (\Gamma_1^{-1} + P_E)^{-1} + \\ & + \sum_{i=1}^k (\Gamma_1^{-1} + P_i)^{-1} (A_1^T M_{2,3}^{-1} M_z M_{2,3}^{-1} A_1)_i (\Gamma_1^{-1} + P_i)^{-1} \end{aligned} \quad (2.53.3)$$

As shown in Appendix D,  $P$  is the covariance matrix obtained by ignoring the contribution of  $Z$ . It should be noted that the covariance matrix evaluated is identical numerically to the weight coefficients matrix as the variance of unit weight is assumed to remain unchanged after the adjustment (it was set initially to one).

## 2.6 Programming Considerations

The analysis in section 2.5 resulted in a solution which was considered feasible due to the banded block diagonal nature of the normal matrix. Yet even the elements within the summation sign involve operations with matrices of immense dimensions which cannot be handled directly even by the largest computer systems available today. Fortunately, the actual situation is much less alarming as those expressions are composed of matrices with a favorable pattern such that the formation and inversion of the large expressions can be performed in parts.

The objective in this section is to analyze the various matrix expressions obtained in section 2.5 and to develop algorithms for their evaluation under the assumption that a computer system of the rank of IBM 360/75 is available with its core size, auxiliary devices (magnetic discs and tapes) and matrix inversion subroutines.

The expressions that will be considered are as follows (see section 2.5):

### Satellite-Borne

1.  $(A_1^T M_{2,3}^{-1} A_1)_i$
2.  $(A_1^T M_{2,3}^{-1} U)_i$
3.  $(\Gamma_1^{-1} + P_1)^{-1} (A_1^T M_{2,3}^{-1} M_z M_{2,3}^{-1} A_1)_i (\Gamma_1^{-1} + P_1)^{-1}$

where  $i$  represents satellite arc # $i$  .

### Earth-Based

4.  $(A_1^T M_3^{-1} A_1)_E$
5.  $(A_1^T M_3^{-1} U)_E$
6.  $(\Gamma_1^{-1} + P_E)^{-1} (A_1^T M_3^{-1} M_z M_3^{-1} A_1)_E (\Gamma_1^{-1} + P_E)^{-1}$

In order to illustrate better the logic of the algorithms developed, the matrices involved in each of the six expressions will be shown diagrammatically emphasizing the submatrices which are full vs. those composed of zeros.



where

$$\begin{aligned} M_{2,3}^* &= A_2^* \Gamma_2^* A_2^{*T} + A_3^* \Gamma_3^* A_3^{*T} \\ \bar{N}_2 &= A_2^* \Gamma_2^* C_2^T \\ N_2 &= C_2^T \Gamma_2^* C_2^T \end{aligned}$$

$$M_{2,3}^1 = \begin{bmatrix} Q_1 & \bar{Q}_2 \\ \bar{Q}_2^T & Q_2 \end{bmatrix}$$

From Uotila, [1967] it follows:

$$Q_1 = (M_{2,3}^* - \bar{N}_2 N_2^1 \bar{N}_2^T)^{-1} = M_{2,3}^{*1} + M_{2,3}^{*1} \bar{N}_2 (N_2 - \bar{N}_2^T M_{2,3}^{*1} \bar{N}_2)^{-1} \bar{N}_2^T M_{2,3}^{*1}$$

The only element in  $M_{2,3}^1$  needed is  $Q_1$  as

$$A_1^T M_{2,3}^1 A_1 = \begin{bmatrix} A_1^T & 0 \end{bmatrix} \begin{bmatrix} Q_1 & \bar{Q}_2 \\ \bar{Q}_2^T & Q_2 \end{bmatrix} \begin{bmatrix} A_1 \\ 0 \end{bmatrix} = A_1^T Q_1 A_1$$

The covariances are blocked as follows:

$$\Gamma_1 = \Sigma_{1,2,3} = \begin{bmatrix} \text{shaded} & \text{shaded} \\ \text{shaded} & \text{shaded} \end{bmatrix}$$

$$\Gamma_2 = \begin{bmatrix} \Sigma_4 & 0 \\ 0 & \Sigma_5 \end{bmatrix} = \begin{bmatrix} \text{shaded} & \text{white} \\ \text{white} & \text{shaded} \end{bmatrix}$$

$$\Gamma_3 = \begin{bmatrix} \Sigma_{6,1} & & & & & & & & 0 \\ & \Sigma_{6,2} & \dots & & & & & & \\ & & & \Sigma_{6,w} & & & & & \\ & & & & \Sigma_7 & & & & \\ 0 & & & & & \Sigma_8 & & & \\ & & & & & & \Sigma_9 & & \end{bmatrix} = \begin{bmatrix} \text{shaded} & & & & & & & & \\ & \text{shaded} & & & & & & & \\ & & \text{shaded} & & & & & & \\ & & & \text{shaded} & & & & & \\ & & & & \text{shaded} & & & & \\ & & & & & \text{shaded} & & & \\ & & & & & & \text{shaded} & & \\ & & & & & & & \text{shaded} & \\ & & & & & & & & \text{shaded} \end{bmatrix}$$

$$\begin{aligned} \Sigma_7 &= \sigma_f^2 \cdot I \\ \Sigma_8 &= \sigma_g^2 \cdot I \\ \Sigma_9 &= \sigma_h^2 \cdot I \end{aligned}$$

Evaluating the  $M_{2,3}^1$  matrix:

$$M_{2,3}^{*1} = (M_3^* + A_2^* \Gamma_2^* A_2^{*T})^{-1} = M_3^1 - M_3^1 A_2^* (\Gamma_2^1 + A_2^{*T} M_3^1 A_2^*)^{-1} A_2^{*T} M_3^1$$







$$A_z = \begin{bmatrix} & & & & 0 \\ & A_{G,z,1} & & & \\ & & A_{G,z,2} & & \\ & & & \dots & \\ & & & & A_{G,z,\ell} \\ A_{H,z,1} & & & & \\ & & A_{H,z,2} & & \\ & & & \dots & \\ & & & & A_{H,z,\ell} \\ & & & & 0 \end{bmatrix} = \begin{array}{|c|} \hline \text{---} \\ \hline \text{---} \\ \hline \text{---} \\ \hline \text{---} \\ \hline \end{array}$$

$$M_z = A_z \Gamma_z A_z^T = \begin{bmatrix} 0 & & 0 \\ & M_G^z & \\ 0 & & M_H^z & 0 \end{bmatrix} = \begin{array}{|c|} \hline \text{---} \\ \hline \text{---} \\ \hline \text{---} \\ \hline \text{---} \\ \hline \end{array}$$

$$M_G^z = \begin{bmatrix} m_{G,z,1} & & 0 \\ & m_{G,z,2} & \\ 0 & & \dots & \\ & & & m_{G,z,\ell} \end{bmatrix}; \quad M_H^z = \begin{bmatrix} m_{H,z,1} & & 0 \\ & m_{H,z,2} & \\ 0 & & \dots & \\ & & & m_{H,z,\ell} \end{bmatrix}$$

$$m_{G,z,j} = A_{G,z,j} \Sigma_{z,j} A_{G,z,j}^T$$

$$m_{H,z,k} = A_{H,z,k} \Sigma_{z,k} A_{H,z,k}^T$$

Using auxiliary submatrices as defined for Expression 1 above, the resulting algorithm is:

$$A_1^T M_{2,3}^{-1} M_z M_{2,3}^{-1} A_1 = A_{G1}^T Q_1 M_z Q_1 A_{G1} + A_{H1}^T Q_1 M_z Q_1 A_{H1} =$$

$$= \sum_j q_{G1,j}^2 m_{G,z,j} A_{G1,j}^T A_{G1,j} + \sum_k q_{H1,k}^2 m_{H,z,k} A_{H1,k}^T A_{H1,k} \quad (2.6.3)$$

Expression 4:  $(A_1^T M_3^{-1} A_1)_E$

Because of the absence of range and range-rate observations the situation is much easier to handle. Parameters  $L_4$ ,  $L_5$  and also the conditions imposed

on  $L_4$  do not figure in the mathematical model for Earth-based observations.

$$A_1 = \begin{bmatrix} A_{E,1,1} \\ A_{E,1,2} \\ \vdots \\ A_{E,1,n} \end{bmatrix} = \begin{array}{|c|c|c|} \hline \text{[stippled]} & \text{[stippled]} & \text{[stippled]} \\ \hline \end{array}$$

$n$  is the number of earth-based exposures in the batch.

$$A_3 = \begin{bmatrix} A_{E,3,1} & & & 0 & & \\ & A_{E,3,2} & & & & \\ & 0 & \dots & & & \\ & & & A_{E,3,n} & & \\ & & & & I & \end{bmatrix} = \begin{array}{|c|c|c|} \hline \text{[stippled]} & & \text{[diagonal]} \\ \hline \text{[stippled]} & & \text{[diagonal]} \\ \hline & & \text{[diagonal]} \\ \hline \text{[stippled]} & & \text{[diagonal]} \\ \hline & & \text{[diagonal]} \\ \hline \end{array}$$

$$A_z = \begin{bmatrix} A_{E,z,1} & & & 0 \\ & A_{E,z,2} & & \\ & 0 & \dots & \\ & & & A_{E,z,n} \end{bmatrix} = \begin{array}{|c|c|c|} \hline \text{[stippled]} & & \\ \hline & \text{[stippled]} & \\ \hline & & \\ \hline & & \text{[stippled]} \\ \hline \end{array}$$

The covariance matrices  $\Gamma_1$ ,  $\Gamma_3$ ,  $\Gamma_z$  are identical to the ones defined for Expressions 1, 2, and 3.

$$M_3^{-1} = \begin{bmatrix} M_{E,3,1}^{-1} & & & 0 \\ & M_{E,3,2}^{-1} & & \\ & 0 & \dots & \\ & & & M_{E,3,n}^{-1} \end{bmatrix} = \begin{array}{|c|c|c|} \hline \text{[stippled]} & & \\ \hline & \text{[stippled]} & \\ \hline & & \\ \hline & & \text{[stippled]} \\ \hline \end{array}$$

$$M_{E,3,1}^{-1} = [A_{E,3,1} \Sigma_{E,1} A_{E,3,1}^T + \sigma_E^2 I]^{-1}$$

Following the same logic as for Expression 1

$$(A_1^T M_3^{-1} A_1)_E = \sum_1 A_{E,1,1}^T M_{E,3,1}^{-1} A_{E,1,1} \quad (2.6.4)$$

Expression 5:  $(A_1^T M_3^{-1} U)_E$

$$U_E = \begin{bmatrix} U_{E,1} \\ U_{E,2} \\ \vdots \\ U_{E,n} \end{bmatrix}$$

Using results from Expression 4, it follows:

$$(A_1^T M_3^{-1} U)_E = \sum_1^{\infty} A_{E,1,i}^T M_{E,3,i}^{-1} U_i \quad (2.6.5)$$

Expression 6:  $(\Gamma_1^T + P_E)^{-1} (A_1^T M_3^{-1} M_z M_3^{-1} A_1)_E (\Gamma_1^T + P_E)^{-1}$

$P_E$  is equivalent to Expression 4 and was treated above.

$$M_z = A_z \Gamma_z A_z^T = \begin{bmatrix} M_{E,z,1} & & & 0 \\ & M_{E,z,2} & & \\ 0 & & \dots & \\ & & & M_{E,z,n} \end{bmatrix}$$

$M_{E,z,i}$  are block diagonal matrices composed of  $(2 \times 2)$  submatrices.

$$A_1^T M_3^{-1} M_z M_3^{-1} A_1 = \sum_1^{\infty} A_{E,1,i}^T M_{E,3,i}^{-1} M_{E,z,i} M_{E,3,i}^{-1} A_{E,1,i} \quad (2.6.6)$$

As stated at the beginning of this section, the algorithms were developed in order to demonstrate the feasibility of the solution as presented in section 2.5 and also to serve as the mathematical basis for the massive computer programming effort, necessary for carrying out an actual reduction of data.

### 3. NUMERICAL INTEGRATION OF THE PHYSICAL LIBRATIONS OF THE MOON

#### 3.1 Introduction

The orientation of the Moon in space or more specifically, the orientation with respect to the ecliptic mean coordinate system of a Moon-fixed selenodetic coordinate system is a problem of primary importance in the solution for a datum on the Moon. As explained in Chapter 1, the problem can be reduced actually to the solution of the physical librations of the Moon. Although a satisfactory solution for the physical librations does exist [Eckhardt, 1970], there are several important aspects which require an entirely different approach.

There has been considerable discussion in the literature [Kopal and Goudas, 1967] on the problems created by the linearization of Euler's dynamic equations prior to their solution. The prevailing opinion is that the unstable solution for one of the terms in the physical libration in longitude ( $\tau$ ) at a particular value of the constant  $f$  (where  $f = \frac{(C-B)B}{(C-A)A}$  and  $A, B, C$  are the principal moments of inertia of the Moon) does not necessarily exist in the actual rotational motion of the Moon, but is due to the linearization. Thus, if a solution of Euler's dynamic equations in their original nonlinearized form is possible, it could avoid the aforementioned problem.

The consistency of the existing solutions for physical librations with the new generation of numerical lunar ephemerides cannot be maintained due to the manner in which these solutions were obtained. The particular solution of Euler's dynamic equations (the forced librations of the Moon) is composed of harmonic terms with arguments which are linear combina-

tions of the arguments in Brown's lunar ephemeris [Koziel, 1948; Eckhardt, 1965]. Even if the solution for the physical librations is not so sensitive to small variations in the lunar ephemeris [Eckhardt, 1971], the fact remains that the present solutions are inconsistent in principle with the best available lunar ephemeris.

As pointed out in section 1.3, it is difficult to evaluate all the effects of the bias introduced by the "center of figure" assumption made in the reduction of the heliometer observations. Thus, a solution which is entirely independent of this assumption could provide a clue as to its real effects.

The adjustment procedure, as developed in Chapter 2, presents a problem of parameterization for the solution of the physical librations (section 2.3). The analysis of observations which are sensitive to the orientation of the Moon and, consequently, to the physical librations of the Moon, requires the definition of a minimal number of mutually independent physical librations parameters. It is also advantageous for these parameters to be explicitly present in the mathematical model in order to enhance its linearization.

There are two additional aspects which have been neglected so far. The existing solutions ignore the motion of the ecliptic coordinate system and do not account for the direct gravitational effect of the Sun. The effect of these approximations is marginal in view of uncertainties in the present knowledge of the dynamical figure of the Moon and the quality of presently available optical observations. However, as shown in this chapter, the incorporation of these effects in the solution requires little additional effort and in view of observations of a superior quality which are becoming available (like laser ranging to the Moon) it appears that the objective in any new attempt at solving the physical librations problem should be to obtain as complete a solution as possible.

The solution for the physical librations in this chapter is presented in three main sections:

- (i) Derivation of the equations of rotational motion of the

Moon in the form of second order differential equations of the physical libration angles and the subsequent solution of those equations by numerical integration.

(ii) Development of the adjustment model for observations which are sensitive to the physical libration angles.

(iii) Development of the mathematical theory for a least squares fit of one set of physical libration angles into another.

The solution in this chapter is based on the following three postulates:

(i) The Moon is regarded as perfectly rigid [Eckhardt, 1970].

(ii) The translatory motion of the Moon's mass center about the geocenter is assumed perfectly known and taken directly from the LE-16 lunar ephemeris [O'Handley, et al., 1969].

(iii) The effect of the spherical harmonics of the lunar gravitational field of degree higher than the second is neglected.

## 3.2 Equations of Rotational Motion of the Moon

### 3.21 Euler's Dynamic Equations.

The differential equations of rotational motion of a rigid body about its mass center as referred to an inertially oriented system are known in the literature as Euler's dynamic equations. A brief account is brought of the derivation of these equations for the rotation of the Moon.

Two right-handed Cartesian coordinate systems are considered, both centered at the mass center of the Moon:

- X Y Z - inertially oriented coordinate system (see section 2.1).
- x y z - selenodetic coordinate system where x,y,z coincide with the principal axes of the Moon.

Principal axes of a rigid body are defined such that the moment of inertia tensor is a  $3 \times 3$  diagonal matrix where the three diagonal elements A,B,C are the principal moments of inertia with respect to axes x,y,z, respectively.

The two coordinate systems X Y Z and x y z momentarily coincide for the purpose of this analysis.

The rotational (angular) velocity of the Moon with respect to the x y z rotating system is expressed by the vector  $\vec{\omega}$ . The components of  $\vec{\omega}$  along x,y,z are the rotational velocities around the x,y,z axes, respectively. In matrix notation

$$\omega = \begin{bmatrix} \omega_x \\ \omega_y \\ \omega_z \end{bmatrix} .$$

The angular momentum of the Moon in its rotation with respect to the x y z system is denoted by vector  $\vec{h}$  and defined as

$$\vec{h} = \int_m dm \vec{r} \times \vec{\omega} \times \vec{r} \quad (3.21.1)$$

where

$\vec{r}$  is the position vector of a mass element  $dm$

$M$  is the total mass of the Moon

Using matrix notation for the vector cross product and substituting the moment of inertia tensor of the Moon,  $h$  assumes the following form:

$$h = \begin{bmatrix} h_x \\ h_y \\ h_z \end{bmatrix} = \begin{bmatrix} A & -F & -E \\ -F & B & -D \\ -E & -D & C \end{bmatrix} \cdot \begin{bmatrix} \omega_x \\ \omega_y \\ \omega_z \end{bmatrix} \quad (3.21.2)$$

The coordinate system  $x y z$  was defined to coincide with the principal axes of the Moon which for the products of inertia  $D, E$  and  $F$  would mean that:

$$D = E = F = 0 \quad .$$

The expression for  $h$  simplifies further to

$$h = \begin{bmatrix} A \cdot \omega_x \\ B \cdot \omega_y \\ C \cdot \omega_z \end{bmatrix} \quad (3.21.3)$$

The angular momentum of the Moon in its rotation with respect to the inertial  $X Y Z$  system is denoted by  $\vec{H}$ . The following important relation holds between  $\vec{H}$ ,  $\vec{h}$  and  $\vec{\omega}$  [Smart, 1951]:

$$\vec{H} = \vec{h} + \vec{\omega} \times \vec{h} \quad . \quad (3.21.4)$$

$\dot{\vec{H}}$  and  $\dot{\vec{h}}$  are the time derivatives of  $H$  and  $h$ , respectively.

In the matrix notation, considering  $A, B, C$  as time invariant, the expression for  $\dot{\vec{H}}$  can be written as follows (see Appendix E):

$$\begin{bmatrix} \dot{H}_x \\ \dot{H}_y \\ \dot{H}_z \end{bmatrix} = \begin{bmatrix} A \dot{\omega}_x \\ B \dot{\omega}_y \\ C \dot{\omega}_z \end{bmatrix} + \begin{bmatrix} 0 & -\omega_z & \omega_y \\ \omega_z & 0 & -\omega_x \\ -\omega_y & \omega_x & 0 \end{bmatrix} \cdot \begin{bmatrix} A \omega_x \\ B \omega_y \\ C \omega_z \end{bmatrix} \quad (3.21.5)$$

Moment of a force  $\vec{T}$  acting on the Moon is denoted by  $\vec{Q}$  and is defined as

$$\vec{Q} = \frac{1}{M} \int_M dm \vec{R} \times \vec{T} \quad (3.21.6)$$

where  $\vec{R}$  is the selenocentric position vector of the mass element  $dm$ .

The second law of Newton applied to rotational motion states that the moment of a force acting on a rigid body is equal to the derivative with respect to time of the angular momentum of the body. As in the case of Newton's second laws for translatory motion, the moment and the angular momentum are referred to fixed (inertial) axes - in our case - X, Y, Z.

$$\vec{Q} = \dot{\vec{H}} .$$

In the matrix notation denoting the components of  $\vec{Q}$  along X, Y, Z as L, M, N, respectively, it follows:

$$\begin{bmatrix} L \\ M \\ N \end{bmatrix} = \begin{bmatrix} A \dot{\omega}_x \\ B \dot{\omega}_y \\ C \dot{\omega}_z \end{bmatrix} + \begin{bmatrix} (C - B) \omega_y \omega_z \\ -(C - A) \omega_x \omega_z \\ (B - A) \omega_x \omega_y \end{bmatrix} \quad (3.21.7)$$

Three moment of inertia ratios are defined as follows:

$$\alpha = \frac{C - B}{A} \quad \beta = \frac{C - A}{B} \quad \gamma = \frac{B - A}{C}$$

The differential equations written now in their final form are known as Euler's dynamic equations:

$$\begin{bmatrix} \dot{\omega}_x \\ \dot{\omega}_y \\ \dot{\omega}_z \end{bmatrix} + \begin{bmatrix} \alpha & 0 & 0 \\ 0 & -\beta & 0 \\ 0 & 0 & \gamma \end{bmatrix} \cdot \begin{bmatrix} \omega_y \omega_z \\ \omega_x \omega_z \\ \omega_x \omega_y \end{bmatrix} = \begin{bmatrix} L/A \\ M/B \\ N/C \end{bmatrix} . \quad (3.21.8)$$

The external forces acting on the Moon are primarily the gravitational attraction of the Earth and that of the Sun. The moment caused by the attraction of the planets is insignificant and in this analysis it is neglected.

The potential of the Moon at a distant point and for a unit mass can be expressed by Mac Cullaugh's formula:

$$V = k^2 \left[ \frac{M}{r} + \frac{1}{2r^3} (A + B + C - 3I) \right] \quad (3.21.9)$$

where

M is the mass of the Moon

r is the distance between the mass centers of the Moon and the disturbing body

A, B, C are the principal moments of inertia of the Moon (about the x, y, z axes)

I is the moment of inertia about an axis defined by the mass centers of the Moon and the disturbing body.

The position of the disturbing body in the x y z (rotating) system is  $x_D, y_D, z_D$  such that  $r^2 = x_D^2 + y_D^2 + z_D^2$ .

In terms of A, B, C and  $x_D, y_D, z_D$ , the moment I can be expressed as follows:

$$I = \frac{1}{r^2} (A \cdot x_D^2 + B \cdot y_D^2 + C \cdot z_D^2)$$

The potential of the Moon for the total mass D of the disturbing body is then

$$V = \frac{k^2 DM}{r} + \frac{k^2 D}{2r^3} \left[ A + B + C - \frac{3}{r^2} (A x_D^2 + B y_D^2 + C z_D^2) \right] \quad (3.21.10)$$

In this formula the effect of harmonic terms of the Moon's gravitational field of a degree higher than the second are neglected. The error introduced in the moment caused by the Earth is in the ninth significant digit while for the Sun it causes an error in the fifteenth significant digit [Eckhardt, 1970].

If a differential rotation  $\delta\theta$  is introduced to the Moon, the work done by the disturbing moment is equal to the change in potential of the Moon. Inspecting the expression for  $V$  it is obvious that the only term that depends on the Moon's orientation is  $I$ . Thus, the variation in  $V$  is obtained as follows:

$$\begin{aligned}\delta V &= -\frac{3k^2D}{r^5} \cdot (A \cdot x_D \cdot \delta x_D + B \cdot y_D \cdot \delta y_D + C \cdot z_D \cdot \delta z_D) \\ &= -\frac{3k^2D}{r^5} \cdot [A \cdot x_D \quad B \cdot y_D \quad C \cdot z_D] \cdot \begin{bmatrix} \delta x_D \\ \delta y_D \\ \delta z_D \end{bmatrix}\end{aligned}\quad (3.21.11)$$

$\delta x_D$ ,  $\delta y_D$ ,  $\delta z_D$  are related to  $\delta\theta$  according to the following expression:

$$\begin{bmatrix} \delta x_D \\ \delta y_D \\ \delta z_D \end{bmatrix} = \begin{bmatrix} 0 & -\delta\theta_z & \delta\theta_y \\ \delta\theta_z & 0 & -\delta\theta_x \\ -\delta\theta_y & \delta\theta_x & 0 \end{bmatrix} \cdot \begin{bmatrix} x_D \\ y_D \\ z_D \end{bmatrix} = - \begin{bmatrix} 0 & -z_D & y_D \\ z_D & 0 & -x_D \\ -y_D & x_D & 0 \end{bmatrix} \cdot \begin{bmatrix} \delta\theta_x \\ \delta\theta_y \\ \delta\theta_z \end{bmatrix}$$

The work done by a moment  $\vec{Q}$  along the angle of rotation  $\delta\vec{\theta}$  is equal to the dot product of the two vectors and is denoted by  $\delta U$ :

$$\delta U = [L \quad M \quad N] \cdot \begin{bmatrix} \delta\theta_x \\ \delta\theta_y \\ \delta\theta_z \end{bmatrix}\quad (3.21.12)$$

According to the law of conservation of energy and for an arbitrary rotation  $\delta\vec{\theta}$

$$\delta V + \delta U = 0\quad (3.21.13)$$

Substituting (3.21.11) and (3.21.12) in (3.21.13) it follows:

$$[L \ M \ N] = \frac{3k^2 D}{r^5} [A \cdot x_0 \ B \cdot y_0 \ C \cdot z_0] \begin{bmatrix} 0 & z_0 & -y_0 \\ -z_0 & 0 & x_0 \\ y_0 & -x_0 & 0 \end{bmatrix} \quad (3.21.14)$$

$$\begin{bmatrix} L \\ M \\ N \end{bmatrix} = \frac{3k^2 D}{r^5} \cdot \begin{bmatrix} (C - B) y_0 z_0 \\ -(C - A) x_0 z_0 \\ (B - A) x_0 y_0 \end{bmatrix}$$

$$\begin{bmatrix} L/A \\ M/B \\ N/C \end{bmatrix} = \frac{3k^2 D}{r^5} \cdot \begin{bmatrix} \alpha & 0 & 0 \\ 0 & -\beta & 0 \\ 0 & 0 & \gamma \end{bmatrix} \begin{bmatrix} y_0 z_0 \\ x_0 z_0 \\ x_0 y_0 \end{bmatrix} \quad (3.21.15)$$

Denoting the mass of the Earth by E and that of the Sun by S, Euler's equations can be written now with an explicit right hand part:

$$\begin{bmatrix} \dot{\omega}_x \\ \dot{\omega}_y \\ \dot{\omega}_z \end{bmatrix} = \begin{bmatrix} \alpha & 0 & 0 \\ 0 & -\beta & 0 \\ 0 & 0 & \gamma \end{bmatrix} \cdot \left( \frac{3k^2 E}{r_E^5} \begin{bmatrix} yz \\ xz \\ xy \end{bmatrix}_E + \frac{3k^2 S}{r_S^5} \begin{bmatrix} yz \\ xz \\ xy \end{bmatrix}_S - \begin{bmatrix} \omega_y \omega_z \\ \omega_x \omega_z \\ \omega_x \omega_y \end{bmatrix} \right) \quad (3.21.16)$$

It would be of interest to compare the perturbing effect of the Sun to that of the Earth.

(a) Gravity coefficients

$$\frac{k^2 S}{r_S^3} \cong \frac{.99 \cdot 10^{21}}{1.5^3 \cdot 10^{24}} \cong .00029 \text{ day}^{-2}$$

$$\frac{k^2 E}{r_E^3} \cong \frac{.298 \cdot 10^{16}}{3.84^3 \cdot 10^{15}} \cong .0525 \text{ day}^{-2}$$

$$\frac{.00029}{.0525} \cong \frac{1}{200} = 0.5\%$$

(b) Range for  $\frac{yz}{r^2}$ ,  $\frac{xz}{r^2}$ ,  $\frac{xy}{r^2}$

	$\left  \frac{yz}{r^2} \right $	$\left  \frac{xz}{r^2} \right $	$\left  \frac{xy}{r^2} \right $
Sun	<.026	<.026	<.707
Earth	<.014	<.12	<.12

(c) Total effect in L, M, N in  $[\text{day}^{-2}]$  :

Moment	Earth	Sun	Sun/Earth
$L/[3(C-B)]$	$<.00073$	$<.0000075$	$\sim 1. \%$
$M/[3(C-A)]$	$<.0063$	$<.0000075$	$\sim 0.1\%$
$N/[3(B-A)]$	$<.0063$	$<.000205$	$\sim 3.2\%$

The ratios between the Earth and the Sun in generating the disturbing moment as calculated should be viewed as an estimate of the order of magnitude only. It is realized that at zero libration in longitude ( $y_e = 0$ ) or at zero libration in latitude ( $z_e = 0$ ) N and M, respectively, are composed solely of the effect of the Sun. Generally, however, the Earth dominates the Sun in generating the L and M components of the disturbing moment. In N the effect of the Sun can be considered as marginal. Programming the inclusion of the Sun in Euler's dynamic equations is simple and the extra computer time needed to evaluate and include the contribution of the Sun at each step of the integrations is negligible. In order to keep the approximations and neglected effects in the derivation to a minimum without having to pay an unreasonable price Euler's dynamic equations are extended to include the effect of the Sun.

### 3.22 Transformation of Euler's Dynamic Equations.

Euler's dynamic equations have been derived (Equation 3.21.16) without referring explicitly to the Eulerian orientation angles of the Moon  $\varphi, \psi, \theta$ . However, it is the Eulerian angles which are of interest, rather than the rotational velocities  $\omega_x, \omega_y, \omega_z$ , as they define the orientation of the selenodetic coordinate system with respect to the mean of date ecliptic coordinate system (see section 2.1). The mean of date (MOD) ecliptic coordinate system is defined by the instantaneous (of date) plane of the mean orbit of the Earth around the Sun (mean ecliptic) and the instantaneous mean vernal equinox [Mueller, 1969]. Denoting the MOD ecliptic

coordinate system by XYZ and the selenodetic coordinate system by xyz, the transformation from XYZ into xyz is obtained by a sequence of three rotations through the Eulerian angles as follows:

$$\begin{bmatrix} x \\ y \\ z \end{bmatrix} = R_3(\varphi) R_1(-\theta) R_3(\psi) \cdot \begin{bmatrix} X \\ Y \\ Z \end{bmatrix} = G_T \begin{bmatrix} X \\ Y \\ Z \end{bmatrix} \quad (3.22.1)$$

In this section, Euler's dynamic equations are transformed into second order differential equations of the Eulerian angles of the Moon. The first step in the transformation of Euler's dynamic equations is made by rotating the time derivatives of the Eulerian angles ( $\dot{\varphi}$ ,  $\dot{\psi}$ ,  $\dot{\theta}$ ) into the x y z system. The resulting components are equivalent to the rotational velocities of the Moon about the x,y,z, axes (see Figure 3.1).

$$\begin{bmatrix} \omega_x \\ \omega_y \\ \omega_z \end{bmatrix} = R_3(\varphi) R_1(\theta) \cdot \begin{bmatrix} -\dot{\theta} \\ 0 \\ \dot{\psi} \end{bmatrix} + \begin{bmatrix} 0 \\ 0 \\ \dot{\varphi} \end{bmatrix} =$$

$$= \begin{bmatrix} 0 & -\sin\varphi \sin\theta & -\cos\varphi \\ 0 & -\cos\varphi \sin\theta & \sin\varphi \\ 1 & \cos\theta & 0 \end{bmatrix} \cdot \begin{bmatrix} \dot{\varphi} \\ \dot{\psi} \\ \dot{\theta} \end{bmatrix} \quad (3.22.2)$$

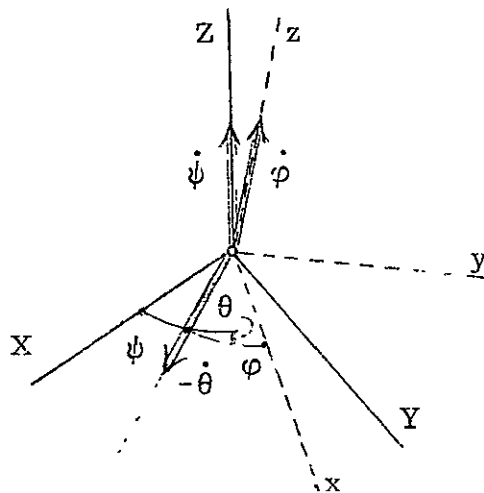


Figure 3.1 Euler's Geometric Equations Diagram

These equations are known as Euler's geometric equations. The implicit assumption made in deriving them is that the vector  $\vec{\omega}$  represents the total rotational motion of the Moon, i.e., that the X Y Z system is motionless (inertial). The equations developed in section 3.21 and in particular the relation between the rate of angular momentum and moments of external forces hold for a XYZ system which is inertial in the Newtonian sense. Traditionally, the motion of the MOD ecliptic system has been neglected because of the small magnitudes involved and mainly because of difficulties in obtaining an analytical solution of Euler's dynamic equations.

If the MOD ecliptic system has a rotational motion of its own with respect to the Newtonian Reference Frame, denoted as  $\vec{e}$ , the total rotational motion of the Moon will be the sum of the two motions, i.e.,  $\vec{\omega} + \vec{e}$ . As stated above, in order to keep the approximations to a minimum, the implication of the motion of the MOD ecliptic coordinate system in transforming and solving Euler's dynamic equations is analysed.

There is, of course, the possibility to relate the x y z system to another coordinate system like the mean equatorial system of 1950.0. However, as it is shown in section 3.23 there are considerable advantages in using the mean ecliptic as the reference system, mainly due to the Cassini laws.

The motion of the MOD ecliptic coordinate system consists of slow rotation of the plane XY (the plane of the ecliptic) by rotational velocity  $\pi$  about an axis contained in the plane of the ecliptic at longitude  $\Pi$ , and a comparatively fast rotation about the Z axis by the rate  $-p$  (regression of the vernal equinox), (see Figure 3.2).

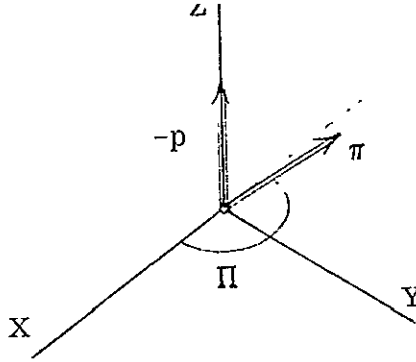


Figure 3.2 Motion of the MOD Ecliptic Coordinate System

The expressions for  $\Pi$ ,  $\pi$  and  $p$  as a function of time given by Newcomb are as follows [Mueller, 1969]:

$$\Pi = 173^\circ 57'.06 + 54'.77 \cdot t$$

$$\pi = 0'.4711 - 0'.0007 \cdot t$$

$$p = 50'.2564 + 0'.222 \cdot t$$

where

$t$  is in tropical centuries since 1900.

$\pi$  and  $p$  are annual motions.

The components of the rotational velocity vector of the MOD ecliptic system  $\vec{e}$  along the X, Y, Z axes, denoted by  $e_x$ ,  $e_y$ ,  $e_z$  are as follows:

$$\begin{bmatrix} e_x \\ e_y \\ e_z \end{bmatrix} = R_3(-\Pi) \begin{bmatrix} \pi \\ 0 \\ 0 \end{bmatrix} + \begin{bmatrix} 0 \\ 0 \\ -p \end{bmatrix} = \begin{bmatrix} \pi \cos \Pi \\ \pi \sin \Pi \\ -p \end{bmatrix}$$

Euler's geometric equations extended now to include the vector  $\vec{e}$ , are

$$\begin{bmatrix} \dot{\omega}_x \\ \dot{\omega}_y \\ \dot{\omega}_z \end{bmatrix} = R_3(\varphi) \cdot R_1(-\theta) \left( \begin{bmatrix} -\dot{\theta} \\ 0 \\ \dot{\psi} \end{bmatrix} + R_3(\psi) \cdot \begin{bmatrix} e_x \\ e_y \\ e_z \end{bmatrix} \right) + \begin{bmatrix} 0 \\ 0 \\ \dot{\varphi} \end{bmatrix} \quad (3.22.3)$$

Euler's geometric equations differentiated with respect to time, where  $\vec{e}$  is regarded as time invariant, are

$$\begin{bmatrix} \dot{\omega}_x \\ \dot{\omega}_y \\ \dot{\omega}_z \end{bmatrix} = \left[ \frac{\partial R_3(\varphi)}{\partial \varphi} \cdot \dot{\varphi} \cdot R_1(-\theta) + R_3(\varphi) \cdot \frac{\partial R_1(-\theta)}{\partial \theta} \cdot \dot{\theta} \right] \cdot \left( \begin{bmatrix} -\dot{\theta} \\ 0 \\ \dot{\psi} \end{bmatrix} + R_3(\psi) \cdot \begin{bmatrix} e_x \\ e_y \\ e_z \end{bmatrix} \right)$$

$$+ R_3(\varphi) \cdot R_1(-\theta) \cdot \begin{bmatrix} -\ddot{\theta} \\ 0 \\ \ddot{\psi} \end{bmatrix} + \begin{bmatrix} 0 \\ 0 \\ \ddot{\varphi} \end{bmatrix} + R_3(\varphi) \cdot R_1(-\theta) \cdot \frac{\partial R_3(\psi)}{\partial \psi} \cdot \dot{\psi} \cdot \begin{bmatrix} e_x \\ e_y \\ e_z \end{bmatrix} \quad (3.22.4)$$

The terms containing  $\ddot{\varphi}$ ,  $\ddot{\psi}$ ,  $\ddot{\theta}$  are developed further as follows:

$$R_3(\varphi) \cdot R_1(-\theta) \cdot \begin{bmatrix} -\ddot{\theta} \\ 0 \\ \ddot{\psi} \end{bmatrix} + \begin{bmatrix} 0 \\ 0 \\ \ddot{\varphi} \end{bmatrix} = \begin{bmatrix} 0 & -\sin\varphi\sin\theta & -\cos\varphi \\ 0 & -\cos\varphi\sin\theta & \sin\varphi \\ 1 & \cos\theta & 0 \end{bmatrix} \cdot \begin{bmatrix} \ddot{\varphi} \\ \ddot{\psi} \\ \ddot{\theta} \end{bmatrix} = W \cdot \begin{bmatrix} \ddot{\varphi} \\ \ddot{\psi} \\ \ddot{\theta} \end{bmatrix}$$

The inverse of W obtained analytically is:

$$-W^{-1} = \begin{bmatrix} \sin\varphi\cot\theta & \cos\varphi\cot\theta & 1 \\ -\sin\varphi\csc\theta & -\cos\varphi\csc\theta & 0 \\ -\cos\varphi & \sin\varphi & 0 \end{bmatrix} \quad (3.22.5)$$

The expressions for  $\begin{bmatrix} \dot{\omega}_x \\ \dot{\omega}_y \\ \dot{\omega}_z \end{bmatrix}$  from Equation 3.22.4

are substituted in Euler's dynamic equations (3.21.16). All the terms in  $[\dot{\omega}_x, \dot{\omega}_y, \dot{\omega}_z]^T$  except the ones containing  $[\ddot{\varphi}, \ddot{\psi}, \ddot{\theta}]^T$  are transposed to the right hand side. Then both sides are premultiplied by  $W^{-1}$  and result in

$$\begin{aligned}
\begin{bmatrix} \ddot{\phi} \\ \ddot{\psi} \\ \ddot{\theta} \end{bmatrix} &= W^1 \cdot \left\langle \begin{bmatrix} \alpha & 0 & 0 \\ 0 & -\beta & 0 \\ 0 & 0 & \gamma \end{bmatrix} \cdot \left( \frac{3k_E^2 E}{r_E^5} \cdot \begin{bmatrix} yz \\ xz \\ xy \end{bmatrix}_E + \frac{3k_S^2 S}{r_S^5} \cdot \begin{bmatrix} yz \\ xz \\ xy \end{bmatrix}_S - \begin{bmatrix} \omega_y & \omega_z \\ \omega_x & \omega_z \\ \omega_x & \omega_y \end{bmatrix} \right) \right. \\
&\quad - \left[ \frac{\partial R_3(\varphi)}{\partial \varphi} \cdot R_1(-\theta) \cdot \dot{\phi} + R_3(\varphi) \cdot \frac{\partial R_1(-\theta)}{\partial \theta} \cdot \dot{\theta} \right] \cdot \left( \begin{bmatrix} -\dot{\theta} \\ 0 \\ \dot{\psi} \end{bmatrix} + R_3(\psi) \cdot \begin{bmatrix} e_x \\ e_y \\ e_z \end{bmatrix} \right) \\
&\quad - R_3(\varphi) \cdot R_1(-\theta) \cdot \frac{\partial R_3(\psi)}{\partial \psi} \cdot \dot{\psi} \cdot \begin{bmatrix} e_x \\ e_y \\ e_z \end{bmatrix} \rangle \quad (3.22.6)
\end{aligned}$$

In the above equations the vector  $\begin{bmatrix} \omega_y & \omega_z \\ \omega_x & \omega_z \\ \omega_x & \omega_y \end{bmatrix}$  is expressed in terms of  $\varphi, \psi, \theta, \dot{\phi}, \dot{\psi}, \dot{\theta}$  through equation (3.22.3).

The only quantities that have not been treated yet are the selenodetic position of the Earth  $\begin{bmatrix} x \\ y \\ z \end{bmatrix}_E$  and that of the Sun  $\begin{bmatrix} x \\ y \\ z \end{bmatrix}_S$ .

The geocentric ephemeris of the Moon and of the Sun can be obtained from the DE-69 ephemeris in the mean equatorial (mean equator and equinox) coordinate system of 1950.0. The transformation from this 1950.0 system to the MOD ecliptic coordinate system can be performed through a series of rotations through the precession angles  $z, \zeta_0, \theta$  and through the obliquity of the ecliptic angle  $\epsilon$  [Mueller, 1969]. (In this paragraph,  $\theta$  is different from the Eulerian angle  $\theta$ ). The transformation is carried out as follows:

$$\begin{bmatrix} X \\ Y \\ Z \end{bmatrix} = R_1(\epsilon) R_3(-z) R_2(\theta) R_3(-\zeta_0) \cdot \begin{bmatrix} X \\ Y \\ Z \end{bmatrix}_{\alpha, \delta} = R_T \cdot \begin{bmatrix} X \\ Y \\ Z \end{bmatrix}_{\alpha, \delta}$$

where the subscripts  $\alpha$  and  $\delta$  denote the equatorial system of 1950.0 .

The selenocentric coordinates of the Earth mass center in any coordinate system are the same as the geocentric coordinates of the Moon, only with opposite signs. In the differential equations (3.22.6), the coordinates of the Earth appear always in products of two (xy, yz, xz), so changing the sign of all three coordinates does not make any difference in these products. Therefore, the ephemerides of the Moon can be used as given in DE-69 without reversing their sign. In a similar manner the selenocentric coordinates of the Sun are obtained as the differences between the geocentric coordinates of the Moon and those of the Sun.

The transformation from the MOD ecliptic system to the selenodetic coordinate system was shown to consist of three rotations (Equation 3.22.1). So combining the two transformations, the coordinates of the Earth or of the Sun in the selenodetic xyz system are obtained as follows:

$$\begin{bmatrix} x \\ y \\ z \end{bmatrix} = G_T R_T \begin{bmatrix} X \\ Y \\ Z \end{bmatrix}_{\alpha, \delta}$$

where

$G_T$  was defined in Equation (3.22.1)

and

$$R_T = R_3(\varphi) R_1(-\theta) R_3(\psi) .$$

This completes the transformation of Euler's dynamic equations (3.21.16) into the second order differential equations of the Eulerian orientation angles  $\varphi, \psi, \theta$  (3.22.6). The second derivatives of  $\varphi, \psi, \theta$  are expressed in (3.22.6) in terms of the angles  $\varphi, \psi, \theta$ , their first derivatives with respect to time, information from the DE-69 ephemeris and a number of constants ( $\alpha, \beta, \gamma$ , etc.).

The solution of equations (3.22.6) is possible using available computer subroutines for numerical integration of ordinary differential equations.

By analogy to the numerical integration of orbits of planets and satellites, the solution for the Eulerian angles  $\varphi, \psi, \theta$  obtained by the numerical integration of Equation (3.22.6) can be regarded as an integration of Cowell's type and, consequently, Equation (3.22.6) is referred in this study as Cowell's equations of motion of the Eulerian angles of the Moon.

### 3.23 Differential Equations of the Physical Libration Angles.

The equations of motion (3.22.6) as derived in section 3.22 can be integrated numerically and this was done successfully for a variety of initial epochs. There are, however, certain refinements of these equations which, without adding much labor in terms of computer programming, introduce definite improvements in the solution.

As in any numerical solution of differential equations, the number of "correct" significant digits in the integrated quantities is crucial. Correct is set in quotation marks as all the numerical integration subroutine can detect and take care of, are the local discretization and round off errors at each step of the integration. No reliable and general way of monitoring the cumulative effect of these errors exists. In textbooks and reports one is advised to experiment with functions which are close in nature to the actual differential equation and which have an analytical solution. One principle generally accepted in numerical integration is that the smaller the number of "correct" significant digits needed in the integrated quantities, the better the chances are of obtaining a solution without running into numerical problems or having to spend excessive computer time.

Long before electronic computers were available for numerical solution of differential equations Encke devised a modification of the "raw" equations such that in order to achieve the same absolute accuracy, fewer "correct" significant digits are required in the integration. Encke introduced a differential equation of a reference function which has an analytical solution

and is close in nature to the original [Brouwer and Clemence, 1961, p. 176] . The quantity integrated is then the difference between the two functions. If the reference is chosen close enough, the magnitude of the differences integrated is much smaller than the original function.

Encke's artifice is particularly applicable to Euler's dynamic equations in view of Cassini's laws for the rotation of the Moon. The mathematical interpretation of Cassini's laws is that the Eulerian angles can be approximated by power series of the independent argument (time). Actually these series are combinations of the elements of the mean orbit of the Moon around the geocenter as referred to the MOD ecliptic coordinate system. The implication of Cassini's laws is that the Eulerian angles  $\varphi, \psi, \theta$  and their first and second time derivatives can be presented as power series of time with known coefficients plus small periodic terms (perturbations). The main property of these perturbations of interest in this case is their small magnitude. For example, the perturbations in  $\varphi$  and in  $(\varphi + \psi - \pi)$  are of the order of two minutes of arc. Those in  $\psi$  can reach a magnitude of less than one degree.

Thus, after an appropriate modification is made, the quantities to be integrated numerically for the solution of Euler's dynamic equations are the small periodic perturbations in the following Eulerian angle combinations:

$$\varphi + \psi - \pi, \quad \psi \quad \text{and} \quad \theta$$

It is easily seen that these perturbations are the physical librations of the Moon as follows:

$$\begin{array}{l} \tau \\ \sigma \\ \rho \end{array} \left[ \begin{array}{l} \text{the physical} \\ \text{librations in} \end{array} \right. \left[ \begin{array}{l} \text{longitude} \\ \text{node} \\ \text{inclination} \end{array} \right] \text{ are equivalent to the } \left[ \begin{array}{l} \varphi + \psi - \pi \\ \psi \\ \theta \end{array} \right. \text{ perturbations in}$$

Unlike numerical integration of satellite trajectories where occasional rectifications of the Encke reference orbit are necessary in order to keep

the perturbations to the reference orbit small, in this case the reference Eulerian angles (the power series) are stable in the sense that the perturbations  $\tau, \sigma, \rho$  are composed solely of periodic terms of constant amplitude.

The two parameters of the mean lunar orbit needed to separate the physical libration angles from Euler's angles are the mean longitude  $L_D$  and the longitude of the node  $\Omega_D$ .

According to [AENA Supplement, 1961] and in general notation

$$\begin{aligned} L_D &= L_0 + L_1(T-T_0) + L_2(T-T_0)^2 + L_3(T-T_0)^3 \\ \Omega_D &= \Omega_0 + \Omega_1(T-T_0) + \Omega_2(T-T_0)^2 + \Omega_3(T-T_0)^3 \end{aligned} \quad (3.23.1)$$

where  $(T-T_0)$  is the time interval since the standard epoch  $T_0$ .

Through Cassini's laws and the definition of the physical libration angles, the Eulerian angles can be expressed as follows:

$$\begin{aligned} \varphi &= L_D + \pi - \psi + \tau \\ \psi &= \Omega_D + \sigma \\ \theta &= I_D + \rho \end{aligned} \quad (3.23.2)$$

where

$I_D$  is the mean inclination of the Moon's equator to the ecliptic.

From the above relations

$$\begin{aligned} L_D + \pi + \tau &= \varphi + \psi \\ \Omega_D + \sigma &= \psi \\ I_D + \rho &= \theta \end{aligned} \quad \text{or} \quad \begin{bmatrix} \tau \\ \sigma \\ \rho \end{bmatrix} = \begin{bmatrix} \varphi + \psi \\ \psi \\ \theta \end{bmatrix} - \begin{bmatrix} L_D + \pi \\ \Omega_D \\ I_D \end{bmatrix}$$

Differentiating with respect to time, it follows:

$$\begin{bmatrix} \dot{\tau} \\ \dot{\sigma} \\ \dot{\rho} \end{bmatrix} = \begin{bmatrix} \dot{\varphi} + \dot{\psi} \\ \dot{\psi} \\ \dot{\theta} \end{bmatrix} - \begin{bmatrix} \dot{L}_D \\ \dot{\Omega}_D \\ 0 \end{bmatrix}$$

A second differentiation yields

$$\begin{bmatrix} \ddot{\tau} \\ \ddot{\sigma} \\ \ddot{\rho} \end{bmatrix} = \begin{bmatrix} \ddot{\psi} + \ddot{\psi} \\ \ddot{\psi} \\ \ddot{\eta} \end{bmatrix} - \begin{bmatrix} \ddot{L}_D \\ \ddot{\Omega}_D \\ 0 \end{bmatrix}. \quad (3.23.3)$$

The derivatives of  $L_D$  and  $\Omega_D$  are obtained by formal differentiation of the power series with respect to time :

$$\dot{L}_D = L_1 + 2L_2(T-T_0) + 3L_3(T-T_0)^2,$$

$$\dot{\Omega}_D = \Omega_1 + 2\Omega_2(T-T_0) + 3\Omega_3(T-T_0)^2,$$

and

$$\ddot{L}_D = 2L_2 + 6L_3(T-T_0),$$

$$\ddot{\Omega}_D = 2\Omega_2 + 6\Omega_3(T-T_0).$$

This completes the transformation of Euler's dynamic equations from Cowell's form (3.22.6) as presented in section 3.22 to Encke's form (3.23.3). On the left side of the equations (3.23.3) are the second derivatives of the physical libration angles while on the right side there are rather complicated expressions which depend, however, on the angles  $\tau, \sigma, \rho, \dot{\tau}, \dot{\sigma}, \dot{\rho}$ , on power series with known fixed coefficients ( $L_D, \Omega_D$ ), on numerical information from the DE-69 ephemeris and on a number of physical constants ( $k^2 E, k^2 S, \alpha, \beta, \gamma$ , etc.) .

The only additional information needed to solve these equations by numerical integration are the values of  $\tau, \sigma, \rho, \dot{\tau}, \dot{\sigma}, \dot{\rho}$  at some arbitrary standard epoch, the initial values of the numerical integration. The only way these six values can be determined is through analysis of observations which are sensitive to the orientation of the Moon. In a sense these six quantities correspond to the six arbitrary constants in an analytical solution of the three second order differential equations.

### 3.3 Adjustment Theory

The differential equations (3.23.3) developed in section 3.23 and their solution depend on a number of parameters. The purpose of this section is to develop the adjustment theory for the least squares estimation of those parameters so as to provide the means for carrying out the general solution for a datum on the Moon as presented in Chapter 2.

The solution of the differential equations (3.23.3) is performed by numerical integration. In complete analogy to other situations in which differential equations of certain quantities are solved by numerical integration (satellite trajectories, planetary orbits, etc.), the parameterization of this problem is straightforward. The values of the integrated quantities at any intermediate epoch (between the initial and the final epochs of the integration) depend on two sets of parameters as follows:

- (i) The values of the quantities at the initial epoch - in this case, the initial values of the physical libration angles and their time rate, to be referred as initial values.
- (ii) A number of constants which appear explicitly or indirectly in the differential equations - in this case, physical constants associated with the gravitational field of the Moon, to be referred as physical constants.

These two sets of quantities have been chosen as the parameters which govern the solution for the physical librations. Through an adjustment process, these parameters can be estimated following known procedures (orbit determination of satellites from tracking data, for example).

In the following subsections, the general outline of the mathematical model designed to process data sensitive to the physical librations is presented. The derivations necessary for the generation of the so-called state transition and parameter sensitivity matrices are presented also in full detail.

### 3.31 Mathematical Model.

The mathematical model for the adjustment of observational data sensitive to the physical librations of the Moon follows in general ideas and procedures of Warner [1964] and notation as of Uotila [1967].

A general situation to be considered is that the data being processed are sensitive to the physical libration parameters (initial values and physical constants) and also to additional groups of parameters which are irrelevant to the physical librations phenomena. These will be referred as additional constants. The selenodetic coordinates of observed features on the surface of the Moon are an example of such a group of parameters.

For any of the quantities figuring in the mathematical model, the meaning of the superscripts is as follows:

$L^a$	represents	adjusted	quantities
$L^o$		approximate	
$L^b$		observed	
$L$		correction to observed or to approximate	

The quantities involved in the mathematical model are denoted as follows:

#### Parameters

#### Initial Values

$$= \begin{bmatrix} \tau_o \\ \sigma_o \\ \rho_o \\ \dot{\tau}_o \\ \dot{\sigma}_o \\ \dot{\rho}_o \end{bmatrix} ; \quad \gamma = \begin{bmatrix} \delta \tau_o \\ \delta \sigma_o \\ \delta \rho_o \\ \delta \dot{\tau}_o \\ \delta \dot{\sigma}_o \\ \delta \dot{\rho}_o \end{bmatrix} ; \quad \gamma^a = \gamma^o + \gamma$$

where

$\tau_0, \sigma_0, \rho_0$  are the initial values of the physical libration angles at the standard epoch  $T_0$ .

$\dot{\tau}_0, \dot{\sigma}_0, \dot{\rho}_0$  are the initial values of the time rates of the physical libration angles at  $T_0$ .

#### Physical Constants

$$\varphi^0 = \begin{bmatrix} C_{22} \\ \beta \\ C_{20} \end{bmatrix}; \quad \omega = \begin{bmatrix} \delta C_{22} \\ \delta \beta \\ \delta C_{20} \end{bmatrix}; \quad \varphi^a = \varphi^0 + \omega$$

where

$\left. \begin{matrix} C_{20} \\ C_{22} \end{matrix} \right\}$  are second degree harmonics of the gravitational field of the Moon.

$\beta = \frac{C-A}{B}$  is a ratio between the principal moments of inertia of the Moon.

There are other physical constants which figure in equations (3.23.3). However, their values are well known from other sources and it can be shown that the physical librations are insensitive to small variations in these constants. Another consideration against their inclusion in  $\varphi$  is in the fact that these constants have been estimated in the solution for the lunar ephemeris LE-16 [O'Handley, et al., 1969] and the ephemeris is treated here as fixed.

#### Additional Constants

$$\lambda^0 = \begin{bmatrix} \lambda_1 \\ \lambda_2 \\ \cdot \\ \cdot \\ \cdot \\ \lambda_k \end{bmatrix}; \quad \lambda = \begin{bmatrix} \delta \lambda_1 \\ \delta \lambda_2 \\ \cdot \\ \cdot \\ \delta \lambda_k \end{bmatrix}; \quad \lambda^a = \lambda^0 + \lambda$$

As specified above these are parameters which depend on the particular data type, but are irrelevant to the physical librations. They are left in general notation.

### Observations

$$L^b = \begin{bmatrix} L_1 \\ L_2 \\ \cdot \\ \cdot \\ \cdot \\ L_n \end{bmatrix}; \quad L \doteq \begin{bmatrix} \delta L_1 \\ \cdot \\ \cdot \\ \cdot \\ \cdot \\ \delta L_n \end{bmatrix}; \quad L^a = L^b + L$$

### Covariance Matrices

(a priori statistics of  $L^b, \gamma^o, \varphi^o, \lambda^o$ )

$\Sigma_{L^b}$  - observed quantities

$\Sigma_{\gamma^o}$  - initial values

$\Sigma_{\varphi^o}$  - physical constants

$\Sigma_{\lambda^o}$  - additional constants

The mathematical model is defined as the function F

$$F(L^a, \gamma^a, \varphi^a, \lambda^a) = 0 \tag{3.31.1}$$

The function F is linearized under the assumption that  $L, \gamma, \varphi, \lambda$ , are vectors composed of small quantities so that the second degree terms in Taylor's expansion of F can be neglected.

$$\frac{\partial F}{\partial L^a} \cdot L + \frac{\partial F}{\partial \gamma^a} \cdot \gamma + \frac{\partial F}{\partial \varphi^a} \cdot \varphi + \frac{\partial F}{\partial \lambda^a} \cdot \lambda + F^0 = 0 \quad (3.31.2)$$

where

$$F^0 = F(L^b, \gamma^0, \varphi^0, \lambda^0) \quad .$$

The expressions  $\frac{\partial F}{\partial \gamma^a}$  and  $\frac{\partial F}{\partial \varphi^a}$  are developed further in keeping with the nature of the numerical integration process.

$$\frac{\partial F}{\partial \gamma^a} = \frac{\partial F}{\partial [\tau \ \sigma \ \rho \ \dot{\tau} \ \dot{\sigma} \ \dot{\rho}]^T} \cdot \frac{\partial [\tau \ \sigma \ \rho \ \dot{\tau} \ \dot{\sigma} \ \dot{\rho}]^T}{\partial \gamma^a} = A_{PL} \cdot U$$

$$\frac{\partial F}{\partial \varphi^a} = A_{PL} \cdot \frac{\partial [\tau \ \sigma \ \rho \ \dot{\tau} \ \dot{\sigma} \ \dot{\rho}]^T}{\partial \varphi^a} = A_{PL} \cdot Q$$

where

$$A_{PL} = \frac{\partial F}{\partial [\tau \ \sigma \ \rho \ \dot{\tau} \ \dot{\sigma} \ \dot{\rho}]^T}$$

$$U = \frac{\partial [\tau \ \sigma \ \rho \ \dot{\tau} \ \dot{\sigma} \ \dot{\rho}]^T}{\partial \gamma^a}$$

$$Q = \frac{\partial [\tau \ \sigma \ \rho \ \dot{\tau} \ \dot{\sigma} \ \dot{\rho}]^T}{\partial \varphi^a}$$

In the literature U is referred to as the state transition matrix and Q as the parameters sensitivity matrix.

Denoting B for  $\frac{\partial F}{\partial L^a}$  and C for  $\frac{\partial F}{\partial \lambda^a}$  the linearized mathematical model is written as follows:

$$B \cdot L + A_{PL}(U\gamma + Q\varphi) + C \cdot \lambda + F^0 = 0 \quad (3.31.3)$$

Least squares adjustment is applied under the assumption that  $L^b$  is a vector of random quantities with mean  $L^{\mu}$  and variance and covariance matrix  $\Sigma_{\mu}$ .

The well known procedure will result in estimates for the parameters and their variance covariance matrix obtained through the minimization of the function  $\xi$  ( $\xi = L^T \Sigma_L^{-1} L$ ) and in keeping with the constraints imposed by the a priori statistics of the parameters ( $\Sigma_{\gamma^o}, \Sigma_{\varphi^o}, \Sigma_{\lambda^o}$ ).

The matrices B,  $A_{pL}$ , C, and  $F^o$  depend on the particular data type processed while the matrices U and Q are general for all observational types and depend solely on the numerical integration of the physical libration angles. All partial derivatives matrices are evaluated for  $L^b, \gamma^o, \varphi^o, \lambda^o$ .

### 3.32 State Transition and Parameter Sensitivity Matrices.

The state transition and the parameters sensitivity matrices were defined in section 3.31 as

$$U = \frac{\partial [\tau \sigma \rho \dot{\tau} \dot{\sigma} \dot{\rho}]^T}{\partial \gamma^a}$$

and

$$Q = \frac{\partial [\tau \sigma \rho \dot{\tau} \dot{\sigma} \dot{\rho}]^T}{\partial \varphi^a}$$

where

$$\gamma^a = [\tau_o \sigma_o \rho_o \dot{\tau}_o \dot{\sigma}_o \dot{\rho}_o]^T$$

and

$$\varphi^a = [C_{22} \beta C_{20}]^T$$

The only mathematical expressions that relate indirectly the quantities  $[\tau, \sigma, \rho, \dot{\tau}, \dot{\sigma}, \dot{\rho}]$  at a particular epoch to the vectors  $\gamma^a$  and  $\varphi^a$  are the second order differential equations (3.23.3) derived in section 3.23. Of the many methods known for the formation of the matrices U and Q [Escobal, 1965] the one presented by Anderson [1964] will be used as a basis for the developments in this section. In denoting differentiation with respect to  $\gamma^a$  and  $\varphi^a$  the superscript  $^a$  will be omitted hereafter.

The following vectors are defined:

$$\xi = \begin{bmatrix} \tau \\ \sigma \\ \rho \end{bmatrix}; \quad \dot{\xi} = \begin{bmatrix} \dot{\tau} \\ \dot{\sigma} \\ \dot{\rho} \end{bmatrix}; \quad \ddot{\xi} = \begin{bmatrix} \ddot{\tau} \\ \ddot{\sigma} \\ \ddot{\rho} \end{bmatrix}$$

Equations (3.23.3) and the U and Q matrices can be written in the new notation as follows:

$$\begin{bmatrix} \dot{\xi} \\ \ddot{\xi} \end{bmatrix} = \begin{bmatrix} \dot{\xi}(\xi, \dot{\xi}, \varphi) \\ \ddot{\xi}(\xi, \dot{\xi}, \varphi) \end{bmatrix}$$

$$U = \frac{\partial \begin{bmatrix} \xi \\ \dot{\xi} \end{bmatrix}}{\partial \gamma} \quad (3.32.1)$$

$$Q = \frac{\partial \begin{bmatrix} \xi \\ \dot{\xi} \end{bmatrix}}{\partial \varphi} \quad (3.32.2)$$

From the discussion on the nature of the numerical integration process in section 3.31, the following variational equation can be written:

$$\delta \begin{bmatrix} \dot{\xi} \\ \ddot{\xi} \end{bmatrix} = \frac{\partial \begin{bmatrix} \dot{\xi} \\ \ddot{\xi} \end{bmatrix}}{\partial \begin{bmatrix} \xi \\ \dot{\xi} \end{bmatrix}} \cdot \delta \begin{bmatrix} \xi \\ \dot{\xi} \end{bmatrix} + \frac{\partial \begin{bmatrix} \dot{\xi} \\ \ddot{\xi} \end{bmatrix}}{\partial \varphi} \cdot \delta \varphi = \Theta \cdot \delta \begin{bmatrix} \xi \\ \dot{\xi} \end{bmatrix} + \Phi \cdot \delta \varphi \quad (3.32.3)$$

The variation in  $[\xi^T \dot{\xi}^T]^T$  is developed in terms of  $\delta \gamma$  and  $\delta \varphi$ .

$$\delta \begin{bmatrix} \xi \\ \dot{\xi} \end{bmatrix} = \frac{\partial \begin{bmatrix} \xi \\ \dot{\xi} \end{bmatrix}}{\partial \gamma} \cdot \delta \gamma + \frac{\partial \begin{bmatrix} \xi \\ \dot{\xi} \end{bmatrix}}{\partial \varphi} \delta \varphi = U \cdot \delta \gamma + Q \cdot \delta \varphi \quad (3.32.4)$$

Substituting equation (3.32.4) in equation (3.32.3), it follows:

$$\delta \begin{bmatrix} \dot{\xi} \\ \ddot{\xi} \end{bmatrix} = \Theta \cdot U \cdot \delta \gamma + (\Theta \cdot Q + \Phi) \cdot \delta \varphi \quad (3.32.5)$$

But the variation in  $\begin{bmatrix} \dot{\xi} \\ \ddot{\xi} \\ \xi \end{bmatrix}$  can be obtained also by differentiation with respect to time of  $\delta \begin{bmatrix} \dot{\xi} \\ \ddot{\xi} \\ \xi \end{bmatrix}$  which yields

$$\delta \begin{bmatrix} \dot{\xi} \\ \ddot{\xi} \\ \xi \end{bmatrix} = \dot{U} \cdot \delta \gamma + \dot{Q} \cdot \delta \varphi \quad (3.32.6)$$

A variational equation holds for an arbitrary variation in the independent variables so the coefficients in front of  $\delta \gamma$  and  $\delta \varphi$  can be equated one by one. Two first-order differential equations are the result of this operation:

$$\begin{aligned} \dot{U} &= \Theta \cdot U \\ \dot{Q} &= \Theta \cdot Q + \Phi \end{aligned} \quad (3.32.7)$$

Solution of these two sets of differential equations can provide the two matrices  $U$  and  $Q$ . So the problem narrows to the derivation of expressions for the matrices  $\Theta$  and  $\Phi$ , which then can be used to integrate numerically the equations  $\dot{U}$  and  $\dot{Q}$  and result in the determination of the matrices  $U$  and  $Q$  along with the integration of the physical libration angles ( $\xi$ ). The  $\Theta$  and  $\Phi$  have been defined as follows:

$$\Theta = \frac{\partial \begin{bmatrix} \dot{\xi} \\ \ddot{\xi} \\ \xi \end{bmatrix}}{\partial \begin{bmatrix} \dot{\xi} \\ \ddot{\xi} \\ \xi \end{bmatrix}} = \begin{bmatrix} 0 & I \\ \frac{\partial \ddot{\xi}}{\partial \dot{\xi}} & \frac{\partial \ddot{\xi}}{\partial \ddot{\xi}} \end{bmatrix} ; \quad \Phi = \frac{\partial \begin{bmatrix} \dot{\xi} \\ \ddot{\xi} \\ \xi \end{bmatrix}}{\partial \varphi} = \begin{bmatrix} 0 \\ \frac{\partial \ddot{\xi}}{\partial \varphi} \end{bmatrix}$$

Euler's dynamic equations (3.22.6) were formulated for  $[\varphi \psi \theta]$  rather than for  $[\tau \sigma \rho]$  and also the quantities  $[\alpha \beta \gamma]$  rather than  $[C_{22} \beta C_{20}]$  appear in the expressions. So the chain rule for partial differentiation is employed as follows:

$$\frac{\begin{bmatrix} \ddot{\tau} \\ \ddot{\sigma} \\ \ddot{\rho} \end{bmatrix}}{\begin{bmatrix} \tau \\ \sigma \\ \rho \end{bmatrix}} = \frac{\begin{bmatrix} \ddot{\tau} \\ \ddot{\sigma} \\ \ddot{\rho} \end{bmatrix}}{\begin{bmatrix} \dot{\phi} \\ \dot{\psi} \\ \dot{\theta} \end{bmatrix}} \cdot \frac{\begin{bmatrix} \ddot{\phi} \\ \ddot{\psi} \\ \ddot{\theta} \end{bmatrix}}{\begin{bmatrix} \phi \\ \psi \\ \theta \end{bmatrix}} \cdot \frac{\begin{bmatrix} \dot{\phi} \\ \dot{\psi} \\ \dot{\theta} \end{bmatrix}}{\begin{bmatrix} \tau \\ \sigma \\ \rho \end{bmatrix}} \quad (3.32.8)$$

$$\frac{\begin{bmatrix} \ddot{\tau} \\ \ddot{\sigma} \\ \ddot{\rho} \end{bmatrix}}{\begin{bmatrix} \tau \\ \dot{\sigma} \\ \dot{\rho} \end{bmatrix}} = \frac{\begin{bmatrix} \ddot{\tau} \\ \ddot{\sigma} \\ \ddot{\rho} \end{bmatrix}}{\begin{bmatrix} \dot{\phi} \\ \dot{\psi} \\ \dot{\theta} \end{bmatrix}} \cdot \frac{\begin{bmatrix} \ddot{\phi} \\ \ddot{\psi} \\ \ddot{\theta} \end{bmatrix}}{\begin{bmatrix} \dot{\phi} \\ \dot{\psi} \\ \dot{\theta} \end{bmatrix}} \cdot \frac{\begin{bmatrix} \dot{\phi} \\ \dot{\psi} \\ \dot{\theta} \end{bmatrix}}{\begin{bmatrix} \tau \\ \dot{\sigma} \\ \dot{\rho} \end{bmatrix}} \quad (3.32.9)$$

$$\frac{\begin{bmatrix} \ddot{\tau} \\ \ddot{\sigma} \\ \ddot{\rho} \end{bmatrix}}{\begin{bmatrix} C_{22} \\ \beta \\ C_{20} \end{bmatrix}} = \frac{\begin{bmatrix} \ddot{\tau} \\ \ddot{\sigma} \\ \ddot{\rho} \end{bmatrix}}{\begin{bmatrix} \dot{\phi} \\ \dot{\psi} \\ \dot{\theta} \end{bmatrix}} \cdot \frac{\begin{bmatrix} \ddot{\phi} \\ \ddot{\psi} \\ \ddot{\theta} \end{bmatrix}}{\begin{bmatrix} \alpha \\ \beta \\ \gamma \end{bmatrix}} \cdot \frac{\begin{bmatrix} \alpha \\ \beta \\ \gamma \end{bmatrix}}{\begin{bmatrix} C_{22} \\ \beta \\ C_{20} \end{bmatrix}} \quad (3.32.10)$$

The functional relationship between  $[\phi \psi \theta]$  and  $[\tau \sigma \rho]$  is stated again:

$$\begin{bmatrix} \phi \\ \psi \\ \theta \end{bmatrix} = \begin{bmatrix} \tau - \sigma + L_D + \pi - \Omega_D \\ \sigma + \Omega_D \\ \rho + I_D \end{bmatrix} \quad (3.32.11)$$

Equations (3.32.11) are differentiated with respect to time and yield

$$\begin{bmatrix} \dot{\phi} \\ \dot{\psi} \\ \dot{\theta} \end{bmatrix} = \begin{bmatrix} \dot{\tau} - \dot{\sigma} + \dot{L}_D - \dot{\Omega}_D \\ \dot{\sigma} + \dot{\Omega}_D \\ \dot{\rho} \end{bmatrix} \quad (3.32.12)$$

The inverse relationship is derived from equation (3.32.12) and is differentiated once more

$$\begin{bmatrix} \ddot{\tau} \\ \ddot{\sigma} \\ \ddot{\rho} \end{bmatrix} = \begin{bmatrix} \ddot{\varphi} + \ddot{\psi} - \ddot{L}_D \\ \ddot{\psi} - \ddot{\Omega}_D \\ \ddot{\theta} \end{bmatrix} \quad (3.32.13)$$

Now the partial differentiation of  $[\ddot{\tau} \ \ddot{\sigma} \ \ddot{\rho}]^T$  with respect to  $[\ddot{\varphi} \ \ddot{\psi} \ \ddot{\theta}]^T$  can be performed easily:

$$\frac{\partial \begin{bmatrix} \ddot{\tau} \\ \ddot{\sigma} \\ \ddot{\rho} \end{bmatrix}}{\partial \begin{bmatrix} \ddot{\varphi} \\ \ddot{\psi} \\ \ddot{\theta} \end{bmatrix}} = \begin{bmatrix} 1 & 1 & 0 \\ 0 & 1 & 0 \\ 0 & 0 & 1 \end{bmatrix} \quad (3.32.14)$$

From equations(3.32.11) and (3.32.12) it follows:

$$\frac{\partial \begin{bmatrix} \varphi \\ \psi \\ \theta \end{bmatrix}}{\partial \begin{bmatrix} \tau \\ \sigma \\ \rho \end{bmatrix}} = \frac{\partial \begin{bmatrix} \dot{\varphi} \\ \dot{\psi} \\ \dot{\theta} \end{bmatrix}}{\partial \begin{bmatrix} \dot{\tau} \\ \dot{\sigma} \\ \dot{\rho} \end{bmatrix}} = \begin{bmatrix} 1 & -1 & 0 \\ 0 & 1 & 0 \\ 0 & 0 & 1 \end{bmatrix} \quad (3.32.15)$$

From Appendix A and substituting A,B,C in the expressions for  $\alpha, \beta, \gamma$  it follows

$$\begin{aligned} \alpha &= \frac{\beta \cdot (C_{20} + 2 C_{22})}{C_{20} - (2 - 4\beta) \cdot C_{22}} \\ \beta &= \beta \\ \gamma &= \frac{-4\beta C_{22}}{(1 + \beta) \cdot C_{20} - (2 - 2\beta) \cdot C_{22}} \end{aligned} \quad (3.32.16)$$

The squared denominators are defined as auxiliary quantities  $D_1$  and  $D_2$

$$D_1 = [C_{20} - (2 - 4\beta) \cdot C_{22}]^2$$

$$D_2 = [(1 + \beta) \cdot C_{20} - (2 - 2\beta) \cdot C_{22}]^2$$

Differentiating equations (3.32.16) and simplifying the results

$$\frac{\partial \begin{bmatrix} \alpha \\ \beta \\ \gamma \end{bmatrix}}{\partial \begin{bmatrix} C_{22} \\ \beta \\ C_{20} \end{bmatrix}} = \begin{bmatrix} \frac{4\beta(1-\beta) \cdot C_{20}}{D_1} & \frac{C_{20}^2 - 4C_{22}^2}{D_1} & \frac{-4\beta \cdot (1-\beta) \cdot C_{22}}{D_1} \\ 0 & 1 & 0 \\ \frac{-4\beta \cdot (1+\beta) \cdot C_{20}}{D_2} & \frac{-4C_{22} \cdot (C_{20} - 2C_{22})}{D_2} & \frac{4\beta \cdot (1+\beta) \cdot C_{22}}{D_2} \end{bmatrix} \quad (3.32.17)$$

It should be pointed out that the  $\alpha$ ,  $\beta$ ,  $\gamma$  ratios are not independent from each other. They are related by the equation

$$\alpha - \beta + \gamma - \alpha\beta\gamma = 0 \quad (3.32.18)$$

For this reason, the matrix of partials (3.32.17) is of rank two.

Appropriate measures will be taken in the adjustment to avoid singularity.

Equations (3.22.3) and 3.22.6) as derived in section 3.22 are rewritten as a starting point in deriving the three remaining partial derivatives matrices:

$$\frac{\partial \begin{bmatrix} \ddot{\phi} \\ \ddot{\psi} \\ \ddot{\theta} \end{bmatrix}}{\partial \begin{bmatrix} \alpha \\ \beta \\ \gamma \end{bmatrix}} ; \quad \frac{\partial \begin{bmatrix} \ddot{\phi} \\ \ddot{\psi} \\ \ddot{\theta} \end{bmatrix}}{\partial \begin{bmatrix} \dot{\phi} \\ \dot{\psi} \\ \dot{\theta} \end{bmatrix}} ; \quad \frac{\partial \begin{bmatrix} \ddot{\phi} \\ \ddot{\psi} \\ \ddot{\theta} \end{bmatrix}}{\partial \begin{bmatrix} \phi \\ \psi \\ \theta \end{bmatrix}}$$

$$\begin{aligned}
\begin{bmatrix} \ddot{\phi} \\ \dot{\psi} \\ \dot{\theta} \end{bmatrix} &= W^{-1} \left( \begin{bmatrix} \alpha & 0 & 0 \\ 0 & -\beta & 0 \\ 0 & 0 & \gamma \end{bmatrix} \left\langle \frac{3k^2 E}{r_E^5} \begin{bmatrix} yz \\ xz \\ xy \end{bmatrix}_E + \frac{3k^2 E}{r_s^5} \begin{bmatrix} yz \\ xz \\ xy \end{bmatrix}_s - \begin{bmatrix} \omega_2 & \omega_3 \\ \omega_1 & \omega_3 \\ \omega_1 & \omega_2 \end{bmatrix} \right\rangle \right. \\
&- \left[ \frac{\partial R_2(\varphi)}{\partial \varphi} \cdot R_1(-\theta) \cdot \dot{\phi} + R_3(\varphi) \cdot \frac{\partial R_1(-\theta)}{\partial \theta} \cdot \dot{\theta} \right] \cdot \left\langle \begin{bmatrix} -\dot{\theta} \\ 0 \\ \dot{\psi} \end{bmatrix} + R_3(\psi) \begin{bmatrix} e_x \\ e_y \\ e_z \end{bmatrix} \right\rangle \\
&- \left. R_3(\varphi) \cdot R_1(-\theta) \cdot \frac{\partial R_3(\psi)}{\partial \psi} \cdot \dot{\psi} \cdot \begin{bmatrix} e_x \\ e_y \\ e_z \end{bmatrix} \right) \quad (3.22.6)
\end{aligned}$$

$$\begin{bmatrix} \omega_1 \\ \omega_2 \\ \omega_3 \end{bmatrix} = R_3(\varphi) \cdot R_1(-\theta) \left( \begin{bmatrix} -\dot{\theta} \\ 0 \\ \dot{\psi} \end{bmatrix} + R_3(\psi) \cdot \begin{bmatrix} e_x \\ e_y \\ e_z \end{bmatrix} \right) + \begin{bmatrix} 0 \\ 0 \\ \dot{\phi} \end{bmatrix} \quad (3.22.3)$$

From section 3.22, the following relations hold:

$$\begin{bmatrix} x \\ y \\ z \end{bmatrix}_E = M \cdot \begin{bmatrix} X \\ Y \\ Z \end{bmatrix}_E ; \quad \begin{bmatrix} x \\ y \\ z \end{bmatrix}_s = M \cdot \begin{bmatrix} X \\ Y \\ Z \end{bmatrix}_s$$

where

$$M = R_3(\varphi) \cdot R_1(-\theta) \cdot R_3(\psi)$$

The matrix  $W^{-1}$  was derived in section 3.22 as follows:

$$W^{-1} = \begin{bmatrix} \sin \varphi \cot \theta & \cos \varphi \cot \theta & 1 \\ -\sin \varphi \csc \theta & -\cos \varphi \csc \theta & 0 \\ -\cos \varphi & \sin \varphi & 0 \end{bmatrix} \quad (3.22.5)$$

Euler's dynamic equations are written again substituting auxiliary vectors  $T_A$ ,  $T_B$ ,  $T_C$ , and  $T_D$

$$\begin{bmatrix} \ddot{\phi} \\ \ddot{\psi} \\ \ddot{\theta} \end{bmatrix} = W^{-1} \cdot T_D \quad ; \quad T_D = \begin{bmatrix} \alpha & 0 & 0 \\ 0 & \beta & 0 \\ 0 & 0 & \gamma \end{bmatrix} \cdot T_A - T_B P_0 - T_C \quad (3.32.19)$$

where

$$T_A = \frac{3k^2 E}{r_E^5} \cdot \begin{bmatrix} yz \\ -xz \\ xy \end{bmatrix}_E + \frac{3k^2 S}{r_S^5} \cdot \begin{bmatrix} yz \\ -xz \\ xy \end{bmatrix}_S - \begin{bmatrix} \omega_2 & \cdot & \omega_3 \\ -\omega_1 & \cdot & \omega_3 \\ \omega_1 & \cdot & \omega_2 \end{bmatrix} \quad (3.32.20)$$

$$T_B = L_3^c \cdot R_3(\varphi) \cdot R_1(-\theta) \cdot \dot{\phi} - R_3(\varphi) \cdot R_1(-\theta) \cdot L_1^c \cdot \dot{\theta} \quad (3.32.21)$$

(For differentiating rotation matrices, see Appendix E)

$$P_0 = \begin{bmatrix} -\dot{\theta} \\ 0 \\ \dot{\psi} \end{bmatrix} + R_3(\psi) \cdot \begin{bmatrix} e_x \\ e_y \\ e_z \end{bmatrix} \quad (3.32.22)$$

$$T_C = M \cdot L_3 \cdot \dot{\psi} \begin{bmatrix} e_x \\ e_y \\ e_z \end{bmatrix} \quad (3.32.23)$$

A series of intermediate differentiations are performed

$$\frac{\partial [x \ y \ z]^T}{\partial [\varphi \ \psi \ \theta]^T} = \begin{bmatrix} L_3 \cdot M \cdot \begin{bmatrix} X \\ Y \\ Z \end{bmatrix} \\ \vdots \\ M \cdot L_3 \cdot \begin{bmatrix} X \\ Y \\ Z \end{bmatrix} \end{bmatrix} \cdot \begin{bmatrix} X \\ Y \\ Z \end{bmatrix} \cdot \begin{bmatrix} -R_3(\varphi) \cdot R_1(-\theta) \cdot L_1 \cdot R_3(\psi) \cdot \begin{bmatrix} X \\ Y \\ Z \end{bmatrix} \end{bmatrix} = \begin{bmatrix} C_1 \\ C_2 \\ C_3 \end{bmatrix}$$

Two  $3 \times 3$  matrices are evaluated; one for the Earth  $\begin{bmatrix} C_1 \\ C_2 \\ C_3 \end{bmatrix}_e$  and another for the Sun  $\begin{bmatrix} C_1 \\ C_2 \\ C_3 \end{bmatrix}_s$

$$\frac{\partial [\omega_1 \ \omega_2 \ \omega_3]^T}{\partial [\varphi \ \psi \ \theta]^T} = \left[ \mathbb{I}_3 \cdot R_3(\varphi) \cdot R_1(-\theta) \cdot P_0 \quad M \cdot \mathbb{I}_3 \begin{bmatrix} e_x \\ e_y \\ e_z \end{bmatrix} \quad -R_3(\varphi) \cdot R_1(-\theta) \cdot \mathbb{I}_3 \cdot P_0 \right] = \begin{bmatrix} G_1 \\ G_2 \\ G_3 \end{bmatrix}$$

$$\frac{\partial [\omega_1 \ \omega_2 \ \omega_3]^T}{\partial [\varphi \ \psi \ \theta]^T} = R_3(\varphi) \cdot R_1(-\theta) \cdot \begin{bmatrix} 0 & 0 & -1 \\ 0 & 0 & 0 \\ 0 & 1 & 0 \end{bmatrix} + \begin{bmatrix} 0 & 0 & 0 \\ 0 & 0 & 0 \\ 1 & 0 & 0 \end{bmatrix} = \begin{bmatrix} F_1 \\ F_2 \\ F_2 \end{bmatrix}$$

$$\frac{\partial (W^1)}{\partial \varphi} = \begin{bmatrix} \cos \varphi \cot \theta & -\sin \varphi \cot \theta & 0 \\ -\cos \varphi \csc \theta & \sin \varphi \csc \theta & 0 \\ \sin \varphi & \cos \varphi & 0 \end{bmatrix} ; \quad \frac{\partial (W^1)}{\partial \psi} = 0 ;$$

$$\frac{\partial (W^1)}{\partial \theta} = \begin{bmatrix} -\sin \varphi \csc^2 \theta & -\cos \varphi \csc^2 \theta & 0 \\ \sin \varphi \cot \theta \csc \theta & \cos \varphi \cot \theta \csc \theta & 0 \\ 0 & 0 & 0 \end{bmatrix}$$

Now the three partial derivatives matrices necessary for the formation of  $\Theta$  and  $\Phi$  can be evaluated:

$$\frac{\partial [\ddot{\varphi} \ \ddot{\psi} \ \ddot{\theta}]^T}{\partial [\varphi \ \psi \ \theta]^T} = \left[ \frac{\partial (W^1)}{\partial \varphi} \cdot T_0 \quad 0 \quad \frac{\partial (W^1)}{\partial \theta} \cdot T_0 \right] + W^1 \frac{\partial T_D}{\partial [\varphi \ \psi \ \theta]^T} \quad (3.32.24)$$

$$\frac{\partial [\ddot{\varphi} \ddot{\psi} \ddot{\theta}]^T}{\partial [\varphi \psi \theta]^T} = W^{-1} \frac{\partial T_D}{\partial [\dot{\varphi} \dot{\psi} \dot{\theta}]^T} ; \quad (3.32.25)$$

$$\frac{\partial [\ddot{\varphi} \ddot{\psi} \ddot{\theta}]^T}{\partial [\alpha \beta \gamma]^T} = W^{-1} \frac{\partial T_D}{\partial [\alpha \beta \gamma]^T} = W^{-1} \begin{bmatrix} T_A(1) & 0 & 0 \\ 0 & T_A(2) & 0 \\ 0 & 0 & T_A(3) \end{bmatrix} \quad (3.32.26)$$

where

$$\frac{\partial T_D}{\partial [\varphi \psi \theta]^T} = \begin{bmatrix} \alpha & 0 & 0 \\ 0 & \beta & 0 \\ 0 & 0 & \gamma \end{bmatrix} \cdot \frac{\partial T_A}{\partial [\varphi \psi \theta]^T} - \frac{\partial (T_B \cdot P_0)}{\partial [\varphi \psi \theta]^T} - \frac{\partial T_C}{\partial [\varphi \psi \theta]^T} ;$$

$$\begin{aligned} \frac{\partial T_A}{\partial [\varphi \psi \theta]^T} &= \frac{3k^2 E}{r_E^5} \cdot \frac{\partial [yz - xz \ xy]_E^T}{\partial [\varphi \psi \theta]^T} + \frac{3k^2 S}{r_S^5} \cdot \frac{\partial [yz - xz \ xy]_S^T}{\partial [\varphi \psi \theta]^T} \\ &\quad - \frac{\partial [\omega_2 \omega_3 \ -\omega_1 \omega_3 \ \omega_1 \omega_2]^T}{\partial [\varphi \psi \theta]^T} = \\ &= \frac{3k^2 E}{r_E^5} \cdot \begin{bmatrix} C_2 \cdot z + C_3 \cdot y \\ -C_1 \cdot z - C_3 \cdot x \\ C_1 \cdot y + C_2 \cdot x \end{bmatrix}_E + \frac{3k^2 S}{r_S^5} \cdot \begin{bmatrix} C_2 \cdot z + C_3 \cdot y \\ -C_1 \cdot z - C_3 \cdot x \\ C_1 \cdot y + C_2 \cdot x \end{bmatrix}_S - \begin{bmatrix} G_2 \cdot \omega_3 + G_3 \cdot \omega_2 \\ -G_1 \cdot \omega_3 - G_3 \cdot \omega_1 \\ G_1 \cdot \omega_2 + G_2 \cdot \omega_1 \end{bmatrix} ; \end{aligned}$$

$$\frac{\partial (T_B \cdot P_0)}{\partial [\varphi \psi \theta]^T} = \begin{bmatrix} I_{E3} \cdot T_B \cdot P_0 \\ T_B \cdot I_{E3} \cdot R_3(\psi) \cdot \begin{bmatrix} e_x \\ e_y \\ e_z \end{bmatrix} \end{bmatrix} - T_B \cdot I_{E1} \cdot P_0$$

$$\frac{\partial T_C}{\partial [\varphi \psi \theta]^T} = \begin{bmatrix} I_{E3} \cdot T_C \\ M \cdot I_{E3} \cdot I_{E3} \cdot \dot{\psi} \cdot \begin{bmatrix} e_x \\ e_y \\ e_z \end{bmatrix} \end{bmatrix} - R_3(\varphi) \cdot R_1(-\theta) \cdot I_{E1} \cdot R_3(\psi) \cdot I_{E3} \cdot \dot{\psi} \cdot \begin{bmatrix} e_x \\ e_y \\ e_z \end{bmatrix} ;$$

$$\frac{\partial T_p}{\partial [\dot{\phi} \ \dot{\psi} \ \dot{\theta}]^T} = \begin{bmatrix} -\alpha & 0 & 0 \\ 0 & -\beta & 0 \\ 0 & 0 & -\gamma \end{bmatrix} \frac{\partial [\omega_2 \omega_3 - \omega_1 \omega_3 \ \omega_1 \omega_2]^T}{\partial [\dot{\phi} \ \dot{\psi} \ \dot{\theta}]^T} - \frac{\partial (T_B \cdot P_0)}{\partial [\dot{\phi} \ \dot{\psi} \ \dot{\theta}]^T} - \frac{\partial T_c}{\partial [\dot{\phi} \ \dot{\psi} \ \dot{\theta}]^T} ;$$

$$\frac{\partial [\omega_2 \omega_3 - \omega_1 \omega_3 \ \omega_1 \omega_2]^T}{\partial [\dot{\phi} \ \dot{\psi} \ \dot{\theta}]^T} = \begin{bmatrix} F_2 \cdot \omega_3 + F_3 \cdot \omega_2 \\ -F_1 \cdot \omega_3 - F_3 \cdot \omega_1 \\ F_1 \cdot \omega_2 + F_2 \cdot \omega_1 \end{bmatrix} ;$$

$$\frac{\partial (T_B \cdot P_0)}{\partial [\dot{\phi} \ \dot{\psi} \ \dot{\theta}]^T} = [E_3 \cdot R_3(\varphi) \cdot R_1(-\theta) \cdot P_0 \mid 0 \mid -R_3(\varphi) \cdot R_1(-\theta) \cdot E_1 \cdot P_0] + T_B \begin{bmatrix} 0 & 0 & -1 \\ 0 & 0 & 0 \\ 0 & 1 & 0 \end{bmatrix} ;$$

$$\frac{\partial T_c}{\partial [\dot{\phi} \ \dot{\psi} \ \dot{\theta}]^T} = \begin{bmatrix} 0 & \vdots & \frac{1}{\psi} \cdot T_c & \vdots & 0 \end{bmatrix} .$$

This completes the derivation of the  $\Theta$  and  $\Phi$  matrices. No attempt was made to simplify the results and to put them together as the only criterion used to judge the final forms was the efficiency with which they can be coded.

U and Q matrices were generated by numerical integration using the coded  $\Theta$  and  $\Phi$  matrices over an interval of several months. For the same interval another set of U and Q matrices were generated using numerical differentiation [Escobal, 1965]. The agreement found in the corresponding elements of U and Q was usually better than five significant digits. This was considered as an indirect check on the derivation carried out in this section.

### 3.4 Fitting Numerically Integrated Physical Libration Angles Into Existing Solutions

The approach taken by J P L in creating the numerically integrated lunar ephemeris was discussed in section 1.31. Fitting the numerically integrated ephemeris into Brown's ephemeris was defined as the product of minimizing the differences between the position vectors at a series of corresponding epochs along the lunar orbit. There are other criteria that could be used to define the minimizing function; however, it appears that fitting one trajectory into another does not represent conceptual difficulties.

In order to test the proposed method for the solution of Euler's dynamic equations and also to come up with provisional standard epoch values for  $\gamma^0$  (section 3.31) an attempt is made to fit the numerically integrated physical libration angles and time rates into an existing solution.

Eckhardt's solution for the physical libration angles using Koziel's values for  $f = \frac{\alpha}{\beta}$  and  $I_D$  is used to generate "observed" physical libration angles [Eckhardt, 1970]. The basic problem to be clarified prior to the actual fit is the definition of a "best fit" of one set of physical libration angles into another. The main difficulty is in the fact that unlike the case of trajectories, the physical libration angles are used invariably as a means for determining the orientation of the xyz selenodetic coordinate system with respect to the MOD ecliptic system after an appropriate conversion into Eulerian angles. It may be possible to come up with two different sets of physical libration angles that will result in the same transformation matrix from MOD ecliptic into the selenodetic system. If the transformation matrix is the goal, it seems reasonable to seek minimization of the differences between the corresponding elements of the "observed" transformation matrix and the numerically integrated one.

Another approach to the "best fit" problem can be developed by

analyzing the relations between variational rotations around the  $x, y, z$  axes and variations in the physical libration angles. The following two subsections will treat these two approaches.

### 3.41 Spatial Angles Approach.

Two  $xyz$  coordinate systems are considered:

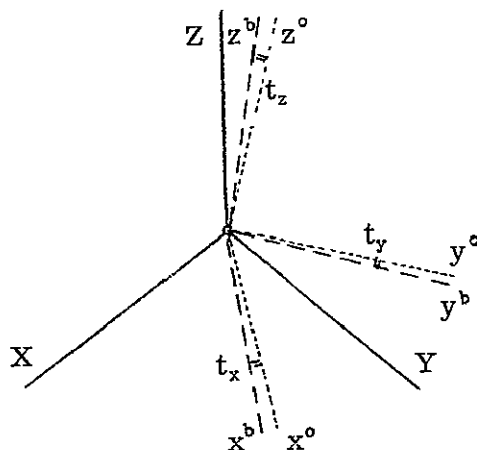


Figure 3.3 Spatial Angles Diagram

(a) An "observed"  $[xyz]^b$  system defined in space by three rotations from the ecliptic mean system  $XYZ$  through Eckhardt's Eulerian angles.

(b) A "computed"  $[xyz]^o$  system defined in the same way like (a) but using the numerically integrated Eulerian angles.

Actually "observed" and "computed" are the physical libration angles  $\tau$ ,  $\sigma$ ,  $\rho$  which are transformed into Eulerian angles through  $L_D$ ,  $\Omega_D$ , and  $I_D$  (section 3.22).

The best fit is defined as the solution for  $\gamma$  and  $\varphi$  (section 3.31) that minimizes the spatial angles  $t_x$ ,  $t_y$ ,  $t_z$  between the "observed" and "computed" axes  $x$ ,  $y$  and  $z$ , respectively (see Figure 3.3).

Mathematically, the two  $xyz$  systems are defined by the respective transformation matrices

$$\begin{bmatrix} x \\ y \\ z \end{bmatrix}_b = R_3(\phi^b) \cdot R_1(-\theta^b) \cdot R_3(\psi^b) \cdot \begin{bmatrix} X \\ Y \\ Z \end{bmatrix} = B \cdot \begin{bmatrix} X \\ Y \\ Z \end{bmatrix} \quad (3.41.1)$$

$$\begin{bmatrix} x \\ y \\ z \end{bmatrix}_o = R_3(\phi^o) \cdot R_1(-\theta^o) \cdot R_3(\psi^o) \cdot \begin{bmatrix} X \\ Y \\ Z \end{bmatrix} = C \cdot \begin{bmatrix} X \\ Y \\ Z \end{bmatrix} \quad (3.41.2)$$

B and C are orthogonal so  $B^{-1} = B^T$  and

$$\begin{bmatrix} X \\ Y \\ Z \end{bmatrix} = B^T \begin{bmatrix} x \\ y \\ z \end{bmatrix}_b$$

Substituting  $\begin{bmatrix} X \\ Y \\ Z \end{bmatrix}$  in the equation for  $\begin{bmatrix} x \\ y \\ z \end{bmatrix}_o$

$$\begin{bmatrix} x \\ y \\ z \end{bmatrix}_o = C \cdot B^T \begin{bmatrix} x \\ y \\ z \end{bmatrix}_b = D \begin{bmatrix} x \\ y \\ z \end{bmatrix}_b \quad (3.41.3)$$

D is an orthogonal transformation matrix from the "observed" to the "computed" xyz system.

D will be the identity matrix in case  $B = C$ , i.e., when the two systems coincide.

Examining the diagonal elements in D

$\left. \begin{array}{l} d_{11} \\ d_{22} \\ d_{33} \end{array} \right\}$  are the cosines of the spatial angles  $t_x, t_y, t_z$  between the axes  $\left\{ \begin{array}{l} x^b \text{ and } x^o \\ y^b \text{ and } y^o \\ z^b \text{ and } z^o \end{array} \right\}$  respectively

For  $D = I$  (identity matrix)

$$d_{11} = d_{22} = d_{33} = 1$$

and the spatial angles are zero

$$t_x = t_y = t_z = 0$$

The adjustment process is defined as the estimation of  $\gamma^a$  and  $\varphi^a$  that will minimize the spatial angles  $t_x, t_y, t_z$  at a series of consecutive epochs.

The following notation is used:

Parameters:

$$\left. \begin{array}{l} \gamma^o \\ \varphi^o \end{array} \right\} \text{nominal} \quad \left\{ \begin{array}{ll} \text{initial values} & \tau_o, \sigma_o, \rho_o, \dot{\tau}_o, \dot{\sigma}_o, \dot{\rho}_o \\ \text{physical constants} & C_{22}, \beta, C_{20} \end{array} \right.$$

$$\left. \begin{array}{l} \gamma^a \\ \varphi^a \end{array} \right\} \text{adjusted}$$

$$\left. \begin{array}{l} \gamma \\ \varphi \end{array} \right\} \text{corrections in the sense} \quad \left\{ \begin{array}{l} \gamma^a = \gamma^o + \gamma \\ \varphi^a = \varphi^o + \varphi \end{array} \right.$$

Quasi Observations:

$$\left[ \begin{array}{c} t_x \\ t_y \\ t_z \end{array} \right]^o \quad \begin{array}{l} \text{spatial angles} \\ \text{calculated by the use of Eckhardt's and the} \\ \text{nominal (based on } \gamma^o, \varphi^o \text{) angles.} \end{array}$$

$$\left[ \begin{array}{c} t_x \\ t_y \\ t_z \end{array} \right]^a \quad \text{adjusted spatial angles.}$$

The mathematical model of the least squares fit can be written now

$$\begin{bmatrix} t_x \\ t_y \\ t_z \end{bmatrix}^a = \begin{bmatrix} t_x \\ t_y \\ t_z \end{bmatrix}^o + \frac{\partial [t_x \ t_y \ t_z]^T}{\partial \begin{bmatrix} \gamma \\ \varphi \end{bmatrix}^a} \cdot \begin{bmatrix} \gamma \\ \varphi \end{bmatrix} \quad (3.41.4)$$

Introducing the U and Q matrices (section 3.32)

$$\begin{bmatrix} t_x \\ t_y \\ t_z \end{bmatrix}^a = \begin{bmatrix} t_x \\ t_y \\ t_z \end{bmatrix}^o + \frac{\partial [t_x \ t_y \ t_z]^T}{\partial [\tau \ \sigma \ \rho \ \tau \ \sigma \ \rho]^T} \cdot [U \ ; \ Q] \cdot \begin{bmatrix} \gamma \\ \varphi \end{bmatrix}$$

In auxiliary notation

$$V_i = L_i + A_{ti} \cdot [U_i \ ; \ Q_i] \cdot \begin{bmatrix} \gamma \\ \varphi \end{bmatrix} \quad (3.41.5)$$

The subscript i indicates the i set of observation equations corresponding to the i epoch.

The function that is minimized is

$$\lambda_1 = \sum_1 t_{xi}^2 + t_{yi}^2 + t_{zi}^2 = \sum_1 V_i^T \cdot V_i \quad (3.41.6)$$

And the solution follows according to Uotila [1967]:

$$\begin{bmatrix} \gamma \\ \varphi \end{bmatrix} = - \left\langle \sum_1 \begin{bmatrix} U_i^T \\ Q_i^T \end{bmatrix} \cdot A_{ti}^T \cdot A_{ti} [U_i \ ; \ Q_i] \right\rangle^{-1} \cdot \sum_1 \begin{bmatrix} U_i^T \\ Q_i^T \end{bmatrix} \cdot A_{ti}^T \cdot L_i \cdot \quad (3.41.7)$$

The matrix  $A_t$  and vector L will be developed explicitly in terms of Eckhardt's and the numerically integrated angles.

Assuming the  $t_x, t_y, t_z$  angles to be small

$$\begin{aligned}
t_x &\cong \sin t_x = \sqrt{1 - d_{11}^2} \\
t_y &\cong \sin t_y = \sqrt{1 - d_{22}^2} \\
t_z &\cong \sin t_z = \sqrt{1 - d_{33}^2}
\end{aligned}$$

$$L_1 = \begin{bmatrix} \sqrt{1 - d_{11}^2} \\ \sqrt{1 - d_{22}^2} \\ \sqrt{1 - d_{33}^2} \end{bmatrix}_1$$

$$A_{t1} = \begin{bmatrix} \frac{\partial [t_x t_y t_z]_1^T}{\partial [\tau \sigma \rho]_1^T} & \vdots & 0 \end{bmatrix}$$

$$\frac{\partial [t_x t_y t_z]_1^T}{\partial [\tau \sigma \rho]_1^T} = \frac{\partial [t_x t_y t_z]_1^T}{\partial [d_{11} d_{22} d_{33}]_1^T} \cdot \frac{\partial [d_{11} d_{22} d_{33}]_1^T}{\partial [\varphi \psi \theta]_1^T} \cdot \frac{\partial [\varphi \psi \theta]_1^T}{\partial [\tau \sigma \rho]_1^T}$$

$$\frac{\partial [t_x t_y t_z]_1^T}{\partial [d_{11} d_{22} d_{33}]_1^T} = \begin{bmatrix} -\frac{d_{11}}{t_x} & 0 & 0 \\ 0 & -\frac{d_{22}}{t_y} & 0 \\ 0 & 0 & -\frac{d_{33}}{t_z} \end{bmatrix}$$

$$\frac{\partial [\varphi \psi \theta]_1^T}{\partial [\tau \sigma \rho]_1^T} = \begin{bmatrix} 1 & -1 & 0 \\ 0 & 1 & 0 \\ 0 & 0 & 1 \end{bmatrix} \quad (\text{from section 3.32})$$

The transformation matrices B and C as defined above are partitioned

$$B = \begin{bmatrix} B_1 \\ B_2 \\ B_3 \end{bmatrix} ; \quad C = \begin{bmatrix} C_1 \\ C_2 \\ C_3 \end{bmatrix} ;$$

$$\begin{bmatrix} d_{11} \\ d_{22} \\ d_{33} \end{bmatrix} = \begin{bmatrix} C_1 \cdot B_1^T \\ C_2 \cdot B_2^T \\ C_3 \cdot B_3^T \end{bmatrix}$$

$$\frac{\partial [d_{11} \ d_{22} \ d_{33}]^T}{\partial [\varphi \ \psi \ \theta]^T} = \begin{bmatrix} \frac{\partial C_1}{\partial \varphi} \cdot B_1^T & \frac{\partial C_1}{\partial \psi} \cdot B_1^T & \frac{\partial C_1}{\partial \theta} \cdot B_1^T \\ \frac{\partial C_2}{\partial \varphi} \cdot B_2^T & \dots & \dots \\ \frac{\partial C_3}{\partial \varphi} \cdot B_3^T & \dots & \frac{\partial C_3}{\partial \theta} \cdot B_3^T \end{bmatrix}$$

$$C = R_3(\varphi) \cdot R_1(-\theta) \cdot R_3(\psi)$$

Matrix  $C$  is differentiated using Lucas matrices  $L_1^c$ ,  $L_2^c$ ,  $L_3^c$  (see Appendix E).

$$\frac{\partial C}{\partial \varphi} = L_3^c \cdot C$$

$$\frac{\partial C}{\partial \psi} = C \cdot L_3^c$$

$$\frac{\partial C}{\partial \theta} = -R_3(\varphi) \cdot R_1(-\theta) \cdot L_1^c \cdot R_3(\psi)$$

The fit over a large number of epochs is simplified and the computer memory requirements are minimal because the normal matrix and also the vector of constants are created by a process of summation. As the numerical integration of Euler's dynamic equations progresses, at pre-determined epochs or at regular time intervals, a layer is added to the normal matrix and to the vector of constants until the whole interval over which the fit is performed has been covered.

### 3.42 Variational Rotations Method.

The variations in the physical libration angles are transformed into variational rotations around the  $x, y, z$  axes of the selenodetic system. The least squares fit is defined then by the minimization of the variational rotations around the  $x, y, z$  axes.

Euler's geometric equations (3.22.2) are used to transform  $\delta\varphi, \delta\psi, \delta\theta$  into  $\delta\xi_x, \delta\xi_y, \delta\xi_z$

$$\begin{bmatrix} \delta\xi_x \\ \delta\xi_y \\ \delta\xi_z \end{bmatrix} = R_3(\omega) \cdot R_1(-\theta) \cdot \begin{bmatrix} -\delta\theta \\ 0 \\ \delta\psi \end{bmatrix} + \begin{bmatrix} 0 \\ 0 \\ \delta\varphi \end{bmatrix}$$

where  $\delta\xi_x, \delta\xi_y, \delta\xi_z$  are variational rotations of the Moon around the  $x, y, z$  axes, respectively.

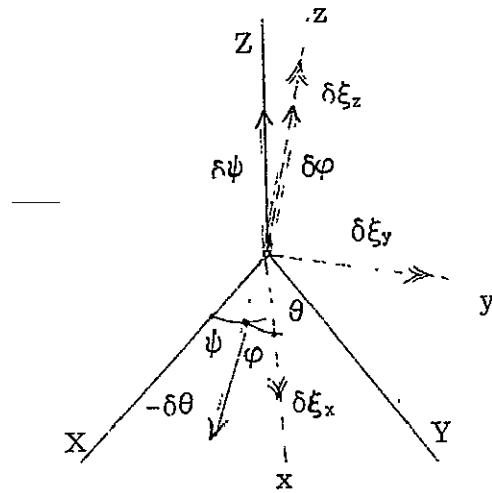


Figure 3.4 Variational Rotations About the xyz Axes

From the relations between  $\varphi$ ,  $\psi$ ,  $\theta$  and  $\tau$ ,  $\sigma$ ,  $\rho$  (section 3.23) and after some regrouping

$$\begin{bmatrix} \delta \xi_x \\ \delta \xi_y \\ \delta \xi_z \end{bmatrix} = \begin{bmatrix} 0 & -\sin\varphi\sin\theta & -\cos\varphi \\ 0 & -\cos\varphi\sin\theta & \sin\varphi \\ 1 & \cos\theta - 1 & 0 \end{bmatrix} \cdot \begin{bmatrix} \delta\tau \\ \delta\sigma \\ \delta\rho \end{bmatrix} = E_M \cdot \begin{bmatrix} \delta\tau \\ \delta\sigma \\ \delta\rho \end{bmatrix}. \quad (3.42.1)$$

The variations in  $\tau$ ,  $\sigma$ ,  $\rho$  are identified in the adjustment process with the differences between Eckhardt's  $\tau$ ,  $\sigma$ ,  $\rho$  and the numerically integrated angles. Through the  $E_M$  matrix these differences are transformed into rotations around x, y and z axes. Thus, the function to be minimized in accordance with the opening statement in this subsection is

$$\lambda_2 = \sum_1 (\delta \xi_{x1}^2 + \delta \xi_{y1}^2 + \delta \xi_{z1}^2)$$

It is interesting at this point to express  $\lambda_2$  in terms of  $\delta\tau, \delta\sigma, \delta\rho$  and compare it with  $\lambda_1$  from 3.41.

$$\begin{aligned} [\delta \xi_x \quad \delta \xi_y \quad \delta \xi_z] \cdot \begin{bmatrix} \delta \xi_x \\ \delta \xi_y \\ \delta \xi_z \end{bmatrix} &= [\delta\tau \quad \delta\sigma \quad \delta\rho] \cdot E_M^T \cdot E_M \cdot \begin{bmatrix} \delta\tau \\ \delta\sigma \\ \delta\rho \end{bmatrix} = \\ &= [\delta\tau \quad \delta\sigma \quad \delta\rho] \cdot \begin{bmatrix} 1 & \cos\theta - 1 & 0 \\ \cos\theta - 1 & 2(1 - \cos\theta) & 0 \\ 0 & 0 & 1 \end{bmatrix} \cdot \begin{bmatrix} \delta\tau \\ \delta\sigma \\ \delta\rho \end{bmatrix} = \\ &= \delta\tau^2 - 2 \cdot (1 - \cos\theta) \cdot \delta\tau \cdot \delta\sigma + 2 \cdot (1 - \cos\theta) \cdot \delta\sigma^2 + \delta\rho^2 \quad (3.42.2) \end{aligned}$$

For the Moon  $\theta$  is a small angle of about  $1^\circ 30'$ , so for the purpose of this comparison only

$$\cos\theta \cong 1 - \frac{\theta^2}{2}$$

The result is then

$$\delta\xi_x^2 + \delta\xi_y^2 + \delta\xi_z^2 = \delta\tau^2 + (\theta \cdot \delta\sigma)^2 + \delta\rho^2 - \theta \cdot \delta\sigma \cdot \delta\tau \cdot \theta$$

Considering the orders of magnitude of  $\tau, \sigma, \rho$  and  $\delta\tau, \delta\sigma, \delta\rho$  the last (fourth) term in the expression obtained is by an order of magnitude smaller than the rest and will be neglected. The sum of squares of the variations ( $\lambda_2$ ) is then in an approximation to the first order

$$\lambda_2 = \delta\xi_x^2 + \delta\xi_y^2 + \delta\xi_z^2 \cong \delta\tau^2 + (\theta \cdot \delta\sigma)^2 + \delta\rho^2 \quad (3.42.3)$$

From 3.41

$$\lambda_1 = t_x^2 + t_y^2 + t_z^2$$

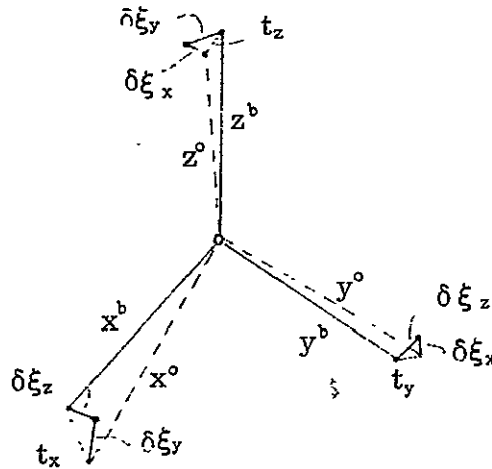


Figure 3.5

### Equivalency Between Spatial Angles and Variational Rotations

The comparizon is made only for a single epoch  $T_1$  in order to simplify the notation; however , the results are valid for any number of epochs.

From inspecting Figure 3.5 and as the  $t_x$   $t_y$   $t_z$  spatial angles are small, it follows that

$$\lambda_1 = t_x^2 + t_y^2 + t_z^2 = (\delta\xi_z^2 + \delta\xi_y^2) + (\delta\xi_z^2 + \delta\xi_y^2) + (\delta\xi_x^2 + \delta\xi_y^2) = 2\lambda_2 \quad (3.42.4)$$

The conclusion to be drawn from the last equation is that within the approximations made in deriving equation (3.42.4) the two methods are equivalent. However, the computational effort involved in applying method 2 is considerably lighter.

The mathematical model for method 2 and the consequent solution follow the same logic as for method 1.

Notation:

$$\begin{bmatrix} \xi_x \\ \xi_y \\ \xi_z \end{bmatrix}^{\circ} \quad \begin{array}{l} \text{rotations around x,y,z computed from Eckhardt's} \\ \text{angles and numerical integration of } \tau, \sigma, \rho \\ \text{based on } (\gamma^{\circ}, \varphi^{\circ}) \end{array}$$

$$\begin{bmatrix} \xi_x \\ \xi_y \\ \xi_z \end{bmatrix}^a \quad \text{- adjusted rotations}$$

$\gamma^{\circ}, \varphi^{\circ}, \gamma^a, \varphi^a, \gamma, \varphi$ , are the same as defined in 3.41 .

$$\begin{bmatrix} \xi_x \\ \xi_y \\ \xi_z \end{bmatrix}^a = \begin{bmatrix} \xi_x \\ \xi_y \\ \xi_z \end{bmatrix}^{\circ} + \frac{\partial[\xi_x \ \xi_y \ \xi_z]^T}{\partial[\tau \ \sigma \ \rho \ \dot{\tau} \ \dot{\sigma} \ \dot{\rho}]^T} [U \ ; \ Q] \begin{bmatrix} \gamma \\ \varphi \end{bmatrix} \quad (3.42.5)$$

From results obtained in this subsection

$$L_1 = \begin{bmatrix} \tau^{\circ} & - & \tau^b \\ \sigma^{\circ} & - & \sigma^b \\ \rho^{\circ} & - & \rho^b \end{bmatrix}_1$$

Using auxiliary notation as in 3.41 an observation equation set  $i$  can be written as follows:

$$V_i = E_{M1} \cdot L_1 + [E_{M1} \mid 0] \cdot [U_1 \mid Q_1] \begin{bmatrix} \gamma \\ \varphi \end{bmatrix} \quad (3.42.6)$$

The solution minimizing  $\lambda_2 = \sum_1 V_i^T V_i$  is

$$\begin{bmatrix} \gamma \\ \varphi \end{bmatrix} = - \left( \sum_1 \begin{bmatrix} U_1^T \\ Q_1^T \end{bmatrix} \cdot \begin{bmatrix} E_{M1}^T \\ 0 \end{bmatrix} \cdot [E_{M1} \mid 0] \cdot [U_1 \mid Q_1] \right)^{-1} \cdot \sum_1 \begin{bmatrix} U_1^T \\ Q_1^T \end{bmatrix} \cdot \begin{bmatrix} E_{M1}^T \\ 0 \end{bmatrix} \cdot E_{M1} \cdot L_1 \quad (3.42.7)$$

Method 2 was used to perform a series of least squares fits into Eckhardt's angles over various periods . Results and diagrams are given in Chapter 5. The residuals after the fit were not subjected to extensive analysis as the purpose of this mathematical development was to demonstrate the compatibility of the new method with conventional solutions and also to obtain provisional initial values for the physical libration angles. The residuals in  $\tau$ ,  $\sigma$ ,  $\rho$  shown in Chapter 5 suggest patterns which may lead eventually to a better understanding of the differences between Eckhardt's solution and the one based on numerical integration. However, such an investigation appears to be well beyond the scope of the present work.

## 4. SIMULATION OF ENVIRONMENT AND OBSERVATIONS

### 4.1 Introduction

In Chapter 4 a sustained effort has been directed towards the creation of a self-consistent simulated environment of the Earth, the Moon and man-made satellites in which a variety of observational activities take place. The celestial bodies involved move and rotate according to the laws of Newton and Kepler; the satellites revolve around the Moon in accordance with the forces acting on them. The observations are generated realistically, while at the same time they are free of any unaccounted effects. The solution presented in Chapter 2 aims at estimating certain parameters which represent existing physical properties of the real Moon; it solves for the initial state vector of a satellite orbiting the Moon and in general the situations treated are rather complex. All this implies that any simulation short of accounting exactly for all the gravitational phenomena taking place (which are solved afterwards) cannot be useful for investigating numerically the feasibility and merits of the theoretical solution proposed in Chapter 2.

Simulation of environment and observations has become a standard tool for testing theories and computational procedures in many fields of science. In a sense, use of simulation in research can be considered indispensable.

Sooner or later any scientific research reaches the stage when the theories and procedures developed have to be tested by exposing them to actually observed phenomena. Discrepancies between theory and observations lead eventually to an improvement of the theory and also to a better understanding of the phenomena involved.

Sound as it is, this approach is rather expensive in time and effort required on the part of the research worker—a great deal of luck is needed too. Observations are never free of unaccounted effects, and it is with a large degree of optimism that one makes the convenient assumption that they are randomly distributed and as such can be handled by statistical analysis.

With the advent of the electronic computer, a new option became available to the research worker. Very complicated situations can be programmed, and observations can be simulated with an absolute knowledge of the effects embodied in them. The simulations are usually designed to follow closely the actual (true life) situation. In the early stages of a study, it is helpful to have a reasonably representative model which is absolutely free of unknown phenomena in order to acquire a better insight into the problems involved and also to develop a feeling for the general behavior of quantities which play an important role in the area of study. For this purpose the simulated model can be rather simple so that the main structure is clearly visible. It is judged qualitatively and not quantitatively. In later stages of the study it becomes more important for the simulated model to follow as closely as possible the true situation. It is necessary for the smooth transition from the simulated to the true environment. This would require a very complicated model up to the inclusion of marginally significant effects.

The problem of designing a simulated model of the Earth-Moon environment was solved by a compromise. It was clear that the scope of the present study does not justify the design of too complicated a model. On the other hand, the results of this study will have to be applied at a latter stage to the true case. The compromise was the design of a moderately complex simulated model that exceeds the needs

of the present study, but holds the promise for future applications in more advanced stages of the research.

Whatever the level of complexity of a simulated model, it has to be fully consistent. Consistency is to be understood here as conceptual as well as numerical. The basic set of constants are to be selected carefully so that the exact relationship among them in accordance with the model of simulation are absolutely valid - no discrepancies or contradictions of any kind and magnitude can be tolerated. Numerically, the quantities generated should contain sufficient number of correct significant digits to conform to the anticipated noise in the observations. For example, if the noise in heliometer observations is believed to be about  $0''.02 - 0''.05$ , the lunar ephemeris needed to simulate the heliometer observations will have to be precise to the degree that will insure observations better than  $''001$ .

There is certain danger in relying too heavily on conclusions reached from the analysis of a simulation. The models used to generate the simulation are occasionally the same ones employed in the reduction procedures. Unless programming errors interfere, the procedures will prove to be invariably successful. However, the first contact with reality, i.e., the use of actual observations will cause a serious shock which in some cases may shatter the whole theoretical structure of the analysis. So, useful and convenient as it is, numerical simulation should be utilized with utmost care and watchfulness. It is the real world that we want to analyze and not the simulated model, no matter how skillfully it has been created.

The design of a simulated model of the Earth-Moon environment presented a unique opportunity to develop some new ideas in astronomy. Instead of formulating and programming models based on concepts and expressions

as published in textbooks, a difficult but promising approach was taken. The theories, models and constants relevant to the Earth-Moon Environment were subjected to intensive study. The objective was to gain a profound understanding of the basic problems and postulates which have served as a starting point in developing the conventional solutions. Another goal was set to determine a minimal set of independent parameters. The astronomical problems were solved then consistently using a new approach. The result is a compact and geometrically well-defined astronomical model. No attempt is made to point out differences or similarities. As this development is confined to the simulated model only, it was felt that there is no need or justification for comparison. Rather a continuous exposition is made, and the theories are developed as if no other ways exist for solving the same problem.

It would be presumptuous to regard the developments in this chapter as applicable to the analysis of actual astronomical observations. However, changes in relevant astronomical models in the future should not be ruled out. The impact of computer technology has left many areas in astronomy unaffected; in many cases the computer has been employed as a mere substitute for the human in performing the calculations without bringing substantial changes in the approach to the problems. Instead of triggering a critical examination of concepts and fundamentals, the computer produced merely amendments to the available procedures.

In the following sections of this Chapter the simulated environment is unfolded step by step beginning with definitions and fundamentals, adopting a set of basic constants, through development of the equations of motion and finally presenting the theory for the generation of the various data types. In order not to refer too often to definitions and facts already stated in Chapters 1 through 3 the liberty is taken to repeat some of those without indulging in lengthy discussions.

## 4.2 Fundamentals of the Simulation

The celestial bodies described in this Chapter carry the names Earth and Moon and in their properties closely correspond to the real Earth and Moon. However, by definition they are part of an abstract model. As such anything related to them is or is based upon abstract assumptions. So in stating the "facts" and "constants" of this model it should be remembered that these are facts and constants existing only in the abstract model created in this Chapter.

The simulated Earth-Moon environment is composed of the Earth, the Moon and one or more man-made satellites usually in the vicinity of the Moon. The mean distance between the Earth and the Moon is of the same order of magnitude as in the real case. The basic framework in the simulation is an inertially oriented right handed Cartesian coordinate system (XYZ). It is defined implicitly by infinitely distant fixed stars so that all the directions to any of these stars from points within the Earth-Moon environment are perfectly parallel. Numerically this coordinate system is chosen identical to the mean ecliptic system of some standard epoch.

An infinitely distant illuminating source serves as the "Sun" in the simulation. It moves on the XY inertial plane in a positive direction (from X to Y) with an angular velocity similar to that of the mean sun. All the illuminating rays of the "Sun" crossing the Earth-Moon environment are perfectly parallel. The "Sun" does not have any gravitational effect on the Earth-Moon environment. The only celestial bodies which exert gravitational attraction are the Earth and the Moon. Man-made satellites in the system have negligibly small masses. The center of mass of the Earth and the Moon (the barycenter of the system) is regarded as an inertial point in space, i.e., it is considered to be stationary or moving at a constant speed in a certain direction.

The particular inertially-oriented system (XYZ) centered at the barycenter is the fundamental coordinate system of the simulated environment. The motion of the Earth, the Moon and any of the man-made satellites is defined with respect to this system. In some cases, however, it may be convenient to transform the motions to non-inertial points like the geocenter or the selenocenter.

The Earth is a perfectly rigid body. Its topography is identical to that of the true Earth. Its reference figure is a rotationally symmetric ellipsoid. Four radio tracking stations measuring range and range-rate and three optical observatories are defined at locations where actual and presently active stations are engaged in observations of the appropriate type. Two additional optical observatories are defined which were used in the past for conducting heliometer observations of the Moon.

An average terrestrial right handed Cartesian coordinate system is defined (UVW) which is fixed to the Earth, centered at its mass center and is oriented so that it coincides with the principal axes of inertia of the Earth. Where such axes are not defined (on the equator of a rotationally symmetric Earth) the UW plane contains a certain point on the Earth's surface (Greenwich). The total motion of the Earth with respect to the fundamental coordinate system is defined by the translatory motion of its center of mass and by the rotation of the average terrestrial system about its origin.

The gravitational field of the Earth is given in terms of a spherical harmonics expansion. The only coefficient in the expansion apart of the central (zero degree) term which is not zero is the  $J_2$ . The three principal moments of inertia of the Earth (A, B, C) are consistent with the value of  $J_2$  and the ratio  $\mu = \frac{C - A}{A}$ . For derivation of a value for  $\mu$  to be adopted in the simulation see Appendix B.

The Moon is a perfectly rigid body. Its topography is that of an exact sphere. The center of the sphere is shifted from the center of

mass. On the front side of the Moon (the side facing the Earth) 30 triangulation points are chosen evenly spaced and in areas on the true Moon where there is an abundance of craterlets of 3-7 km diameter range. The crater Mösting A and also the crater Bruce in Sinus Medii are among the 30 points.

A selenodetic right-handed Cartesian coordinate system is defined (x y z) which is fixed to the lunar body, centered at its center of mass and is oriented so that it coincides with the principal axes of inertia of the Moon. The motion of the Moon is defined in a manner similar to that of the Earth.

The mass of the Moon is related to that of the Earth by a constant. Dynamically, the Moon is a more complicated body than the Earth. It is a triaxial ellipsoid with a set of 12 mass-points superimposed on its triaxial dynamic figure.  $C_{22}$  and  $C_{20}$  are the only non-zero coefficients of spherical harmonics expansion of the triaxial ellipsoid, apart of the zero degree term. The 12 mascons are selected so as to satisfy certain conditions. The conditions are that their total mass and also their first and second moments are all zeros. This was considered necessary in order to retain a basically rough gravity field as far as a close lunar satellite is concerned and at the same time not to complicate unnecessarily the equations of motion of the Moon itself. The three moments of inertia ( $A'$ ,  $B'$ ,  $C'$ ) are consistent with the  $C_{20}$ ,  $C_{22}$  values and also with the ratio  $\beta = \frac{C' - A'}{B'}$  taken identical to the presently accepted value of  $\beta$  for the true Moon.

The man-made satellites are defined as bodies of negligible mass and physical dimensions. No parallax exists between mass center, the calibrated point of the transponder for radio measurements and the principal point of its camera or other sensor. No orientation jets or other physical effects disturb the perfectly gravitational motion. In designing the various satellite orbits no consideration is given to their



E - Earth

M - Moon

B - barycenter

XYZ - fundamental inertial coordinate system

UVW - average terrestrial coordinate system

xyz - selenodetic coordinate system

$\eta, \lambda, \epsilon$  - Eulerian orientation angles of the Earth relating the UVW system to a coordinate system centered at E and parallel to the XYZ system.

$\varphi, \psi, \theta$  - Eulerian orientation angles of the Moon relating the xyz system to a coordinate system centered at M and parallel to the XYZ system.

#### 4.3 Constants of the Simulation

The best known presently values were selected as basic constants. The list of constants adopted by the IAU in its resolution of 1964 was the main source. Additional constants were taken from NASA and JPL publications, also from reports by other scientists or groups working in this area of study.

##### 4.31 The Earth.

$k^2 \cdot E$	=	.297556 $10^{16}$ km <sup>3</sup> /day <sup>2</sup>	- Earth's gravitational constant
$J_2$	=	.0010827	- second degree zonal harmonic
$a_e$	=	6378.16 km	- equatorial semi-diameter of reference ellipsoid
$f$	=	1/298.25	- flattening of reference ellipsoid
$\mu = \frac{C-A}{A}$	=	.00227802	- dynamical "flattening" where A, C are the equatorial and polar moments of inertia
$\omega_s$	=	6.300388098 rad/day	- diurnal rotational speed

No.	Name	Type	U	V	W
1	TUCSON	OPT	-1996.0051	-5042.6961	3360.7748
2	PIC DU MIDI	OPT	4686.1252	11.6385	4321.0499
3	JOHANNESBURG	OPT	5058.2628	2698.0251	-2799.8019
4	GOLDSTONE	RRT	-2351.1949	-4655.5944	3661.0605
5	WOOMERA	RRT	-3978.5840	3724.8986	-3302.3278
6	JOHANNESBURG	RRT	5085.4787	2668.3035	-2768.7011
7	MADRID	RRT	4845.7274	-360.0147	4125.7615
8	BAMBERG	HEL	4051.6351	779.4787	4864.3305
9	KAZAN	HEL	2369.2457	2707.8489	5266.5740

OPT- Optical, RRT- Radio, HEL- Helimeter, U, V, W in kilometers

Table 4.1. Geocentric Cartesian Coordinates of Observatories.

#### 4.32 The Moon.

$$m = \frac{E}{M} = 81.3 \quad - \quad \text{ratio of mass of the Earth to that of the Moon}$$

$$\left. \begin{aligned} C_{20} &= -.000207 \\ C_{22} &= .0000207 \end{aligned} \right\} - \text{second-order harmonics}$$

$$\xi = 3.6696 \quad - \quad \text{ratio of equatorial semi-axis of Earth ellipsoid to mean radius of the Moon}$$

$$\beta = \frac{C' - A'}{B'} = .000629 \quad - \quad \text{ratio between Moon's principal moments of inertia}$$

No.	Mass	x	y	z
1	19.0694	1619.1766	- 433.5269	449.3554
2	-20.0394	1532.2877	559.6170	593.9678
3	15.3805	1497.0175	866.7468	- 151.9861
4	-11.8910	1630.7870	1.0000	- 594.9678
5	11.7378	938.9899	- 940.4899	-1117.7341
6	-12.7844	1110.4827	-1325.4011	- 151.9861
7	2.8233	750.1227	-1302.5808	868.5538
8	- 6.0431	836.9416	- 223.9277	1504.7454
9	10.0246	715.6442	856.8510	1330.9677
10	- 8.0542	582.9365	1609.4737	301.3192
11	8.1149	750.1227	1304.5808	- 869.5538
12	- 8.3384	750.1227	435.5269	-1505.7454
Mass in $10^{-6}$ of Moon's mass; x, y, z in kilometers				

Table 4.2. Mass and Selenodetic Coordinates of Mascons on the Moon.

No.	x	y	z
1	284.7144	- 164.8233	1705.6738
2	267.3828	742.4968	1548.1653
3	298.9995	-1050.4536	1350.2634
4	950.9536	- 484.8089	1369.1476
5	897.8094	293.5282	1457.1998
6	297.0151	1298.3423	1116.7341
7	1013.5746	-1088.6066	894.6916
8	1453.2020	- 75.2901	946.1413
9	1076.7970	844.2392	1069.5859
10	341.1861	-1615.9158	536.6048

11	1506.4731	- 767.8602	390.4892
12	1577.2501	544.9516	478.5874
13	341.1861	1617.9158	536.6048
14	1157.6880	-1287.5193	120.7443
15	1735.3430	1.0000	29.8342
16	1106.4064	1322.5432	211.3220
17	1726.6207	- 150.2785	- 91.4655
18	490.5786	-1611.7874	- 420.9863
19	1499.1838	733.4201	- 479.5874
20	294.7339	1686.6973	- 302.3192
21	1211.2688	-1091.8823	- 594.9678
22	1511.8985	- 131.4927	- 843.1513
23	1004.3727	1244.3842	- 679.6328
24	257.4499	-1221.9682	-1207.8911
25	1155.7211	- 614.8371	-1140.8012
26	1055.5706	741.8690	-1163.5211
27	449.7967	1120.4735	-1250.7900
28	940.5390	83.5052	-1458.1998
29	377.2905	-378.7905	-1653.5386
30	305.4515	368.0022	-1671.2764
x, y, z are in kilometers			

Table 4.3. Selenodetic Coordinates of Triangulation Points on the Moon.

The selenodetic coordinates of the center of the Moon's sphere are as follows:

$$x = -2.5; \quad y = 1.0; \quad z = -0.5 \text{ (in kilometers).}$$

#### 4.33 Illuminating Source "Sun".

The longitude of the "Sun" measured from X in a positive direction (to Y) is given by the angle  $\lambda$  :

$$\lambda = \lambda_0 + \lambda_1 (T - T_0)$$

$$\lambda_0 = 4.8815286 \text{ rad}$$

$$\lambda_1 = .0172027913 \text{ rad/day}$$

T epoch for which  $\lambda$  is required in JD.

$$T_0 = 2415020.0 \text{ JD. standard epoch (1900.0) .}$$

#### 4.34. Initial Values for Position and Orientation of Earth and Moon including Linear and Angular Velocities.

The inertial (barycentric) position and orientation of the Earth and the Moon are obtained from the solution of the differential equations of motion. As shown already, because of the particular configuration of the mass centers of the Earth and Moon with respect to the barycenter, the position of only one of the mass centers has to be solved, that of the other being obtained in a trivial way. Thus the total of  $12 = 2 \times (2 \times 3)$  second-order differential equations is reduced to nine. The solution of these equations requires the determination of eighteen arbitrary constants of the integration. As it is shown in section 4.4, the integration is performed numerically, so the arbitrary constants are actually the initial values of position, orientation angles, and their time rates. The differential equations for the translatory motion of the Moon's mass center are written with respect to the geocenter so that the eighteen initial values that need to be defined are as follows:

- |  |   |  |
|--|---|--|
| $X_0, Y_0, Z_0, \dot{X}_0, \dot{Y}_0, \dot{Z}_0$                             | - | geocentric position and velocity of the Moon   |
| $\varphi_0, \psi_0, \theta_0, \dot{\varphi}_0, \dot{\psi}_0, \dot{\theta}_0$ | - | Eulerian angles and their time rates defining the orientation of the seleno-detic system (x y z) with respect to the inertial (X Y Z) system |

$\eta_0, \lambda_0, \epsilon_0, \dot{\eta}_0, \dot{\lambda}_0, \dot{\epsilon}_0$  - Eulerian angles and their time rates defining the orientation of the average terrestrial system (UVW) with respect to the (XYZ) system.

These eighteen initial values are defined for a given epoch at which the numerical integration begins. In order to be flexible in the choice of such initial epoch no fixed numerical values are given for a particular initial epoch, but rather the method and the equations are given with the aid of which the eighteen initial values for any desired initial epoch ( $T_0$ ) can be evaluated.

#### 4.35. Motion of the Mass Center of the Moon.

$X_0$  } These six values are the geocentric position and velocity  
 $Y_0$  } components of a Moon that moves in a Keplerian orbit. The  
 $Z_0$  } parameters of this orbit are taken identical to the mean  
 $\dot{X}_0$  } orbital elements of the true Moon at epoch  $T_0$ . ( $\Omega_0, \omega_0, \ell_0,$   
 $\dot{Y}_0$  }  $i_0, e_0, n_0$  — longitude of node, argument of perigee, mean  
 $\dot{Z}_0$  } anomaly, inclination, eccentricity, and mean motion). These  
 parameters are explicit functions of time as follows:

$$\begin{bmatrix} \Omega_0 \\ \omega_0 \\ \ell_0 \\ i_0 \\ e_0 \\ n_0 \end{bmatrix} = \begin{bmatrix} 4.523601515 & -0.9242202943 \cdot 10^{-3} & +0.271952 \cdot 10^{-13} & +0.07156 \cdot 10^{-20} \\ 1.311550024 & +0.2868588296 \cdot 10^{-2} & -0.162264 \cdot 10^{-12} & -0.5009 \cdot 10^{-20} \\ 5.168000340 & +0.2280271350 & +0.120256 \cdot 10^{-12} & +0.43616 \cdot 10^{-20} \\ 0.0898 & 0.0 & 0.0 & 0.0 \\ 0.0549 & 0.0 & 0.0 & 0.0 \\ 0.2299715030 & -0.296454 \cdot 10^{-13} & +0.02042 \cdot 10^{-20} & 0.0 \end{bmatrix} \cdot \begin{bmatrix} 1 \\ d \\ d^2 \\ d^3 \end{bmatrix}$$

The coefficients are in radians or radians per day<sup>i</sup> (i = 1, 2, 3); d = T<sub>0</sub> - T<sub>∞</sub> in Julian days; T<sub>∞</sub> = 2415020.0 J.D. The coefficients are from [AENA Supplement, 1961].

The transformation from Keplerian elements to state vector parameters X<sub>0</sub>, Y<sub>0</sub>, Z<sub>0</sub>,  $\dot{X}_0$ ,  $\dot{Y}_0$ ,  $\dot{Z}_0$  is performed using an iterative solution of Kepler's equation and well known formulae as given in textbooks [Mueller, 1964].

#### 4.36 Eulerian Angles of the Moon.

$$\begin{bmatrix} \varphi_0 \\ \psi_0 \\ \theta_0 \\ \dot{\varphi}_0 \\ \dot{\psi}_0 \\ \dot{\theta}_0 \end{bmatrix} = \begin{bmatrix} \omega_0 + \ell_0 + \pi \\ \Omega_0 \\ I_0 \\ \dot{\omega}_0 + \dot{\ell}_0 \\ \dot{\Omega}_0 \\ 0 \end{bmatrix} + \begin{bmatrix} \tau_0 - \sigma_0 \\ \sigma_0 \\ \rho_0 \\ \dot{\tau}_0 - \dot{\sigma}_0 \\ \dot{\sigma}_0 \\ \dot{\rho}_0 \end{bmatrix}$$

where

$$\pi = 3.14\dots \text{radians}$$

$\Omega_0, \omega_0, \ell_0$  are the same as defined for the Moon's Keplerian orbit.

$\dot{\Omega}_0, \dot{\omega}_0, \dot{\ell}_0$  are the time derivatives of the same quantities.

$\tau_0, \sigma_0, \rho_0, \dot{\tau}_0, \dot{\sigma}_0, \dot{\rho}_0$  are the physical libration angles and their time rates at T<sub>0</sub>.

The physical libration angles are obtained from the following expressions:

$$I_0 = 0.026769 \text{ radians}$$

$$\tau_0 = 1''.7 \sin \alpha_1 + 91''.6 \sin \alpha_2 - 1''.4 \sin \alpha_3 + 4''.2 \sin \alpha_4 - 3''.5 \sin \alpha_5 - 16''.9 \sin \alpha_6 + 1''.0 \sin \alpha_7 + 15''.3 \sin \alpha_8 + 10''.0 \sin \alpha_9$$

$$I_0 \dot{\sigma}_0 = -3''.0 \sin \alpha_1 - 10''.6 \sin \alpha_{10} - 23''.8 \sin \alpha_{11} + 2''.5 \sin \alpha_4 - 100''.6 \sin \alpha_6$$

$$\rho_0 = -3''.1 \cos \alpha_1 - 10''.8 \cos \alpha_{10} + 23''.8 \cos \alpha_{11} - 1''.9 \cos \alpha_4 - 98''.4 \cos \alpha_6$$

The coefficients for the physical libration angles are taken from [Eckhardt, 1970].

$\alpha_1 =$	$2F_0 - 2D_0$	$\alpha_7 =$	$2l_0 - l'_0$	$-2D_0$
$\alpha_2 =$	$l'_0$	$\alpha_8 =$	$2l_0$	$-2F_0$
$\alpha_3 =$	$l_0 - l'_0$	$\alpha_9 =$	$2l_0$	$-2D_0$
$\alpha_4 =$	$l_0$	$\alpha_{10} =$		$2F_0$
$\alpha_5 =$	$l_0$	$\alpha_{11} =$	$l_0$	$-2F_0$
$\alpha_6 =$	$l_0$			

Table 4.4 Arguments of the Terms in the Physical Librations Harmonic Series.

The arguments  $\alpha_i$  are linear combinations of the so called Delaunay arguments as given in Table 4.4 .

$l_0, l'_0, F_0, D_0$  are Delaunay arguments composed of parameters of the mean orbits of the Sun and the Moon and are explicit functions of time. They are evaluated for  $T_0$ . The coefficients are taken from [AENA Supplement, 1961].

$$F_0 = \omega_0 + l_0$$

$$l_0 = l_0$$

$$l'_0 = 6.256583523 + .01720196977 \cdot d - .1962403 \cdot 10^{-14} \cdot d^2 - .1075 \cdot 10^{-20} \cdot d^3$$

$$D_0 = 6.121523941 + .2127687117 \cdot d - .18786737 \cdot 10^{-13} \cdot d^2 + .068 \cdot 10^{-20} \cdot d^3$$

The coefficients are in radians or radians per day<sup>i</sup> ( $i = 1, 2, 3$ );  $d = T_0 - T_{00}$  in Julian days;  $T_{00} = 2415020.0$  (1900.0).

$l'_0$  is the mean anomaly of the Sun

$D_0$  is the mean elongation of the Moon from the Sun

For  $\dot{\tau}_0, \dot{\sigma}_0, \dot{\rho}_0$ , the trigonometric series for  $\tau, \sigma, \rho$  are differentiated and the values for  $\dot{l}_0, \dot{l}'_0, \dot{F}_0, \dot{D}_0$  are obtained by differentiation with respect to time of the series for these quantities.

4.37. Eulerian Angles of the Earth.

$$\begin{bmatrix} \eta_0 \\ \lambda_0 \\ \epsilon_0 \\ \dot{\eta}_0 \\ \dot{\lambda}_0 \\ \dot{\epsilon}_0 \end{bmatrix} = \begin{bmatrix} -1.73993589 & 6.300388098 & 0.506407 \cdot 10^{-14} & 0.0 \\ 0.0 & 0.0 & 0.0 & 0.0 \\ 0.4093197475 & -0.6217959 \cdot 10^{-8} & -0.214556 \cdot 10^{-16} & 0.18 \cdot 10^{-21} \\ 6.300388098 & 1.012814 \cdot 10^{-14} & 0.0 & 0.0 \\ 0.0 & 0.0 & 0.0 & 0.0 \\ -0.6217959 \cdot 10^{-8} & -0.429112 \cdot 10^{-16} & 0.36 \cdot 10^{-21} & 0.0 \end{bmatrix} \cdot \begin{bmatrix} 1 \\ d \\ d^2 \\ d^3 \end{bmatrix}$$

The coefficients are in radians or radians per day<sup>i</sup> (i = 1, 2, 3); d = T<sub>0</sub> - T<sub>00</sub> in Julian days; T<sub>00</sub> = 2415020.0 JD (1900.0). The coefficients are taken from [AENA Supplement, 1961] and also from [Mueller, 1969].

#### 4.4 Equations of Motion

The constants and postulates as outlined in sections 4.2 and 4.3 are used to derive the equations of motion of the bodies in the simulated system with respect to the fundamental inertial coordinate system (X Y Z) centered at the barycenter. However in order to generate data sets of the same nature as the ones available for the real Earth-Moon environment and also to generate observational data that will conform with the reduction model as proposed in Chapter 2, various transformations of origin will be introduced to the equations of motion.

The data sets to be generated are as follows (see Figure 4.2):

- (a) Cartesian coordinates of the Moon's mass center with respect to an inertially oriented geocentric coordinate system (X Y Z).
- (b) Eulerian orientation angles of the selenographic coordinate system (x y z) with respect to an inertially oriented selenocentric coordinate system (X Y Z).
- (c) Eulerian orientation angles of the average terrestrial coordinate system (U V W) with respect to an inertially-oriented geocentric coordinate system.
- (d) Cartesian coordinates of a satellite in an inertially oriented selenocentric coordinate system (X Y Z).

The inertially oriented systems in (a), (b), (c), and (d) are all parallel to the fundamental coordinate system as defined in section 4.2.

##### Symbols in the derivation of the equations of motion.

- $k^2$  - universal gravitational constant
- E - mass of the Earth
- $M = \frac{E}{m}$  - mass of the Moon
- A, B, C - principal moments of inertia of the Earth, where  $A = B$
- $A', B', C'$  - principal moments of inertia of the Moon, where  $A' < B' < C'$
- $a_e$  - major semiaxis of Earth reference ellipsoid.

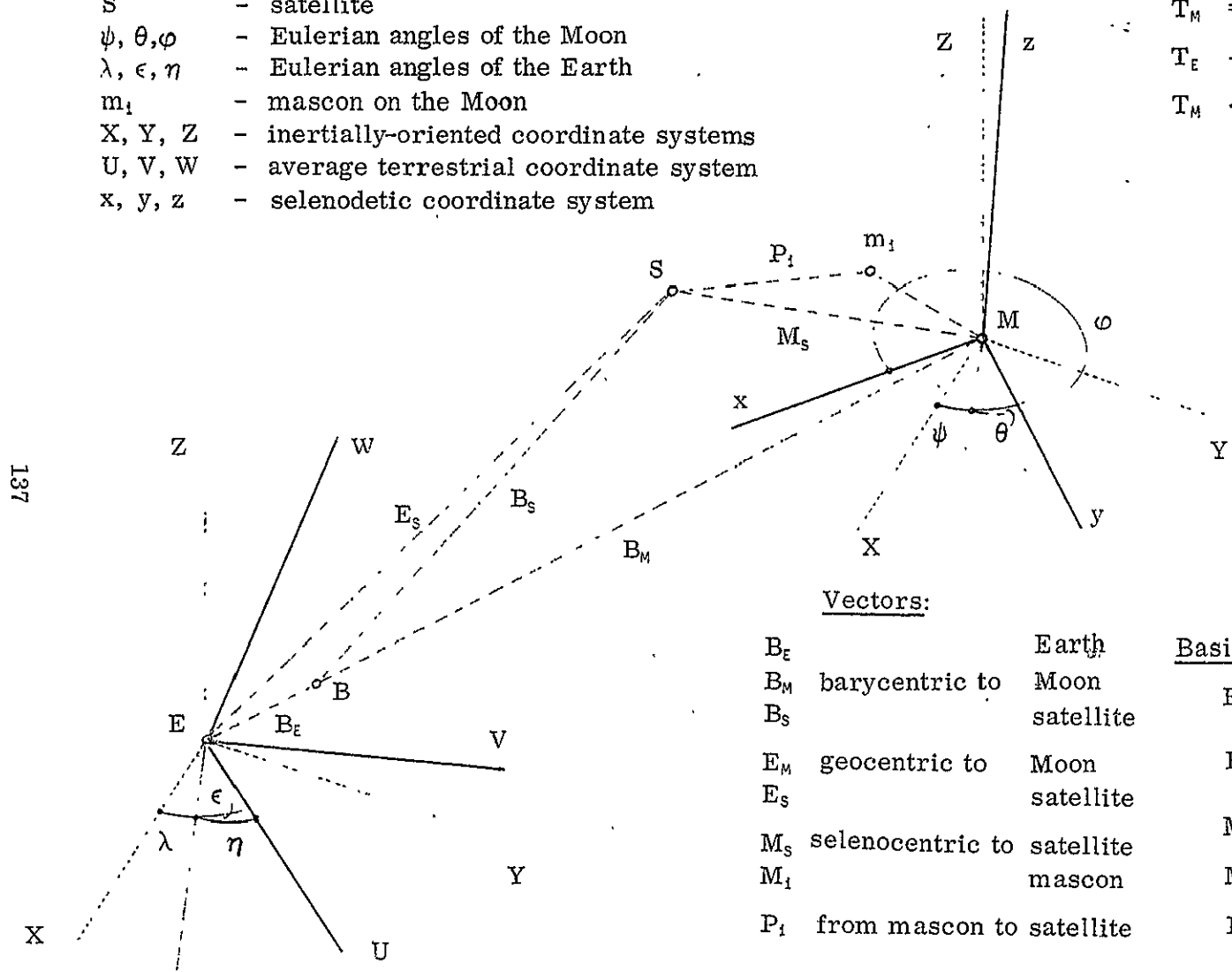
- E - Earth mass center
- M - Moon mass center
- B - barycenter
- S - satellite
- $\psi, \theta, \varphi$  - Eulerian angles of the Moon
- $\lambda, \epsilon, \eta$  - Eulerian angles of the Earth
- $m_1$  - mascon on the Moon
- X, Y, Z - inertially-oriented coordinate systems
- U, V, W - average terrestrial coordinate system
- x, y, z - selenodetic coordinate system

Orthogonal transformation matrices:

$$T_E = R_3(\eta) \cdot R_1(-\epsilon) \cdot R_3(\lambda)$$

$$T_M = R_3(\varphi) \cdot R_1(-\theta) \cdot R_3(\psi)$$

$T_E$  - from XYZ to UVW  
 $T_M$  - from XYZ to xyz



Vectors:

- $B_E$  Earth
- $B_M$  barycentric to Moon
- $B_S$  satellite
- $E_M$  geocentric to Moon
- $E_S$  satellite
- $M_S$  selenocentric to satellite
- $M_1$  mascon
- $P_1$  from mascon to satellite

Basic Vector relations:

$$E_M = B_M - B_E$$

$$B_M = \frac{m}{1+m} \cdot E_M$$

$$M_S = B_S - B_M = B_S - B_E - E_M$$

$$M_1 = T_M^T \cdot M_{11}$$

$$P_1 = B_S - B_M - M_1$$

Figure 4.2. The Simulated Earth-Moon Environment.

$a_m = \frac{a_e}{\xi}$	- radius of Moon reference sphere
$J_2$	- second-order zonal harmonic of the Earth
$C_{20}, C_{22}$	- second-order harmonics of the triaxial (basic) Moon dynamic figure
$\mu = \frac{C - A}{A}$	- dynamic "flattening" of the Earth
$\beta = \frac{C' - A'}{B'}$	- dynamic "flattening" of the Moon
$\mu_i = \frac{m}{M}$	- ratio of mass of i - th mascon with respect to the total mass of the Moon.

#### 4.41 Equations of Motion of the Moon's Mass Center.

The potential of the Earth and the Moon integrated over the masses of the two bodies is given by MacCullagh's formula [ Brouwer and Clemence, 1961, p. 132 ] .

$$V = k^2 \left\{ \frac{E \cdot M}{\rho} + \frac{E}{2\rho^3} [ A' + B' + C' - 3(A' \alpha'^2 + B' \beta'^2 + C' \gamma'^2) ] \right. \\ \left. + \frac{M}{2\rho^3} [ 2A + C - 3(A \cdot \alpha^2 + A \cdot \beta^{*2} + C \gamma^2) ] \right\} \quad (4.41.1)$$

where  $\rho$                       absolute magnitude of vector  $E_m$  (distance Earth-Moon)  
 $\alpha, \beta, \gamma$                     direction cosines of Earth in UVW system  
 $\alpha', \beta', \gamma'$                 direction cosines of Moon in xyz system.

The potential  $V$  is interpreted as being equivalent to the work to be done in bringing the Moon from infinity to its instantaneous position and orientation in the fundamental barycentric coordinate system, while the Earth is kept fixed in its instantaneous position and orientation [Plummer, 1918]. The potential of the mascons is ignored in this analysis which is permissible regarding the specific way by which the mascons were designed (see Appendix C).

Because of the rotational symmetry of the dynamical figure of the Earth the following hold:

$$\alpha^2 + \beta^{*2} + \gamma^2 = 1; \quad \alpha^2 + \beta^{*2} = 1 - \gamma^2$$

$$A(\alpha^2 + \beta^{*2}) + C\gamma^2 = A + (C - A)\gamma^2$$

The expression for the potential V (4.41.1) is transformed in terms of auxiliary expressions in order to facilitate its subsequent differentiation.

$$V = k^2 \left\{ \frac{EM}{\rho} + \frac{E}{2\rho^3} \left[ (A' + B' + C') - 3[\alpha' \beta' \gamma'] \cdot \begin{bmatrix} A' & 0 & 0 \\ 0 & B' & 0 \\ 0 & 0 & C' \end{bmatrix} \begin{bmatrix} \alpha' \\ \beta' \\ \gamma' \end{bmatrix} \right] + \frac{M}{2\rho^3} (C - A)(1 - 3\gamma^2) \right\} \quad (4.41.2)$$

From Appendix A it follows

$$A' + B' + C' = \frac{M a_n^2}{\beta} [- (3 + \beta) C_{20} + (6 - 6\beta) C_{22}] = \frac{E \cdot a_e^2}{m \cdot \beta \cdot \xi^2} \cdot D \quad ; \quad (4.41.3)$$

$$\begin{bmatrix} A' & 0 & 0 \\ 0 & B' & 0 \\ 0 & 0 & C' \end{bmatrix} = \frac{M a_n^2}{\beta} \begin{bmatrix} -C_{20} + (2 - 4\beta) C_{22} & 0 & 0 \\ 0 & -C_{20} + 2 C_{22} & 0 \\ 0 & 0 & -(1 + \beta) C_{20} + (2 - 2\beta) C_{22} \end{bmatrix} = \frac{E \cdot a_e^2}{m \cdot \beta \cdot \xi^2} G \quad ; \quad (4.41.4)$$

$$C - A = E a_e^2 \cdot J_2 \quad . \quad (4.41.5)$$

According to Figure 4.2 and setting  $X = \begin{bmatrix} X_1 \\ X_2 \\ X_3 \end{bmatrix} \equiv E_n$ ,

$X_1, X_2, X_3$  being the vector components of  $E_M$  in the inertial coordinate system, the following expressions hold:

$$\begin{bmatrix} \alpha' \\ \beta' \\ \gamma' \end{bmatrix} = T_M \cdot \frac{X}{\rho} \quad \text{and} \quad \begin{bmatrix} \alpha \\ \beta \\ \gamma \end{bmatrix} = T_E \cdot \frac{-X}{\rho}$$

$\rho$  was defined earlier as  $\rho = (X_1^2 + X_2^2 + X_3^2)^{\frac{1}{2}} = (X^T \cdot X)^{\frac{1}{2}}$ .

Another  $3 \times 3$  matrix is defined:

$$L = \begin{bmatrix} 0 & 0 & 0 \\ 0 & 0 & 0 \\ 0 & 0 & 1 \end{bmatrix} \quad (4.41.6)$$

Substituting the array of new symbols in  $V$  and after some rearrangement

$$\begin{aligned} V &= k^2 E^2 \left[ \frac{1}{m \rho} + \frac{1}{2 \rho^3} \cdot \frac{a_e^2}{m \cdot \beta \cdot \xi^2} \left( D - \frac{3}{\rho^2} X^T T_M^T G T_M X \right) + \right. \\ &\quad \left. + \frac{1}{2 \rho^3} \cdot \frac{a_e^2 \cdot J_2}{m} \left( 1 - \frac{3}{\rho^2} X^T T_E^T L T_E X \right) \right] \\ &= \frac{k^2 E^2}{m} \left[ \frac{1}{\rho} + \frac{a_e^2}{2 \rho^3} \left( \frac{D}{\beta \cdot \xi^2} + J_2 \right) - \frac{3 a_e^2}{2 \rho^5} \left( \frac{X^T T_M^T G T_M X}{\beta \cdot \xi^2} + J_2 X^T T_E^T L T_E X \right) \right] \quad (4.41.7) \end{aligned}$$

This is the final form of the potential which will be differentiated with respect to  $B_M$  and  $B_E$  to obtain the barycentric equations of motion of the Moon and of the Earth.

Let  $\varphi$  be a function of  $X$  and implicitly of  $B_E$  and  $B_M$  (as  $X = B_M - B_E$ )

$$\frac{\partial \varphi}{\partial B_E} = \frac{\partial \varphi}{\partial X} \cdot \frac{\partial X}{\partial B_E} \quad ; \quad \frac{\partial \varphi}{\partial B_M} = \frac{\partial \varphi}{\partial X} \cdot \frac{\partial X}{\partial B_M}$$

$$\frac{\partial X}{\partial B_E} = -I_{(3 \times 3)} \quad ; \quad \frac{\partial X}{\partial B_M} = I_{(3 \times 3)}$$

$$\frac{\partial \varphi}{\partial B_E} = - \frac{\partial \varphi}{\partial X} \quad ; \quad \frac{\partial \varphi}{\partial B_M} = \frac{\partial \varphi}{\partial X}$$

The equations of motion of a body are identified with the second derivatives with respect to time of its position vector and are denoted by the symbol of the position vector with two upper dots.

Thus

$X$  is the position vector of the body  $X$   
 $\dot{X}$  is the velocity vector of  $X$   
 $\ddot{X}$  is the acceleration vector of  $X$  identified with the equations of motion of the body  $X$ .

The equations of motion of the Moon ( $\ddot{B}_M$ ) are obtained as the derivatives of the potential ( $V$ ) with respect to the barycentric position vector of the Moon ( $B_M$ ) divided by the total mass of the Moon ( $M$ ) [Brouwer and Clemence, 1961, p. 132]. Similar procedure is applied for the Earth.

$$\frac{d^2 B_M}{dt^2} = \ddot{B}_M = \frac{1}{M} \cdot \left[ \frac{\partial V}{\partial B_M} \right]^T = \frac{m}{E} \cdot \left[ \frac{\partial V}{\partial X} \right]^T \quad (4.41.8)$$

$$\frac{d^2 B_E}{dt^2} = \ddot{B}_E = \frac{1}{E} \cdot \left[ \frac{\partial V}{\partial B_E} \right]^T = -\frac{1}{E} \cdot \left[ \frac{\partial V}{\partial X} \right]^T \quad (4.41.9)$$

The points  $E$ ,  $B$ , and  $M$  are on a straight line and so it follows

$$X = B_M - B_E \quad (4.41.10)$$

Equation (4.41.10) differentiated twice with respect to time results in the geocentric equations of motion of the Moon :

$$\ddot{X} = \ddot{B}_M - \ddot{B}_E = \left( \frac{m}{E} + \frac{1}{E} \right) \cdot \left[ \frac{\partial V}{\partial X} \right]^T = \frac{m+1}{E} \cdot \left[ \frac{\partial V}{\partial X} \right]^T \quad (4.41.11)$$

Equation (4.41.7) is differentiated with respect to X using rules as developed in Appendix E.

$$\left[ \frac{\partial V}{\partial X} \right]^T = \frac{k^2 E^2}{m} \left[ \frac{X}{\rho^3} - \frac{3 a_e^2 X}{2 \rho^5} \left( \frac{D}{\beta \cdot \xi^2} + J_2 \right) + \frac{15 a_e^2 \cdot X}{2 \rho^7} \left( \frac{X^T T_M^T G T_M X}{\beta \cdot \xi^2} + J_2 X^T T_E^T L T_E X \right) - \frac{3 a_e^2}{2 \rho^5} \left( \frac{2 T_M^T G T_M X}{\beta \cdot \xi^2} + 2 J_2 T_E^T L T_E X \right) \right] \quad (4.41.12)$$

A new set of auxiliaries is defined:

$$\bar{P} = \frac{3 a_e^2}{\beta \cdot \xi^2} T_M^T G T_M ; \quad \bar{Q} = 3 a_e^2 J_2 T_E^T L T_E$$

$$\bar{H} = \frac{3 a_e^2}{2 \beta \cdot \xi^2} D ; \quad \bar{E} = \frac{3 a_e^2 J_2}{2}$$

Rearranging  $\frac{\partial V}{\partial X}$  and substituting the auxiliaries:

$$\begin{aligned} \left[ \frac{\partial V}{\partial X} \right]^T &= - \frac{k^2 E^2}{m} \left[ \frac{1}{\rho^3} + \frac{\bar{H} + \bar{E}}{\rho^5} - \frac{\frac{5}{2} \cdot X X^T (\bar{P} + \bar{Q})}{\rho^7} + \frac{\bar{P} + \bar{Q}}{\rho^5} \right] X \\ &= - \frac{k^2 E^2}{m} \left[ \frac{1}{\rho^3} + \frac{\bar{H} + \bar{E}}{\rho^5} + \frac{(\rho^2 I - \frac{5}{2} X X^T) \cdot (\bar{P} + \bar{Q})}{\rho^7} \right] X \quad (4.41.13) \end{aligned}$$

I is the 3 x 3 identity matrix. Equation (4.41.13) is substituted in (4.41.11)

$$\ddot{X} = \frac{m+1}{E} \cdot \left[ \frac{\partial V}{\partial X} \right]^T = - k^2 E \left( 1 + \frac{1}{m} \right) \left[ \frac{1}{\rho^3} + \frac{\bar{H} + \bar{E}}{\rho^5} + \frac{(\rho^2 I - \frac{5}{2} X X^T) \cdot (\bar{P} + \bar{Q})}{\rho^7} \right] X \quad (4.41.14)$$

These are Cowell's equations of motion of the Moon's mass center with respect to a geocentric inertially oriented coordinate system.

4.42 Equations of Motion of the Selenodetic Coordinate System with Respect to a Selenocentric Inertially Oriented System.

The motion of a rigid body about its center of mass satisfies Euler's dynamic equations (Plummer, 1918, p. 292)

$$\begin{bmatrix} \dot{\omega}_x \\ \dot{\omega}_y \\ \dot{\omega}_z \end{bmatrix} = \begin{bmatrix} \alpha & 0 & 0 \\ 0 & -\beta & 0 \\ 0 & 0 & \gamma \end{bmatrix} \cdot \left( \begin{bmatrix} N_x \\ N_y \\ N_z \end{bmatrix} - \begin{bmatrix} \omega_y \omega_z \\ \omega_x \omega_z \\ \omega_x \omega_y \end{bmatrix} \right). \quad (4.42.1)$$

For this section only,  $\alpha$  and  $\gamma$  are defined as follows:

$$\alpha = \frac{C' - B'}{A'}$$

$A', B', C'$  are principal moments of inertia of the Moon

$$\gamma = \frac{B' - A'}{C'}$$

$$\beta = \frac{C' - A'}{B'}$$

as defined already.

$\begin{bmatrix} \omega_x \\ \omega_y \\ \omega_z \end{bmatrix}$  are rotational velocities of the Moon around axes x, y, and z respectively

$\begin{bmatrix} N_x \\ N_y \\ N_z \end{bmatrix}$  are moments of external forces acting on the Moon around axes x, y and z

As it is the equations of motion (second time derivatives) of the Eulerian angles  $(\varphi, \psi, \theta)$ , which are of interest, Euler's geometric equations are used to relate the rotational velocities  $(\omega_x, \omega_y, \omega_z)$  to the angles  $(\varphi, \psi, \theta)$  and their time derivatives (see Figure 4.3) :

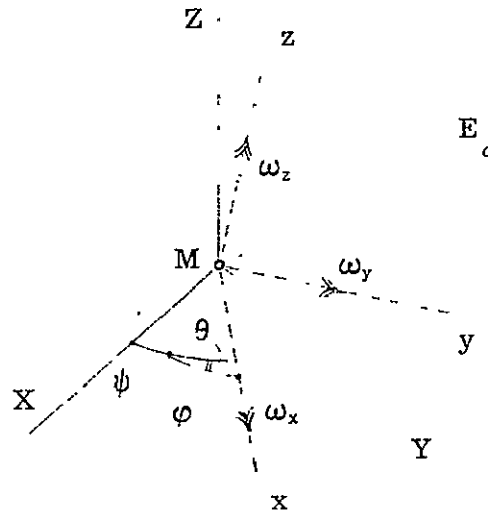


Figure 4.3 Eulerian Angles of the Moon

$$\begin{bmatrix} \omega_x \\ \omega_y \\ \omega_z \end{bmatrix} = \begin{bmatrix} 0 & -\sin\varphi \sin\theta & -\cos\varphi \\ 0 & -\cos\varphi \sin\theta & \sin\varphi \\ 1 & \cos\theta & 0 \end{bmatrix} \cdot \begin{bmatrix} \dot{\varphi} \\ \dot{\psi} \\ \dot{\theta} \end{bmatrix} \quad (4.42.2)$$

Differentiating Euler's geometric equations with respect to time

$$\begin{aligned} \begin{bmatrix} \dot{\omega}_x \\ \dot{\omega}_y \\ \dot{\omega}_z \end{bmatrix} &= \begin{bmatrix} 0 & -\sin\varphi \sin\theta & -\cos\varphi \\ 0 & -\cos\varphi \sin\theta & \sin\varphi \\ 1 & \cos\theta & 0 \end{bmatrix} \cdot \begin{bmatrix} \ddot{\varphi} \\ \ddot{\psi} \\ \ddot{\theta} \end{bmatrix} + \begin{bmatrix} 0 & -\cos\varphi \sin\theta & \sin\varphi \\ 0 & \sin\varphi \sin\theta & \cos\varphi \\ 0 & 0 & 0 \end{bmatrix} \cdot \dot{\varphi} \cdot \begin{bmatrix} \dot{\varphi} \\ \dot{\psi} \\ \dot{\theta} \end{bmatrix} + \\ &+ \begin{bmatrix} 0 & -\sin\varphi \cos\theta & 0 \\ 0 & -\cos\varphi \cos\theta & 0 \\ 0 & -\sin\theta & 0 \end{bmatrix} \cdot \dot{\theta} \cdot \begin{bmatrix} \dot{\varphi} \\ \dot{\psi} \\ \dot{\theta} \end{bmatrix} \quad (4.42.3) \end{aligned}$$

Regrouping

$$\begin{bmatrix} \dot{\omega}_x \\ \dot{\omega}_y \\ \dot{\omega}_z \end{bmatrix} = \begin{bmatrix} 0 & -\sin\varphi \sin\theta & -\cos\varphi \\ 0 & -\cos\varphi \sin\theta & \sin\varphi \\ 1 & \cos\theta & 0 \end{bmatrix} \begin{bmatrix} \ddot{\varphi} \\ \ddot{\psi} \\ \ddot{\theta} \end{bmatrix} + \begin{bmatrix} -\sin\varphi \cos\theta & -\cos\varphi \sin\theta & \sin\varphi \\ -\cos\varphi \cos\theta & \sin\varphi \sin\theta & \cos\varphi \\ -\sin\theta & 0 & 0 \end{bmatrix} \begin{bmatrix} \dot{\psi} \dot{\theta} \\ \dot{\psi} \dot{\varphi} \\ \dot{\theta} \dot{\varphi} \end{bmatrix} \quad (4.42.4)$$

This expression (4.42.4) is substituted into Euler's dynamic equations (4.42.1),

the matrix in front of  $\begin{bmatrix} \ddot{\varphi} \\ \ddot{\psi} \\ \ddot{\theta} \end{bmatrix}$  is inverted and the second term is transposed to the right hand side. The results are the equations of motion of the angles  $\varphi, \psi, \theta$ :

$$\begin{bmatrix} \ddot{\varphi} \\ \ddot{\psi} \\ \ddot{\theta} \end{bmatrix} = \begin{bmatrix} 0 & -\sin\varphi \sin\theta & -\cos\varphi \\ 0 & -\cos\varphi \sin\theta & \sin\varphi \\ 1 & \cos\theta & 0 \end{bmatrix}^{-1} \begin{bmatrix} \alpha & 0 & 0 \\ 0 & -\beta & 0 \\ 0 & 0 & \gamma \end{bmatrix} \begin{bmatrix} N_x - \omega_y \omega_z \\ N_y - \omega_x \omega_z \\ N_z - \omega_x \omega_y \end{bmatrix} - \begin{bmatrix} -\sin\varphi \cos\theta & -\cos\varphi \sin\theta & \sin\varphi \\ -\cos\varphi \cos\theta & \sin\varphi \sin\theta & \cos\varphi \\ -\sin\theta & 0 & 0 \end{bmatrix} \begin{bmatrix} \dot{\psi} \dot{\theta} \\ \dot{\psi} \dot{\varphi} \\ \dot{\theta} \dot{\varphi} \end{bmatrix} \quad (4.42.5)$$

The moments  $N_x, N_y, N_z$  are functions of the mass of the disturbing body (the Earth) and its position with respect to the x,y,z system.

The position of the Earth in the selenodetic system  $\begin{bmatrix} x \\ y \\ z \end{bmatrix}$  can be obtained from the geocentric ephemeris of the Moon given in the XYZ system. A change in sign and a transformation through the Eulerian angles ( $\varphi, \psi, \theta$ ) is necessary to perform the conversion as follows:

$$\begin{bmatrix} x \\ y \\ z \end{bmatrix} = T_M \cdot (-X)$$

where

$$T_M = R_3(\rho) \cdot R_1(-\theta) \cdot R_3(\psi) \quad \begin{array}{l} \text{as defined in earlier} \\ \text{sections of this chapter} \end{array}$$

$X$  is the geocentric position of the Moon in the XYZ system

$\rho$  is the distance between the centers of mass of the Earth and the Moon.

The moments of the external forces are obtained as follows:

$$\begin{bmatrix} N_x \\ N_y \\ N_z \end{bmatrix} = \frac{3 \cdot k^2 E}{\rho^5} \begin{bmatrix} y \cdot z \\ x \cdot z \\ x \cdot y \end{bmatrix} \quad (4.42.6)$$

The moments of inertia  $A'$ ,  $B'$ ,  $C'$  can be expressed in terms of the second degree harmonics as follows (see Appendix A):

$$\begin{bmatrix} A' \\ B' \\ C' \end{bmatrix} = \frac{E a c^2}{m \cdot \beta \cdot \xi^2} \begin{bmatrix} -C_{20} + (2 - 4\beta) \cdot C_{22} \\ -C_{20} \quad \quad \quad 2 \cdot C_{22} \\ -(1 + \beta) \cdot C_{20} + (2 - 2\beta) \cdot C_{22} \end{bmatrix} \quad (4.42.7)$$

All quantities on the right side have been numerically defined as basic constants of the simulation in Section 4.3 and also

$$\alpha = \frac{C' - B'}{A'} ; \quad \gamma = \frac{B' - A'}{C'}$$

Performing the inversion in equations (4.42.5) analytically and substituting (4.42.6) it follows:

$$\begin{bmatrix} \ddot{\varphi} \\ \ddot{\psi} \\ \ddot{\theta} \end{bmatrix} = \begin{bmatrix} \cos \theta \sin \varphi / \sin \theta & \cos \theta \cos \varphi / \sin \theta & 1 \\ -\sin \varphi / \sin \theta & -\cos \varphi / \sin \theta & 0 \\ -\cos \varphi & \sin \varphi & 0 \end{bmatrix} \cdot \begin{bmatrix} \alpha & 0 & 0 \\ 0 & -\beta & 0 \\ 0 & 0 & \gamma \end{bmatrix} \cdot \left\langle \frac{3k^2 E}{\rho^5} \begin{bmatrix} y \cdot z \\ x \cdot z \\ x \cdot y \end{bmatrix} \right. \\ \left. - \begin{bmatrix} \omega_y \omega_z \\ \omega_x \omega_z \\ \omega_x \omega_y \end{bmatrix} \cdot \begin{bmatrix} -\sin \varphi \cos \theta & -\cos \varphi \sin \theta & \sin \varphi \\ -\cos \varphi \cos \theta & \sin \varphi \sin \theta & \cos \varphi \\ -\sin \theta & 0 & 0 \end{bmatrix} \cdot \begin{bmatrix} \dot{\psi} & \dot{\theta} \\ \dot{\psi} & \dot{\varphi} \\ \dot{\theta} & \dot{\varphi} \end{bmatrix} \right) \quad (4.42.8)$$

$\begin{bmatrix} \omega_x \\ \omega_y \\ \omega_z \end{bmatrix}$  are functions of  $\varphi, \psi, \theta, \dot{\varphi}, \dot{\psi}, \dot{\theta}$ , through Euler's geometric equations.

Equations (4.42.8) are Cowell's equations of rotational motion of the Moon about its mass center. On the right side of these equations there are functions of the following quantities:

$\varphi, \psi, \theta, \dot{\varphi}, \dot{\psi}, \dot{\theta}, X_1, X_2, X_3, \rho$  and also

$k^2 E, a_e, m, \beta, \xi, C_{20}, C_{22}$

The first group is composed of quantities that are being integrated as shown in this section and also in 4.41. The second group is composed of basic constants of the simulation.

#### 4.43 Equations of Motion of the Average Terrestrial Coordinate System with Respect to a Geocentric Inertially-Oriented Coordinate System.

The approach is similar to that applied to the motion of the Moon.



Euler's dynamic equations assume the following form:

$$\begin{bmatrix} \dot{\omega}_U \\ \dot{\omega}_V \end{bmatrix} = \mu \left\{ \frac{3k^2 E}{m \cdot \rho^3} \cdot \begin{bmatrix} VW \\ -UW \end{bmatrix} - \begin{bmatrix} \omega_V & \omega_W \\ -\omega_U & \omega_W \end{bmatrix} \right\} \quad (4.43.1)$$

As a result of  $\gamma = 0$  it follows:

$$\begin{aligned} \dot{\omega}_W &= 0 \\ \omega_W &= \text{constant} = \omega_3 \quad \text{an adopted constant in the simulation.} \end{aligned}$$

Euler's geometric equations (see Figure 4.4)

$$\begin{bmatrix} \omega_U \\ \omega_V \\ \omega_W \end{bmatrix} = \begin{bmatrix} 0 & -\sin \eta \sin \epsilon & -\cos \eta \\ 0 & -\cos \eta \sin \epsilon & \sin \eta \\ 1 & \cos \epsilon & 0 \end{bmatrix} \cdot \begin{bmatrix} \dot{\eta} \\ \dot{\lambda} \\ \dot{\epsilon} \end{bmatrix} \quad (4.43.2)$$

From the third equation in (4.43.2)

$$\omega_W = \dot{\eta} + \cos \epsilon \dot{\lambda} \quad (4.43.3)$$

but  $\omega_W = \omega_3 = \text{constant}$ ; so it follows:

$$\dot{\omega}_W = 0 = \ddot{\eta} + \cos \epsilon \ddot{\lambda} - \sin \epsilon \dot{\epsilon} \dot{\lambda} \quad (4.43.4)$$

$$\ddot{\eta} = \sin \epsilon \dot{\epsilon} \dot{\lambda} - \cos \epsilon \ddot{\lambda}$$

Now the first two geometric equations (4.43.2) are differentiated and regrouped

$$\begin{bmatrix} \dot{\omega}_U \\ \dot{\omega}_V \end{bmatrix} = \begin{bmatrix} -\sin \eta \sin \epsilon & -\cos \eta \\ -\cos \eta \sin \epsilon & \sin \eta \end{bmatrix} \cdot \begin{bmatrix} \ddot{\lambda} \\ \ddot{\epsilon} \end{bmatrix} + \begin{bmatrix} -\sin \eta \cos \epsilon & -\cos \eta \sin \epsilon & \sin \eta \\ -\cos \eta \cos \epsilon & \sin \eta \sin \epsilon & \cos \eta \end{bmatrix} \cdot \begin{bmatrix} \dot{\lambda} \dot{\epsilon} \\ \dot{\lambda} \dot{\eta} \\ \dot{\epsilon} \dot{\eta} \end{bmatrix}$$

From equation (4.43.3) it follows:

$$\dot{\eta} = \omega_3 - \cos \epsilon \dot{\lambda} \quad (4.43.5)$$

The coordinates of the disturbing body (the Moon) are obtained as follows:

$$\begin{bmatrix} U \\ V \\ W \end{bmatrix} = T_E \cdot X$$

where

$U, V, W$  - are the vector components of the moon mass center in the average terrestrial coordinate system.

$T_E = R_3(\eta) \cdot R_1(-\epsilon) \cdot R_3(\lambda)$  as defined earlier.

The same mathematical procedure is followed as for the Moon and the expression is

$$\begin{aligned} \begin{bmatrix} \ddot{\lambda} \\ \ddot{\epsilon} \end{bmatrix} &= \begin{bmatrix} -\sin\eta \sin\epsilon & -\cos\eta \\ -\cos\eta \sin\epsilon & \sin\eta \end{bmatrix} \cdot \left( \frac{3 \cdot k^2 E \cdot \mu}{m \cdot \rho^5} \begin{bmatrix} VW \\ -UW \end{bmatrix} + \mu \cdot \omega_3 \begin{bmatrix} \cos\eta \sin\epsilon & -\sin\eta \\ -\sin\eta \sin\epsilon & -\cos\eta \end{bmatrix} \cdot \begin{bmatrix} \dot{\lambda} \\ \dot{\epsilon} \end{bmatrix} \right. \\ &\quad \left. + \begin{bmatrix} \sin\eta \cos\epsilon & \cos\eta \sin\epsilon & -\sin\eta \\ \cos\eta \cos\epsilon & -\sin\eta \sin\epsilon & -\cos\eta \end{bmatrix} \cdot \begin{bmatrix} \dot{\lambda} \dot{\epsilon} \\ \dot{\lambda} (\omega_3 - \cos\epsilon \dot{\lambda}) \\ \dot{\epsilon} (\omega_3 - \cos\epsilon \dot{\lambda}) \end{bmatrix} \right) \quad (4.43.6) \end{aligned}$$

The inversion is performed and after some regrouping the final form is

$$\begin{aligned} \begin{bmatrix} \ddot{\lambda} \\ \ddot{\epsilon} \end{bmatrix} &= \begin{bmatrix} -\sin\eta/\sin\epsilon & -\cos\eta/\sin\epsilon \\ -\cos\eta & \sin\eta \end{bmatrix} \cdot \left( \frac{3 k^2 E \mu}{m \cdot \rho^5} \cdot \begin{bmatrix} VW \\ -UW \end{bmatrix} + \right. \\ &\quad \left. + \begin{bmatrix} \sin\eta \cos\epsilon & \cos\eta \sin\epsilon & -\sin\eta \\ \cos\eta \cos\epsilon & -\sin\eta \sin\epsilon & -\cos\eta \end{bmatrix} \cdot \begin{bmatrix} \dot{\lambda} \dot{\epsilon} \\ \dot{\lambda} [\omega_3 (1+\mu) - \cos\epsilon \dot{\lambda}] \\ \dot{\epsilon} [\omega_3 (1+\mu) - \cos\epsilon \dot{\lambda}] \end{bmatrix} \right) \quad (4.43.7) \\ \ddot{\eta} &= \sin\epsilon \cdot \dot{\epsilon} \cdot \dot{\lambda} - \cos\epsilon \ddot{\lambda} \end{aligned}$$

These are Cowell's equations of motion of the Earth about its mass center. On the right side there are functions of the following quantities:  $\eta, \lambda, \epsilon, \dot{\eta}, \dot{\lambda}, \dot{\epsilon}, X_1, X_2, X_3, \rho$  which are integrated functions and also  $k^2 E, m, \mu, \omega_3$  which are constants of the simulation.

#### 4.44 Equations of Motion of a Satellite with Respect to a Selenocentric Inertially Oriented Coordinate System.

The approach is somewhat similar to the one used for the geocentric motion of the Moon's mass center.

Additional symbols in this section are:

		<u>Components in Inertially Oriented System</u>
$R = E_s$	$\rho_e = (R_1^2 + R_2^2 + R_3^2)^{\frac{1}{2}} = (R^T \cdot R)^{\frac{1}{2}}$	vector from Earth to satellite
$S = M_s$	$\rho_m = (S_1^2 + S_2^2 + S_3^2)^{\frac{1}{2}} = (S^T \cdot S)^{\frac{1}{2}}$	vector from Moon to satellite
$P_i \equiv P_1$	$\rho_1 = (P_{i1}^2 + P_{i2}^2 + P_{i3}^2)^{\frac{1}{2}} = (P_i^T \cdot P_i)^{\frac{1}{2}}$	vector from mascon to satellite

The potential of the Earth and the Moon at a point in space and for a unit mass is defined as follows:

$$V = k^2 \left\{ \frac{E}{\rho_e} + \frac{1}{2\rho_e^3} (C - A)(1 - 3\gamma^2) + \frac{M}{\rho_m} + \frac{1}{2\rho_m^3} [A' + B' + C' - 3(A'\alpha'^2 + B'\beta'^2 + C'\gamma'^2)] + M \cdot \sum_1 \frac{\mu_1}{\rho_1} \right\} \quad (4.44.1)$$

Substituting the auxiliaries L, D and G defined in section 4.41 ,

$$V = k^2 E \cdot \left\langle \frac{1}{\rho_e} + \frac{1}{2\rho_e^3} a e^2 J_2 (1 - 3\gamma^2) + \frac{1}{m} \left\{ \frac{1}{\rho_m} + \frac{1}{2\rho_m^3} \left[ \frac{3a_e^2 D}{\beta \cdot \xi^2} - \frac{3a_e^2}{\beta \cdot \xi^2} \cdot [\alpha' \beta' \gamma'] \cdot G \cdot \begin{bmatrix} \alpha' \\ \beta' \\ \gamma' \end{bmatrix} \right] + \sum_1 \frac{\mu_1}{\rho_1} \right\} \right\rangle \quad (4.44.2)$$

where

$$\begin{bmatrix} \alpha' \\ \beta' \\ \gamma' \end{bmatrix} = T_M \cdot S \qquad \begin{bmatrix} \alpha \\ \beta \\ \gamma \end{bmatrix} = T_E \cdot R$$

The auxiliaries L, D and G are substituted in (4.44.2):

$$V = k^2 E \left[ \frac{1}{\rho_e} + \frac{J_2 a_e^2}{2 \rho_e^3} - \frac{3 a_e^2 J_2}{2 \rho_e^5} \cdot R^T T_E^T L T_E R + \frac{1}{m} \left( \frac{1}{\rho_m} + \frac{a_e^2 D}{2 \beta \xi^2 \rho_m^3} - \frac{3 a_e^2}{2 \beta \xi^2 \rho_m^5} S^T T_M^T G T_M S + \sum_1 \frac{\mu_1}{\rho_1} \right) \right] \quad (4.44.3)$$

In general V is a function of the vectors R, S and P<sub>1</sub>

$$V = f_1(R) + f_2(S) + \sum_1 f_{(2+1)}(P_1) \quad (4.44.4)$$

Applying the chain rule in partial differentiation and noting th

$$\begin{aligned} B_S &= B_E + R \\ B_S &= B_M + S \\ B_S &= B_M + M_1 + P_1 \end{aligned}$$

the differentiation of V can be performed in parts as follow

$$\frac{\partial f_1}{\partial B_S} = \frac{\partial f_1}{\partial R} \cdot \frac{\partial R}{\partial B_S} ; \quad \frac{\partial R}{\partial B_S} = I \quad \text{so} \quad \frac{\partial f_1}{\partial B_S} = \frac{\partial f_1}{\partial R}$$

where I is the identity matrix. Following the same pattern

$$\frac{\partial f_2}{\partial B_S} = \frac{\partial f_2}{\partial S}$$

and also

$$\frac{\partial f_{2+i}}{\partial B_s} = \frac{\partial f_{2+i}}{\partial P_1}$$

The equations of motion of the satellite with respect to the barycenter are obtained in a way similar to those of the Moon and the Earth:

$$\left[ \ddot{B}_s \right]^T = \frac{\partial V}{\partial B_s} = \frac{\partial f_1}{\partial R} + \frac{\partial f_2}{\partial S} + \frac{\partial f_{2+i}}{\partial P_1} \quad (4.44.5)$$

The functions  $f_1(R)$ ,  $f_2(S)$  and  $f_{(2+i)}(P_i)$  are written explicitly

$$\begin{aligned} V = & k^2 E \left( \frac{1}{\rho_e} + \frac{a_e^2 J_2}{2 \rho_e^3} - \frac{3 a_e^2 J_2}{2 \rho_e^5} R^T T_E^T L T_E R \right) \\ & + \frac{k^2 E}{m} \left( \frac{1}{\rho_m} + \frac{a_e^2 D}{2 \beta \xi^2 \rho_m^3} - \frac{3 a_e^2}{2 \beta \xi^2 \rho_m^5} S^T T_M^T G T_M S \right) \\ & + \frac{k^2 E}{m} \sum_i \frac{\mu_i}{\rho_i} \quad (4.44.6) \end{aligned}$$

Differentiating functions  $f_1, f_2, f_{2+i}$  ( $i = 1, \dots, 12$ ) by  $R, S$  and  $P_i$ , respectively

$$\begin{aligned} \ddot{B}_s = & -k^2 E \left\{ \left( \frac{1}{\rho_e^3} + \frac{3 a_e^2 J_2}{2 \rho_e^5} - \frac{15 a_e^2 J_2}{2 \rho_e^7} R R^T T_E^T L T_E + \frac{3 a_e^2 J_2}{\rho_e^5} T_E^T L T_E \right) R + \right. \\ & + \frac{1}{m} \left[ \left( \frac{1}{\rho_m^3} + \frac{3 a_e^2 D}{2 \beta \xi^2 \rho_m^5} - \frac{15 a_e^2}{2 \beta \xi^2 \rho_m^7} S S^T T_M^T G T_M - \frac{3 a_e^2}{\beta \xi^2 \rho_m^5} T_M^T G T_M \right) S + \right. \\ & \left. \left. + \sum_i \frac{\mu_i}{\rho_i^3} P_i \right] \right\} \quad (4.44.7) \end{aligned}$$

Substituting the auxiliaries  $\bar{P}, \bar{Q}, \bar{E}, \bar{H}$  as defined in section 4.41

$$\begin{aligned} \ddot{B}_s = & -k^2 E \left\{ \left( \frac{1}{\rho_e^3} + \frac{\bar{E}}{\rho_e^5} + \frac{(\rho_e^2 I - \frac{5}{2} R R^T) \bar{Q}}{\rho_e^7} \right) R + \frac{1}{m} \left[ \frac{1}{\rho_m^3} + \frac{\bar{H}}{\rho_m^5} + \frac{(\rho_m^2 I - \frac{5}{2} S S^T) \bar{P}}{\rho_m^7} \right] S + \right. \\ & \left. + \frac{1}{m} \sum_i \frac{\mu_i}{\rho_i^3} P_i \right\} \quad (4.44.8) \end{aligned}$$

These are the barycentric equations of motion of the satellite. However

$$\begin{aligned} \mathbf{S} &= \mathbf{B}_s - \mathbf{B}_M \\ \ddot{\mathbf{S}} &= \ddot{\mathbf{B}}_s - \ddot{\mathbf{B}}_M \end{aligned} \quad (4.44.9)$$

where  $\ddot{\mathbf{B}}_M$  are the barycentric equations of motion of the Moon. Expressions for  $\ddot{\mathbf{B}}_M$  as obtained in section 4.1 (part of equation (4.41.11)) are substituted in equation (4.44.9) and result in

$$\begin{aligned} \ddot{\mathbf{S}} = -k^2 \mathbf{E} \left\{ \frac{1}{m} \left[ \frac{1}{\rho_m^3} + \frac{\overline{\mathbf{H}}}{\rho_m^5} + \frac{(\rho_m^2 \mathbf{I} - \frac{5}{2} \mathbf{S} \mathbf{S}^T) \overline{\mathbf{P}}}{\rho_m^7} \right] \mathbf{S} + \frac{1}{m} \frac{\mu_1}{\rho_1^3} \mathbf{P}_1 + \right. \\ \left. + \left[ \frac{1}{\rho_e^3} + \frac{\overline{\mathbf{E}}}{\rho_e^5} + \frac{(\rho_e^2 \mathbf{I} - \frac{5}{2} \mathbf{R} \mathbf{R}^T) \overline{\mathbf{Q}}}{\rho_e^7} \right] \mathbf{R} \right. \\ \left. - \left[ \frac{1}{\rho^3} + \frac{\overline{\mathbf{H}} + \overline{\mathbf{E}}}{\rho^5} + \frac{(\rho^2 \mathbf{I} - \frac{5}{2} \mathbf{X} \mathbf{X}^T) (\overline{\mathbf{P}} + \overline{\mathbf{Q}})}{\rho^7} \right] \mathbf{X} \right\} \end{aligned} \quad (4.44.10)$$

These are Cowell's equations of motion of a satellite with respect to a selenocentric inertially oriented coordinate system. As shown before, the right side of the equations is composed of functions of the integrated quantities, i. e.,  $\mathbf{S}$ ,  $\mathbf{X}$ ,  $\varphi$ ,  $\psi$ ,  $\theta$ ,  $\eta$ ,  $\lambda$ ,  $\epsilon$  and of constants as adopted for the simulation.

#### 4.45 Numerical Integration of the Equations of Motion.

The equations of motion derived in 4.41 through 4.44 are second-order differential equations of a rather complex form. Their analytical solution, if possible at all, is a task well beyond the scope of this work. Particular real cases have been solved after introducing many simplifying assumptions. The cost was enormous in terms of time spent by the best talents in dynamical astronomy.

As the solutions are needed for the purpose of simulating a synthetic physical environment there is no justification whatsoever not to resort to more convenient, yet, over a short time interval, not less accurate, methods. The availability of the electronic computer makes the simultaneous solution of the 9 or even 12 second-order differential equations by numerical integration a straightforward process. The simultaneous solution is needed as the three (or four) sets of equations (4.41.14, 4.42.8, 4.43.7, 4.44.10) share information on the right sides of the equations.

Control over the accuracy of a numerical integration process is exercised through the so called local error criteria. However there are other means by which the potential accuracy of the process can be enhanced. One such method is to reduce the number of significant digits in the integrated quantities and still maintain the absolute accuracy needed. This can be done by modifying the original equations of motion from Cowell's to Encke's type. A reference case of motion is defined which has an analytical solution of its equation of motion. The differences between Cowell's equations and the equations of motion of the reference case are called Encke's equations of motion. The new quantities integrated are the perturbations of the reference case of motion. By proper choice of the reference case and favorable nature of the original equations of motion the perturbations can be reduced to a small magnitude, and consequently a fewer number of significant digits, compared to the full quantities, will result in the same degree of absolute accuracy. This is particularly appropriate to the cases of the Moon's motion, its orientation, and the orientation of the Earth for the following reasons:

(a) The lunar orbit is very close to a Keplerian orbit. (b) The Eulerian angles of the Moon follow very closely Cassini's laws. (c) The deviations of the rotation of the Earth from secular motions such as precession, diurnal spin, mean inclination are much smaller than the full quantities.

The perturbations in all three cases are periodic in nature, or, if there are some secular effects left in, because of the particular choice of constants and initial values, over short periods of time (one to three years) their accumulated effect will remain small enough not to require a rectification of the reference case of motion.

The application of Encke's modification to the equations of motion of the lunar satellite is not so clearly advantageous, as the nature of the perturbations is less predictable and for a very close lunar satellite (Apollo-type orbit) after one revolution the perturbations may be as large as the full components of the

selenocentric radius vector. However, an efficient computer subroutine was developed (SKEPTR) with the help of which the rectification of the reference Keplerian orbit can be performed in a fraction of a second with absolutely no loss in accuracy. Through occasional or even frequent rectifications of the reference orbit, the magnitude of the perturbations can be kept below a predetermined level, thus enhancing the use of Encke-type equations of motion for a satellite of the Moon as well.

The transition from Cowell- to Encke-type equations is straightforward.

Using general notation:

$$\begin{aligned}\ddot{\mathbf{X}} &= \ddot{\mathbf{f}}(\mathbf{X}, \dot{\mathbf{X}}) && \text{are Cowell's equations of motion} \\ \ddot{\mathbf{X}}_0 &= \ddot{\mathbf{f}}_0(\mathbf{X}_0, \dot{\mathbf{X}}_0) && \text{are the reference case equations of motion.}\end{aligned}$$

There has to be an analytical solution for  $\mathbf{X}_0$  as a function of time which satisfies the differential equations  $\ddot{\mathbf{X}}_0$ . Thus defining

$$\begin{aligned}\delta &= \mathbf{X} - \mathbf{X}_0 && \text{as the perturbations vector it follows by differentiation} \\ \ddot{\delta} &= \ddot{\mathbf{X}} - \ddot{\mathbf{X}}_0 = \ddot{\mathbf{f}}(\mathbf{X}, \dot{\mathbf{X}}) - \ddot{\mathbf{f}}_0(\mathbf{X}_0, \dot{\mathbf{X}}_0) && \text{which are Encke's equations of motion.}\end{aligned}$$

The main condition for the effectiveness of the transition to Encke's equations is to choose the function  $\mathbf{f}_0$  sufficiently close to  $\mathbf{f}$  so that  $\delta$  remains small. In case  $\delta$  grows beyond a certain limit, the reference case is rectified, the values  $\mathbf{X}_0, \dot{\mathbf{X}}_0$  are set equal to  $\mathbf{X}, \dot{\mathbf{X}}$ , and the process is carried on.

In what follows the reference cases for the four sets of equations of motion are discussed.

(a) Geocentric motion of the Moon.

$$\begin{aligned}\ddot{\mathbf{f}}(\mathbf{X}) &= -k^2 E \left( 1 + \frac{1}{m} \right) \left[ \frac{1}{\rho^3} + \frac{\overline{H} + \overline{E}}{\rho^5} + \frac{(\rho^2 \mathbf{I} - \frac{5}{2} \mathbf{X} \mathbf{X}^T)(\overline{P} + \overline{Q})}{\rho^7} \right] \mathbf{X} \\ &= -k^2 E \left( 1 + \frac{1}{m} \right) \left( \frac{\mathbf{X}}{\rho^3} + \mathbf{K} \right) && \text{which are Cowell's equations. (4.41.14)}\end{aligned}$$

$\mathbf{K}$  stands for the second and third terms in the square brackets multiplied by  $\mathbf{X}$ .

The reference case is defined as a Keplerian orbit:

$$\ddot{\mathbf{f}}_0(\mathbf{X}_0) = -k^2 E \left(1 + \frac{1}{m}\right) \frac{\mathbf{X}_0}{\rho_0^3} \quad (4.45.1)$$

where  $\mathbf{X}_0$  is the geocentric position vector of the reference Moon in a Keplerian orbit around the Earth.

$$\ddot{\delta} = \ddot{\mathbf{f}}(\mathbf{X}) - \ddot{\mathbf{f}}_0(\mathbf{X}_0) = -k^2 E \left(1 + \frac{1}{m}\right) \left[ \left( \frac{\mathbf{X}}{\rho^3} - \frac{\mathbf{X}_0}{\rho_0^3} \right) + \mathbf{K} \right] \quad \text{Encke's equations.} \quad (4.45.2)$$

The mean elements of the lunar orbit are used to generate  $\mathbf{X}_0$ .

(b) Eulerian angles of the Moon.

It is known from observations of the actual Moon that in its rotation about its mass center it follows Cassini's laws very closely. The reference Moon, thus, is defined as following these laws exactly, the angles  $\varphi_0, \psi_0, \theta_0$  and their time derivatives  $\dot{\varphi}_0, \dot{\psi}_0, \dot{\theta}_0$  being explicit functions of time. As the integration is not carried out over extensive periods of time, the perturbations can absorb some small secular effects. So the reference equations of motion  $\ddot{\mathbf{f}}_0$  are defined as follows:

$$\ddot{\mathbf{f}}_0 = \begin{bmatrix} \ddot{\varphi}_0 \\ \ddot{\psi}_0 \\ \ddot{\theta}_0 \end{bmatrix} = \begin{bmatrix} 0 \\ 0 \\ 0 \end{bmatrix}; \quad \begin{bmatrix} \dot{\varphi}_0 \\ \dot{\psi}_0 \\ \dot{\theta}_0 \end{bmatrix} = \begin{bmatrix} \dot{\varphi}_0 \\ \dot{\psi}_0 \\ 0 \end{bmatrix}; \quad \begin{bmatrix} \varphi_0 \\ \psi_0 \\ \theta_0 \end{bmatrix} = \begin{bmatrix} \varphi_{00} + \dot{\varphi}_0 t \\ \psi_{00} + \dot{\psi}_0 t \\ \theta_0 \end{bmatrix} \quad (4.45.3)$$

The four constants  $\varphi_{00}, \dot{\varphi}_0, \psi_{00}, \dot{\psi}_0$ , are derived from the mean elements of the lunar orbit where terms in  $\iota_0, \omega_0$  and  $\Omega_0$  with powers of  $t$  higher than the first are deleted and  $\theta_0$  is set equal to  $I_0$  (see Section 4.3).

Subtracting (4.45.3) from (4.42.8) it follows:

$$\delta = \begin{bmatrix} \varphi \\ \ddot{\psi} \\ \ddot{\theta} \end{bmatrix} - \begin{bmatrix} \varphi_0 \\ \ddot{\psi}_0 \\ \ddot{\theta}_0 \end{bmatrix} = \begin{bmatrix} \varphi \\ \ddot{\psi} \\ \ddot{\theta} \end{bmatrix} \quad \text{which are Encke's} \\ \text{equations of motion.} \quad (4.45.4)$$

It is evident that in this case, formally, the Encke equations are identical to Cowell's. It is only the initial values  $(\delta, \dot{\delta})$  used and further integrated which make the difference.

(c) Eulerian angles of the Earth.

The rotational motion of the Earth is dominated by the diurnal spin about the W axis. So the reference case to be chosen may be even simpler than that for the Moon.

$$\ddot{\mathbf{i}}_0 = \begin{bmatrix} \ddot{\eta}_0 \\ \ddot{\lambda}_0 \\ \ddot{\epsilon}_0 \end{bmatrix} = \begin{bmatrix} 0 \\ 0 \\ 0 \end{bmatrix}; \quad \begin{bmatrix} \dot{\eta}_0 \\ \dot{\lambda}_0 \\ \dot{\epsilon}_0 \end{bmatrix} = \begin{bmatrix} \omega_3 \\ 0 \\ 0 \end{bmatrix}; \quad \begin{bmatrix} \eta_0 \\ \lambda_0 \\ \epsilon_0 \end{bmatrix} = \begin{bmatrix} \eta_{00} + \omega_3 t \\ 0 \\ \epsilon_0 \end{bmatrix}. \quad (4.45.5)$$

The constants  $\eta_{00}$ ,  $\epsilon_0$  are taken from the expressions in section 4.3 where for  $\epsilon_0$  all terms except the constant and for  $\eta_0$  the terms beyond the one having  $t$  in the first power have been deleted;  $\omega_3$  is an adopted constant. Here too the Encke equations are identical to Cowell's, the only difference being in the initial values of the integration.

(d) Selenocentric motion of a satellite.

The reference case of the satellite orbit is chosen as a Keplerian orbit having the following equations of motion:

$$\ddot{\mathbf{i}}_0(S_0) = -k^2 E \left( \frac{S_0}{m \rho_{n0}^3} \right) \quad (4.45.6)$$

where  $S_0$  is the selenocentric position vector of a satellite in a Keplerian orbit around the Moon and

$$\rho_{n0} = (S_0^T S_0)^{\frac{1}{2}}$$

Equation (4.45.6) is subtracted from (4.44.10) and the result is

$$\ddot{\delta} = \ddot{f} - \ddot{f}_0 = -k^2 E \left[ \frac{1}{m} \left( \frac{S}{\rho_m^3} - \frac{S_0}{\rho_{m0}^3} \right) + K \right]. \quad \text{Encke's equations, (4.45.7)}$$

As mentioned before, too rapid growth in  $\delta$  may preclude the advantages of a transition to Encke-type equations for a satellite of the Moon.

(e) Encke transformation [see Brouwer and Clemence, 1961, p. 177].

Establishing Encke-type equations in cases (a) and (d) may lead to a considerable loss in significant figures when the quantities subtracted are close in value. In case (a),  $[(X/\rho^3) - (X_0/\rho_0^3)]$  is such a set of differences, and in case (d) there are even two such sets of differences:  $\left(\frac{S}{\rho_m^3} - \frac{S_0}{\rho_{m0}^3}\right)$  and  $\left(\frac{R}{\rho_e^3} - \frac{X}{\rho^3}\right)$ . It should be remembered that  $X, S, R, X_0, S_0$  are all column vectors.

To overcome this problem, Encke has devised a simple transformation:

$$\begin{aligned} \delta &= X - X_0 \\ \frac{X}{\rho^3} - \frac{X_0}{\rho_0^3} &= \frac{\delta - FX}{\rho_0^3} \end{aligned}$$

where

$$\begin{aligned} F &= 1 - \frac{1}{(1 + 2q)^{3/2}} \\ q &= \frac{1}{\rho_0^2} \left[ X_0 + \frac{1}{2} \delta \right]^T \delta \end{aligned}$$

$F$  is usually a small number; however, the number of significant digits carried in  $\delta$  through the numerical integration is not lost. This procedure is applied in all three cases in (a) and (d).

#### 4.5 Total Librations of the Moon.

The disc of the true Moon as seen by an observer on Earth appears to be oscillating about its center. This phenomena is called libration of the Moon and is a combination of a true oscillation of the Moon with respect to its mass center called physical libration and an apparent one due to the eccentricity and inclination of the Moon's geocentric orbit and the diurnal motion of the observer about the geocenter called geometrical and topocentric libration, respectively. This distinction is made mainly for the purpose of evaluating the components as in the end all three are summed up to result in the total libration of the Moon.

In the simulated environment all the quantities necessary to establish the geometric relationship between an observer on Earth and the selenodetic coordinate system can be obtained from the results of the numerical solution of the equations of motion. In this section the equations are derived for the direct evaluation of the total librations of the Moon.

Total libration in longitude and latitude are defined (Figure 4.5) by the polar angles  $l_T$ ,  $b_T$  of the selenodetic vector to the observer Y. Position angle is measured counterclockwise from the plane defined by  $\vec{OP}$  and  $\vec{OW}'$  up to the plane defined by  $\vec{OP}$  and  $\vec{Pz}'$ . It is denoted as  $P_p$ .

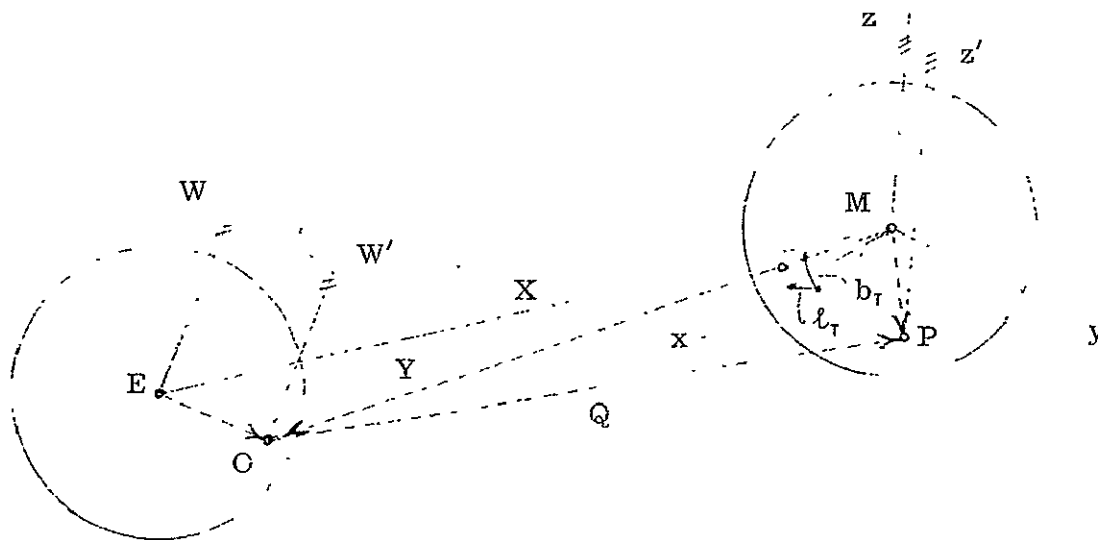


Figure 4.5. Total Librations of the Moon.

The following vectors are defined :

X	geocentric position vector of the Moon	} In components of the XYZ system.
Q	topocentric (observer) vector to point P	
$W_E$	unit vector of spin axis (W) of the Earth	
$W_M$	unit vector of spin axis (z) of the Moon	
O	position of observer in the UVW system	
P	position of point P on the Moon in xyz system.	

Two orthogonal transformation matrices are defined:

- $T_E$  from XYZ to UVW systems
- $T_M$  from XYZ to xyz systems

The computational procedure set to evaluate  $l_T$ ,  $b_T$  and  $P_p$  is as follows:

$$Y = T_M^T \cdot (T_E^T \cdot O - X)$$

$$l_T = \tan^{-1} \left( \frac{Y_y}{Y_x} \right)$$

$$b_T = \sin^{-1} \left( \frac{Y_z}{|Y|} \right)$$

$$V_1 = Q \times W_E$$

$$V_2 = Q \times W_M$$

$$|P_p| = \cos^{-1} \left( \frac{V_1 \cdot V_2}{|V_1| \cdot |V_2|} \right)$$

To determine the sign of  $P_p$  another vector is evaluated:

$$V_z = W_M \times W_E$$

$$s = V_z^T \cdot Q$$

If  $s$  is positive,  $P_p$  is positive and vice versa.

#### 4.6 Observations

One of the purposes of creating the simulated environment was to have the capacity of generating absolute observations for any desired epoch. As in the case of the environment itself, certain simplifications are introduced for the observations too so that a purely geometric situation be created with no consideration being given at this stage to physical and instrumental problems encountered when dealing with actual observations.

The following additional assumptions are made in generating the simulated observations:

- (a) No atmosphere (troposphere, ionosphere) exists around the earth.
- (b) The velocity of electromagnetic wave propagation (including light) is infinite. This excludes any relativity theory implications.
- (c) No distortion whatsoever is caused by using man-made observing instruments or recording materials.
- (d) No solar radiation pressure exists.

Thus the observations are the result of the instantaneous geometric situation defined by positions and velocities of points in space. The equivalent of these idealized observations in the real world would be the fully corrected and compensated actual observations. The random noise left or, in other words, the total of the unknown or unaccounted effects would be the only difference between those observations and the absolute observations generated in the simulation.

##### 4.61 Optical Observations.

Optical observations are defined in the most general way. No matter by which means the observations were obtained, they can be reduced to a bundle of rays emanating from a point to be called the projection center. Each ray in the bundle points from the projection center to a particular point on the Moon (30 such points have been defined on the Earth side of

the Moon, section 4.3). The rays in the bundle are related to a reference Cartesian system ( $B_1, B_2, B_3$ ) which is centered at the projection center and is oriented with respect to the inertial coordinate system by means of three Eulerian angles ( $\varphi_1, \varphi_2, \varphi_3$ ). The a priori covariance matrix of these angles will provide the distinction between an oriented and a floating (unoriented) bundle of rays. This concept allows a uniform treatment of all optical observations obtained from Earth-based or satellite photography and from direct angular observations taken on board a spacecraft (Apollo).

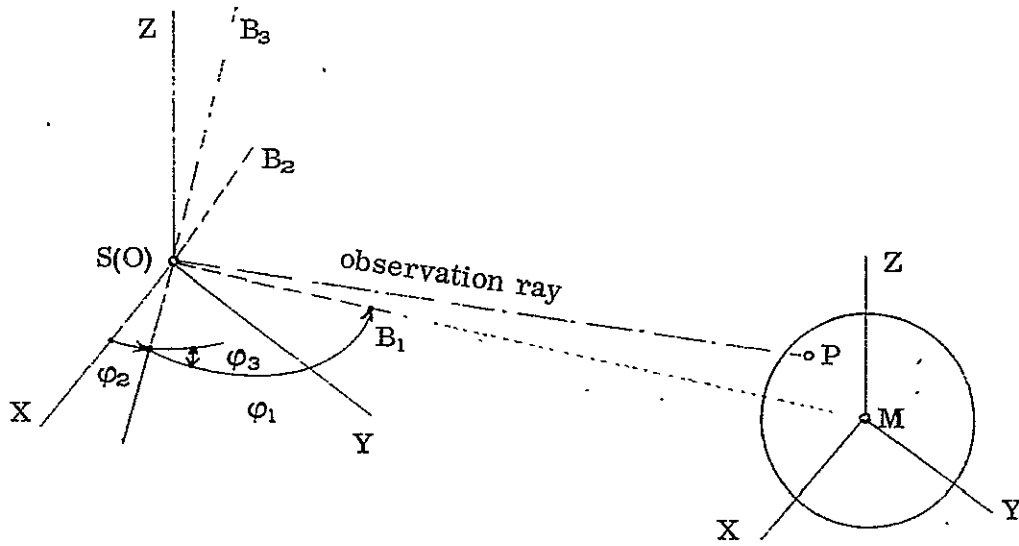


Figure 4.6. Reference Frame for Optical Observations.

- S or O Projection center on a satellite (S) or on the Earth (O)
- M Selenocenter
- P Point on the Moon being observed
- XYZ Inertially oriented coordinate systems
- $B_1B_2B_3$  Reference frame for the optical observations
- $\varphi_1 \varphi_2 \varphi_3$  Eulerian angles relating  $B_1B_2B_3$  to XYZ.

### Conditions for a Valid Optical Observation Ray

In order to be generated, an optical ray has to satisfy all of the following conditions:

- (i) At the Earth station it is night (the "Sun" is  $18^\circ$  below the horizon).
- (ii) The observation ray is at least  $20^\circ$  above the station horizon.
- (iii) The angle between the observation ray and the Sun rays is smaller than  $120^\circ$  (to prevent glare).
- (iv) The observed point is on the front side of the Moon's disc (front side defined with respect to the projection center) and  $20^\circ$  off the lunar limb.
- (v) The observed point is illuminated ( $5^\circ$  from the terminator in the illuminated portion of the disc).
- (vi) The observation ray is within the "aperture frame" - (to simulate photography).

As the constraining angles defined in the conditions are fairly conservative, the station's zenith (and horizon) can be defined by the geocentric radius vector to the station rather than by the normal to the reference ellipsoid.

The rays in the bundle are referred to the  $B_1 B_2 B_3$  system through two angles ( $\nu_1, \kappa_1$ ) or through three unit vector components (direction cosines) ( $u_{1,1}, u_{1,2}, u_{1,3}$ ).

As the orientation of  $B_1 B_2 B_3$  with respect to XYZ is arbitrary a standard orientation is defined common for all situations:

$B_1$  - points to the Moon's mass center.

$B_2$  - is parallel to the XY plane.

$B_3$  - completes the right handed Cartesian system.

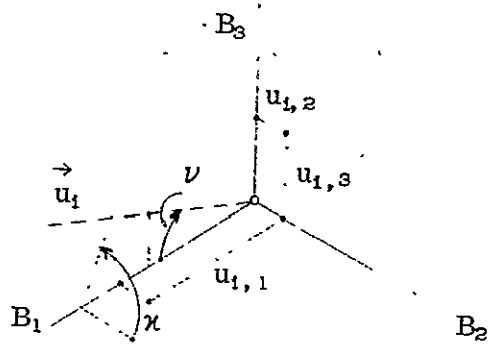


Figure 4.7. Optical Observations

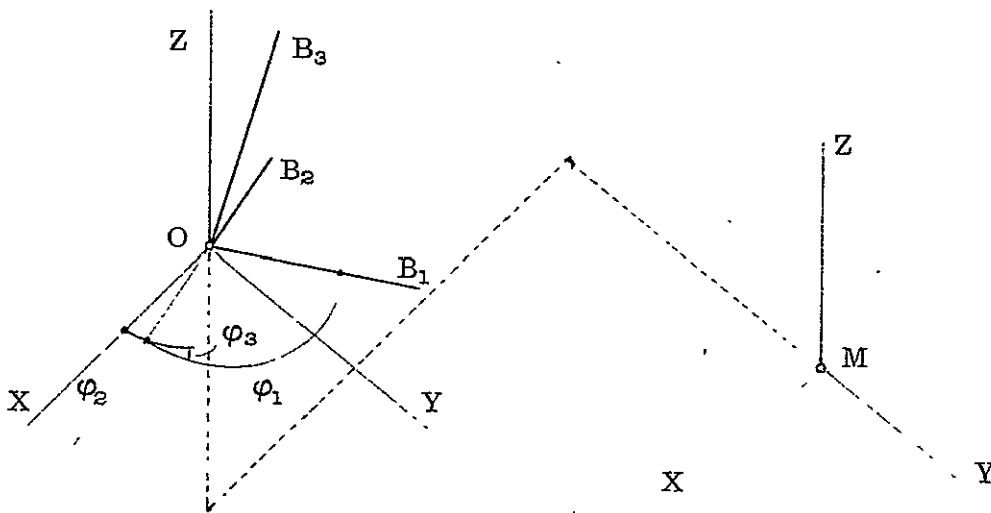


Figure 4.8. Determining the Eulerian Angles  $\varphi_1, \varphi_2, \varphi_3$

The Eulerian orientation angles of  $B_1B_2B_3$  ( $\varphi_1, \varphi_2, \varphi_3$ ) are defined then by the selenocentric position of the projection center (O) as follows:

$$\varphi_1 = \frac{\pi}{2}$$

$$\varphi_2 = \tan^{-1} \left( \frac{Q_y}{Q_x} \right) + \frac{\pi}{2}$$

$$\varphi_3 = \sin^{-1} \left( \frac{Q_z}{|Q|} \right)$$

where  $Q$  is the vector from  $M$  to  $O$  in component of the  $XYZ$  system (see also Figure 4.6). Using these angles the transformation matrix from the  $XYZ$  system to the  $B_1 B_2 B_3$  system is defined in the usual way:

$$T_B = R_3(\varphi_1) \cdot R_1(-\varphi_3) \cdot R_3(\varphi_2)$$

Flow of Computations for the Establishment of the Bundle of Rays.

(a) For the particular epoch for which the bundle is to be generated the geocentric position of the Moon, the Moon's orientation, the Earth's orientation and if a satellite is involved, the selenocentric position of the satellite, are all assumed known. The positions of the observing stations on Earth are known in  $UVW$  components. The positions of the points to be observed on the Moon are known in the  $x y z$  system (see Figure 4.9).

- $O_b$  - observing station in  $UVW$  components
  - $P$  - Moon point in  $x y z$  components
  - $X$  - geocentric Moon position
  - $Q_s$  - observation rays
  - $Q_o$  - observation rays
  - $S$  - selenocentric position
  - $O$  - of projection center
  - $N$  - illuminating vector (Sun)
  - $U$  - observation ray in  $B_1 B_2 B_3$  components
- } in  $X Y Z$  components

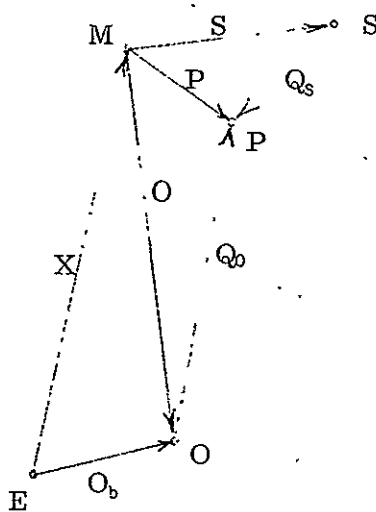


Figure 4.9 Vector Diagram of Optical Observations

$T_E$ ,  $T_M$ , as before, are transformation matrices from the XYZ system to UVW and xyz systems, respectively.

(b) All the vectors are transformed into XYZ system and the unit vectors of the observation rays are computed as follows:

$$O = T_E^T \cdot O - X$$

$$Q_0 = T_M^T \cdot P - O$$

$$Q_s = T_M^T \cdot P - S$$

(c) Check on observing conditions is carried out by vector operations in which the spatial angle between any two vectors is obtained from their dot product. This angle is compared to the appropriate criteria as set above (conditions i through vi).

(d) The observation ray is established in the  $B_1 B_2 B_3$  system, after the  $T_B$  matrix has been calculated. The unit vector of an observation ray (U) is a function of the observed angles  $\nu$  and  $\kappa$  according to the following relations:

$$U = \begin{bmatrix} u_1 \\ u_2 \\ u_3 \end{bmatrix} = \begin{bmatrix} \cos \nu \\ \sin \nu \cos \kappa \\ \sin \nu \sin \kappa \end{bmatrix}$$

The reverse relationship follows directly (see Figure 4.7)

$$\nu = \cos^{-1} (u_1)$$

$$\kappa = \tan^{-1} \left( \frac{u_3}{u_2} \right)$$

The unit vector  $U$  is obtained by the following transformation

$$\dot{U}^* = T_B \cdot Q_s$$

or

$$\dot{U}^* = T_B \cdot Q_0$$

and the division of the  $\dot{U}^*$  vector by its absolute value

$$U = \frac{\dot{U}^*}{|\dot{U}^*|}$$

#### 4.62 Range and Range Rate Observations from an Earth Station to a Satellite of the Moon.

The range between a radio tracking station on Earth (O in Figure 4.10) and a satellite of the Moon (S) can be derived from the following quantities which are either defined as constants (Section 4.3) or are obtained as a result of the numerical integration of the equations derived in Section 4.4. These are:

$$\begin{bmatrix} X \\ \dot{X} \end{bmatrix} \quad \text{the geocentric state vector of the Moon}$$

$$\begin{bmatrix} S \\ \dot{S} \end{bmatrix} \quad \text{the selenocentric state vector of the satellite}$$

$$\begin{bmatrix} \eta \\ \lambda \\ \epsilon \\ \dot{\eta} \\ \dot{\lambda} \\ \dot{\epsilon} \end{bmatrix}$$

the Eulerian angles of the Earth and their time rates

O the station position vector in UVW components.

The evaluation of the range-rate between the tracking station and the satellite requires in addition to the previously mentioned quantities the knowledge of the linear velocity of the station referred to a geocentric inertially oriented XYZ system, to be denoted as  $\dot{P}$ .

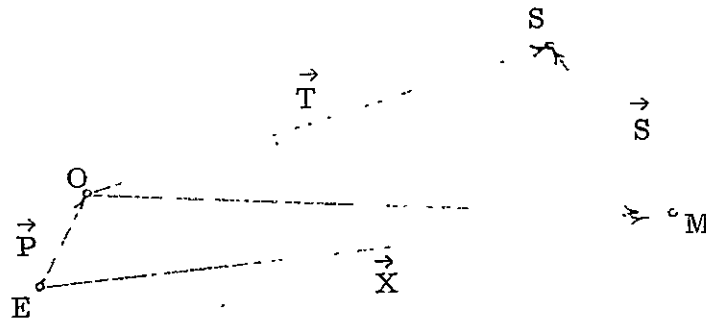


Figure 4.10. Range and Range-Rate Diagram.

- E geocenter
- O tracking station on Earth
- M Moon's mass center
- S satellite

The vector  $\dot{P}$  is obtained as follows:

Euler geometric equations relate the instantaneous rotational velocities of the Earth around axes UVW to the quantities  $\dot{\eta}$ ,  $\dot{\lambda}$ ,  $\dot{\epsilon}$  (see section 4.43)

$$\begin{bmatrix} \dot{\omega}_U \\ \dot{\omega}_V \\ \dot{\omega}_W \end{bmatrix} = \begin{bmatrix} 0 & -\sin \eta \sin \epsilon & -\cos \eta \\ 0 & -\cos \eta \sin \epsilon & \sin \eta \\ 1 & \cos \epsilon & 0 \end{bmatrix} \cdot \begin{bmatrix} \dot{\eta} \\ \dot{\lambda} \\ \dot{\epsilon} \end{bmatrix}$$

$$\dot{P} = T_E^T \cdot \left( \begin{bmatrix} \dot{\omega}_U \\ \dot{\omega}_V \\ \dot{\omega}_W \end{bmatrix} \times O \right)$$

where

$T_E = R_3(\eta) \cdot R_1(-\epsilon) \cdot R_3(\lambda)$  as defined before is the transformation matrix from the XYZ system to the UVW system.

In order to have all the vectors involved in the computation referred to the XYZ system vector O is transformed into vector P:

$$P = T_E^T \cdot O \quad .$$

The range and the range-rate can be calculated at any desired density along the satellite orbit from the following expressions

$$r = |T| \quad \text{range from O to S}$$

$$\dot{r} = \frac{T^T \cdot \dot{T}}{r} \quad \text{range rate from O to S}$$

where

$$\mathbf{T} = \mathbf{X} + \mathbf{S} - \mathbf{P}$$

$$\dot{\mathbf{T}} = \dot{\mathbf{X}} + \dot{\mathbf{S}} - \dot{\mathbf{P}}$$

$$r = (\mathbf{T}^T \cdot \mathbf{T})^{\frac{1}{2}}$$

$$\dot{r} = \frac{\dot{\mathbf{T}}^T \cdot \mathbf{T}}{r}$$

The sign of  $\dot{r}$  is defined as positive for  $r$  increasing (S getting away of O).

Conditions for the Existence of Range and Range-Rate Observations.

The conditions considered are two:

- (i) The satellite is at least  $10^\circ$  above the tracking station horizon.
- (ii) The T vector passes no closer than 60 kilometers from the Moon's surface.

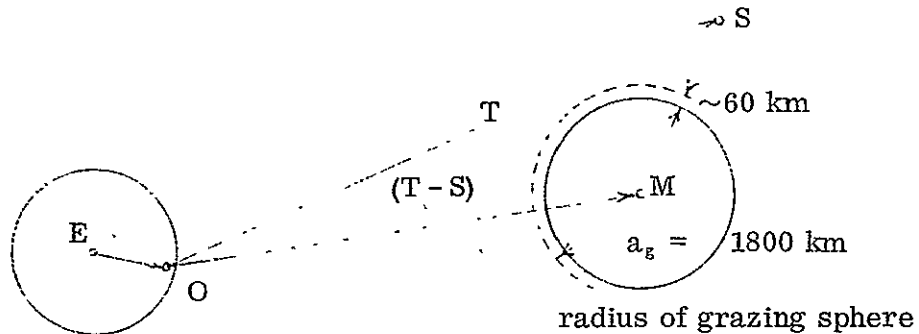


Figure 4.11. Conditions for Existence of Range and Range-Rate Observations

The two conditions are checked as follows:

$$\text{check (i)} = \frac{\mathbf{P}^T \cdot \mathbf{T}}{|\mathbf{P}| \cdot |\mathbf{T}|} - \sin 10^\circ$$

$$\xi = \sin^{-1} \left( \frac{a_g}{|\mathbf{T}-\mathbf{S}|} \right)$$

$$\text{check (ii)} = \frac{P^T \cdot (T-S)}{|P| \cdot |T-S|} - \xi$$

The constraints  $10^\circ$  and 60 km were chosen arbitrarily. Any other set of values derived from experience can be easily substituting in the scheme.

As in the case of the other observation types only those observations are retained which meet the two conditions.

## 5. NUMERICAL EXPERIMENTS

### 5.1 Introduction

The main purpose of this study is to develop a method for the solution of an optimal datum on the Moon from conventional data types. This is accomplished mainly in Chapters 2 and 3 where the models of solution for a datum as well as a new method for the solution of the physical librations of the Moon are presented. Section 2.6 in Chapter 2 goes as far as to display a detailed algorithm to serve as a basis for the extensive computer programming necessary to carry out a complete numerical solution. The complexity of the solution and the number of different types of observations and parameters involved as reflected in section 2.6 clearly indicate that programming the complete solution and running an extensive experimentation program is a task of considerable magnitude well beyond the scope of the present study. However, there are certain elements in the solution which, although mathematically correct, need some numerical confirmation of their feasibility and usefulness. This is true, in particular, regarding the newly proposed method for the solution of the physical librations of the Moon. It is true also for the novel approach taken in treating the Earth-bound optical observations. It seems desirable to have some results which would demonstrate that the numerical solution for the permanent parameters (see section 2.3 in Chapter 2) is possible and the correlations between those parameters are tolerable. Chapter 5 is designed to provide this numerical support for the theory developed in the aforementioned chapters, although it should not be regarded as a complete numerical solution for a datum on the Moon from a combination of Earth-bound and satellite-borne observations.

In the development of a simulated environment and observations, as shown in Chapter 4, particular care is taken to avoid any inconsistencies and obtain simulated data which are realistic and closely correspond to the real situation. All the equations derived in Chapter 4 have been fully programmed in a way such that generating the various data sets is easy and straightforward. So it is clear that the additional effort necessary to bring to completion the extensive numerical experimentation, although time consuming, involves mainly computer programming of mathematical expressions developed in this study and a large number of computer runs. Such a task could be easily handled by a person whose knowledge extends no further than computer programming.

The following three problems are treated in Chapter 5:

- (i) A least squares fit of the numerically integrated physical librations to angles simulated according to Chapter 4 is performed and analyzed.
- (ii) A least squares fit as in (i) above, is performed to angles generated according to Eckhardt's [1970] model and using real lunar and solar ephemerides as given in the DE-69 tape [O'Handley, et al. 1969].
- (iii) A datum solution is obtained consisting of the following:
  - a. Coordinates of a network of 22 triangulation points on the Moon.
  - b. Physical libration angles and time rates at a standard epoch (1969.0).
  - c. The constants  $C_{20}$ ,  $C_{22}$ ,  $\beta$  featuring the low degree terms in the gravitational field of the Moon.

Simulated Earth-bound optical observations are used for this solution.

## 5.2 Fitting Numerically Integrated to Simulated Physical Libration Angles

The main objective in this section is to demonstrate the feasibility of the adjustment model as developed in section 3.3 and to test the numerical efficiency of the algorithm in recovering the "errors" introduced in the nominal parameters. The correlation matrix is regarded as an indicator of the capability of the procedure to separate the various parameters being estimated.

There is another problem which is investigated. The solution for physical libration in longitude, where the value of the constant  $f$  is 0.662, presents a nonlinearity problem as mentioned in section 3.1. Koziel has reported that there appear to be two minima in the solution depending on the starting value of  $f$  [Kopal and Goudas, 1967]. Two different sets of starting values for  $f$  are used to find out if they both converge to the same adjusted value of  $f$ .

As there is no previous experience in similar solutions, the assumption for linearity of the function  $\lambda_2$  (see section 3.42) over the corrections to the starting (approximate) parameters is tested. This assumption is the basis and justification for the linearization of the mathematical model. The test is performed by iterating the least squares solution and denoting the speed of convergence to the final (in this case the theoretical) parameters and also by examining the residuals after each iteration. In the following paragraph, a short account is given of the numerical tools developed for the purpose of this experimentation.

A simulated ephemeris of the Earth and the Moon was created for a period of one year beginning at 2440222.5 JD (1969.0) and up to 2440592.5 JD. The mathematical formulation and constants used follow exactly those given in Chapter 4. The subroutine used to integrate numerically the differential equations of motion is the so called DVDQ - a variable

step, variable order Adams integrator [Krogh, F. T., 1969]. The geocentric position and velocity of the Moon, the Eulerian angles and time rates for the Moon and for the Earth were created and recorded at half daily intervals. In order to facilitate interpolation for the 18 quantities at epochs which fall between the tabulated values, a fifth-order modified Everett interpolation formula was employed [O'Handley, et al., 1969, p. 25]. For this purpose, the second and fourth differences of the tabulated quantities were modified to include linear combinations of the sixth and eighth differences. Subsequent tests of the differences between interpolated quantities and directly integrated ones showed that the interpolation is satisfactory and produces results which are correct within the nominal number of "correct" significant figures obtained in the integration of the differential equations. The final product was a three dimensional matrix of  $3 \times 18 \times 740$  quantities which contained, in double precision, all the information necessary to obtain the position and orientation of the Moon and the orientation of the Earth for any epoch during the year 1969 with a precision of 0.0001 km and 0.0001 km/day for the lunar ephemeris and 0.003 and 0.003 "/day for the orientation angles and time rates of the Earth and the Moon. This ephemeris is used to obtain the selenocentric position of the Earth needed in the integration of the physical librations (see equation 3.23.3 in section 3.23) and also as a source for "observed" physical libration angles needed in performing the least squares fit according to section 3.42.

Programs developed for the integration of the physical librations of the real Moon are used in this experiment, the only difference being that the gravitational constant of the Sun is set to zero (no Sun which exerts gravitational attraction exists in the simulated environment) and also the motion of the ecliptic MOD system is set to zero. The last provision is justified by the fact that the reference XYZ frame in the simulated environment was chosen to be the ecliptic system of 1969.0 which is inertial by definition (see section 4.2 in Chapter 4).

The mean longitude and the longitude of node of the Moon needed in the transformation between the Eulerian angles and the physical librations of the Moon are determined through the following expressions:

$$\begin{aligned} L_D &= 1.196721511 + 0.2299715022 \cdot (T - 2440222.5) \\ \Omega_D &= 0.080512750 - 0.0009242189 \cdot (T - 2440222.5) \end{aligned}$$

where  $L_D$  and  $\Omega_D$  are the mean longitude and the longitude of node in radians and  $T$  is the epoch in Julian days (see Section 4.35).

The mean inclination of the lunar equator to the XY plane ( $I_D$ ) is defined as follows:

$$I_D = 0.026769 \text{ radians}$$

The nominal (theoretically exact) values for the six initial values of the physical librations for 2440222.5 JD and the three physical constants ( $C_{22}$ ,  $\beta$ ,  $C_{20}$ ) are as follows (see Section 4.36):

$$\begin{aligned} \tau &= -0.000060718 & \dot{\tau} &= 0.000027449 & C_{22} &= 0.0000207 \\ \sigma &= -0.008818575 ; & \dot{\sigma} &= 0.005304188 ; & \beta &= 0.0006290 \\ \rho &= 0.000606182 & \dot{\rho} &= 0.000062452 & C_{20} &= -0.0002070 \end{aligned}$$

where  $\tau$ ,  $\sigma$ ,  $\rho$  are in radians,  $\dot{\tau}$ ,  $\dot{\sigma}$ ,  $\dot{\rho}$  are in radians per day and  $C_{22}$ ,  $\beta$ ,  $C_{20}$  are dimensionless.

The value of  $f$  that corresponds to the chosen physical parameters is

$$f = 0.6668$$

which is quite close to the critical value of  $f$  (0.662).

Three types of adjustment were performed as follows:

(i) The nominal (absolute) physical constants were used as starting values while the initial values for 244022.5 of the physical librations were shifted. The normal equations were generated and solved only for the six initial values.

(ii) The absolute initial values of the physical libration angles were used as starting values while  $C_{22}$  and  $\beta$  were shifted from their absolute values. The normal equations were generated and solved for  $C_{22}$  and  $\beta$  alone.

(iii) All the parameters with the exception of  $C_{20}$  were shifted from their nominal values. The normal equations were generated and solved for the 8 parameters (initial values,  $C_{22}$  and  $\beta$ ). Two cases were run with different starting values to test the convergence in both to the same solution and also to test if starting with  $f$  values on either side of the critical  $f(0.662)$  will have any adverse effect on the solution.

The following is a display of the results of the three adjustment experiments:

(i) The starting (approximate) values were set at the following:

$$\begin{array}{rcl}
 \tau = -0.0001 & \dot{\tau} = 0.00001 & C_{22} \\
 \sigma = -0.01 & \dot{\sigma} = 0.01 & \beta \\
 \rho = 0.0 & \dot{\rho} = 0.0001 & C_{20}
 \end{array}
 \begin{array}{l}
 \\
 \\
 \\
 \end{array}
 \begin{array}{l}
 \\
 \text{equal to the} \\
 \text{nominal}
 \end{array}$$

After three iterations all the residuals in  $\tau$ ,  $\sin \theta \cdot \sigma$  and  $\rho$  were smaller than 1/10000 of a second of arc and the adjusted values of the six initial angles and time rates were brought back to the nominal values. Computer time for the run on the IBM 360/75 was 4.4 minutes. The inverted normal matrix (weight coefficients matrix) and the corresponding correlation matrix after the third iteration are as follows:

	$\tau$	$\sigma$	$\rho$	$\dot{\tau}$	$\dot{\sigma}$	$\dot{\rho}$
$\tau$	7.8D-3	1.9D-4	-3.4D-6	-1.3D-5	1.7D-5	-8.1D-6
$\sigma$	0.00	7.5D-0	-4.7D-3	1.3D-5	-7.9D-2	-2.4D-2
$\rho$	-0.00	-0.02	5.2D-3	7.9D-6	2.0D-2	1.4D-5
$\dot{\tau}$	-0.33	0.01	0.25	1.9D-7	6.4D-5	6.2D-8
$\dot{\sigma}$	0.00	-0.07	<u>0.68</u>	0.35	1.7D-1	3.1D-4
$\dot{\rho}$	-0.01	<u>-0.71</u>	0.02	0.01	0.06	1.5D-4

The upper right triangular submatrix is the weight matrix, while the lower left triangular matrix is the correlation matrix without the diagonal elements. This pattern in presenting the weight and the correlation matrices will be used hereafter. The solution appears satisfactory in all respects. There are, however, somewhat larger correlations between  $\dot{\rho}$  and  $\sigma$  and also between  $\dot{\sigma}$  and  $\rho$ .

(ii) The starting initial values and  $C_{20}$  were set equal to the nominal while  $C_{22}$  and  $\beta$  were shifted as follows:

$$\begin{aligned} C_{22} &= 0.0000217 \\ \beta &= 0.000619 \end{aligned}$$

The corresponding  $f$  value is  $f = 0.653$ .

After two iterations, the residuals in all three angles throughout the year (1969) were smaller than  $0.0006$  and the adjusted parameters were back at the nominal, differing at the seventh significant figure for  $C_{22}$  and in the tenth significant figure for  $\beta$ . There is no doubt that a third iteration would have brought all the residuals to zero and the parameters to the exact nominal values. The weight coefficient and correlation matrices after the second iteration were as follows:

$$\begin{array}{cc} & \begin{array}{cc} C_{22} & \beta \end{array} \\ \begin{array}{c} C_{22} \\ \beta \end{array} & \begin{array}{|cc|} \hline 3.1D-7 & -1.4D-6 \\ \hline -0.42 & 3.7D-5 \\ \hline \end{array} \end{array}$$

The two parameters appear to be separated at a tolerable level. The solution for  $C_{22}$  and  $\beta$  crossed the critical value in  $f$  without any deterioration in the solution (from  $f = 0.653$  to  $f = 0.667$ ).

(iii) The starting values for case (a) were as follows:

$$\begin{aligned} \tau &= -0.0001 & \dot{\tau} &= 0.00002 & C_{22} &= 0.00002 \\ \sigma &= -0.009 & ; & \dot{\sigma} &= 0.004 & ; \beta &= 0.000627 \\ \rho &= 0.0005 & \dot{\rho} &= 0.00008 & C_{20} &= 0.000207 \text{ (nominal)} \end{aligned}$$

The  $f$  value corresponding to the starting physical parameters is  $f = 0.676$ .

After three iterations (4.1 minutes computer time on the IBM 360/75) the residuals in all three angles were smaller than 0!0005 and also all the 8 parameters were back at the nominal values. The correlation matrix after the third iteration is presented below:

$\tau$							
0.03	$\sigma$						
-0.06	-0.02	$\rho$					
<u>-0.78</u>	-0.03	0.11	$\dot{\tau}$				
-0.10	-0.08	<u>0.68</u>	0.16	$\dot{\sigma}$			
-0.05	-0.45	0.02	0.06	-0.07	$\dot{\rho}$		
<u>-0.76</u>	-0.11	0.08	<u>0.99</u>	0.13	0.06	$C_{22}$	
0.01	<u>0.77</u>	-0.01	0.00	-0.04	0.00	-0.10	$\beta$

The large correlations, as exhibited in solution (i), show up in this solution too. However, the correlation between  $C_{22}$  and  $\dot{\tau}$  is of a much more disturbing magnitude (0.9889) and places a question mark on the capability of the procedure to separate the two parameters. In spite of the high correlation between  $C_{22}$  and  $\dot{\tau}$ , the solution for these two parameters converged satisfactorily. It appears that this is another of those cases where a high degree of correlation between parameters does not seem to affect their solution adversely.

As it is shown in the next section, this phenomena is common to the true case also, i.e., it is not typical to the simulated environment.

The starting values for case (b) were set as follows:

$$\begin{array}{lll}
 \tau = -0.00003 & \dot{\tau} = 0.000035 & C_{22} = 0.000024 \\
 \sigma = -0.007 & ; \quad \dot{\sigma} = 0.007 & \beta = 0.000633 \\
 \rho = 0.00075 & \dot{\rho} = 0.00004 & C_{20} = -0.000207
 \end{array}$$

The  $f$  value corresponding to the  $C_{22}$ ,  $\beta$ ,  $C_{20}$  as chosen is  $f = 0.624$ .

After three iterations, all the residuals fell below 0.0003 and the parameters were back at the nominal values. The correlation matrix is almost identical to the one displayed for case (a). To illustrate the pattern of the residuals after the first and the second iterations, the residuals in  $\tau$  are plotted in Figure 5.1. The residuals in  $\sin \theta \cdot \sigma$  and in  $\rho$ , not shown in Figure 5.1, fell below the 0.5 level already after the first iteration and exhibited, in general, a monthly period. A similar monthly period in addition to a secular or a very long periodic effect show in the  $\tau$  residuals (Figure 5.1).

Three preliminary conclusions can be drawn from the results presented in this section as follows:

- (i) The adjustment procedure developed in Chapter 3 is capable of solving for the parameters of the physical librations.
- (ii) The critical value of  $f$  does not affect the solution in any perceptible way and there appears to be definitely a single minimum.
- (iii) The separation between the parameters  $C_{22}$  and  $\dot{\tau}$  appears to be poor although the adjustment procedure converges to the correct solution. The correct values of  $C_{22}$  and  $\dot{\tau}$  were known in this case as they are parameters in the simulation.

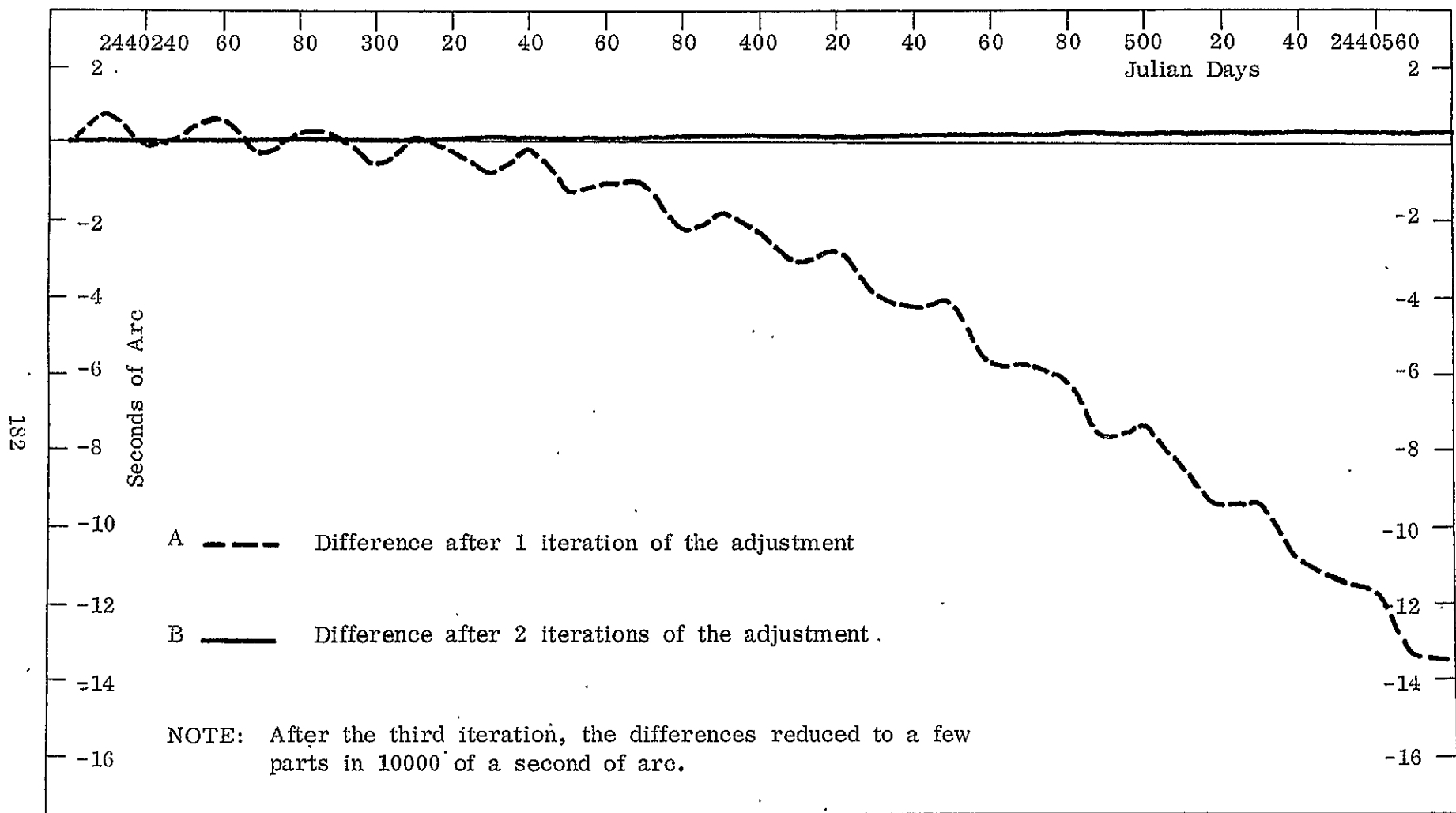


Figure 5.1 Differences Between Numerically Integrated and Simulated  $\tau$  Angles (physical librations in longitude).

### 5.3 Fitting Numerically Integrated to Eckhardt's Physical Libration Angles

In the introduction to Chapter 4, a warning was issued against relying too much on conclusions reached from processing simulated data alone. In the case of the new solution for the physical librations, it was felt that if there is some hidden incompatibility of the procedure as applied to the real world, this study may be seriously compromised if not completely devalidated. For this reason, a large amount of time was spent in testing the solution for the physical librations of the real Moon. Technically, this was not too difficult as an excellent ephemeris of the real Moon was at hand (LE-16) and also a good and frequently used version of the physical librations was available too [Eckhardt, 1970]. The objective of this section was set to compare the new solution for the physical librations with Eckhardt's, or more specifically to fit the numerically integrated to Eckhardt's physical libration angles. Numerically, the treatment was similar to the one used in section 5.2, only here the gravitational attraction of the Sun (the real Sun) and also the motion of the ecliptic MOD coordinate system were included in the solution. As mentioned in section 5.2, the programs used were literally the same. Only several constants had to be changed in the main program (the program which calls the integrating subroutines).

The problem in dealing with real data is that the "true" solution is unknown and actually it remains unknown in spite of good estimates of the solution which may be obtained. Also, when differences are examined, it is occasionally a matter of opinion who is right and who is wrong. In this case, a hypothesis was suggested to explain some of the observed phenomena.

The experiments were performed in two stages:

(i) A least squares fit was performed over one year (from 2440222.5 JD and up to 2440588.5 JD) of Eckhardt's angles and a variety of starting values were used with several different sets of solved and fixed parameters.

(ii) The residuals of the experiments in (i) above prompted a soul-searching operation at the end of which some modifications and "corrections" were applied to Eckhardt's expressions for  $\tau$ , the physical libration in longitude. Then another set of least squares fits were performed which, as it is shown at the end of this section, confirmed the assumptions made and brought some more light into the problem of the physical librations of the Moon. It turned out that the problem was hidden in the troublesome term in the harmonic series for  $\tau$  (argument  $-(2F-2\ell_0)$  and coefficient of  $15''3$  according to Eckhardt [1970]). The coefficient of this term is extremely sensitive to small variations in  $f$  and as  $f$  is not known too well, the value of this coefficient has a large uncertainty [Kopal and Goudas, 1967].

One important result in so far as the numerical integration procedure is concerned was that the normal matrices behaved in very much the same way as in the simulated case (section 5.2) and, actually, for fits over one year to Eckhardt's angles there was little difference in the covariance matrices of the estimated parameters. As stated in Chapter 3, the objectives of this study do not include analysis of the differences between the numerically integrated physical libration angles and those obtained from conventional solutions; therefore, as soon as positive conclusions could be reached about the feasibility and compatibility of the numerical solution of the physical librations of the Moon, the harmonic analysis of the differences was halted.

In the following paragraphs of this section, a brief description of the experiments is presented together with the numerical results.

(i) Eight different cases of adjustment were run as follows:

In cases 1 through 4, the gravitational effect of the Sun and the motion of the ecliptic were set to zero and the starting values of the physical parameters ( $C_{22}$ ,  $\beta$ ,  $C_{20}$ ) were set so that  $f = 0.633$  and  $\beta = 0.0006268$  which are the so-called Koziel's values [Kopal and Goudas, 1967].

In the second group of cases 5 through 8, the effects of the Sun and the motion of the ecliptic were included and the values of  $C_{22}$  and  $C_{20}$  used were the ones adopted by NASA in the so-called Apollo gravitational model of the Moon [Ransford, et al., 1970].

In each of the two groups, the nine normal equations generated were solved in four different ways as follows:

- (a) Only initial values solved (6).
- (b) Initial values and  $C_{22}$  solved (7).
- (c) Initial values and  $\beta$  solved (7).
- (d) All the parameters with the exception of  $C_{20}$  solved (8).

If a parameter was not solved, like  $C_{20}$  in all cases or  $C_{22}$  in case (c), for example, its value was kept fixed in the solution.

The solutions of cases 4 and 8 were iterated two more times to find out if significant changes in the solutions would occur.

The results of the eight cases of adjustment are displayed in Table 5.1; the correlation matrices are given in Tables 5.2 and 5.3 and the residual differences between the numerically integrated and Eckhardt's  $\tau$  angles are presented in Figure 5.2. The residuals in  $\sin\theta \cdot \sigma$  and in  $\rho$  are not displayed as they behaved after the various adjustments quite satisfactorily. There were no differences larger than 3" in absolute magnitude and they were evenly distributed with respect to the zero line. The residuals in  $\tau$  exhibited some unusual persistence and could not be brought to order, no matter what starting values or solution combination were used. The

Sol. No.	$\tau$	$\sigma$	$\rho$	$\dot{\tau}$	$\dot{\sigma}$	$\dot{\rho}$	$C_{22}$	$\beta$	f
Start	-0.000070687	-0.008406005	0.000607810	0.000028399	0.005360716	0.000059528	0.00002302	0.0006268	.633
1	23967	8578287	608580	28130	5363364	59440	2302*	6268*	.633
2	26125	8576564	608424	28262	5362402	59427	2315	6268*	.631
3	24416	8400416	609138	28160	5363646	59446	2302*	6275	.633
4	26241	8401163	608999	28272	5362826	59435	2313	6275	.632
Start	-0.000026241	-0.008401163	0.000608999	0.000028272	0.005362826	0.000059435	0.00002313	0.0006275	.632
4 <sup>+2</sup>	25563	8401807	609046	28232	5363123	59439	2309	6275	.632
Start	-0.000070687	-0.008406005	0.000607810	0.000028399	0.005360716	0.000059528	0.00002070	0.0006268	.667
5	+0.000017248	8570615	611982	25632	5380387	59748	2070*	6268*	.667
6	-0.000049625	8535498	608102	29033	5356752	59422	2385	6268*	.626
7	+0.000016689	8377966	612588	25663	5380708	59755	2070*	6275	.667
8	-0.000049765	8396385	608555	29042	5357078	59429	2384	6273	.626
Start	-0.000050000	-0.008400000	0.000609000	0.000028000	0.005360000	0.000059400	0.00002384	0.0006274	.626
8 <sup>+2</sup>	26200	8405344	609252	28349	5361191	59483	2335	6273	.632

\* These parameters were held fixed in the solution.

+2 Results after two more iterations of the appropriate case (4 or 8)

For cases 1 through 4<sup>+2</sup>  $C_{20}$  was held fixed at -0.0002048.

For cases 5 through 8<sup>+2</sup>  $C_{20}$  was held fixed at -0.000207.

Table 5.1 Starting and Adjusted Physical Libration Parameters for Solutions Numbers 1 Through 8.

$\tau$					
0.00	$\sigma$				
-0.00	-0.02	$\rho$			
-0.35	0.01	0.25	$\dot{\tau}$		
0.00	-0.07	<u>0.68</u>	0.35	$\dot{\sigma}$	
0.00	<u>-0.70</u>	0.01	0.01	0.06	$\dot{\rho}$

No. 1

$\tau$					
-0.03	$\sigma$				
0.11	-0.03	$\rho$			
<u>-0.88</u>	0.03	-0.12	$\dot{\tau}$		
0.12	-0.07	<u>0.68</u>	-0.12	$\dot{\sigma}$	
0.05	<u>-0.70</u>	-0.02	-0.06	0.07	$\dot{\rho}$
<u>-0.88</u>	0.03	-0.13	<u>0.998</u>	-0.14	-0.06

No. 2

$C_{22}$

$\tau$					
-0.08	$\sigma$				
-0.02	0.10	$\rho$			
-0.30	<u>0.60</u>	0.27	$\dot{\tau}$		
0.00	-0.03	<u>0.67</u>	0.23	$\dot{\sigma}$	
-0.01	-0.44	0.02	0.02	0.06	$\dot{\rho}$
-0.11	<u>0.77</u>	0.14	<u>0.78</u>	0.01	0.01

No. 3

$\beta$

$\tau$					
-0.03	$\sigma$				
0.11	0.10	$\rho$			
<u>-0.88</u>	0.04	-0.11			
0.12	-0.03	<u>0.68</u>	-0.12	$\dot{\sigma}$	
0.05	-0.44	0.02	-0.06	0.07	$\dot{\rho}$
<u>-0.87</u>	-0.01	-0.13	<u>0.996</u>	-0.14	-0.06
-0.02	<u>0.77</u>	0.15	0.03	0.02	0.01

No. 4

$C_{22}$

$\beta$

Table 5.2 Correlation Matrices for Cases 1 Through 4.

$\tau$					
0.00	$\sigma$				
0.00	-0.02	$\rho$			
-0.29	0.01	0.25	$\dot{\tau}$		
0.00	-0.07	<u>0.68</u>	0.35	$\dot{\sigma}$	
0.00	<u>-0.70</u>	0.01	0.01	0.06	$\dot{\rho}$

No. 5

$\tau$					
-0.03	$\sigma$				
0.11	-0.03	$\rho$			
<u>-0.84</u>	0.04	-0.12	$\dot{\tau}$		
0.11	-0.07	<u>0.68</u>	-0.12	$\dot{\sigma}$	
0.05	<u>-0.71</u>	-0.02	-0.06	-0.07	$\dot{\rho}$
<u>-0.83</u>	0.04	-0.13	<u>0.998</u>	-0.14	-0.07

No. 6

$C_{22}$

$\tau$					
-0.07	$\sigma$				
-0.02	0.10	$\rho$			
-0.25	<u>0.61</u>	0.26	$\dot{\tau}$		
0.00	-0.03	<u>0.67</u>	0.22	$\dot{\sigma}$	
-0.01	-0.44	0.02	0.02	0.06	$\dot{\rho}$
-0.10	<u>0.77</u>	0.14	<u>0.79</u>	0.01	0.01

No. 7

$\beta$

$\tau$					
-0.03	$\sigma$				
0.10	0.10	$\rho$			
<u>-0.84</u>	0.04	-0.11	$\dot{\tau}$		
0.11	-0.03	<u>0.68</u>	-0.12	$\dot{\sigma}$	
0.05	-0.44	0.02	-0.06	0.07	$\dot{\rho}$
<u>-0.83</u>	-0.01	-0.13	<u>0.996</u>	-0.14	-0.07
-0.01	<u>0.77</u>	0.15	0.02	0.02	0.01

No. 8

$C_{22}$

$\beta$

Table 5.3 Correlation Matrices for Cases 5 Through 8.

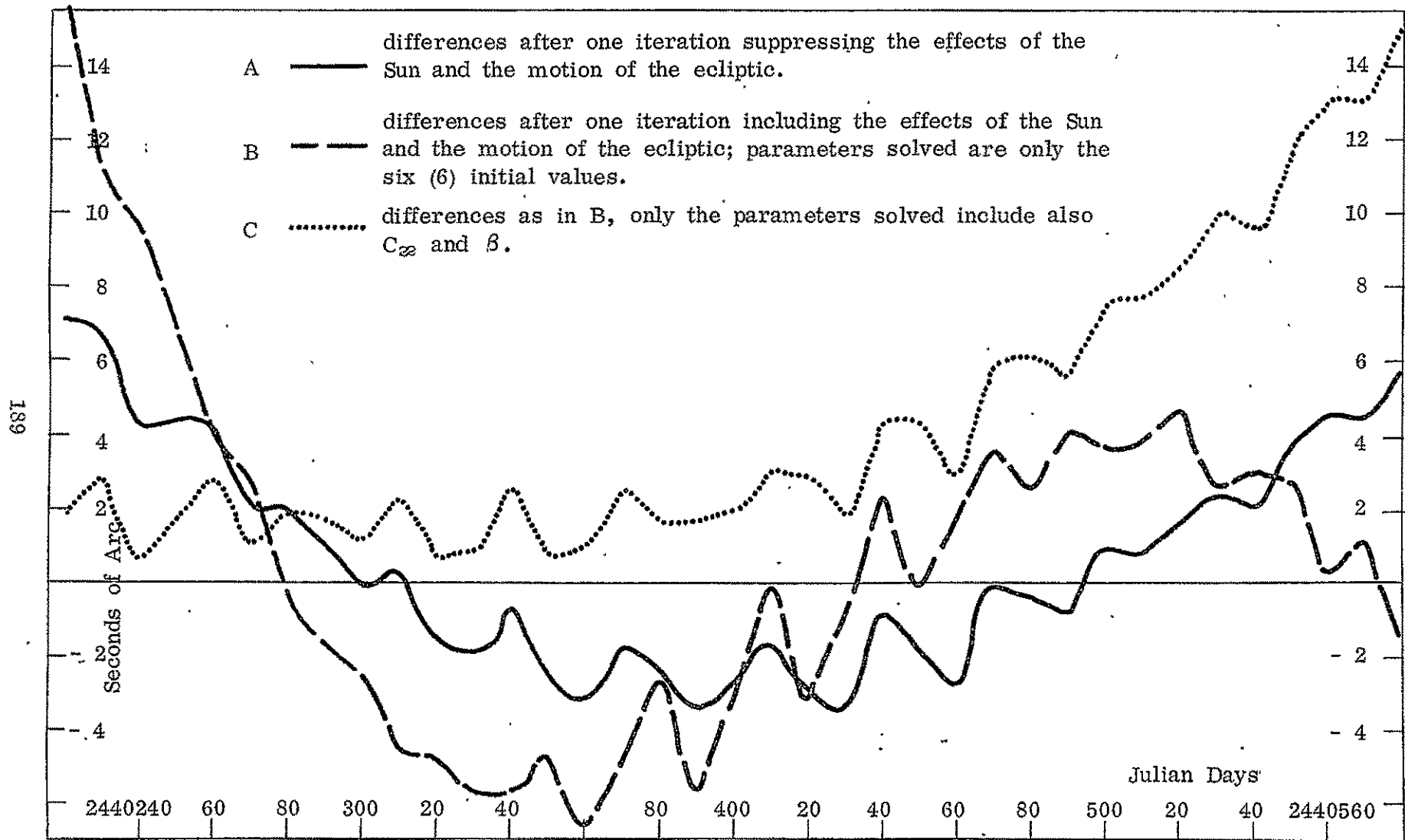


Figure 5.2 Differences Between Numerically Integrated and Eckhardt's  $\tau$  Angles.

correlation matrices are almost exactly the same as those in section 5.2, only here the large correlations are slightly larger. As in section 5.2, the main problem remains the separation between  $\dot{\tau}$  and  $C_{22}$  (correlation 0.996). As could be expected, the Sun and the motion of the ecliptic do not have significant effect as far as the correlation matrices are concerned. In the solutions, however, and mainly in the solution for initial values for  $\tau$  and for  $\dot{\tau}$  and also for the constant  $C_{22}$ , there are two distinct subgroups, i. e., 5 and 7 vs. 6 and 8 (see Table 5.1). The answer lies in the parameters chosen to be solved and those left fixed. In cases 5 and 7,  $C_{22}$  was held fixed at 0.0000207 while in cases 6 and 8, it was solved for. Another reason for the unusual behavior of the solutions 5 through 8 as compared to those of 1 through 4 was that the corrections in  $C_{22}$  required to fit to Eckhardt's angles were apparently too large and more than one iteration was necessary to overcome the nonlinear behavior of the minimized function  $\lambda_2$  (see section 3.42). Thus, case 8 was iterated two more times (denoted as  $8^{+2}$  in Table 5.1) and converged to a solution very close in initial values and in  $f$  to the solution obtained after two more iterations of case 4 (denoted as  $4^{+2}$  in Table 5.1). There were no significant changes in the correlation matrices of cases  $4^{+2}$  and  $8^{+2}$  as compared to the ones of cases 4 and 8, respectively.

The conclusions reached after running all the experiments in (i) were that in  $\sigma$  and in  $\rho$ , the numerical solution for the physical librations of the Moon is quite satisfactory. Actually, the small magnitude of the differences was surprising and encouraging. The only problem remaining was in the solution for  $\tau$ , in view of the large differences and, moreover, in view of their pattern. It was not clear at all if graph A in Figure 5.2 would continue to grow indefinitely which is improbable in view of the laws of Cassini and the long history of observations of the Moon. The experiments undertaken to clarify this problem are presented in the following paragraphs.

(ii) If a solution exists for the numerically integrated physical libration angles all one has are six initial values for some standard epoch and three (actually two) physical parameters which govern the integration. Theoretically, if the solution is perfect and the integrating subroutine does not have any cumulative numerical errors, the physical libration angles could be obtained by numerical integration for any desired epoch, even an epoch which is beyond the interval in time used to obtain the solution. The question thus arises if using an actual solution which is not perfect, an "extrapolation" of the kind described above can be performed without losing control over the integrated angles. In the present case, the initial values and physical constants obtained after the second iteration of case 8<sup>22</sup> above were used to perform an integration over approximately four years (1400 days). The results of this integration in terms of differences between the numerically integrated and Eckhardt's angles are given in Figure 5.3. Two interesting phenomena are evident:

- (a) The solutions in  $\sigma$  and in  $\rho$  (from case 8<sup>22</sup>) are good and could safely be "extrapolated" over three years (beyond 2440588.5 JD). There is some secular trend in  $\rho$  but on the whole, the solution is satisfactory and brings a partial answer to the question if a numerical solution could be used over extended periods of time.
- (b) The residuals in  $\tau$  exhibit a clearly periodic character as suggested by Eckhardt [1971]. Actually, the period of the large differences is almost exactly three years, same as the period of the problematic term in  $\tau$ . It seems quite likely that if the initial epoch for the one year fits performed in (i) above was chosen to be 2440750, the residuals in that experiment would have been an exact mirror image of the ones displayed in Figure 5.2.

In order to investigate the cause for the periodic differences in  $\tau$ ,

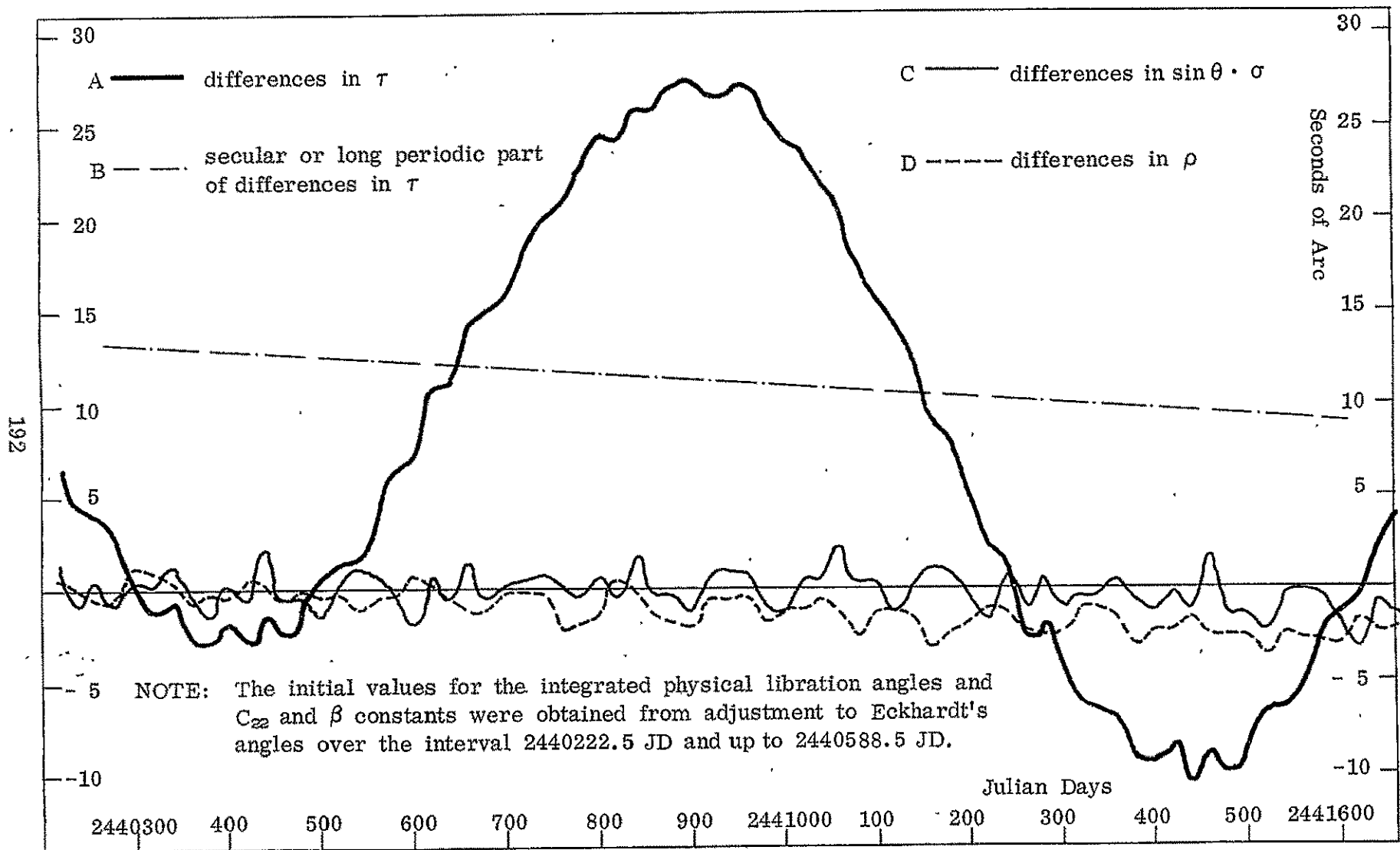


Figure 5.3 Differences Between Numerically Integrated and Eckhardt's Physical Libration Angles.

an adjustment was run over the 1400 days beginning at 2440222.5 JD, only to discover that the parameters changed insignificantly and the residuals in  $\tau$  remained the same. Now it was clear that there is some defect in Eckhardt's model and the value of the coefficient of the term  $(2F-2\ell_0)$  should be checked. A careful search in the literature revealed that Kopal [1970, p.41] reporting on Eckhardt's solution as of 1965, gives the coefficient of that term as  $31''.1$ , much larger than  $15''.3$  as given by Eckhardt in his later solution [Eckhardt, 1970, p.267]. The difference of  $15''.8$  was increased slightly in view of the amplitude of the A graph in Figure 5.3 and a least squares fit was performed to Eckhardt's angles where the term in the harmonic series for  $\tau$  has been increased up to  $32''.3$ . Two iterations of the adjustment over 1200 days, beginning at 2440222.5 JD were run (computer time on the IBM 360/75 was 8.3 minutes). The solution for the parameters (the six initial values,  $C_{22}$  and  $\beta$  were solved) is given in what follows while the residuals are displayed in Figure 5.4.

$$\begin{array}{lll}
 \tau = -0.000032358 & \dot{\tau} = 0.000028992 & C_{22} = 0.00002302 \\
 \sigma = -0.008383211 & \dot{\sigma} = 0.005370362 & \beta = 0.0006274 \\
 \rho = 0.000615345 & \dot{\rho} = 0.000059711 & C_{20} = -0.000205 \text{ (nominal)} \\
 & & f = 0.633
 \end{array}$$

The correlation matrix of the 8 parameters is given below:

$\tau$								
-0.14								
0.13	$\sigma$							
-0.41	0.13							
0.22	0.23	$\rho$						
0.13	-0.15	-0.35	$\dot{\tau}$					
-0.40	-0.50	<u>0.69</u>	-0.53	$\dot{\sigma}$				
-0.09	0.19	0.21	-0.34	0.30	$\dot{\rho}$			
	0.72	-0.41	<u>0.986</u>	-0.57	-0.35	$C_{22}$		
	<u>0.72</u>	0.33	0.08	0.01	0.03	0.02	$\beta$	

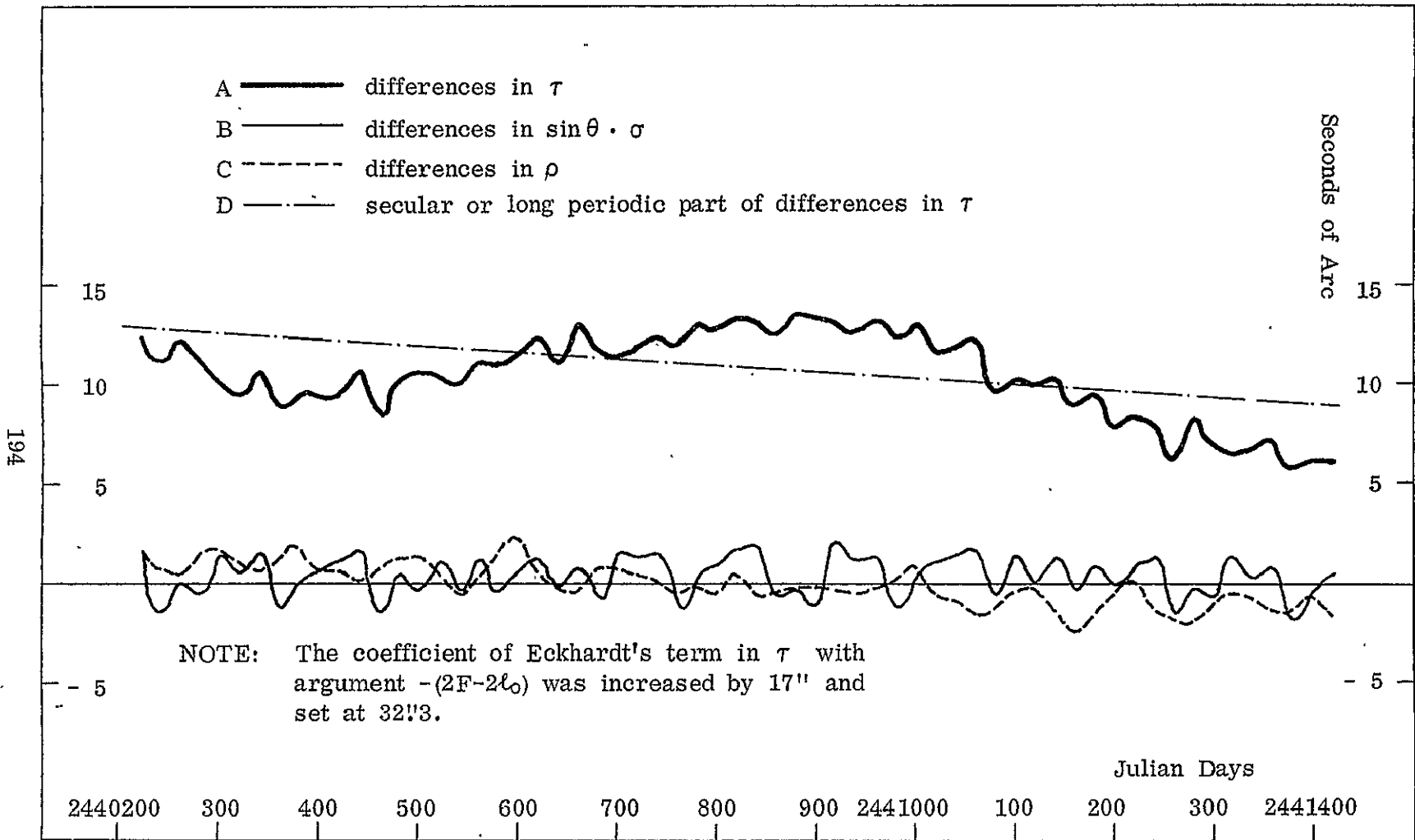


Figure 5.4 Differences Between Numerically Integrated and Eckhardt's Modified Physical Libration Angles.

The correlation matrix compared to the ones in (i) shows a significant increase in the smaller correlations while there is some mellowing in the larger ones. For instance, the 0.996 correlation between  $\dot{\tau}$  and  $C_{22}$  is down to 0.986, still large but less alarming. It is not clear exactly what caused these changes although the fitting interval is considerably longer and may be related to this phenomena.

The residuals in  $\tau$  still remained far from the zero line and as can be seen in Figure 5.4, the coefficient of Eckhardt's term  $(2F-2\ell_0)$  could be increased by some 2 to 3 seconds of arc to eliminate completely the periodic part. A second search in the literature revealed that there may be effects of a very long period (18.6 years, for example) which may be the ones causing the remaining large difference in  $\tau$  [Eckhardt, 1970, p.274]. By inspection, the coefficient and the zero point of an additive harmonic term with a period of 18.6 years (6794 days) were determined as follows:

$$\Delta\tau = 12'' \cdot \sin(360^\circ \cdot \frac{T - 2438700}{6794})$$

where T in Julian days is the epoch for which  $\tau$  is evaluated.

Eckhardt's model was corrected by introducing the additive term in  $\tau$  and increasing the coefficient of the  $(2F-2\ell_0)$  term to 35!3 and a single iteration of the adjusting program was run. The solution shifted slightly from the previous one as follows:

$$\begin{array}{lll} \tau = -0.000035338 & \dot{\tau} = 0.000029111 & C_{22} = 0.00002303 \\ \sigma = -0.008481583 & \dot{\sigma} = 0.005366544 & \beta = 0.0006274 \\ \rho = 0.000613573 & \dot{\rho} = 0.000059654 & C_{20} = -0.000205 \text{ (nominal)} \\ & & f = 0.633 \end{array}$$

The correlation matrix was almost exactly the same as in the previous case of 1200 days. The residuals are displayed in Figure 5.5. Finally, the residuals in  $\tau$  are distributed uniformly about the zero line. There is

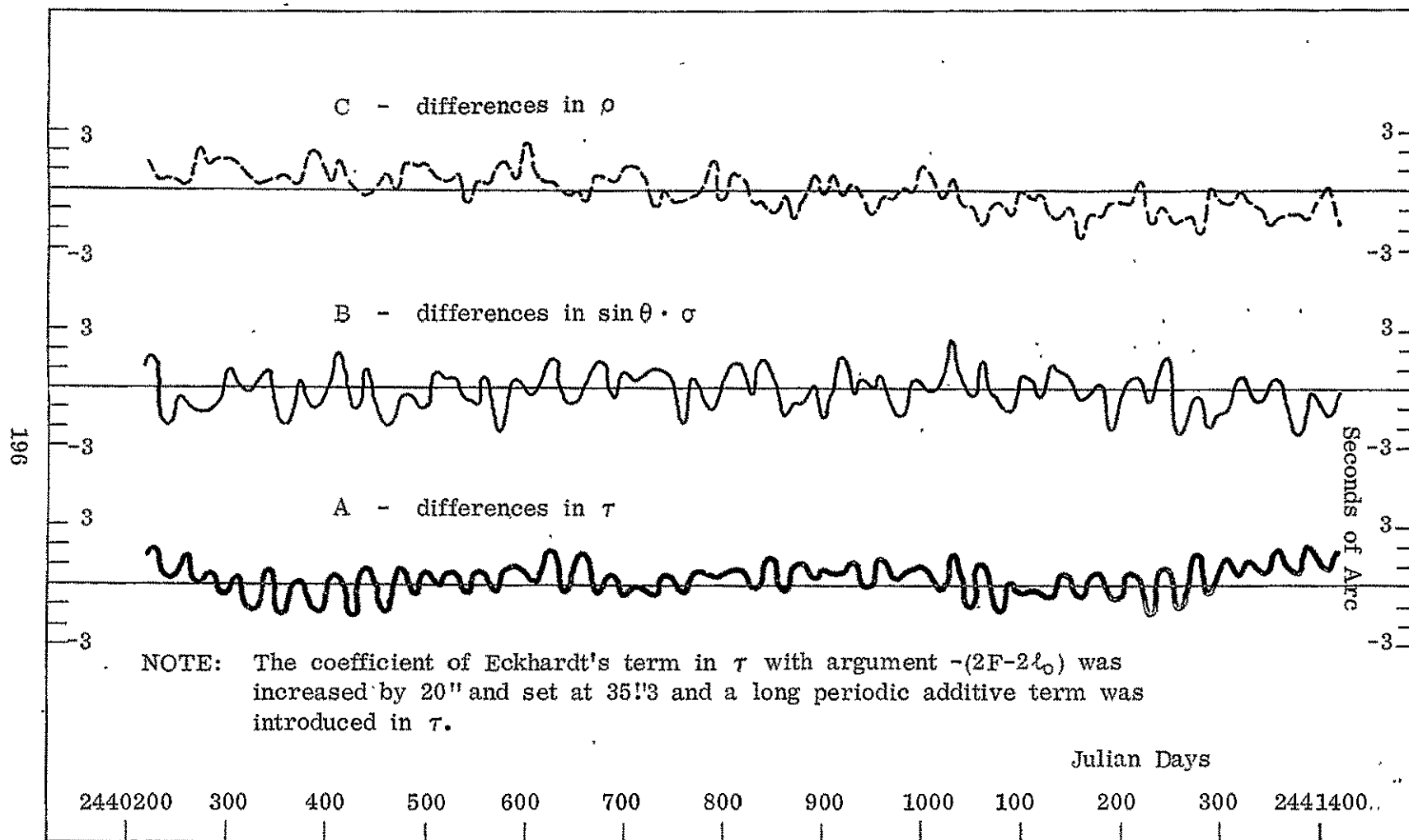


Figure 5.5 Differences Between Numerically Integrated and Eckhardt's Corrected Physical Libration Angles.

still evidence of short periodic effects, the dominant being a clear one-month period (27.3 days). The residuals in  $\rho$  display some secular tendency of about 2" per 1200 days. It is possible to go on and correct additional terms in Eckhardt's model by rigorous harmonic analysis of the remaining differences although the real value of such an improvement is questionable. The fact remains that two totally different solutions agree over a period of more than three years to better than three seconds of arc. Until observations with noise level corresponding to less than 30 meters on the lunar surface become available (1" measured from the selenocenter is roughly equivalent to 10 meters on the surface of the Moon) there is no point in correcting the presently available solution of Eckhardt except for the  $(2F-2L_0)$  term and the additive long periodic term introduced above.

During the various phases of the experimentation reported in this section, the mathematical developments presented in Chapter 3 and programs written accordingly were checked repeatedly to uncover any possible error. After the numerous tests run with this program and the satisfactory results as reported in this section, it can be stated with confidence that the procedure for the solution of the physical librations of the Moon as developed in this study and programmed is fully capable of solving the problem. It remains to obtain real data and process it according to the theory developed in Chapter 2, in order to fully utilize the potentials of the new method.

5.4 Selenodetic Control Solutions From Simulated  
Earth-Bound Optical Observations

In this section, a series of experiments designed to analyze the quality of various solutions for a control network on the Moon from simulated Earth-bound optical observations are presented. As the data imply (Earth-bound observations), the control extends only to features on the front side of the Moon.

The selection of the triangulation points (features on the lunar surface) was done so that two different control networks are defined, each consisting of twenty-two points.

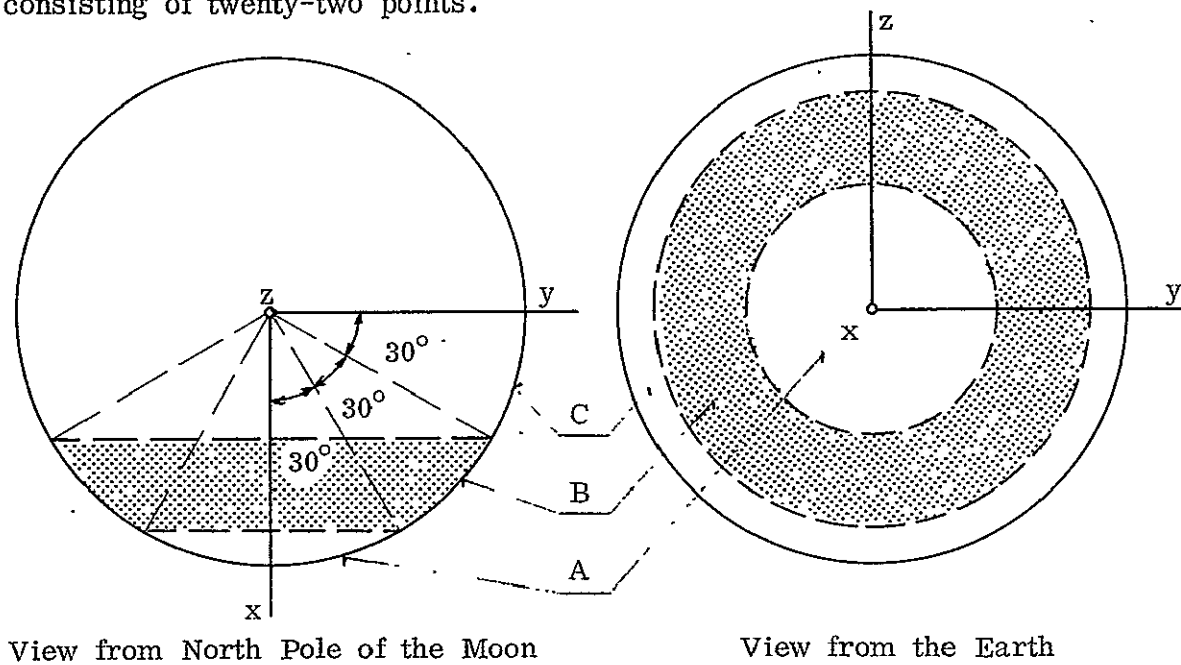


Figure 5.6 Typical Areas for Positioning Triangulation  
Points on the Moon.

The two networks are defined as follows (see Figure 5.6):

- a. Network I includes points from areas A and C.
- b. Network II includes points from areas A and B.

This distinction is made in order to enable experimentation with solutions of "center and limb" networks (I) vs. "limbless" networks (II). In a way, the heliometer observations which traditionally have been used for the solution of the physical libration constants can be regarded as an extreme case of a network of type I where there is only one point in area A (Mösting A) while the points in area C are all on the limb itself. Network II can be associated to the set of 150 triangulation points solved by Schrutka Rechtenstamm (1958) in which there are very few points in the limb area C.

From a total of 30 points as defined in the simulated environment (section 4.32), 14 points are common to both networks (I and II) and the remaining 16 points are split evenly between the two networks (see Figure 5.7).

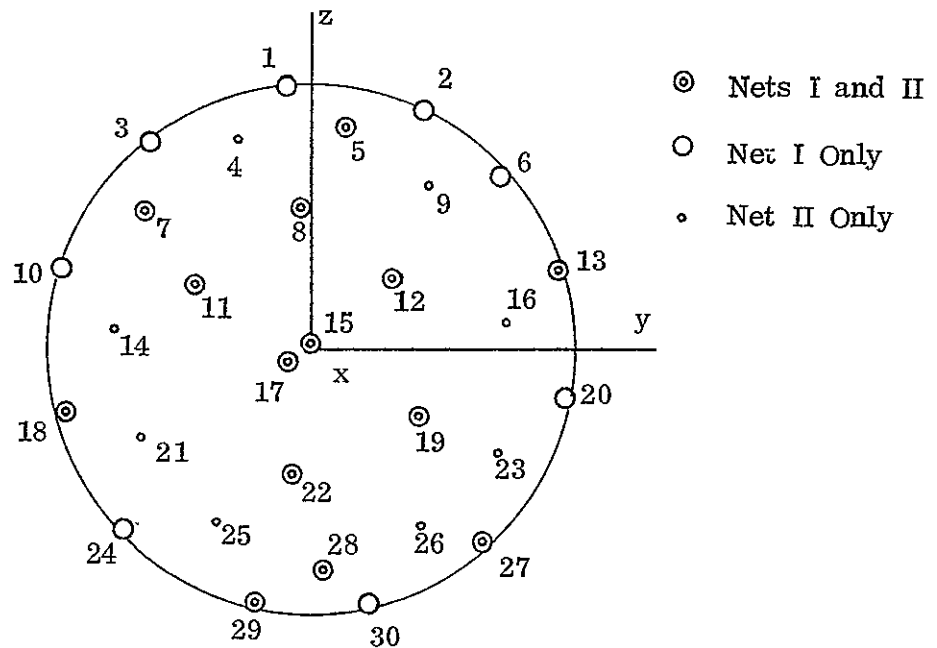


Figure 5.7 Distribution of Points in Control Networks I and II.

Optical observations conducted from the Earth have to be obtained at epochs of extreme libration offsets in order to allow a fair solution (see section 1.2). For this purpose, the total geocentric librations (total

libration as seen from the geocenter) for the year 1969 were generated and then fifteen epochs with large librations evenly distributed along the year were selected as the approximate observation epochs. Another criterion in selecting the approximate epochs was the phase of the Moon. In order to have a maximum number of rays per bundle, the epochs were selected around Full Moon. The observatories at Pic Du Midi and at Johannesburg were defined as the observing stations (see section 4.31) and then it was left to the program to choose the exact epoch of the optical bundle, one for each station, in the proximity of the epochs discussed above so that the observing conditions would be optimal.

In this way, a total of thirty optical bundles were created which contained from twenty-two and up to thirty rays per bundle. The exact librations and other auxiliary data, in addition to the optical observations themselves, were recorded. From this raw data two sets of thirty bundles each were created according to the control points figuring the networks I or II. It should be remembered that all of these calculations are based on the simulated ephemeris for the year 1969 as described in section 5.2.

The libration subpoints (intersection with the lunar surface of the vector from the observing stations to the selenocenter) of the thirty bundles are shown in Figure 5.8.

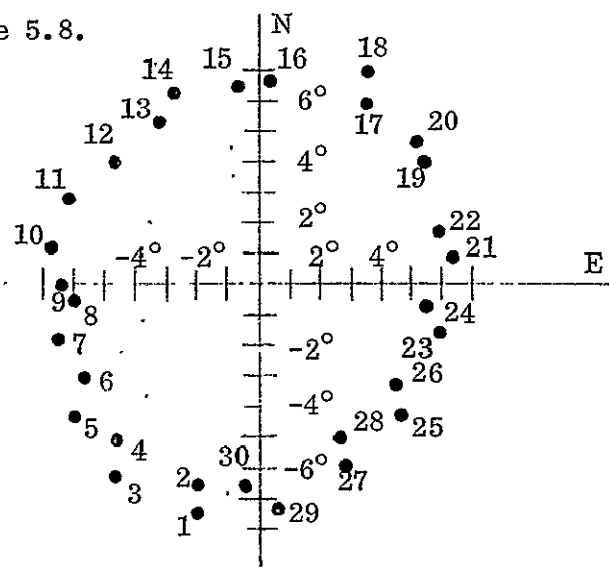


Figure 5.8 Libration Subpoints of the Thirty Optical Bundles.

The adjustment procedure for processing Earth-bound data as developed in Chapter 2 was programmed and applied to the simulated optical data for a solution of selenodetic control. Before going into detailed discussions on the various experiments carried out with the simulated optical data, the logic of the adjustment program is outlined briefly.

The backbone of the adjustment program is the numerical integration program for the physical librations of the Moon discussed in sections 5.2 and 5.3. The sequence of steps is as follows:

1. The integrating program is operated up to the "next" epoch at which a bundle was observed.
2. The integration is arrested and the information generated by the integrating program for that epoch (physical libration angles, state transition and parameter sensitivity matrices) together with information gathered by the optical bundle are used in evaluating the partial derivatives as developed in section 2.4.
3. A layer of the normal matrix, the constant vector and the considered parameters contribution matrix is generated and added to the corresponding matrices where layers from previous bundles have been accumulated.
4. The integration is resumed until the epoch of the "next" bundle and so on, until all the bundles in the batch have been processed. It should be remembered (section 2.52) that the normal matrix generated is that of the permanent parameters only, the solution for the auxiliary parameters being "folded in".
5. The a priori covariances of the permanent parameters are added to the normal matrix followed by inversion and subsequent evaluation of the solution vector (corrections to the starting values of the permanent parameters) and the

full covariance matrix of the corrected (adjusted) parameters. Full covariances mentioned above imply the inclusion of the effect of the considered parameters (see Appendix D).

This complex procedure is not particularly fast, not even on the IBM 360/75 computer. It takes about twenty seconds to process a bundle of twenty rays with intervals between bundles of sixty days.

In the remaining paragraphs of this section, the experiments carried out are described, followed by results and discussion. First the a priori covariances of the parameters used in the various solutions are presented. The units of the a priori covariances (and also of the a posteriori covariances) are as follows:

- km<sup>2</sup> - kilometer squared for coordinates of the triangulation points.
- sec<sup>2</sup> - seconds of arc squared for initial values of the physical librations and also for the physical constants (C<sub>22</sub>, β, C<sub>20</sub>).
- sec<sup>2</sup>/day<sup>2</sup> - seconds squared per day squared for initial values of the physical libration angular velocities (ḡ etc.).

The values for the covariances were selected carefully to conform with the level of uncertainties in the present knowledge of the various quantities.

$$\Sigma_1 = 10.0 \cdot I(66 \times 66) \text{ [km}^2\text{] coordinates of triangulation points}$$

$$\Sigma_2 = \begin{bmatrix} \Sigma_{2,1} & 0 \\ 0 & \Sigma_{2,2} \end{bmatrix} \text{ physical librations initial values}$$

$$\Sigma_{2,1} = 1000.0 \cdot I(3 \times 3) \text{ [sec}^2\text{]}$$

$$\Sigma_{2,2} = 250.0 \cdot I(3 \times 3) \text{ [sec}^2\text{/day}^2\text{]}$$

$$\Sigma_3 = \begin{bmatrix} 0.25 & 0 & 0 \\ 0 & 4.0 & 0 \\ 0 & 0 & 0.0001 \end{bmatrix} \text{ [sec}^2\text{] physical constants (C}_{22}\text{, } \beta\text{, C}_{20}\text{)}$$

$$\left. \begin{aligned} \Sigma_6 &= 0.2 \cdot I(3 \times 3) \text{ [sec}^2\text{] low} \\ \Sigma_6 &= 0.1 \cdot I(3 \times 3) \text{ [sec}^2\text{] normal} \\ \Sigma_6 &= 0.02 \cdot I(3 \times 3) \text{ [sec}^2\text{] high} \end{aligned} \right\} \text{ quality orientation parameters}$$

$$\left. \begin{aligned} \sigma_7^2 &= 0.1 \text{ [sec}^2\text{] low} \\ \sigma_7^2 &= 0.02 \text{ [sec}^2\text{] normal} \\ \sigma_7^2 &= 0.01 \text{ [sec}^2\text{] high} \end{aligned} \right\} \text{ quality optical observations}$$

$$\Sigma_{10} = T_M \begin{bmatrix} 0.004 & 0 & 0 \\ 0 & 0.04 & 0 \\ 0 & 0 & 0.04 \end{bmatrix} \text{ [km}^2\text{]} \quad \text{considered parameters}$$

where  $T_M$  is an orthogonal transformation matrix from the selenodetic to the inertial coordinate systems. It should be remembered that the magnitude and character of  $\Sigma_{10}$  are determined primarily from the uncertainties in the lunar ephemeris.

#### Experiment (i).

The first experiment was designed to test the quality of the solution for selenodetic control by analysing the covariance matrix (the inverted normal matrix augmented by the effect of the considered parameters) of the permanent parameters. The starting values of all the parameters involved were kept at their theoretically known (from the simulation) values. In a way the covariance matrix obtained in such a solution could be regarded as a result of the last in a series of iterative adjustment solutions where the one before the last iteration has brought the parameters very close to their final values. The specific objectives of this experiment were threefold:

- (a) To determine the rate of improvement in the quality of the solution with the gradual introduction of more data.

- (b) To evaluate the effect of variations in the quality of the optical observations on the solution for the permanent parameters.
- (c) To check if there is a significant difference in the quality of the solutions of Network I vs. Network II.

The 30 bundles were processed in a particular order, to enhance the achievement of the above objectives and to save in computer time needed for the experiment. The 30 bundles were divided into 5 batches of 6 bundles each, as follows:

batch No. 1 consisted of bundles 1, 6, 11, 16, 21, 26

batch No. 2 consisted of bundles 2, 7, 12, 17, 22, 27

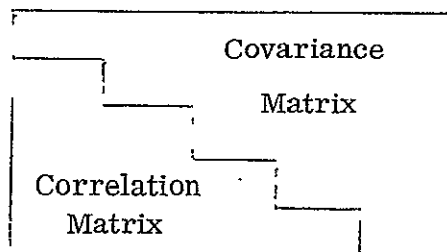
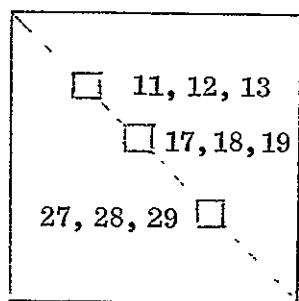
...

batch No. 5 consisted of bundles 5, 10, 15, 20, 25, 30.

As can be seen in Figure 5.8 because of the particular pattern of the libration subpoints of the bundles each batch as defined above could be used to obtain an independent solution. A solution based on a batch consisting of bundles 1 through 6, on the other hand, would certainly run into numerical problems and would produce meaningless results because of the extremely narrow resection basis.

Test (a). A series of 5 solutions were obtained. Starting with a solution from batch No. 1 alone, additional batches (Nos. 2, 3, 4, 5) were introduced in the subsequent solutions so that in the fifth solution the normal matrix was formed from processing all 30 optical bundles. Tables 5.4, 5.5, and 5.6 present samples of the results.

Table 5.4 presents diagonal submatrices of the covariance matrix and the corresponding correlations of the solution based on all 30 bundles. The correlations appear tolerable where a clear pattern of the higher correlations can be observed as follows: The x coordinates are correlated among themselves and the same applies also to the y and z coordinates, respectively. One possible reason for this phenomena is that the orientation of the selenodetic coordinate system is part of the general solution (physical libra-



Parts of Covariance/Correlation Matrix on this Page

11			12			13			
0.483	0.009	-0.001	0.303	0.009	-0.000	0.271	-0.001	-0.001	11
0.061	0.047	0.000	-0.019	0.046	0.000	-0.037	0.018	0.001	
-0.008	0.001	0.015	0.001	0.000	0.012	0.001	0.000	0.010	
0.624	-0.128	0.016	0.488	-0.023	-0.001	0.309	-0.007	-0.003	12
0.060	0.953	0.002	-0.146	0.050	0.000	-0.039	0.019	0.001	
-0.004	0.018	0.818	-0.009	0.018	0.014	-0.001	0.000	0.011	
0.529	-0.229	0.008	0.600	-0.238	-0.012	0.544	-0.012	-0.002	13
-0.009	0.679	0.025	-0.077	0.669	0.015	-0.135	0.015	-0.000	
-0.008	0.023	0.664	-0.031	0.022	0.755	-0.023	-0.010	0.015	
x	y	z	x	y	z	x	y	z	
17			18			19			
0.480	-0.007	0.001	0.283	-0.002	0.002	0.309	-0.007	0.001	17
-0.044	0.058	-0.000	0.040	0.023	-0.001	-0.027	0.050	0.000	
0.014	-0.002	0.014	-0.001	-0.000	0.012	0.002	-0.000	0.012	
0.551	0.226	-0.013	0.551	0.008	-0.005	0.261	0.035	0.000	18
-0.022	0.740	-0.013	0.083	0.017	-0.000	-0.008	0.022	0.000	
0.028	-0.033	0.818	-0.059	-0.030	0.016	0.004	-0.001	0.011	
0.639	-0.162	0.024	0.505	-0.007	0.041	0.485	-0.027	0.000	19
-0.045	0.954	-0.012	0.214	0.765	-0.045	-0.177	0.047	0.000	
0.008	0.017	0.822	0.005	0.006	0.780	0.006	0.014	0.014	
x	y	z	x	y	z	x	y	z	
27			28			29			
0.490	-0.013	-0.000	0.300	-0.019	0.001	0.294	-0.010	0.002	27
-0.144	0.017	0.001	-0.005	0.018	-0.000	-0.000	0.015	-0.000	
-0.005	0.042	0.014	-0.000	0.001	0.011	0.000	0.001	0.011	
0.629	-0.059	-0.003	0.466	-0.007	0.002	0.297	-0.004	0.002	28
-0.161	0.840	0.046	-0.062	0.028	-0.000	0.004	0.018	-0.001	
0.017	-0.020	0.800	0.025	-0.017	0.014	0.001	-0.000	0.011	
0.604	-0.003	0.006	0.625	0.034	0.014	0.484	-0.001	0.001	29
-0.106	0.859	0.049	-0.048	0.813	-0.026	-0.010	0.017	-0.001	
0.021	-0.028	0.755	0.020	-0.028	0.828	0.009	-0.033	0.014	
x	y	z	x	y	z	x	y	z	

Table 5.4 Covariance and Correlation Matrices for Solution of Network I From 30 Bundles. Triangulation Points.

$\tau$	$\sigma$	$\rho$	$\dot{\tau}$	$\dot{\sigma}$	$\dot{\rho}$	$C_{22}$	$\beta$	$C_{20}$	
0.470 03	0.520 00	0.380 00	-0.230 01	-0.570 00	0.590 00	-0.650 01	0.420 00	-0.260-03	$\tau$
0.760-03	0.100 04	0.940 00	-0.230-02	0.140-01	-0.640 01	0.220-02	-0.120 00	0.870-07	$\sigma$
0.530-02	0.500-02	0.110 02	0.120-02	0.290 02	0.170 00	0.230-01	0.220 00	0.920-06	$\rho$
-0.430 00	-0.280-03	0.150-02	0.630-01	0.990-01	-0.170-01	0.860-01	-0.160-02	0.340-05	$\dot{\tau}$
-0.170-02	0.290-04	0.550 00	0.250-01	0.250 03	0.490 00	-0.950-02	0.300 00	-0.380-06	$\dot{\sigma}$
0.240-01	-0.180 00	0.440-01	-0.600-01	0.270-01	0.130 01	-0.180-01	0.530 00	-0.730-06	$\dot{\rho}$
-0.760 00	0.180-03	0.180-01	0.870 00	-0.150-02	-0.410-01	0.150 00	-0.750-04	-0.390-05	$C_{22}$
0.350-01	-0.650-02	0.120 00	-0.110-01	0.340-01	0.830 00	-0.340-03	0.310 00	-0.300-08	$\beta$
-0.120-02	0.280-06	0.280-04	0.140-02	-0.240-05	-0.640-04	-0.990-03	-0.530-06	0.100-03	$C_{20}$

206

17			18			19			
-0.520-01	-0.780 00	-0.340-01	-0.240 00	-0.400 00	-0.950-02	0.900-01	-0.750 00	-0.320-01	$\tau$
-0.340-03	-0.110-02	0.320-01	0.130-02	-0.120-01	0.550-01	0.760-03	-0.790-02	0.110-02	$\sigma$
-0.960-01	0.420-01	-0.770-01	0.410-01	0.140-01	-0.240-01	-0.530-01	0.380-01	-0.810-01	$\rho$
0.290-01	0.100 00	0.430-01	0.250-01	0.470-01	0.390-01	0.120-01	0.970-01	0.220-01	$\dot{\tau}$
0.160-02	-0.230-02	-0.120 00	-0.580-02	-0.140-01	0.220-01	-0.360-02	-0.100-01	-0.140 00	$\dot{\sigma}$
-0.620-01	0.740-01	-0.260 00	0.740-01	0.870-01	-0.330 00	-0.110 00	0.110 00	-0.810-01	$\dot{\rho}$
-0.340-02	0.520 00	0.450-01	0.150 00	0.250 00	0.230-01	-0.830-01	0.490 00	0.330-01	$C_{22}$
-0.990-01	0.780-01	-0.240 00	0.220-01	0.850-01	-0.280 00	-0.100 00	0.110 00	-0.910-01	$\beta$
-0.540-05	0.810-03	0.710-04	0.240-03	0.400-03	0.360-04	-0.130-03	0.770-03	0.510-04	$C_{20}$
x	y	z	x	y	z	x	y	z	
27			28			29			
0.170 00	-0.360 00	-0.100-01	-0.180-02	-0.600 00	-0.190-01	-0.610-01	-0.300 00	-0.740-02	$\tau$
0.340-02	-0.350-01	-0.290-01	0.380-02	-0.320-01	0.130-01	0.460-02	-0.480-01	0.180-01	$\sigma$
0.840-01	0.210-02	-0.400-01	0.550-01	0.180-01	-0.520-01	0.120 00	-0.590-02	-0.230-01	$\rho$
-0.150-01	0.350-01	-0.110-01	0.120-01	0.710-01	0.210-01	0.620-02	0.240-01	0.160-01	$\dot{\tau}$
-0.160-01	-0.410-01	-0.730-01	-0.180-01	-0.380-01	-0.720-01	-0.220-01	-0.550-01	-0.130-01	$\dot{\sigma}$
-0.980-01	0.230 00	0.140 00	-0.790-01	0.230 00	-0.120 00	-0.280-01	0.280 00	-0.120 00	$\dot{\rho}$
-0.990-01	0.230 00	0.160-02	-0.570-02	0.400 00	0.230-01	0.500-01	0.190 00	0.120-01	$C_{22}$
-0.420-01	0.200 00	0.100 00	-0.740-01	0.200 00	-0.110 00	-0.270-01	0.240 00	-0.110 00	$\beta$
-0.150-03	0.360-03	0.250-05	-0.890-05	0.620-03	0.370-04	0.780-04	0.300-03	0.190-04	$C_{20}$

Table 5.5 Covariance and Correlation Matrices for Solution of Net I From 30 Bundles.

Physical Libration Parameters.

tions initial values). On the other hand the coordinates of an individual triangulation point are almost completely noncorrelated. Another typical result to be noted in Table 5.4 is that the x coordinates are determined much less accurately as compared to y and z. Also for points near the zero meridian of the Moon (points with small y coordinates) like points Nos. 11, 12, 17, 19 and 28 (see Figure 5.7) the coordinate z is better determined than y. Points on the limb like 13 and 18 have larger than average uncertainties in x; however their y coordinates are as well determined as their z coordinates. This phenomena is sometimes referred to as the "poor planimetry and fair altimetry" of the limb points on the Moon and vice versa for points in the central region.

Table 5.5 presents the portion of the covariance/correlation matrix of the 30 bundles solution pertaining to the physical libration initial values and the physical constants. At the top the covariances and correlations of the physical libration parameters are presented while at the middle and at the bottom the correlations between the physical libration parameters and the coordinates of some of the triangulation points are shown. The striking feature of the solution for the physical libration parameters is the poor quality of  $\tau$  and the complete insensitivity of the data to  $\sigma$  and  $\dot{\sigma}$ . As can be seen in the table the covariances of  $\sigma$  and  $\dot{\sigma}$  remained after the solution at their a priori values indicating that the solution could not bring any improvement in  $\sigma$  and in  $\dot{\sigma}$ . The improvement in  $\tau$  is from  $1000 \text{ sec}^2$  down to  $472 \text{ sec}^2$  which is not too impressive, considering the large amount of good data involved (optical observations of normal accuracy). It is hard to find a good explanation for this phenomena. One reason may be that one year is too short a period for a solution of a quantity ( $\sigma$ ) defined by the intersection of two planes which form an angle of only  $1.5^\circ$ . As for  $\tau$  it should be remembered that in longitude a selenocentric angle of  $10''$  is about 85 meters on the lunar equator and much less in northern or southern

Without Considered Parameters Effect

	x	y	z	x	y	z	
1	C.562584D CC	0.163333D-01	C.143511D-01	0.618283D CC	0.165249D-01	0.150504D-01	2
3	0.676374D CC	C.175525D-01	0.163297D-01	C.473733D CC	0.254711D-01	C.134444D-01	5
6	0.609828D CC	C.161221D-01	C.154263D-01	0.487897D CC	0.282217D-01	C.148515D-01	7
8	C.480355D CC	C.444248D-01	C.140485D-01	C.694399D CC	0.170668D-01	0.171152D-01	10
11	0.482887D CC	0.466761D-01	0.150172D-01	0.487856D CC	0.501683D-01	C.137219D-01	12
13	C.544261D CC	C.154761D-01	0.147903D-01	0.481852D CC	0.581563D-01	C.142864D-01	15
17	0.479942D CC	0.577590D-01	0.144488D-01	C.551096D CC	0.173817D-01	0.155690D-01	18
19	C.485216D CC	0.472284D-01	C.136118D-01	C.596558D CC	0.159762D-01	C.155148D-01	20
22	C.470524D CC	C.480731D-01	C.141866D-01	C.765189D CC	0.177341D-01	C.173345D-01	24
27	0.489847D CC	0.171649D-01	C.136552D-01	0.466157D CC	0.277558D-01	0.135506D-01	28
29	0.483512D CC	C.167973D-01	C.136111D-01	0.533234D CC	0.165523D-01	C.140026D-01	30
T	0.472491D C3	C.999740D C3	C.109292D C2	0.632028D-01	0.248994D C3	0.129954D 01	
	0.153251D CC	0.212494D 00	C.999998D-04	$\hat{\tau}$	$\hat{\sigma}$	$\hat{\rho}$	
	$C_{22}$	$\beta$	$C_{20}$				

Including Considered Parameters Effect

1	0.625898D CC	0.167121D-01	C.162300D-01	C.710932D CC	0.170971D-01	C.172169D-01	2
3	C.736631D CC	C.175356D-01	C.191806D-01	0.532098D CC	0.260196D-01	C.148171D-01	5
6	0.701103D CC	C.163948D-01	0.177119D-01	C.539170D CC	0.286490D-01	C.166866D-01	7
8	0.540241D CC	0.455234D-01	0.155942D-01	0.745345D CC	0.169368D-01	0.200498D-01	10
11	0.534801D CC	0.477995D-01	C.168795D-01	0.549398D CC	0.515697D-01	C.151288D-01	12
13	0.606834D CC	C.155563D-01	0.166886D-01	0.540493D CC	C.598804D-01	0.158776D-01	15
17	C.536743D CC	C.594767D-01	0.160965D-01	C.604126D CC	0.175109D-01	0.177350D-01	18
19	0.542828D CC	C.486771D-01	0.149772D-01	C.687961D CC	0.157927D-01	C.178423D-01	20
22	0.523661D CC	0.496237D-01	C.157616D-01	C.844837D CC	0.177777D-01	C.203830D-01	24
27	0.542246D CC	C.174342D-01	C.150754D-01	C.520372D CC	0.286634D-01	C.149459D-01	28
29	0.543744D CC	0.172671D-01	C.150639D-01	C.597391D CC	0.168387D-01	C.156928D-01	30
T	0.472382D C3	C.999744D C3	0.143185D C2	0.649896D-01	0.249007D C3	C.171579D 01	
	0.153286D CC	C.383895D 00	C.999998D-04	$\hat{\tau}$	$\hat{\sigma}$	$\hat{\rho}$	
	$C_{22}$	$\beta$	$C_{20}$				

Table 5.6 Diagonal Elements of Covariance Matrix for Solution of Net I from 30 Bundles.

latitudes. So it appears that the poor determination of  $\tau$  and the somewhat poorer solutions for  $y$  (Table 5.4) of points near the zero meridian are interrelated. Actually this is clearly demonstrated by the high correlations between  $\tau$  and the  $y$  coordinates of points 17, 19 and 28 (see Figure 5.7). One encouraging result in the somewhat grim picture is the tolerable correlation between  $\dot{\tau}$  and  $C_{22}$  which in Sections 5.2 and 5.3 was a cause for considerable concern. Actually the solution for  $\dot{\tau}$  has a comfortingly small covariance corresponding to a standard deviation of about 0.25 sec/day, much better than in the solution for  $\dot{\rho}$ .  $\beta$  is also well determined corresponding to a solution good to almost four significant figures.

Table 5.6 displays the diagonal elements of the covariance matrix without and with the inclusion of the effect of the considered parameters. It is somewhat surprising to find out that it is the  $x$  coordinates which are affected mostly by the considered parameters while in  $y$  and in  $z$  there are much smaller effects. This is surprising because the uncertainties ( $\Sigma_{10}$ ) in the  $x$  direction were set at about  $\pm 60$  meters (one- $\sigma$ ) while in  $y$  and in  $z$  they were  $\pm 200$ m. It is possible that the constraints in orientation of the bundles ( $\sigma \cong \pm 0.3$ ) together with the great abundance of data reduced markedly the effect of the considered parameters on  $y$  and on  $z$ . The considered parameters seem to have little or no effect on the covariances of the physical libration initial values and the physical constants.

Table 5.7 presents the improvement in the solution with the introduction of the second, third, etc. batches into the solution. One pattern which is typical for almost all the coordinates as well as for the physical libration parameters (with the exception of  $\sigma$  and of  $\dot{\sigma}$ ) is the sharp improvement between the one and two-batches-solution. After that the degree of improvement levels off. The preliminary conclusion to be drawn from this result is that a greater abundance of data does not necessarily mean a significant improvement in the solution.

	x	y	z	x	y	z	
18	0.176139D 01	0.692431D-01	0.781185D-01	0.144416D 01	0.125875D 00	0.684813D-01	19
21	0.142548D 01	0.101262D 00	0.735069D-01	0.141730D 01	0.127616D 00	0.703892D-01	22
23	0.144555D 01	0.887345D-01	0.685858D-01	0.141691D 01	0.994833D-01	0.710220D-01	25
26	0.143456D 01	0.933615D-01	0.681500D-01	0.151367D 01	0.672012D-01	0.691305D-01	27
28	0.143714D 01	0.875665D-01	0.685596D-01	0.179471D 01	0.699043D-01	0.736899D-01	29
T	0.761160D 03	0.999774D 03	0.540728D 02	0.168057D 00	0.249078D 03	0.501924D 01	
C <sub>22</sub>	0.220457D 00	0.161944D 01	0.100000D-03	C <sub>20</sub> $\hat{t}$	$\hat{\sigma}$	$\hat{\rho}$	
18	0.107611D 01	0.380048D-01	0.404382D-01	0.929329D 00	0.825495D-01	0.359487D-01	19
21	0.919201D 00	0.643828D-01	0.389790D-01	0.908628D 00	0.840264D-01	0.370990D-01	22
23	0.934644D 00	0.544991D-01	0.359559D-01	0.907293D 00	0.628216D-01	0.374737D-01	25
26	0.920359D 00	0.579767D-01	0.357077D-01	0.965538D 00	0.373945D-01	0.362165D-01	27
28	0.915188D 00	0.534729D-01	0.359611D-01	0.103168D 01	0.378328D-01	0.369663D-01	29
T	0.635183D 03	0.999765D 03	0.296760D 02	0.119890D 00	0.249041D 03	0.284320D 01	
C <sub>22</sub>	0.192321D 00	0.822275D 00	0.999999D-04	C <sub>20</sub> $\hat{t}$	$\hat{\sigma}$	$\hat{\rho}$	
18	0.816252D 00	0.268857D-01	0.275705D-01	0.730151D 00	0.685491D-01	0.244570D-01	19
21	0.718152D 00	0.518794D-01	0.270988D-01	0.710210D 00	0.699181D-01	0.254827D-01	22
23	0.732519D 00	0.428245D-01	0.244108D-01	0.705672D 00	0.504493D-01	0.257947D-01	25
26	0.716904D 00	0.460269D-01	0.242196D-01	0.745879D 00	0.269098D-01	0.246058D-01	27
28	0.708000D 00	0.418380D-01	0.244544D-01	0.771500D 00	0.269052D-01	0.248375D-01	29
T	0.570443D 03	0.999762D 03	0.211910D 02	0.101739D 00	0.249032D 03	0.230396D 01	
C <sub>22</sub>	0.177436D 00	0.631398D 00	0.999999D-04	C <sub>20</sub> $\hat{t}$	$\hat{\sigma}$	$\hat{\rho}$	
18	0.691025D 00	0.212260D-01	0.212420D-01	0.614186D 00	0.592240D-01	0.185525D-01	19
21	0.600603D 00	0.439205D-01	0.207311D-01	0.593363D 00	0.603483D-01	0.193786D-01	22
23	0.616607D 00	0.357920D-01	0.185267D-01	0.589397D 00	0.425605D-01	0.196382D-01	25
26	0.600975D 00	0.386148D-01	0.183475D-01	0.619596D 00	0.211823D-01	0.186678D-01	27
28	0.590793D 00	0.347138D-01	0.185258D-01	0.632686D 00	0.209602D-01	0.187284D-01	29
T	0.522466D 03	0.999759D 03	0.164086D 02	0.874166D-01	0.249019D 03	0.185380D 01	
C <sub>22</sub>	0.165965D 00	0.451218D 00	0.999999D-04	C <sub>20</sub> $\hat{t}$	$\hat{\sigma}$	$\hat{\rho}$	
18	0.622028D 00	0.179735D-01	0.176676D-01	0.541140D 00	0.540372D-01	0.149676D-01	19
21	0.526608D 00	0.394302D-01	0.169913D-01	0.520053D 00	0.550847D-01	0.157245D-01	22
23	0.543576D 00	0.317395D-01	0.149534D-01	0.515901D 00	0.381435D-01	0.159698D-01	25
26	0.527542D 00	0.344197D-01	0.147755D-01	0.540827D 00	0.177959D-01	0.150734D-01	27
28	0.516342D 00	0.306875D-01	0.149338D-01	0.547017D 00	0.175002D-01	0.150526D-01	29
T	0.494429D 03	0.999757D 03	0.139085D 02	0.791805D-01	0.249011D 03	0.166974D 01	
C <sub>22</sub>	0.159349D 00	0.371249D 00	0.999999D-04	C <sub>20</sub> $\hat{t}$	$\hat{\sigma}$	$\hat{\rho}$	

Table 5.7 Diagonal Elements of Covariance Matrix for Solutions from 6, 12, 18, 24 and 30 Bundles

	x	y	z	x	y	z	
3	0.463113D 01	0.186486D 00	0.192943D 00	0.358093D 01	0.182831D 00	0.152612D 00	5
6	0.584570D 01	0.208276D 00	0.229464D 00	0.361450D 01	0.186515D 00	0.163935D 00	7
8	0.361376D 01	0.240105D 00	0.156227D 00	0.428456D 01	0.162096D 00	0.181024D 00	10
11	0.359220D 01	0.243932D 00	0.164080D 00	0.362549D 01	0.257973D 00	0.153211D 00	12
13	0.423848D 01	0.165112D 00	0.175685D 00	0.360609D 01	0.282465D 00	0.157245D 00	15
17	0.359350D 01	0.280665D 00	0.158587D 00	0.425398D 01	0.165835D 00	0.181364D 00	18
19	0.359321D 01	0.247121D 00	0.152536D 00	0.531090D 01	0.205469D 00	0.227252D 00	20
22	0.354576D 01	0.249167D 00	0.156906D 00	0.540598D 01	0.190744D 00	0.199975D 00	24
27	0.366144D 01	0.157071D 00	0.155708D 00	0.357152D 01	0.187622D 00	0.153061D 00	28
29	0.432876D 01	0.169945D 00	0.170661D 00	0.433676D 01	0.168874D 00	0.170141D 00	30
T	0.864332D 03	0.999785D 03	0.145248D 03	0.251119D 00	0.249157D 03	0.132445D 02	
C <sub>22</sub>	0.236584D 00	0.280966D 01	0.100000D-03	C <sub>20</sub>	$\bar{r}$	$\bar{\sigma}$	$\bar{\rho}$
3	0.186023D 01	0.711855D-01	0.809387D-01	0.146455D 01	0.819187D-01	0.683792D-01	5
6	0.287926D 01	0.768543D-01	0.926366D-01	0.147935D 01	0.854870D-01	0.731122D-01	7
8	0.149505D 01	0.114147D 00	0.702323D-01	0.172677D 01	0.662794D-01	0.783872D-01	10
11	0.147992D 01	0.117628D 00	0.735201D-01	0.149870D 01	0.124273D 00	0.689157D-01	12
13	0.184077D 01	0.679281D-01	0.754342D-01	0.149534D 01	0.138369D 00	0.708470D-01	15
17	0.148750D 01	0.137662D 00	0.714199D-01	0.169615D 01	0.693115D-01	0.785084D-01	18
19	0.147172D 01	0.119245D 00	0.685125D-01	0.255675D 01	0.735290D-01	0.905539D-01	20
22	0.144895D 01	0.121051D 00	0.705838D-01	0.242239D 01	0.740679D-01	0.841223D-01	24
27	0.150877D 01	0.675709D-01	0.691330D-01	0.145541D 01	0.861721D-01	0.686226D-01	28
29	0.176533D 01	0.703094D-01	0.738040D-01	0.177893D 01	0.690315D-01	0.734495D-01	30
T	0.717898D 03	0.999763D 03	0.540291D 02	0.142740D 00	0.249067D 03	0.529807D 01	
C <sub>22</sub>	0.207876D 00	0.157308D 01	0.999999D-04	C <sub>20</sub>	$\bar{r}$	$\bar{\sigma}$	$\bar{\rho}$
3	0.118557D 01	0.223830D-01	0.323516D-01	0.100513D 01	0.344744D-01	0.237653D-01	5
6	0.208276D 01	0.261167D-01	0.402626D-01	0.100475D 01	0.376600D-01	0.272102D-01	7
8	0.103927D 01	0.603613D-01	0.252909D-01	0.110493D 01	0.204262D-01	0.306441D-01	10
11	0.101896D 01	0.633497D-01	0.276529D-01	0.103967D 01	0.684002D-01	0.243492D-01	12
13	0.127405D 01	0.218825D-01	0.282660D-01	0.103829D 01	0.795470D-01	0.258190D-01	15
17	0.103045D 01	0.790430D-01	0.262290D-01	0.107194D 01	0.233938D-01	0.307317D-01	18
19	0.100616D 01	0.645545D-01	0.240084D-01	0.185620D 01	0.230818D-01	0.388211D-01	20
22	0.987108D 00	0.661174D-01	0.255584D-01	0.160794D 01	0.250617D-01	0.346017D-01	24
27	0.100052D 01	0.223797D-01	0.240157D-01	0.972210D 00	0.381573D-01	0.239573D-01	28
29	0.112661D 01	0.236477D-01	0.273544D-01	0.113887D 01	0.222685D-01	0.270261D-01	30
T	0.623770D 03	0.999757D 03	0.388401D 02	0.105959D 00	0.249045D 03	0.370085D 01	
C <sub>22</sub>	0.186822D 00	0.113533D 01	0.999999D-04	C <sub>20</sub>	$\bar{r}$	$\bar{\sigma}$	$\bar{\rho}$

Table 5.8 Effect on the Solution of Different Optical Observation Accuracies

Test (b). Only one batch (6 bundles) was used to generate normal matrices at three different quality levels of optical observations: low, normal and high. As it could be expected, the quality of the solution is directly proportional to the quality of the optical data. In Table 5.8 the diagonal elements of the covariance matrix are presented for the three solutions beginning at the top with the low quality optical data and ending at the bottom with the solution from the high quality data. The results of this test clearly indicate that the general quality of the solution for selenodetic control strongly depends on the quality of the optical observations. It should be noted that optical observations of a higher quality imply that not only the directions in a bundle relative to each other are known better but also that the orientation of the bundle has smaller uncertainties.

Test (c). A parallel solution to the one discussed in (a) above was run with 30 bundles simulated for Control Network II. At all levels of the solution (6, 12, etc. bundles) the differences in the covariances were found to be insignificant and what is more important no clear pattern could be detected in the differences. It is possible that the reason for this similarity is in the positions of the points chosen for Net I and for Net II. As it can be seen in Figure 5.7 the points chosen for the two networks do not follow exactly the definition of "center and limb" vs. "center only" networks as stated at the beginning of this section. The deviations from these rules may have removed the distinction between the two networks and consequently may have produced two different networks but of the same intermediate type.

#### Experiment (ii).

The second experiment had a more limited objective. Three tests were run to find out the extent to which the adjustment program is capable of recovering shifts introduced in the starting parameters (approximate values of the parameters). In a manner similar to that employed in Section 5.2 the three tests were designed as follows:

- (a) Only the coordinates of the triangulation points were shifted from their known absolute values (simulated coordinates).
- (b) Only the physical libration initial values and the parameters  $C_{22}$  and  $\beta$  were shifted while the coordinates were left at their absolute values.
- (c) All the permanent parameters (with the exception of  $C_{20}$ ) were shifted.

Even before examining the results it should be clear by now from the discussions presented in (i) above that no spectacular results can be expected from the program and the particular Earth-bound simulated data. This is true in particular considering the fact that only one iteration of the adjustment per test case was performed and the data used consisted of only one batch of 6 bundles of optical data.

Test (a). Table 5.9 presents the absolute coordinates of the triangulation points and the solution vector (negative) after one iteration of the adjustment. The starting (shifted) coordinates were set simply by removing from the absolute coordinates the decimal fraction. So the degree of recovery can be assessed by comparing the negative value of the solution vector with the fractional part of the corresponding absolute coordinate. The degree of recovery of the shifts is impressive, more so considering the low quality of the solution as exhibited by the covariances (see (i) above). A general pattern can be recognized in the difference in the degree of recovery of the x coordinates as compared to that in y and in z. It can be seen in Table 5.9 that in x the recovery is much less efficient. As stated earlier the main reason for this as well as for the higher uncertainties in the solution for x lies in the poor geometry of the optical observations of the Moon conducted from the Earth.

Test (b). Only the starting values of the physical libration parameters were shifted as follows:

$$\begin{array}{lll}
 \Delta \tau = 4''.27 & \Delta \dot{\tau} = -1.54''/\text{day} & \Delta C_{22} = 0''.21 \\
 \Delta \sigma = 45''.09 & ; \quad \Delta \dot{\sigma} = -62.70''/\text{day} ; & \Delta \beta = -0''.41 \\
 \Delta \rho = -5''.40 & \Delta \dot{\rho} = -2.57''/\text{day} & \Delta C_{20} = 0''.00
 \end{array}$$

Solution Vector

	x	y	z	x	y	z	
1	-0.2491957 00	0.3101670 00	-0.6716820 00	0.4512320-01	-0.5090600 00	-0.1645110 00	2
3	-0.4873230 00	0.4390740 00	-0.2635030 00	-0.3418440 00	-0.5406490 00	-0.1975840 00	5
6	0.3390170 00	-0.3545130 00	-0.7345390 00	-0.1245630 00	0.5943230 00	-0.6887960 00	7
8	0.2139880 00	0.2768100 00	-0.1397550 00	0.2160750 00	0.9044010 00	-0.6007560 00	10
11	-0.2890360-01	0.8466370 00	-0.4857660 00	0.1717670 00	-0.9637410 00	-0.5836460 00	12
13	0.2166890 00	-0.9280990 00	-0.6017100 00	0.8728060-01	-0.1329570-01	-0.8301960 00	15
17	-0.1672220 00	0.2048720 00	0.4681040 00	-0.1280610 00	0.7752670 00	0.9875630 00	18
19	0.2280090 00	-0.4330690 00	0.5900060 00	-0.2580440 00	-0.7103170 00	0.3211860 00	20
22	-0.4241280 00	0.4789410 00	0.1551740 00	-0.9368160-02	0.9545610 00	0.8933470 00	24
27	-0.3318220 00	-0.4867260 00	0.7929960 00	-0.9496580-01	-0.5175810 00	0.2045170 00	28
29	0.1296450 00	0.7770900 00	0.5435990 00	-0.1547550-01	-0.1537190-01	0.2802520 00	30
T	-0.1221540 00	0.5497170-02	-0.6251510-01	-0.2673450-03	-0.1851670-01	-0.5030320-02	
C <sub>22</sub>	-0.2252110-02	-0.1936830-01	-0.9008430-07	C <sub>20</sub>	†	‡	δ

214

Absolute (Simulated) Coordinates of Triangulation Points

	x	y	z	x	y	z	
1	284.7144	-164.8233	1705.6738	267.3828	742.4968	1548.1653	2
3	298.9905	-1050.4536	1350.2634	897.8094	293.5282	1457.1998	5
6	297.0151	1298.3423	1116.7341	1013.5746	-1088.6066	894.6916	7
8	1453.2020	-75.2901	946.1413	341.1861	-1615.9158	536.6048	10
11	1506.4731	-767.8602	390.4892	1577.2501	544.9516	478.5874	12
13	341.1861	1617.9158	536.6048	1735.3430	1.	29.8342	15
17	1726.6207	-150.2785	-91.4655	490.5786	-1611.7874	-420.9863	18
19	1499.1838	733.4201	-479.5874	294.7339	1686.6973	-302.3192	20
22	1511.8985	-121.4927	-843.1513	257.4409	-1221.9682	-1207.8911	24
27	449.7967	1120.4735	-1250.7900	940.5390	83.5052	-1458.1998	28
29	377.2905	-378.7905	-1653.5386	305.4515	368.0022	-1671.2764	30

Table 5.9. Solution Vector for Test (a) in Experiment (ii)

Coordinates of Triangulation Points

	x	y	z
1	0.4955070-01	0.1464670-01	-0.6755610-02
3	0.5639680-01	0.1288930-01	0.5069450-03
6	0.6329310-02	0.9495640-02	-0.1901100-01
8	0.6369970-01	0.1983280-01	-0.5729260-01
11	0.5831670-01	0.1520750-01	-0.5289880-01
13	-0.1734040-01	0.6958680-02	-0.2373500-01
17	0.3660910-01	0.1320600-01	-0.6739250-01
19	-0.3971020-02	0.8442020-02	-0.6528710-01
22	-0.2703040-02	0.5016090-02	-0.5833880-01
27	-0.7364130-01	-0.7189580-02	-0.2440090-01
29	-0.8224540-01	-0.1039940-01	-0.7548570-02
2	0.2614170-01	0.1274030-01	-0.1366030-01
5	0.6221300-01	0.1982200-01	-0.3532250-01
7	0.6254660-01	0.1557500-01	-0.2977550-01
10	0.1891510-01	0.8283830-02	0.3006380-02
12	0.4461550-01	0.1746470-01	-0.6627710-01
15	0.3953220-01	0.1438860-01	-0.6898750-01
18	-0.1080770-01	0.8055180-03	-0.3733860-02
20	-0.3794870-01	0.7484650-03	-0.2297280-01
24	-0.7456660-01	-0.6454700-02	0.4016780-02
28	-0.5097740-01	-0.5217150-02	-0.3581790-01
30	-0.9813790-01	-0.1092560-01	-0.1133170-01

Parameters of Physical Librations

	$\tau$	$\sigma$	$\rho$
Solution	0.4093290 01	-0.5416810-01	0.1771080 01
Shift	-4."27	-45!"09	5!"40
	$\dot{\tau}$	$\dot{\sigma}$	$\dot{\rho}$
Solution	-0.1654280 01	-0.5471280-01	-0.1954230 01
Shift	1.54 "/day	62.70 "/day	2.57 "/day
	$C_{22}$	$\beta$	$C_{20}$
Solution	0.1551930-01	-0.2222570 00	0.6507590-06
Shift	-0!"21	0!"41	0!"00

Table 5.10 Solution Vector for Test (b) in Experiment (ii)

Table 5.10 presents the elements of the solution vector. The recovery is excellent for  $\tau$  and  $\dot{\tau}$ ; it is fair for  $\dot{\rho}$  and  $\beta$ ; it is poor for  $\rho$  and  $C_{22}$ ; and it is non-existent for  $\sigma$  and  $\dot{\sigma}$ . This is rather surprising as the covariances (not shown) are very much the same as in the cases discussed in (i) above.  $\rho$  is not as well determined as one would have expected but on the other hand  $\tau$  is really excellent, much better than indicated by the covariance of the solution for  $\tau$ . No final conclusions can be reached from this experiment as it is felt that one or two more iterations would have brought the physical libration parameters closer to their absolute values. However, the problem with the inability of the procedure to solve for  $\sigma$  and for  $\dot{\sigma}$  remains and further investigation is necessary in order to determine the exact cause of this disturbing phenomena. The shifts introduced in  $\sigma$  and in  $\dot{\sigma}$  were set actually larger than the a-priori covariances ( $1000 \text{ sec}^2$ ,  $250 \text{ sec}^2/\text{day}^2$ ) in order to find out if any correction in the right direction would occur. It did not produce any results and the solution remained insensitive to the shifts in  $\sigma$  and  $\dot{\sigma}$ . The coordinates of the triangulation points received "corrections" - generally small - which is another way of demonstrating the small but nevertheless existing correlations between the physical libration parameters and the coordinates of the triangulation points. It should be noted by examining the solution vector that the "corrections" or actually errors introduced in  $z$  are slightly larger than those in  $y$  probably due to the error remaining after the adjustment in the value of  $\rho$  (the physical libration in inclination).

Test (c). The shifts in all the permanent parameters were set as for cases (a) and (b) put together. Table 5.11 presents the solution vector and the absolute coordinates of the points (as in Table 5.9) as well as the shifts introduced in the physical libration parameters. There is no significant difference between cases (c) and (a) as far as the recovery of shifts in the coordinates are concerned and the same applies to cases (c) and (b) for the

Solution Vector

	x	y	z	x	y	z	
1	-0.200808D 00	0.824526D 00	-0.678571D 00	0.705724D-01	-0.496463D 00	-0.178005D 00	2
3	-0.432900D 00	0.451851D 00	-0.263232D 00	-0.280111D 00	-0.521331D 00	-0.233920D 00	5
6	0.344812D 00	-0.344246D 00	-0.753193D 00	-0.637059D-01	0.609942D 00	-0.718852D 00	7
8	0.279927D 00	0.297119D 00	-0.196453D 00	0.238025D 00	0.912547D 00	-0.597833D 00	10
11	0.259190D-01	0.862415D 00	-0.539065D 00	0.216077D 00	-0.946419D 00	-0.650471D 00	12
13	0.197241D 00	-0.920370D 00	-0.625250D 00	0.126360D 00	0.148574D-02	-0.899227D 00	15
17	-0.131186D 00	0.278351D 00	0.400670D 00	-0.136340D 00	0.776199D 00	0.983971D 00	18
19	0.227196D 00	-0.424527D 00	0.525079D 00	-0.295157D 00	-0.708580D 00	0.298213D 00	20
22	-0.426854D 00	0.483852D 00	0.967144D-01	-0.790565D-01	0.948349D 00	0.897496D 00	24
27	-0.409014D 00	-0.494354D 00	0.768983D 00	-0.147572D 00	-0.522653D 00	0.168347D 00	28
29	0.457082D-01	0.766990D 00	0.535345D 00	-0.114885D 00	-0.262701D-01	0.269267D 00	30
T	0.392739D 01	-0.485298D-01	0.171527D 01	-0.165366D 01	-0.735039D-01	-0.195694D 01	
C <sub>22</sub>	0.145543D-01	-0.240210D 00	0.610297D-06	C <sub>20</sub>	$\hat{t}$	$\hat{\sigma}$	$\hat{\rho}$

Absolute (Simulated) Coordinates of Triangulation Points

	x	y	z	x	y	z	
1	284.7122	-166.8223	1705.6738	267.3828	742.2968	1546.1452	2
3	298.0006	-1610.4536	1350.2634	897.8094	293.5292	1457.1098	5
6	297.0151	1208.3423	1116.7341	1013.5746	-1098.6066	894.6016	7
8	1453.2020	-75.2001	946.1413	341.1861	-1615.9155	526.6046	10
11	1506.4731	-767.8602	300.4802	1577.2501	544.9516	478.5174	12
13	341.1861	1617.9158	536.6048	1735.3430	1.	24.8342	15
17	1726.6207	-150.2785	-01.4655	490.5786	-1611.7874	-420.9863	18
19	1499.1838	733.4201	-470.5874	294.7339	1696.6973	-302.3192	20
22	1511.8985	-131.4927	-843.1513	257.4409	-1221.5682	-1207.8911	24
27	449.7467	1120.4735	-1250.7900	940.5300	83.5052	-1458.1098	28
29	377.2005	-378.7005	-1653.5386	305.4515	368.0022	-1671.2764	30

Table 5.11 Solution Vector for Test (c) in Experiment (ii)

physical libration parameters. It is another proof of the relative independence in the solution for the coordinates of the points in the control network on one hand and the solution for the parameters of the physical librations on the other. The covariance matrix (not shown) is almost exactly the same as for cases shown in (i) above.

It would be premature and rather presumptuous to state that definite conclusions can be drawn from the few experiments with simulated data performed in this section. As it was declared in the introduction to this chapter the main purpose was to demonstrate the feasibility of the adjustment program and to develop a feeling for the many problems that lie ahead. With a large degree of reservation it can be stated that from the experiments described in this section it appears that the coordinates of a selenodetic control network can be solved rather efficiently from processing Earth-based optical observations and scaling the network by the lunar ephemeris. The solution for the physical libration parameters is less spectacular and there remains the problem of the inability of the procedure to solve for  $\sigma$  and  $\dot{\sigma}$ . In general however the results demonstrate convincingly that the theory developed in Chapter 2 is sound and it is possible to solve simultaneously for the coordinates of the control network points and for the orientation parameters of the selenodetic coordinate system.

## 6. SUMMARY AND CONCLUSIONS

This study was undertaken to solve the problem of determination of an optimal selenodetic control network on the Moon. Selenodetic control is defined by the coordinates of a network of well identifiable features on the lunar surface with respect to a selenodetic Cartesian coordinate system which is fixed to the lunar crust, is centered at its mass center and is oriented along the three principal axes of inertia of the Moon. The solution of this problem, although closely related to the dynamical properties of the Moon, is not a comprehensive datum solution for the Moon which by definition includes in addition to the fundamental selenodetic control also the parameters of the lunar gravitational field and the elements of its general geometric figure.

In order not to compromise the generality and rigor of the solution, the method, as developed in this study, is fully consistent with the theoretical and numerical models for the motion of the Moon in space. For this purpose, the definition of the selenodetic coordinate system and its orientation in space are given particular attention. Actually, the parameters of orientation of the selenodetic system with respect to the mean ecliptic coordinate system were made an integral part of the solution for selenodetic control.

The solution in this study is based on processing optical, range and range-rate data obtained from photography or direct angular observations of the Moon and range or range-rate measurements from tracking stations on Earth to satellites orbiting the Moon. As all the observations are either taken directly from the Earth or are related to it (a satellite photographing the Moon is tracked from stations on Earth) the geocentric ephemeris of the lunar mass center and also the geocentric coordinates of

the stations engaged in relevant observational activities are incorporated in the solution. In order not to expand unnecessarily the scope of the study, the geocentric lunar ephemeris and coordinates of observing stations on Earth are kept as fixed quantities in the solution although their uncertainties are reflected in the covariances of the solved parameters.

In the solution, the Moon is regarded as a rigid body rotating in space in a complicated manner under the influence of the gravitational attraction of the Earth and the Sun, the effect of the planets being neglected. The orientation of the Moon in space is defined through three Eulerian angles relating the selenodetic coordinate system to the mean ecliptic system. The value of these angles (or rather the so-called physical libration angles) at any epoch constitutes the solution for the orientation of the Moon. Around the Moon in space there are a variety of sensors engaged in optical observations of the Moon. An optical observation is defined as the direction in space from a projection center (the sensor) to a particular feature on the lunar surface. The optical observations are usually grouped in bundles, i.e., directions emanating simultaneously from the same projection center. These optical observations modeled in terms of the parameters of the solution are processed by a weighted least squares adjustment procedure and result in estimates for the following parameters and their covariances:

- a. the selenodetic coordinates of a selected number of features on the lunar surface;
- b. six parameters of orientation of the Moon in space (physical libration initial values);
- c. three parameters featuring the low degree terms (second degree) in the lunar gravitational field.

In case the projection center is on board a spacecraft, in addition to the optical data, range and range-rate measurements from the Earth to the spacecraft are incorporated in the adjustment process. A standard orbit determination procedure is applied to the range and range-

rate data which results in estimates for the selenocentric state vector of the spacecraft and also in estimates of parameters of the gravitational field of the Moon. As the position of the spacecraft is identified with the projection center and also some of the parameters of the gravitational field of the Moon figure in the model for the optical observations, it is necessary for the optical data taken from the satellite to be processed simultaneously with the range and range-rate measured from Earth to the satellite.

In order to test numerically the mathematical procedures developed in this study, a simulated environment was created which reflects very closely the true world. The Earth, the Moon and a variety of satellites move and rotate in this simulated environment strictly according to the laws of Newton and Kepler. The observational material generated is absolutely free of any unaccounted phenomena and although certain simplifications were introduced, it simulates very closely real observations that could be obtained through photography or by Doppler tracking as the case may be.

A number of experiments run with the simulated data served as a test for the mathematical development in this study and provided also a sample of the quality of results that could be expected from processing real data with the same characteristics. Tests of the new model for the physical librations of the Moon demonstrated that the adjustment procedure is capable of estimating the parameters of physical libration and with one exception, the correlations between the parameters are tolerable.

Experiments were run also with real data in which the model for the physical librations was compared to an existing model. The results of the comparison indicated a surprising similarity although the approaches taken in developing the two models were entirely different.

A complete selenodetic control solution was attempted using as source data thirty simulated bundles of optical rays taken from the Earth. The results confirmed once more the limitations of the Earth bound data. The

covariance matrices indicated a comparatively poor determination of the coordinates of the lunar features with standard deviations in the hundreds of meters. The parameters of the physical librations of the Moon were not determined much better, i. e. , the standard deviations of the initial values of the physical librations were of the order of tens of seconds of arc. The primary reason is that the attempted solution was limited to Earth bound data thus only letting the poor geometry and the great distance have their say. There is little doubt that the inclusion of satellite-borne optical data would have changed the situation entirely.

There are many problem areas which can be seen as a natural continuation of the present study. Actually, at almost every step in the course of the research, there were new questions raised, new avenues of research laid open, tempting and promising, interesting and previously unknown answers, just around the corner. A great deal of restraint had to be applied in order to keep the present study within the predetermined scope and time limits. The main problem areas are outlined in the form of questions and brief comments:

- a. What is the comparative value of optical observations obtained from a low orbiting spacecraft (perigee of less than 100 miles) as compared to observations from a high spacecraft (perigee of more than 1000 miles)? There are two conflicting aspects, i. e. , the scale of the photographs taken vs. the perturbing effect of the fine (and not so well-known) features of the lunar gravitational field.
- b. Are the covariances of the coordinates of the lunar features as obtained in the sample solution indicative of the uncertainties in the relative position of the points in the control network or they only indicate that the coordinate system itself is poorly defined while the relative positions are much better? It appears that applying inner adjustment constraints to the solution may bring an answer to this question [Meissl, 1971].

- c. What is the quality of a solution for the physical libration parameters from analysis of heliometer observations as compared to the solution from ordinary optical observations as proposed in this study? It would be of great interest to find out if the vast number of heliometer observations accumulated over more than a century could be put to use in deriving a new solution for the physical librations.
- d. As in any other theoretical study, it is extremely interesting to find out what new problems will be brought up when an attempt is made to use real data for a selenodetic control solution.

At the end, the main characteristics of the solution for selenodetic control, as developed in this study, are summarized:

- a. The solution is consistent with the motion of the Moon in space.
- b. The solution for the orientation of the Moon in space is part of the general solution.
- c. Optical data obtained from the Earth or from a spacecraft are processed uniformly, thus avoiding inconsistencies between solutions based on either of the two sources of data.
- d. All the observations needed for the solution (optical, range, and range-rate) are processed simultaneously in a weighted least squares procedure where the parameters are constrained according to their apriori covariances.
- e. The adjustment procedure can be programmed for use with available electronic computers where the core size required and the computer time for processing the data are reasonable and make the application of the solution to processing real data a feasible proposition.

## APPENDIX A

### Equivalency of MacCullagh's Formula to a Spherical Harmonics Expansion

The problem treated in this Appendix is to compare expressions for the potential of a triaxial ellipsoid using MacCullagh's formula with that of a spherical harmonics expansion.

MacCullagh's formula (Jeffreys, "The Earth", p. 176):

$$V = k^2 \left( \frac{M}{\rho} + \frac{A + B + C - 3I}{2\rho^3} \right) \quad (\text{A. 1})$$

Spherical harmonics expansion:

$$V = \frac{k^2 M}{\rho} \left[ 1 + \left( \frac{a}{\rho} \right)^2 \left( P_2 \cdot C_{20} + P_{22} \cdot C_{22} \cos 2\lambda \right) \right] \quad (\text{A. 2})$$

The second order harmonics  $C_{21}, S_{21}, S_{22}$  are equal to zero, which means that the axes (x, y, z) are identical with the principal axes of inertia.

Symbols used and their meaning:

$k^2$      gravitational constant

$M$      mass of the body

$a$      scaling quantity (usually taken as equal to the major semiaxis of the reference ellipsoid)

$C_{20}$  } coefficients of the second order in a spherical harmonics

$C_{22}$  } expansion of the gravitational potential

$P_2$  } Legendre polynomials

$P_{22}$  }

$\rho, \lambda, \phi$      polar coordinates of point (Q) at which the potential is evaluated with respect to the principal axes of the body (x, y, z).

The following relations hold between the polar coordinates of a point Q and its Cartesian coordinates:

$$\mathbf{r} = \begin{bmatrix} x \\ y \\ z \end{bmatrix}_Q = \rho \cdot \begin{bmatrix} \alpha \\ \gamma \\ \delta \end{bmatrix}_Q; \quad \begin{bmatrix} \alpha \\ \gamma \\ \delta \end{bmatrix} = \begin{bmatrix} \cos \varphi \cos \lambda \\ \cos \varphi \sin \lambda \\ \sin \varphi \end{bmatrix}$$

where  $\alpha, \gamma, \delta$  are the direction cosines of  $Q$  (see Figure A.1).

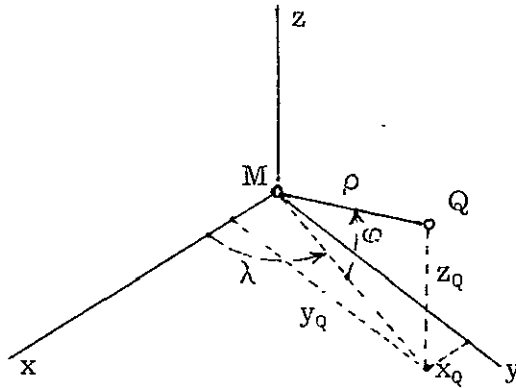


Figure A.1 Polar Coordinates of Point Q.

$I$  is defined as the moment of inertia of the body about an axis defined by  $\alpha, \gamma, \delta$  as follows:

$$I = A\alpha^2 + B\gamma^2 + C\delta^2 = [\alpha \ \gamma \ \delta] \cdot \begin{bmatrix} A & 0 & 0 \\ 0 & B & 0 \\ 0 & 0 & C \end{bmatrix} \begin{bmatrix} \alpha \\ \gamma \\ \delta \end{bmatrix} = \frac{1}{\rho^2} \mathbf{r}^T \begin{bmatrix} A & 0 & 0 \\ 0 & B & 0 \\ 0 & 0 & C \end{bmatrix} \mathbf{r} \quad (\text{A.3})$$

The Legendre polynomials are expressed as a function of the latitude  $\varphi$  [Mueller, 1964]:

$$\begin{aligned} P_2 &= \frac{1}{2} (3 \sin^2 \varphi - 1) \\ P_{22} &= 3 \cos^2 \varphi \end{aligned} \quad (\text{A.4})$$

The principal moments of inertia are related to the spherical harmonics coefficients by the following formulae [Mueller, 1964]:

$$C_{20} = \frac{1}{Ma^2} \left( \frac{A+B}{2} - C \right) \quad (\text{A.5})$$

$$C_{22} = \frac{1}{Ma^2} \frac{B-A}{4}$$

$\beta = \frac{C-A}{B}$  is a ratio between the moments of inertia A, B and C.

The relationship in (A.5) can be reversed so that A, B and C are expressed in terms of  $C_{20}$ ,  $C_{22}$  and  $\beta$ :

$$\begin{bmatrix} 1 & 1 & -2 \\ -1 & 1 & 0 \\ 1 & \beta & -1 \end{bmatrix} \begin{bmatrix} A \\ B \\ C \end{bmatrix} = Ma^2 \begin{bmatrix} 2 \cdot C_{20} \\ 4 \cdot C_{22} \\ 0 \end{bmatrix} ; \quad (\text{A.6})$$

$$\begin{bmatrix} 1 & 1 & -2 \\ -1 & 1 & 0 \\ 1 & \beta & -1 \end{bmatrix}^{-1} = \frac{1}{2\beta} \begin{bmatrix} -1 & (1-2\beta) & 2 \\ -1 & 1 & 2 \\ -(1+\beta) & (1-\beta) & 2 \end{bmatrix} . \quad (\text{A.7})$$

So finally:

$$\begin{bmatrix} A \\ B \\ C \end{bmatrix} = \frac{Ma^2}{\beta} \begin{bmatrix} -C_{20} & + C_{22} \cdot (2 - 4\beta) \\ -C_{20} & + C_{22} \cdot 2 \\ -C_{20} \cdot (1 + \beta) & + C_{22} \cdot (2 - 2\beta) \end{bmatrix} \quad (\text{A.8})$$

The following intermediate developments are necessary for the comparison of (A.1) and (A.2):

$$\sin^2 \varphi = \frac{z^2}{\rho^2}; \quad \cos^2 \varphi = 1 - \frac{z^2}{\rho^2} = \frac{x^2 + y^2}{\rho^2}$$

$$\cos 2\lambda = \cos^2 \lambda - \sin^2 \lambda; \quad \sin \lambda = \frac{y}{\sqrt{x^2 + y^2}}; \quad \sin^2 \lambda = \frac{y^2}{x^2 + y^2}; \quad \cos^2 \lambda = 1 - \frac{y^2}{x^2 + y^2}$$

$$P_2 = \frac{1}{2} (3 \sin^2 \varphi - 1) = \frac{1}{2\rho^2} (3z^2 - x^2 - y^2 - z^2) = \frac{1}{2\rho^2} (2z^2 - x^2 - y^2)$$

$$P_{22} = \frac{3}{\rho^2} (x^2 + y^2)$$

$$\cos 2\lambda = 1 - \frac{2y^2}{x^2 + y^2} = \frac{x^2 + y^2 - 2y^2}{x^2 + y^2} = \frac{x^2 - y^2}{x^2 + y^2}.$$

In what follows the spherical harmonics expression (A. 2) is to be transformed by substitutions so that finally it is expressed in terms of the same quantities as MacCullagh's formula (A. 1):

$$V = \frac{k^2 M}{\rho} \left\{ 1 + \frac{a^2}{\rho^2} \left[ \frac{1}{2\rho^2} (2z^2 - x^2 - y^2) \cdot \frac{A+B-2C}{2Ma^2} + \frac{3(x^2 + y^2)}{\rho^2} \cdot \frac{(B-A)}{4Ma^2} \cdot \frac{(x^2 - y^2)}{(x^2 + y^2)} \right] \right\}.$$

After rearrangement

$$V = k^2 M \left\{ \frac{1}{\rho} + \frac{1}{M\rho^3} \cdot \frac{1}{4\rho^2} \left[ x^2 \cdot (-4A+2B+2C) + y^2(2A-4B+2C) + z^2(2A+2B-4C) \right] \right\}.$$

Adding and subtracting in the square brackets the expression

$$x^2 6A + y^2 6B + z^2 6C$$

the result is

$$V = k^2 M \left\{ \frac{1}{\rho} + \frac{1}{M\rho^3} \left[ \frac{x^2 + y^2 + z^2}{4\rho^2} (2A + 2B + 2C) - \frac{6}{4\rho^2} (x^2 A + y^2 B + z^2 C) \right] \right\}$$

but

$$\rho^2 = x^2 + y^2 + z^2$$

so finally

$$V = k^2 M \left\{ \frac{1}{\rho} + \frac{1}{2M\rho^3} \cdot \left( A + B + C - \frac{3}{\rho^2} [xyz] \cdot \begin{bmatrix} A & 0 & 0 \\ 0 & B & 0 \\ 0 & 0 & C \end{bmatrix} \cdot \begin{bmatrix} x \\ y \\ z \end{bmatrix} \right) \right\}. \quad (\text{A. 9})$$

The expression (A. 9) is identical with MacCullagh's formula (A. 1) where I has been substituted by (A. 3). This completes the proof of the equivalency of (A. 1) and (A. 2). It holds only where in both expressions for the potential the terms beyond the second degree have been neglected.

## APPENDIX B

### Derivation of a Numerical Value for the Ratio between the Equatorial and Polar Moments of Inertia of the Earth.

In analysing the motion of the average terrestrial system with respect to the center of mass of the Earth the following ratio is needed in the integration (see Chapter 4, Section 4.43):

$$\mu = \frac{C - A}{A}$$

where C and A are the polar and the equatorial moments of inertia of the Earth. In the literature the values given for  $\mu$  vary in the third significant figure and there is no clear indication of the method used to derive this constant [Plummer, 1918; Jeffreys, 1970].

In what follows two methods are used for deriving a numerical value for  $\mu$ :

Method (i) - From Woolard's expressions for nutation in obliquity using the constant of nutation adopted by the IAU in 1964 [Woolard, 1953].

Method (ii) - Using formulae given by Jeffreys [1970] and evaluating the value of  $\mu$  for constants adopted by IAU in 1964.

The constants to be used are

$k^2_M = 4902.86593 \text{ km}^3 \text{ sec}^{-2}$  gravitational constant of the Moon

$N = 9''.210$  coefficient of major term in nutation in obliquity for the epoch 1900.0

$\omega_z = .0000729211507 \text{ rad/sec}$  spin velocity of the Earth

$a = 384400.0$  km. mean distance to the Moon

$\dot{\Omega} = 1.06969941 \cdot 10^{-8}$  rad/sec rate of change of the node of the lunar orbit.

$a_e = 6378.16$  km. major semiaxis of Earth reference ellipsoid

$f = 1/298.25$  flattening of the reference ellipsoid

$k^2 E = 398603 \text{ km}^3 \text{ sec}^{-2}$  gravitational constant of the Earth.

### Method (i)

From Woolard's "Astronomical Papers" p. 124 for the solution of Poisson's equations for the motion of the Earth, through integration of the term " $\sin \Omega$ ", the following expression is obtained [Woolard, 1953, p. 124]:

$$-k^2 M \cdot \frac{3}{\omega_3} \cdot \frac{C-A}{C} \cdot \frac{1}{a^3} \cdot \frac{-0.041166}{\dot{\Omega}} \cdot \cos \Omega = 9.21 \cdot \cos \Omega$$

$$\frac{C-A}{C} = \frac{9.21}{206264.8062} \cdot \frac{1.06969941 \cdot 10^{-8}}{.041166} \cdot \frac{-0.729211507 \cdot 10^{-4}}{3} \cdot \frac{384400^3}{4902.86593}$$

$$\frac{C-A}{C} = .00326731.$$

### Method (ii)

From Jeffreys [1970, p. 189] a formula for  $\frac{C-A}{C}$  is given as follows:

$$\frac{C-A}{C} = \frac{f - \frac{m}{2}}{1 - \frac{2}{5} \sqrt{1 + \eta_a}}$$

where

$$\eta_a = \frac{5m}{2f} - 2$$

$$m = \frac{\omega_z^2 a_e^2 b}{k^2 E} \quad \text{and} \quad b = (1-f) a_e \text{ is the minor semi-axis of the}$$

reference ellipsoid.

The constants listed at the beginning of this Appendix are substituted in the above expression and result in the following:

$$m = .003449801472$$

$$\eta_a = .572258243$$

and finally

$$\frac{C - A}{C} = .003266166 .$$

The difference between the values obtained is in the fourth significant digit and as the constant  $N = 9.21$  is based on astronomic observations and as it is important to remain consistent with the set of constants adopted by IAU in 1964 ( $N$  being one of them) the value for  $\frac{C-A}{C}$  to be adopted is 0.003267.

A simple algebraic manipulation results in  $\mu = \frac{C-A}{A}$  :

$$\mu = .00327802.$$

Compared to the dynamic flattening of the Moon ( $\beta = \frac{C-A}{B} = .000629$ )  $\mu$  is about five times larger.

## APPENDIX C

### Design of a set of Mascons on the Moon.

Dynamically the simulated Moon is a triaxial ellipsoid with a set of 12 mass concentrations laying on the surface of the Moon sphere. They are superimposed on the basic triaxial figure.

The mascons had to be designed in a way such that they do not alter the low degree terms of the spherical harmonics expansion (up to and including the second degree). This would mean that the total contribution of the mascons to the mass of the Moon, to its first moments and to its second moments and products of inertia is zero.

The 12 mascons were all chosen to lay on the front (Earth side) of the Moon at locations which correspond to mascon models as solved and reported recently.

Mathematically this is an overdetermined problem as the 12 masses have to satisfy a total of nine independent conditions. The symbols used are:

$m_i$  — mass of  $i$  mascon

$x_i, y_i, z_i$  — Cartesian coordinates of mascon in the selenodetic system  $(x, y, z)$ .

The nine conditions are as follows:

zero degree term	1	$\Sigma m_i = 0$
	2	$\Sigma m_i x_i = 0$
first degree terms	3	$\Sigma m_i y_i = 0$
	4	$\Sigma m_i z_i = 0$

$\Sigma$  is the summation symbol over the  $i$  mascons

	$C_{20} = 0$	5	$\Sigma m_i \left( z_i^2 - \frac{x_i^2 + y_i^2}{2} \right)$
	$C_{21} = 0$	6	$\Sigma m_i x_i z_i$
second degree terms	$C_{22} = 0$	7	$\Sigma m_i (x_i^2 - y_i^2)$
	$C_{21} = 0$	8	$\Sigma m_i y_i z_i$
	$C_{22} = 0$	9	$\Sigma m_i x_i y_i$

The condition equations are linear in the parameters and so the solution follows directly.

The mathematical model is given by

$$BM + W = 0$$

where

$$B = \begin{bmatrix} 1 & 1 & \dots & \dots & \dots & 1 \\ x_1 & x_2 & \dots & \dots & \dots & x_{12} \\ y_1 & \dots & \dots & \dots & \dots & y_{12} \\ z_1 & \dots & \dots & \dots & \dots & z_{12} \\ z_1^2 - \frac{x_1^2 + y_1^2}{2} & \dots & \dots & \dots & \dots & z_{12}^2 - \frac{x_{12}^2 + y_{12}^2}{2} \\ \vdots & \dots & \dots & \dots & \dots & \vdots \\ x_1 y_1 & x_2 y_2 & \dots & \dots & \dots & x_{12} y_{12} \end{bmatrix}; \quad M = \begin{bmatrix} \delta m_1 \\ \delta m_2 \\ \delta m_3 \\ \vdots \\ \delta m_{12} \end{bmatrix}; \quad W = \begin{bmatrix} w_1 \\ w_2 \\ \vdots \\ \vdots \\ w_9 \end{bmatrix}$$

$\delta m_1, \delta m_2, \dots$  are corrections to initial values for the masses  $m_{01}, m_{02}, \dots, m_{012}$ .

The least squares solution for M is

$$M = -P^{-1}B^T (BP^{-1}B^T)^{-1} W$$

where P is the weight matrix for M (in this case it was defined as the identity matrix). Two of the masses were set to predetermined initial values while the rest (ten masses) were set to zero.

Three consecutive iterations of the adjustment problem were run. The

second and third iterations produced identical results and the vector  $W$  after the third iteration contained quantities smaller than  $10^{-15}$ .

## APPENDIX D

### Considered Parameters in a Least Squares Adjustment Process

Parameters in a least squares adjustment process are estimated either as free variables, i.e., without conditions (functional or weight constraints) being imposed on their solution or as observed quantities having an a priori estimate of their covariances. These a priori covariances constrain the solution of the parameters and figure also in their weight coefficients matrix. In what follows the second case is treated where a priori information on the parameters does exist.

In order to solve for the parameters one should have reasons to expect that the data processed are of a type and quality such that the estimates of the parameters are going to be improved after the adjustment, i.e., the trace of the a posteriori covariance matrix (the scaled weight coefficients matrix) will be smaller as compared to the trace of the a priori covariance matrix. There are cases, however, where for various reasons some of the parameters have to be held fixed through the adjustment or even if they can be allowed to vary it is realized beforehand that no improvements in their a priori values can be expected as a result of the adjustment. If this is the case, such parameters are treated as constants. There is one major flaw in such an approach:

In estimating the covariances of the parameters that are being adjusted, the effect of uncertainties in the "fixed" parameters on these estimated covariances is implicitly ignored. This implicit omission is seldom justified as the "fixed" parameters themselves have been obtained, most probably, earlier through an

adjustment process and have a covariance matrix associated with them.

The problem to be treated in this appendix is to derive expressions for the contribution of uncertainties in "fixed" parameters on the estimated covariance matrix of other parameters which are being solved for in a least squares adjustment process. The development here is a generalization of the method of "Considered Parameters" as used by JPL and outlined by Anderson [1964].

The mathematical model used is in accordance with the so called "Generalized Approach" in which all the quantities involved are treated as observables with associated a priori covariance estimates [Uotila, 1967].

The following notation is used:

$L^b$  - observables which are subject to adjustment

$X^b$  - observables which although possessing a covariance matrix are held fixed

$\Sigma$  } a priori covariance }  $L^b$ , respectively.  
 $\Sigma_x$  } matrix of }  $X^b$

The mathematical model  $F$  is then

$$F = F(L^a, X^b) = 0 \quad (D.1)$$

where  $L^a$  are the adjusted observables.

$$L^a = L^b + V \quad (D.2)$$

The mathematical model is linearized under the assumption that  $F$  is fairly linear over  $V$

$$F = BV + W = 0 \quad (D.3)$$

where

$$B = \frac{\partial F}{\partial L^a} \quad \text{and} \quad W = F(L^b, X^b)$$

In what follows the sequence of formulae is well known from Uotila [1967] and is presented, therefore, without comments:

$$\varphi = V^T \Sigma^{-1} V - 2\lambda^T (BV + W) \quad (D.4)$$

$$\frac{1}{2} \left[ \frac{\partial \varphi}{\partial V} \right]^T = 0 = \Sigma^{-1} V - B^T \lambda$$

$$\begin{bmatrix} -\Sigma^{-1} & B^T \\ B & 0 \end{bmatrix} \cdot \begin{bmatrix} V \\ \lambda \end{bmatrix} = \begin{bmatrix} 0 \\ -W \end{bmatrix} \quad (D.5)$$

$$V = -\Sigma B^T (B \Sigma B^T)^{-1} W = -\Sigma B^T M^{-1} W \quad (D.6)$$

$$L^a = L^b + V = L^b - \Sigma B^T M^{-1} W \quad (D.7)$$

Two fixed vectors  $L^o$ ,  $X^o$  are defined which are close in value or even identical to  $L^b$ ,  $X^b$  so that

$$L^b = L^o + L$$

$$L^a = L^o + L^*$$

$$X^b = X^o + X$$

The vectors  $L$ ,  $L^*$ ,  $X$  have the same covariance matrices like  $L^b$ ,  $L^a$ ,  $X^b$ , respectively as  $X^o$  and  $L^o$  are constant vectors.

Using the partial derivatives matrix  $B$

$$W = W^o + BL + B_x X \quad (D.8)$$

where

$$W^o = F(L^o, X^o) \quad \text{and} \quad B_x = \frac{\partial F}{\partial X}$$

The equation for  $L^a$  is written again

$$L^o + L^* = L^o + L - \Sigma B^T M^{-1} W^o - \Sigma B^T M^{-1} B L - \Sigma B^T M^{-1} B_x X$$

$$L^* = -\Sigma B^T M^{-1} W^o + [I - \Sigma B^T M^{-1} B] L - \Sigma B^T M^{-1} B_x X \quad (D.9)$$

The only elements on the right side which possess covariance matrices are  $L$  and  $X$ . An assumption is made that no elements in  $L^b$  are correlated to any elements in  $X^b$ . The covariance matrix of  $L^*$  (or  $L^a$ ) is evaluated according to the law of propagation of covariances.

$$\Sigma_{L^*} = [I - \Sigma B^T M^{-1} B] \Sigma [I - B^T M^{-1} B \Sigma] + \Sigma B^T M^{-1} B_x \Sigma_x B_x^T M^{-1} B \Sigma \quad (D.10)$$

Setting

$$M_x = B_x \Sigma_x B_x^T$$

and also as

$$[I - \Sigma B^T M^{-1} B] \Sigma [I - B^T M^{-1} B \Sigma] = [I - \Sigma B^T M^{-1} B] \Sigma$$

it follows that

$$\Sigma_{L^*} = \Sigma_{L^a} = [I - \Sigma B^T M^{-1} B] \Sigma + \Sigma B^T M^{-1} M_x M^{-1} B \Sigma \quad (D.11)$$

This is the expression for the estimate of the total covariance matrix of  $L^a$  where the first term on the right side is the covariance matrix of  $L^a$  obtained without considering the contribution of  $X^b$ .

In practice the vector of observables  $L^b$  is usually partitioned into

$L_1^b$  - the actual observations

and

$L_e^b$  - the parameters.

The solution for the corrected observations is occasionally of no interest and is "folded in" the solution for the parameters.

An assumption is made again that there is no correlation between  $L_1^b$  and  $L_e^b$

$$V = \begin{bmatrix} V_1 \\ V_2 \end{bmatrix}; \quad L^b = \begin{bmatrix} L_1^b \\ L_e^b \end{bmatrix}; \quad \Sigma = \begin{bmatrix} \Sigma_1 & 0 \\ 0 & \Sigma_2 \end{bmatrix}; \quad B = [B_1 \quad B_2]$$

The solution for  $V$  as obtained above is then

$$\begin{bmatrix} V_1 \\ V_2 \end{bmatrix} = - \begin{bmatrix} \Sigma_1 & 0 \\ 0 & \Sigma_2 \end{bmatrix} \cdot \begin{bmatrix} B_1^T \\ B_2^T \end{bmatrix} \cdot \left\{ [B_1 \quad B_2] \cdot \begin{bmatrix} \Sigma_1 & 0 \\ 0 & \Sigma_2 \end{bmatrix} \cdot \begin{bmatrix} B_1^T \\ B_2^T \end{bmatrix} \right\} \cdot W \quad (D. 12)$$

$$M_1 = B_1 \Sigma_1 B_1^T \quad ; \quad M_2 = B_2 \Sigma_2 B_2^T$$

$$V_2 = - \Sigma_2 B_2^T (M_1 + M_2)^{-1} W \quad (D. 13)$$

A matrix inversion identity is used according to Uotila [1967].

$$(M_1 + M_2)^{-1} = (M_1 + B_2 \Sigma_2 B_2^T)^{-1} = M_1^{-1} - M_1^{-1} B_2 (\Sigma_2^{-1} + B_2^T M_1^{-1} B_2)^{-1} B_2^T M_1^{-1} \quad (D. 14)$$

Through a trivial matrix manipulation it follows:

$$V_2 = - (\Sigma_2^{-1} + B_2^T M_1^{-1} B_2)^{-1} B_2^T M_1^{-1} \cdot W \quad (D. 15)$$

The covariance matrix of  $L^a$  is partitioned as follows:

$$\Sigma_{L^a} = \begin{bmatrix} \Sigma_{L^a 1} & \Sigma_{L^a 12} \\ \Sigma_{L^a 12}^T & \Sigma_{L^a 2} \end{bmatrix}$$

where  $\Sigma_{L^a 12}$  are the covariances between  $L_1^a$  and  $L_2^a$ .  $\Sigma_{L^a 2}$  is the lower right submatrix in  $\Sigma_{L^a}$ . The expression for  $\Sigma_{L^a}$  is developed further to obtain  $\Sigma_{L_2^a}$  explicitly.

$$\begin{aligned} \Sigma_{L^a} &= \begin{bmatrix} \Sigma_1 & 0 \\ 0 & \Sigma_2 \end{bmatrix} - \begin{bmatrix} \Sigma_1 & 0 \\ 0 & \Sigma_2 \end{bmatrix} \begin{bmatrix} B_1^T \\ B_2^T \end{bmatrix} \cdot (M_1 + M_2)^{-1} [B_1 B_2] \cdot \begin{bmatrix} \Sigma_1 & 0 \\ 0 & \Sigma_2 \end{bmatrix} \\ &+ \begin{bmatrix} \Sigma_1 & 0 \\ 0 & \Sigma_2 \end{bmatrix} \begin{bmatrix} B_1^T \\ B_2^T \end{bmatrix} \cdot (M_1 + M_2)^{-1} M_x (M_1 + M_2)^{-1} [B_1 B_2] \cdot \begin{bmatrix} \Sigma_1 & 0 \\ 0 & \Sigma_2 \end{bmatrix} \end{aligned}$$

Skipping several obvious steps

$$\begin{aligned} \Sigma_{L_2^a} &= \Sigma_2 - \Sigma_2 B_2^T (M_1 + M_2)^{-1} B_2 \Sigma_2 + \\ &+ \Sigma_2 B_2^T (M_1 + M_2)^{-1} M_x (M_1 + M_2)^{-1} B_2 \Sigma_2 \end{aligned} \quad (D.16)$$

Using the matrix inversion identity mentioned above

$$(\Sigma_2^{-1} + B_2^T M_1^{-1} B_2)^{-1} = \Sigma_2 - \Sigma_2 B_2^T (M_1 + M_2)^{-1} B_2 \Sigma_2$$

It was shown already that

$$\Sigma_2 B_2^T (M_1 + M_2)^{-1} = (\Sigma_2^{-1} + B_2^T M_1^{-1} B_2)^{-1} B_2^T M_1^{-1}$$

so after setting  $K = (\Sigma_2^{-1} + B_2^T M_1^{-1} B_2)^{-1}$  the covariance matrix for  $L_2^a$  can be written as

$$\Sigma_{t^a_2} = K + K B_2^T M_1^{-1} M_x M_1^{-1} B_2 K \quad . \quad (D.17)$$

As for the  $\Sigma_{t^a}$  matrix, here also  $K$  is the covariance matrix of the  $L_2^a$  parameters obtained if the contribution of uncertainties in  $X^b$  is ignored.

APPENDIX E

Rules for Differentiation of Matrices

- (a) Partial derivative of a scalar function  $\phi$  with respect to a vector  $X$  is the row vector  $Y$ .

$$Y = \frac{\partial \phi}{\partial X} = \left[ \frac{\partial \phi}{\partial X_1} \quad \frac{\partial \phi}{\partial X_2} \quad \frac{\partial \phi}{\partial X_3} \quad \dots \quad \frac{\partial \phi}{\partial X_n} \right]$$

- (b) Partial derivative of a matrix  $A$  by a scalar  $c$  is a matrix  $C$ .

$$C = \frac{\partial A}{\partial c}$$

where each element in  $C$  is the partial derivative by  $c$  of the corresponding element in  $A$ .

- (c) Partial derivative of a vector  $Y$  with respect to a vector  $X$  is a matrix  $C$ .

$$C = \frac{\partial Y}{\partial X} = \begin{bmatrix} \frac{\partial Y_1}{\partial X_1} & \frac{\partial Y_1}{\partial X_2} & \dots & \dots & \dots & \frac{\partial Y_1}{\partial X_n} \\ \frac{\partial Y_2}{\partial X_1} & \dots & \dots & \dots & \dots & \dots \\ \cdot & \dots & \dots & \dots & \dots & \dots \\ \cdot & \dots & \dots & \dots & \dots & \dots \\ \cdot & \dots & \dots & \dots & \dots & \dots \\ \cdot & \dots & \dots & \dots & \dots & \dots \\ \frac{\partial Y_n}{\partial X_1} & \dots & \dots & \dots & \dots & \frac{\partial Y_n}{\partial X_n} \end{bmatrix}$$

$$\left[ \frac{\partial Y}{\partial X_1} \quad \frac{\partial Y}{\partial X_2} \quad \dots \quad \dots \quad \dots \quad \frac{\partial Y}{\partial X_n} \right]$$

(d) Partial derivative of a matrix A by a vector X is a three dimensional matrix C.

$$C = \frac{\partial A}{\partial X}$$

A is partitioned into column vectors

$$A = [A_1 A_2 A_3 \dots A_n]$$

The layers of C are obtained by differentiating sequentially the columns of A

$$C_1 = \frac{\partial A_1}{\partial X}$$

where  $C_1$  are layers of the three dimensional matrix C and are matrices obtained according to (c) above.

(e) Partial derivative of the product of a matrix A and a vector Y by a vector X is a matrix C.

$$C = \frac{\partial (A \cdot Y)}{\partial X}$$

According to case (c)

$$C = \left[ \frac{\partial (A \cdot Y)}{\partial X_1} \quad \frac{\partial (A \cdot Y)}{\partial X_2} \quad \dots \quad \frac{\partial (A \cdot Y)}{\partial X_n} \right]$$

$$C = C_1 + A \cdot C_2$$

where

$$C_1 = \left[ \frac{\partial A}{\partial X_1} \cdot Y \quad \frac{\partial A}{\partial X_2} \cdot Y \quad \dots \quad \frac{\partial A}{\partial X_n} \cdot Y \right]$$

and

$$C_2 = \frac{\partial Y}{\partial X}$$

In what follows two particular vector forms are differentiated applying the rules as developed above.

- (f) Partial derivative of the vector form A by the vector X is the matrix C.

$$A = \frac{D}{(X^T \cdot X)^{1/2}} \cdot X$$

where D is a matrix which is not a function of X .

$$C = \frac{\partial A}{\partial X}$$

$$C = \frac{D}{(X^T \cdot X)^{1/2}} + C_1$$

$$C_1 = -\frac{j \cdot D \cdot X \cdot X^T}{(X^T \cdot X)^{(j+2)/2}}$$

If instead of D there is the scalar d which like D is not a function of X the resulting matrix C is

$$C = \frac{d \cdot I}{(X^T \cdot X)^{1/2}} - \frac{j \cdot d \cdot X \cdot X^T}{(X^T \cdot X)^{(j+2)/2}}$$

- (g) Partial derivative of the vector form A by a vector X is the matrix C.

$$A = X \cdot X^T \cdot D \cdot X$$

where  $D$  is a matrix which is not a function of  $X$

$$C = \frac{\partial A}{\partial X}$$

This can be treated like case (e)

$$C = \frac{\partial [ (XX^T) \cdot (D \cdot X) ]}{\partial X} = C_1 + C_2$$

where

$$C_2 = XX^T D \quad ;$$

$$C_1 = \left[ \begin{array}{c|c|c|c} \frac{\partial (XX^T)}{\partial X_1} \cdot DX & \frac{\partial (XX^T)}{\partial X_2} \cdot DX & \dots & \frac{\partial (XX^T)}{\partial X_n} \cdot DX \end{array} \right]$$

$$\frac{\partial (XX^T)}{\partial X_i} = \begin{bmatrix} 0 & 0 & 0 & \dots & X & \dots & 0 \\ \vdots & \vdots & \vdots & \dots & \vdots & \dots & \vdots \\ \vdots & \vdots & \vdots & \dots & \vdots & \dots & \vdots \\ \vdots & \vdots & \vdots & \dots & \vdots & \dots & \vdots \\ X^T & \vdots & \vdots & \dots & \vdots & \dots & \vdots \\ \vdots & \vdots & \vdots & \dots & \vdots & \dots & \vdots \\ 0 & \vdots & \vdots & \dots & \vdots & \dots & \vdots \end{bmatrix} + \begin{bmatrix} 0 \\ 0 \\ \vdots \\ \vdots \\ X^T \\ \vdots \\ 0 \end{bmatrix} \begin{matrix} 1 \\ 2 \\ \vdots \\ \vdots \\ 1 \\ \vdots \\ n \end{matrix}$$

$$C_1 = XX^T D^T + X^T D X I$$

$$C = XX^T (D + D^T) + X^T D X I$$

(h) Rotation matrices  $R_i(\varphi)$   $i = 1, 2, 3$  are differentiated with respect to the angle of rotation  $\varphi$  using auxiliary matrices  $L_{c_i}$  as given by Lucas [1963].

Rotation matrices about the three Cartesian axes, respectively are:

$$R_1(\varphi) = \begin{bmatrix} 1 & 0 & 0 \\ 0 & \cos \varphi & \sin \varphi \\ 0 & -\sin \varphi & \cos \varphi \end{bmatrix}; \quad R_2(\varphi) = \begin{bmatrix} \cos \varphi & 0 & -\sin \varphi \\ 0 & 1 & 0 \\ \sin \varphi & 0 & \cos \varphi \end{bmatrix}; \quad R_3(\varphi) = \begin{bmatrix} \cos \varphi & \sin \varphi & 0 \\ -\sin \varphi & \cos \varphi & 0 \\ 0 & 0 & 1 \end{bmatrix}$$

Lucas' auxiliary matrices used to differentiate the rotation matrices are:

$$L_{c_1} = \begin{bmatrix} 0 & 0 & 0 \\ 0 & 0 & 1 \\ 0 & -1 & 0 \end{bmatrix}; \quad L_{c_2} = \begin{bmatrix} 0 & 0 & -1 \\ 0 & 0 & 0 \\ 1 & 0 & 0 \end{bmatrix}; \quad L_{c_3} = \begin{bmatrix} 0 & 1 & 0 \\ -1 & 0 & 0 \\ 0 & 0 & 0 \end{bmatrix}$$

The differentiation is straightforward:

$$\frac{\partial R_1(\varphi)}{\partial \varphi} = L_{c_1} \cdot R_1(\varphi) = R_1(\varphi) \cdot L_{c_1}$$

In the case of a negative rotation  $(-\varphi)$

$$\frac{\partial R_1(-\varphi)}{\partial \varphi} = L_{c_1} \cdot R_1(-\varphi) \cdot (-1) = -L_{c_1} R_1(-\varphi)$$

### Products of Vectors in Three Dimensional Space

#### Performed by Equivalent Matrix Operations

- (a) Dot product of vector A and vector B is equal to the scalar c.

$$c = \vec{A} \cdot \vec{B}$$

$$c = A^T \cdot B = B^T \cdot A = [A_1 A_2 A_3] \cdot \begin{bmatrix} B_1 \\ B_2 \\ B_3 \end{bmatrix}$$

(b) Vector product of vector A and vector B is equal to vector C.

$$\vec{C} = \vec{A} \times \vec{B} = -\vec{B} \times \vec{A}$$

$$\begin{bmatrix} C_1 \\ C_2 \\ C_3 \end{bmatrix} = \begin{bmatrix} 0 & -A_3 & A_2 \\ A_3 & 0 & -A_1 \\ -A_2 & A_1 & 0 \end{bmatrix} \cdot \begin{bmatrix} B_1 \\ B_2 \\ B_3 \end{bmatrix} = \begin{bmatrix} 0 & B_3 & -B_2 \\ -B_3 & 0 & B_1 \\ B_2 & -B_1 & 0 \end{bmatrix} \cdot \begin{bmatrix} A_1 \\ A_2 \\ A_3 \end{bmatrix}$$

## APPENDIX F

### Orbit Determination Routine for a Satellite of the Moon in the Simulated Environment

During the past decade with the advent of space exploration and the availability of electronic computers many and highly sophisticated orbit determination routines were developed. To mention only a few, O.D. (orbit determination) routines were programmed and used successfully by JPL, Langley R. C., MSC, TRW, etc. The difference between the various routines, where it does exist, is mainly in the types of data being processed and the particular application the routine was designed for.

None of the above programs was found appropriate for use in the simulated environment. In general, they are much too complicated and have an extensive list of parameters which are irrelevant to the simulation. The observables are real and so extensive error modeling is included in the routines. On the other hand, if such an O.D. routine is to be used with the simulated data, the mathematical model of the simulation would have to be altered to conform with the particular model implied in the O.D. routine.

Because of all the above reasons, it was considered essential to design and program an O.D. routine which will be capable of processing the simulated range and range-rate data and will solve for initial state vector and a set of physical parameters consistent in form with the ones used in generating the data themselves. The approach taken follows very closely that of JPL's ODP as reported by Warner [1964] and by Anderson [1964]. It is based also on theory as presented in textbooks like [Brouwer and Clemence, 1961] and [Escobal, 1965].

The essential elements in the O.D. routine are two:

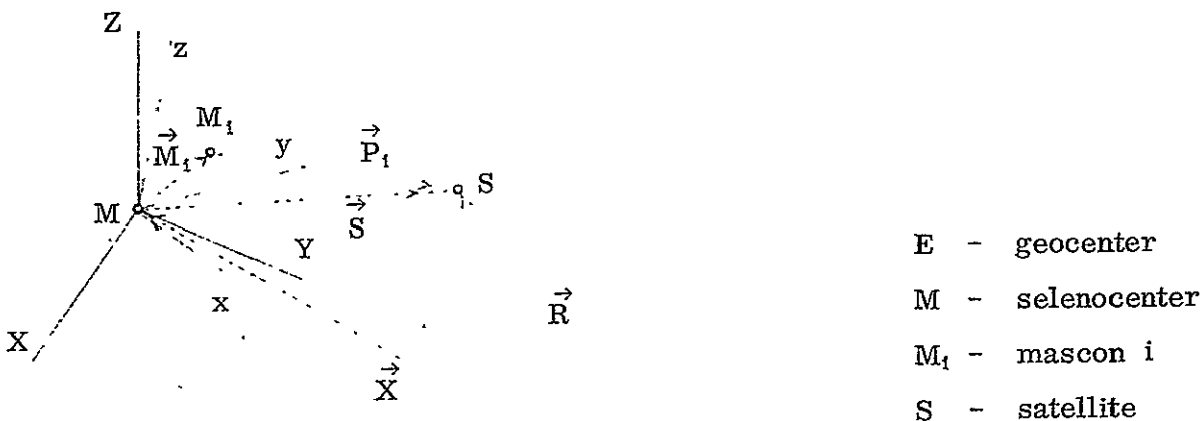
- (a) Numerical integrator of the equations of motion of the satellite.
- (b) Generator of partial derivatives of the state vector with respect to the initial state vector (state transition matrix) and to the parameters of interest (parameter sensitivity matrix).

The mathematical formulation for (a) is given actually in section 4.44 of Chapter 4. The expressions for (b) are developed in this Appendix using as a starting point Cowell's equations of motion of a satellite in the simulated environment as given in section 4.44. The notation to be used in this Appendix is identical to the one used throughout Chapter 4.

Cowell's Equation of Motion of a Satellite

(See Figure F. 1).

$$\begin{aligned} \ddot{\mathbf{S}} = & -k^2 E \left\{ \frac{1}{m} \left[ \frac{1}{\rho_m^3} + \frac{\bar{H}}{\rho_m^5} + \frac{(\rho_m^2 I - \frac{5}{2} \bar{S} \bar{S}^T) \bar{P}}{\rho_m^7} \right] \cdot \mathbf{S} + \frac{1}{m} \sum_i \mu_i \frac{\mathbf{P}_i}{\rho_i^3} \right. \\ & + \left. \left[ \frac{1}{\rho_e^3} + \frac{\bar{E}}{\rho_e^5} + \frac{(\rho_e^2 I - \frac{5}{2} \mathbf{R} \cdot \mathbf{R}^T) \bar{Q}}{\rho_e^7} \right] \cdot \mathbf{R} \right. \\ & \left. - \left[ \frac{1}{\rho^3} + \frac{\bar{H} + \bar{E}}{\rho^5} + \frac{(\rho^2 I - \frac{5}{2} \mathbf{X} \mathbf{X}^T) \cdot (\bar{P} + \bar{Q})}{\rho^7} \right] \cdot \mathbf{X} \right\} \end{aligned} \tag{4.44.10}$$



E

Figure F.1. Vector Diagram for a Satellite of the Moon.

$$\rho = (X^T X)^{\frac{1}{2}}$$

$$\rho_m = (S^T S)^{\frac{1}{2}}$$

$$\rho_e = (R^T R)^{\frac{1}{2}}$$

$$\rho_i = (P_i^T P_i)^{\frac{1}{2}}$$

$$T_M = R_3(\varphi) \cdot R_1(-\theta) \cdot R_3(\psi) .$$

$T_M$  is orthogonal transformation matrix from XYZ into xyz.

$M_i$  is the position vector of the i-th mascon in xyz system.

$k^2 E$  is the Earth gravitational constant.

$m = \frac{E}{M}$  ratio of mass of the Earth to mass of the Moon.

$$R = S + X$$

$$P_i = S - T_M^T \cdot M_i$$

$$\bar{P} = \frac{3 a_e^2}{\beta \xi^2} T_M^T \cdot G \cdot T_M ;$$

$$G = \begin{bmatrix} -C_{20} + (2-4\beta) C_{22} & 0 & 0 \\ 0 & -C_{20} + 2 C_{22} & 0 \\ 0 & 0 & -(1+\beta) C_{20} + (2-2\beta) C_{22} \end{bmatrix}$$

$$\bar{H} = \frac{3 a_e^2}{2\beta \cdot \xi^2} [ -(3 + \beta) C_{20} + (6 - 6\beta) C_{22} ] .$$

$\bar{Q}$ ,  $\bar{E}$ ,  $a_e$ ,  $\xi$  are quantities which are not functions of  $\begin{bmatrix} S \\ \dot{S} \end{bmatrix}$ ,  $p_1$  and  $p_2$ .

$p = \begin{bmatrix} p_1 \\ p_2 \end{bmatrix}$  are the physical parameters as follows:

$$p_1 = [C_{22} \beta \ C_{20}]^T$$

$$p_2 = [\mu_1 \ \mu_2 \ \mu_3 \ \dots \ \mu_k]^T$$

where

$C_{20}, C_{22}$  are second degree spherical harmonics of the gravitational field of the Moon.

$\beta = \frac{C - A}{B}$  where A, B, C are the principle moments of inertia of the Moon.

$\mu_i$  is the ratio of the mass of the i-th mascon to the total mass of the Moon.

Most of the above is copied from Section 4.44.

The two matrices sought in this Appendix are:

$$U_s = \frac{\partial \begin{bmatrix} \dot{S} \\ S \end{bmatrix}}{\partial \begin{bmatrix} \dot{S} \\ S \end{bmatrix}_0} \quad \text{the state transition matrix}$$

and

$$Q_s = \begin{bmatrix} Q_{s1} & Q_{s2} \end{bmatrix} = \begin{bmatrix} \frac{\partial \begin{bmatrix} \dot{S} \\ S \end{bmatrix}}{\partial p_1} & \frac{\partial \begin{bmatrix} \dot{S} \\ S \end{bmatrix}}{\partial p_2} \end{bmatrix} \quad \text{the parameter sensitivity matrix}$$

As the state vector at a particular epoch  $\begin{bmatrix} \dot{S} \\ S \end{bmatrix}$  is the result of the numerical integration of the equations of motion  $\ddot{S}$ , the differentiation of  $\begin{bmatrix} \dot{S} \\ S \end{bmatrix}$  with respect to the initial state vector  $\begin{bmatrix} \dot{S} \\ S \end{bmatrix}_0$  and the parameters  $p_1, p_2$  is carried out through differentiation of  $\ddot{S}$  with respect to  $\begin{bmatrix} \dot{S} \\ S \end{bmatrix}_0, p_1$  and  $p_2$ . As shown by Anderson [1964] two sets of linear differential equations can be derived as follows:

$$\dot{\bar{U}}_s = \Theta \cdot \bar{U}_s \quad (\text{F.1})$$

$$\dot{\bar{Q}}_s = \Theta \cdot \bar{Q}_s + \Phi \quad (\text{F.2})$$

where

$$\Theta = \frac{\partial \begin{bmatrix} \dot{\bar{S}} \\ \ddot{\bar{S}} \end{bmatrix}}{\partial \begin{bmatrix} \bar{S} \\ \dot{\bar{S}} \end{bmatrix}_0} \quad \text{and} \quad \Phi = \frac{\partial \begin{bmatrix} \dot{\bar{S}} \\ \ddot{\bar{S}} \end{bmatrix}}{\partial p}$$

The derivation of these equations as applied to the rotation of the Moon is presented in section 3.32 of Chapter 3.

$$\Theta = \begin{bmatrix} 0 & I \\ \frac{\partial \ddot{\bar{S}}}{\partial \bar{S}} & 0 \end{bmatrix} \quad \Phi = [\Phi_1 \ \Phi_2] = \begin{bmatrix} 0 & 0 \\ \frac{\partial \ddot{\bar{S}}}{\partial p_1} & \frac{\partial \ddot{\bar{S}}}{\partial p_2} \end{bmatrix}$$

In what follows the derivation of expressions for the three partial derivatives matrices  $\frac{\partial \ddot{\bar{S}}}{\partial \bar{S}}$ ,  $\frac{\partial \ddot{\bar{S}}}{\partial p_1}$ ,  $\frac{\partial \ddot{\bar{S}}}{\partial p_2}$  is presented. Rules for differentiation of matrix forms are outlined in Appendix E. As in the case of the matrices derived in section 3.32, the expressions are simplified only in so far as this is required for enhancing the coding in FORTRAN computer language.

The matrix  $\frac{\partial \ddot{\bar{S}}}{\partial \bar{S}}$ :

$$\begin{aligned} \frac{\partial \ddot{\bar{S}}}{\partial \bar{S}} = & -k^2 E \left\{ \frac{1}{m} \left[ \frac{I}{\rho_m^3} - \frac{3SS^T}{\rho_m^5} + \frac{\bar{H} \cdot I}{\rho_m^5} - \frac{5\bar{H}SS^T}{\rho_m^7} + \frac{\bar{P}}{\rho_m^5} - \frac{5\bar{P}SS^T}{\rho_m^7} \right. \right. \\ & - \frac{5SS^T(\bar{P} + \bar{P}^T)}{2\rho_m^7} + \frac{35SS^T\bar{P}SS^T}{2\rho_m^9} - \frac{5S^T\bar{P}SI}{2\rho_m^7} + \sum_1 \left( \frac{\mu_i I}{\rho_i^3} - \frac{3\mu_i P_i P_i^T}{\rho_i^5} \right) \left. \right\} \\ & + \frac{I}{\rho_e^3} - \frac{3RR^T}{\rho_e^5} + \frac{\bar{E}I}{\rho_e^5} - \frac{5\bar{E}RR^T}{\rho_e^7} + \frac{\bar{Q}}{\rho_e^5} - \frac{5\bar{Q}RR^T}{\rho_e^7} - \frac{5RR^T(\bar{Q} + \bar{Q}^T)}{2\rho_e^7} \\ & + \left. \frac{35RR^T\bar{Q}RR^T}{2\rho_e^9} - \frac{5R^T\bar{Q}RI}{2\rho_e^7} \right\}. \end{aligned} \quad (\text{F.3})$$

Slight regrouping is in order and the final form is as follows:

$$\begin{aligned}
 \frac{\partial \ddot{\mathbf{S}}}{\partial \mathbf{S}} = & -k^2 E \left( \frac{1}{m} \left\{ \left[ \frac{\mathbf{I}}{\rho_n^3} + \frac{\overline{\mathbf{H}} \cdot \mathbf{I}}{\rho_n^5} + \frac{(\rho_n^2 \mathbf{I} - \frac{5}{2} \mathbf{S}\mathbf{S}^T) \overline{\mathbf{P}}}{\rho_n^7} \right] \right. \right. \\
 & - \left[ \frac{3 \cdot \mathbf{I}}{\rho_n^5} + \frac{5 \overline{\mathbf{H}} \mathbf{I}}{\rho_n^7} + \frac{5(\rho_n^2 \mathbf{I} - \frac{7}{2} \mathbf{S}\mathbf{S}^T) \overline{\mathbf{P}}}{\rho_n^9} \right] \mathbf{S}\mathbf{S}^T \\
 & - \left. \frac{5}{2\rho_n^7} (\mathbf{S}^T \overline{\mathbf{P}} \mathbf{S} \mathbf{I} + \mathbf{S}\mathbf{S}^T \overline{\mathbf{P}}^T) + \sum_1 \mu_1 \left( \frac{\mathbf{I}}{\rho_1^3} - \frac{3 \mathbf{P}_1 \mathbf{P}_1^T}{\rho_1^5} \right) \right\} \\
 & + \left[ \frac{\mathbf{I}}{\rho_e^3} + \frac{\overline{\mathbf{E}} \mathbf{I}}{\rho_e^5} + \frac{(\rho_e^2 \mathbf{I} - \frac{5}{2} \mathbf{R}\mathbf{R}^T) \overline{\mathbf{Q}}}{\rho_e^7} \right] \\
 & - \left[ \frac{3 \mathbf{I}}{\rho_e^5} + \frac{5 \overline{\mathbf{E}} \mathbf{I}}{\rho_e^7} + \frac{5(\rho_e^2 \mathbf{I} - \frac{7}{2} \mathbf{R}\mathbf{R}^T) \overline{\mathbf{Q}}}{\rho_e^9} \right] \mathbf{R}\mathbf{R}^T \\
 & - \left. \frac{5}{2\rho_e^7} (\mathbf{R}^T \overline{\mathbf{Q}} \mathbf{R} \mathbf{I} + \mathbf{R}\mathbf{R}^T \overline{\mathbf{Q}}^T) \right\} \right). \tag{F.4}
 \end{aligned}$$

The matrix  $\frac{\partial \ddot{\mathbf{S}}}{\partial \mathbf{p}_1}$  :

$$\mathbf{p}_1 = [\mathbf{C}_{22} \quad \beta \quad \mathbf{C}_{20}]^T$$

In section 3.32 the following two partial derivative matrices are derived.

$$\Gamma = \frac{\partial [\varphi \quad \psi \quad \theta \quad \dot{\varphi} \quad \dot{\psi} \quad \dot{\theta}]^T}{\partial [\tau \quad \sigma \quad \rho \quad \dot{\tau} \quad \dot{\sigma} \quad \dot{\rho}]^T} = \begin{bmatrix} 1 & -1 & 0 & & & \\ 0 & 1 & 0 & & 0 & \\ 0 & 0 & 1 & & & \\ & & & 1 & -1 & 0 \\ & 0 & & 0 & 1 & 0 \\ & & & 0 & 0 & 1 \end{bmatrix} \tag{F.5}$$

and

$$Q_M = \frac{\partial [\tau \quad \sigma \quad \rho \quad \dot{\tau} \quad \dot{\sigma} \quad \dot{\rho}]^T}{\partial p_1} \quad (F.6)$$

$$\begin{bmatrix} K \\ L \end{bmatrix} = \Gamma \cdot Q_M$$

where

$$K = \frac{\partial [\varphi \quad \psi \quad \theta]^T}{\partial p_1} \quad (F.7)$$

The differentiation is performed as follows:

$$\begin{aligned} \frac{\partial \ddot{S}}{\partial p_1} = & -k^2 E \left\{ \frac{1}{m} \left[ \frac{I}{\rho^5} \cdot \frac{\partial \bar{H}}{\partial p_1} \cdot S + \frac{(\rho^2 I - \frac{5}{2} SS^T)}{\rho^7} \frac{\partial (\bar{P} \cdot S)}{\partial p_1} + \sum_i \mu_i \frac{\partial \left( \frac{\rho_i}{\rho^3} \right)}{\partial p_1} \right] \right. \\ & \left. + \frac{I}{\rho^5} \cdot \frac{\partial \bar{H}}{\partial p_1} \cdot X + \frac{(\rho^2 I - \frac{5}{2} XX^T)}{\rho^7} \frac{\partial (\bar{P} \cdot X)}{\partial p_1} \right\} \quad (F.8) \end{aligned}$$

The following intermediaries are needed:

$$\frac{\partial \bar{H}}{\partial p_1} = \frac{3a_e^2}{2\beta\xi^2} \left[ (6-6\beta) \quad \frac{3(C_{20} - 2C_{22})}{\beta} \quad -(3+\beta) \right]$$

$$\frac{\partial (\bar{P} \cdot S)}{\partial p_1} = \begin{bmatrix} \frac{\partial \bar{P}}{\partial C_{22}} \cdot S \\ \frac{\partial \bar{P}}{\partial \beta} \cdot S \\ \frac{\partial \bar{P}}{\partial C_{20}} \cdot S \end{bmatrix}$$

$\frac{\partial (\bar{P} \cdot X)}{\partial p_1}$  is obtained similarly substituting X for S.

$$\frac{\partial \bar{P}}{\partial C_{22}} = \frac{3a_e^2}{\beta\xi^2} \left[ T_M^T \cdot \frac{\partial G}{\partial C_{22}} \cdot T_M + 2T_M^T G \frac{\partial T_M}{\partial C_{22}} \right]$$

$$\frac{\partial \bar{P}}{\partial \beta} = \frac{3a_e^2}{\xi^2} \left[ T_M^T \cdot \frac{\partial (G/\beta)}{\partial \beta} \cdot T_M + \frac{2}{\beta} \cdot T_M^T G \frac{\partial T_M}{\partial \beta} \right]$$

$$\frac{\partial \bar{P}}{\partial C_{20}} = \frac{3a_p^2}{\beta \xi^2} \left[ T_M^T \frac{\partial G}{\partial C_{20}} \cdot T_M + 2 T_M^T G \cdot \frac{\partial T_M}{\partial C_{20}} \right]$$

where

$$\frac{\partial G}{\partial C_{22}} = \begin{bmatrix} 2-4\beta & 0 & 0 \\ 0 & 2 & 0 \\ 0 & 0 & 2-2\beta \end{bmatrix}; \quad \frac{\partial (G/\beta)}{\partial \beta} = \frac{(C_{20} - 2C_{22})}{\beta} \cdot I$$

and

$$\frac{\partial G}{\partial C_{20}} = \begin{bmatrix} -1 & 0 & 0 \\ 0 & -1 & 0 \\ 0 & 0 & -(1+\beta) \end{bmatrix}$$

The partial derivatives of  $T_M$  are evaluated as follows:

$$\frac{\partial T_M}{\partial p_1} = \frac{\partial T_M}{\partial (\varphi \psi \theta)^T} \cdot K \quad (K \text{ was defined above})$$

$$A_1 = \frac{\partial T_M}{\partial \varphi} = L^{c_3} \cdot T_M$$

$$A_2 = \frac{\partial T_M}{\partial \psi} = T_M \cdot L^{c_3}$$

$$A_3 = \frac{\partial T_M}{\partial \theta} = -R_3(\varphi) \cdot L^{c_1} \cdot R_1(-\theta) \cdot R_3(\psi)$$

(see appendix F)

$$\frac{\partial T_M}{\partial C_{22}} = A_1 \cdot K_{1,1} + A_2 \cdot K_{2,1} + A_3 \cdot K_{3,1}$$

$$\frac{\partial T_M}{\partial \beta} = A_1 \cdot K_{1,2} + A_2 \cdot K_{2,2} + A_3 \cdot K_{3,2}$$

$$\frac{\partial T_M}{\partial C_{20}} = A_1 K_{1,3} + A_2 K_{2,3} + A_3 K_{3,3}$$

$$\frac{\partial \left( \frac{P_1}{\rho_1^3} \right)}{\partial p_1} = - \left[ \frac{1}{\rho_1^3} - \frac{3 P_1 P_1^T}{\rho_1^5} \right] \cdot [A_1^T \cdot M_1 ; A_2^T \cdot M_1 ; A_3^T \cdot M_1]$$

The last expression is based on the following identity

$$A_1^T = \left[ \frac{\partial T_M}{\partial C_{22}} \right]^T = \frac{\partial T_M^T}{\partial C_{22}}$$

The matrix  $\frac{\partial \ddot{S}}{\partial p_2}$ :

$$\frac{\partial \ddot{S}}{\partial p_2} = -\frac{k^2 E}{m} \left[ \frac{P_1}{\rho_1^3} \quad \frac{P_2}{\rho_2^3} \quad \dots \quad \frac{P_k}{\rho_k^3} \right]$$

This completes the derivation of all the expressions necessary to evaluate  $\Theta$  and  $\Phi$ . Using numerical integration, the matrices  $U$  and  $Q$  are evaluated along the orbit together with the state vector itself. In case the number of parameters (number of columns in  $Q$ ) is excessive, the differential equations  $\dot{Q} = \Theta Q + \Phi$  can be solved by quadrature using Simpson's or other appropriate methods (see Anderson, 1964).

## REFERENCES

- AENA Supplement. (1961). Explanatory Supplement to the Astronomical Ephemeris and the AENA. H. M. Stationery Office, London.
- AENA. (1968). "Supplement to the American Ephemeris 1968" (The Introduction of the IAU System of Astronomical Constants).
- Anderson, J.D. (1964). "Theoretical Basis of the JPL Orbit Determination Program." JPL TM 312-409, Pasadena.
- Arthur, D.W.G. (1962). "On the Problems of Selenodetic Photogrammetry." Communications of the LPL No. 8, Vol. 1.
- Arthur, D.W.G. (1968). Communications of the LPL No. 127-131, Vol. 7, Part 5.
- Boeing. (1969). "Post Mission Analysis of Photo Data from the Lunar Orbiter Missions." Boeing, D2-100815-4.
- Breece, S., Hardy, M., and Marchant, M. (1964). "Horizontal and Vertical Control for Lunar Mapping, Part 2." AMS, T R No. 29, March.
- Brouwer, D., and Clemence, G. (1961). Methods of Celestial Mechanics. Academic Press, New York.
- Brown, D. C. (1968). "A Unified Lunar Control Network." Photogrammetric Engineering, Vol. 34, No. 12, December.
- Brown, D. C. (1969). Saga, A Computer Program for Short Arc Geodetic Adjustment of Satellite Observations. DBA Systems Inc., Melbourne, Florida. AD-691 835.
- Brown, E. W. (1896). An Introductory Treatise on the Lunar Theory. Reprinted by Dover Publications, Inc., New York, 1960.
- Cary, C. N. and Sjogren, W. L. (1968). "Gravitational Inconsistency in the Lunar Theory Confirmed by Radio Tracking." Science, 160, p. 875.
- Doyle, F.J. (1968). "Photogrammetric Geodesy on the Moon". Presented at the annual meeting of The American Society of Photogrammetry, March.
- Eckert, W. J., et al. (1954). Improved Lunar Ephemeris 1952-1959. U. S. Government Printing Office, Washington, D. C.
- Eckert, W. M. (1965). "On the Motions of the Perigee and Node and the Distribution of Mass in the Moon." The Astronomical Journal, Vol. 70, pp. 787-792.

- Eckhardt, D. H. (1965). "Computer Solutions of the Forced Physical Libration of the Moon." The Astronomical Journal, Vol. 70, No. 7, pp. 466-471, September.
- Eckhardt, D. H. (1970). "Lunar Libration Tables." The Moon, Vol. 1, No. 2, February.
- Eckhardt, D. H. (1971). Private Communication.
- Edgar, R. F. (1964). "Turbulence and Resolution in Astronomical Photography." University of Manchester, Department of Astronomy, T N No. 4, January.
- Escobal, P. R. (1965). Methods of Orbit Determination. John Wiley and Sons, New York.
- Fajemirokun, F. A. (1971). "Application of New Observational Systems for Selenodetic Control." The Ohio State University, Department of Geodetic Science, Report No. 157.
- Franz, J. (1898). "Die Figure des Mondes." Astro. Beob. Königsberg, 38.
- Franz, J. (1901). "Ortsbestimmung von 150 Mondkratern." Mitteilungen der Königlichen Universitäts-Sternwarte zu Breslau, Vol. 1, pp. 1-51.
- Garthwaite, K., et al. (1970). "A Preliminary Special Perturbation Theory for the Lunar Motion." The Astronomical Journal, 75, No. 10, December, p. 1133.
- Haines, E. L. (1969). "Selenodesy and Lunar Dynamics." JPL Document No. 900-278, Vol. 1, Pasadena.
- Hallert, B. (1962). "Geometrical Quality of Lunar Mapping by Photogrammetric Methods." GIMRADA RN No. 9, September.
- Hathaway, J. D. (1967). DOD Selenodetic Control System 1966. AMS Final Report, NASA Defense Purchase Request No. T-37794(G), January.
- Hayn, F. (1904). "Selenographische Koordinaten." Leipzig Sachs<sup>8</sup> Gesell. der Wiss. II Abb.
- Hopmann, J. (1967). "The Accuracy of the Information on Absolute Heights on the Moon, and the Problem of its Figure." Mantles of the Earth and Terrestrial Planets, S. K. Runcorn, (ed.), John Wiley and Sons, New York.
- Jeffreys, H. (1970). The Earth. (5th Edition), Cambridge University Press, London.

- Kopal, Z. and Goudas, C. (eds). (1967). Measure of the Moon. D. Reidel Publishing Company, Dordrecht, Holland.
- Kopal, Z. (1969). The Moon. D. Reidel Publishing Company., Dordrecht, Holland.
- Koziel, K. (1948). Acta Astronomica, 4. p. 61, June 27.
- Krogh, F. T. (1969). VODQ/SVDQ/DVDQ - Variable Order Integrators for the Numerical Solution of Ordinary Differential Equations. Section 314, JPL, Pasadena.
- Kuiper, G. P., Arthur, D.W.G., et al. (1969). Research Directed Toward a Photo-Telescopic Selenodetic Measuring Program. Final Report, AFCRL-69-0537, December. AD-702 526.
- Lorell, J. (1969). "Lunar Orbiter Gravity Analysis." JPL TR 32-1387, Pasadena, June, 15.
- Lucas, J. (1963). "Differentiation of Orientation Matrix." Photogrammetric Engineering, Vol. 29, No. 7, July.
- Meissl, P. (1971). Private Communication.
- Melbourne, W. G., et al. (1968). "Constants and Related Information for Astrodynamic Calculations 1968." JPL TR 32-1306, Pasadena.
- Meyer, D. L. and Ruffin, B. W., (1965). "Coordinates of Lunar Features, Group I and II Solutions." ACIC Technical Paper No. 15, March.
- Mills, C. A. and Sudbury, P. V. (1968). "Absolute Coordinates of Lunar Features, III." Icarus, Vol. 9, pp. 538-561, June 5.
- Moutsoulas, M. (1970). "Physical Libration of the Moon in Longitude." The Moon, Vol. 1, No. 3, April.
- Moutsoulas, M. (1970b). "Star Calibrated Moon Photography." The Moon, Vol. 1, No. 2, February.
- Mueller, I.I. (1964). Introduction to Satellite Geodesy. Frederick Ungar Publishing Company, New York.
- Mueller, I.I. (1969). Spherical and Practical Astronomy as Applied to Geodesy. Frederick Ungar Publishing Company, New York.
- Mueller, I.I. (1969b). "A General Review and Discussion on Geodetic Control of the Moon." Report of the Department of Geodetic Science, No. 127, December.
- Mulholland, J. D. (1968). "Proceedings of the JPL Seminar on Uncertainties in the Lunar Ephemeris." JPL TR 32-1247, Pasadena, May.

- Mulholland, J. D. (1969). "Proceedings of the Symposium on Observation, Analysis and Space Research Applications of the Lunar Motion." JPL TR 32-1386, Pasadena.
- Mulholland, J. D. (1969b). "Apollo 10 Range Data Provide Additional Support for LE-16." JPL SPS 37-58 II, pp. 229-230.
- NASA, MSC. (1966). "Lunar Control Uncertainties." Memorandum.
- NASA. (1967). 1967 Summer Study of Lunar Science and Exploration. NASA, S P - 157.
- O'Handley, D. A., et al. (1969). "JPL Development Ephemeris, No. 69." JPL TR 32-1465, Pasadena, December.
- Plummer, H. C. (1918). An Introductory Treatise on Dynamical Astronomy. Reprinted by Dover Publications, Inc., New York, 1960.
- Ransford, G.A. (1969). Private Communication.
- Ransford, G. A., et al. (1970). "Lunar Landmark Locations Apollo 8, 10, 11, and 12 Missions." NASA, Technical Note MSCS-249.
- Rinner, K., et al. (1967). Systematic Investigation of Geodetic Networks in Space. U. S. Army Research and Development Group (Europe), May.
- Saunders, S. A. (1904). "The Determination of Selenographic Positions III." Memoirs Royal Astron. Soc., Vol. 57, Part 1.
- Schrutka-Rechtenstamm, G. (1956). "Neureduction der acht von J. Franz und der vier von F. Hayn Gemessenen Mondkraterpositionen." Sitzungsberichte Osterr. Arks. Wiss. Math-Naturw. Kl., Abt. II, Vol. 165.
- Schrutka-Rechtenstamm, G. (1958). "Neureduction der 150 Mondpunkte der Breslauer Messungen Von J. Franz." Sitz. Osterr. Akad. Wiss. Math-Naturw. Kl., Abt. II, Vol. 167.
- Sjorgen, W. L. (1968). "Lunar Orbiter Ranging Data Analysis." JPL TR 32-1247, Pasadena, May.
- Smart, E. H. (1951). Advanced Dynamics of a Solid Body. Vol. 2., MacMillan Company, London.
- TOPOCOM. (1969). "Lunar Orbiter IV Test and Evaluation Study for the Development of an Improved Lunar Geodetic Control." NASA, W-12476.
- Uotila, U. A. (1967). Introduction to Adjustment Computations with Matrices. The Ohio State University, Department of Geodetic Science, unpublished.
- Van Flandern, T. C. (1970). Private Communication.

Warner, M. R. (1964). "The Orbit Determination Program of the JPL." JPL TM 33-168, Pasadena.

Woolard, E. W. (1953). "Theory of the Rotation of the Earth Around its Center of Mass." Astronomical Papers of the AENA, Vol. XV, Part 1.

The abbreviations used in the list of References are as follows:

ACIC	Astronautical Chart and Information Center
AENA	American Ephemeris and Nautical Almanac
AFCLR	Air Force Cambridge Research Laboratories
AMS	Army Map Service
DOD	Department of Defense
IAU	International Astronomical Union
JPL	Jet Propulsion Laboratory
LPL	Lunar and Planetary Laboratory
RN	Research Note
TM	Technical Memorandum
TN	Technical Note
TR	Technical Report